The Fire Performance of Timber Floors in Multi-Storey Buildings

A thesis submitted in partial fulfilment
of the requirements for the
Degree in Doctor of Philosophy

By
James William O'Neill

Supervised by
Professor Andrew H. Buchanan
Dr. Anthony K. Abu
Dr. David M. Carradine

Department of Civil and Natural Resources Engineering
University of Canterbury
Christchurch, New Zealand

December 2013

ABSTRACT

This research investigated the fire performance of unprotected timber floors, focussing on composite joist floors, composite box floors and timber-concrete composite floors. The study of these floors was conducted using the finite element software ABAQUS using a thermo-stress analysis in three dimensions, and with experimental fire tests of floor assemblies. The major goal of this research was to develop a simplified design approach for timber floors, validated against the numerical and experimental work.

Four furnace tests were conducted on unprotected timber floor systems in the full-scale furnace at the BRANZ facilities in New Zealand. The tested floors were one-way strip floors with pinned support conditions exposed to the ISO 834 standard fire for varying durations of 30 – 105 minutes. The floors were loaded under standard office loading conditions of 3.0kPa live and 1.0kPa superimposed dead loading. The charring rates of the LVL timber members were found to range from 0.66 – 0.86 mm/min across all specimens. When designed to resist a similar load level both the composite joist and box floor types had a similar response to the fire loads, however the joist floors exhibited increased upward burning through the beam members in the latter stages of testing which may contribute to earlier failure times for smaller floor geometries.

A sequentially coupled thermal-stress analysis was conducted to determine the effects of a fire on floor assemblies under load. Firstly a thermal analysis was performed to determine the temperature profile of the floor assemblies for the duration of modelling, and then a stress analysis was performed using the temperature profile as input into the structural model. With regards to the thermal modelling, a proposed set of effective values was used to account for the mass transfer processes occurring in the timber. The thermal modelling predicted the charring damage of the floors tested in the experiments to within a few millimetres of precision, and the simplified assumptions made in relation to fire inputs, boundary conditions, mesh refinement and effective material parameters were accurate to the desired level of precision. A sensitivity study was conducted comparing different mesh sizes, time step sizes, material model approaches and software suites to determine any shortfalls which may be encountered in the analysis. It was found that a material model adopting a latent heat approach was the most adequate for modelling timber in fires using these effective values, and mesh sizes of up to 6 mm produced relatively precise results.

The structural modelling predicted the displacement response and failure times of the floors to within 20% of the experimental data, and the simplified assumptions made in relation to fire inputs, boundary conditions, mesh refinement and effective material properties were once again accurate to the desired level of precision. A modification to the reduction in tension strength at elevated temperatures was proposed to better predict the observed behaviour. A sensitivity study concluded that the material model definition plays a vital role in the output of the modelling. Non-standard fire exposures were also modelled for completeness.

A simplified design method to estimate the fire resistance of unprotected floor assemblies was also developed. The method uses a bi-linear charring rate the assumption of a zero strength layer in the timber. The method was compared to the experimental data from this research and others around the world. The results were also compared to other charring rate methodologies from around the world.

ACKNOWLEDGEMENTS

I would like to express my gratitude to my supervisor Professor Andrew Buchanan, whose guidance and support over the years has fuelled my efforts to explore the fields of fire and timber engineering. His mentoring and encouragement has opened many avenues for me in my professional career, and I am extremely grateful to him for this.

I would also like to acknowledge my supervisor Dr Anthony Abu, who has provided me with countless hours of support and guidance during my work. His persistent attitude and consistently high standards have left a great impression on me and my work, and I hold him in the highest regard.

I would like to thank my supervisor Dr David Carradine who has been such a positive force in my postgraduate study and a great friend for many years, he has always inspired me to do better. His expertise in experimental work and prompt reviewing has been instrumental in allowing me to complete my research in my allotted timeframe, and having him as a supervisor has been a privilege.

A very special thanks to Associate Professor Peter Moss, whose invaluable expertise and guidance have helped shape my work over the past years. Peter has been a fountain of engineering knowledge at my disposal and his constructive feedback has been a privilege to receive.

A special thanks to my friend Norman Werther from whom I have learned so much. His related research and constant input into my own work has been a great help, and I wish him the very best in his own endeavours.

It is important to acknowledge the STIC Initiative for funding my research and in particular Dr Robert Finch for always paying the bills I racked up over the years. I would also like to thank my colleagues at the University of Auckland and the University of Technology in Sydney, and the staff from Nelson Pine and Carter Holt Harvey for their input into my research. I would like to thank the fabricators McIntosh Laminates and Hunter Laminates for facilitating the experimental portions of my work.

Thanks to the Department of Civil Engineering at the University of Canterbury, it has been a fantastic environment to conduct my study. In particular I would like to acknowledge Elizabeth Ackermann for her tireless administration efforts on my behalf which is much appreciated.

I would also like to thank the Fire Engineering group at the University of Canterbury, in particular Dr Michael Spearpoint and Associate Professor Charley Fleischmann for facilitating technical meetings and providing a wealth of support and feedback on my work.

Thanks to the staff at BRANZ, and in particular Paul Bano-Chapman for his extremely valuable input and patience, and technicians Rick and Paul for their aid during the fire tests.

A very special thanks to my civil engineering colleagues at the University of Canterbury, in particular Dennis Pau, Sam McHattie, Andrew Baird, Varun Joshi, Tobias Smith and all the others who have come and gone throughout the years. Our technical discussions and endless debate have assisted me greatly in completing my research to a high standard.

Thanks to the people at SP Trätek for their encouragement and aid during the start of my research. In particular I would like to acknowledge Dr Birgit Östmann, Dr Jürgen König and Dr Joachim Schmid who gave me such valuable direction and advice when formulating my research.

Also thanks to the people at ETH Zurich for hosting me earlier on in my research, in particular Professor Andrea Frangi for his advice and encouragement, which helped shape my early research.

I would like to thank my brother Richard, who has provided me with much needed financial backing in recent years to enable me to finish this work, it is much appreciated.

Finally, I would like to thank my parents Francesco and Julia for their undying support and enthusiasm during my many years of study. They have always been my inspiration to better myself and achieve my dreams, and I dedicate this work to them.

TABLE OF CONTENTS

LIST OF FIGURES

LIST OF TABLES

NOMENCLATURE

Roman Characters

a	Distance between loading and support points, four point bending (m)
A	Section area (mm^2)
A_p	Perpendicular bearing area (mm^2)
A_s	Shear area (mm^2)
A_t	Total internal area of compartment surfaces (m^2)
A_v	Area of vertical openings (m^2)
b	Distance between loading points, four point bending (m)
c_p	Specific heat (J/kgK)
d_{char}	Charring depth (mm)
d_{slab}	Slab depth (mm)
d_{zero}	Zero strength layer (mm)
E	Modulus of elasticity (MPa)
E_d	Design load (kPa)
$E_{d,fire}$	Fire design load (kPa)
f_b'	Characteristic bending strength (MPa)
f_p'	Characteristic compression strength perpendicular to grain (MPa)
f_s'	Characteristic shear strength (MPa)
F_v	Opening factor (m$^{1/2}$)
G	Modulus of rigidity (MPa)
G_l	Dead load (kPa)
G_{self}	Self-weight (kPa)
H_v	Height of vertical openings (m)
I	Second moment of area (mm^4)
k	Thermal conductivity (W/mK)
k_0	Zero strength layer modification factor
k_1	Load duration factor
k_3	Bearing area factor
k_4	Parallel support factor
k_5	Grid system factor

k_8	Load sharing factor
k_{24}	Size factor
L	Span length (m)
L_b	Bearing length (mm)
M^*	Moment demand (kNm)
M^*_{fire}	Moment demand for the fire design (kNm)
M_n	Nominal bending strength capacity (kNm)
N^*_b	Bearing strength demand (kN)
N_{nb}	Nominal bearing strength capacity (kN)
P_{fire}	Point load for the fire design (kN)
Q_l	Live load (kPa)
$\dot{Q}$	Rate of internal heat generation (W/m^3)
$Q_{centroid}$	First moment of area about the section centroid (mm^3)
SDL	Superimposed dead load (kPa)
t	Time (s)
t_b	Bearing thickness (mm)
t_w	Web thickness (mm)
t^*	Fictitious time (hours)
t^*_{max}	Time for maximum gas temperature (hours)
T	Temperature (K)
V^*	Shear demand (kN)
V_n	Nominal shear strength capacity (kN)
w	Uniformly distributed load (kN/m)
w_{fire}	Fire uniformly distributed load (kN/m)
W_t	Tributary width (m)
x	Dimension in the x-direction (m)
x_1	Time modification factor
y	Dimension in the y-direction (m)
z	Dimension in the z-direction (m)
Z_b	Elastic section modulus (mm^3)

Greek Characters

β	Nominal charring rate (mm/min)
$\beta_{overall}$	Calculated overall charring rate (mm/min)
δ	Differential operator
ρ	Density (kg/m^3)
θ_g	The gas temperature in the compartment (°C)
θ_{max}	The maximum gas temperature (°C)
ψ_l	Load reduction factor
υ	Poisson's ratio
$\emptyset$	Strength reduction factor

1 INTRODUCTION

1.1 Timber as a Building Material

Although timber floor systems have provided the basis for flooring needs for centuries, the development of the skyscraper and with it the proliferation of steel and concrete floor systems has made the use of less efficient traditional timber floor systems obsolete. However with the advent of high performance wood materials such as glue laminated timber and laminated veneer lumber, timber floors are once again a viable alternative to using steel or concrete. This raises the question of the performance of these floors in fires. Due to the nature of the non-combustible materials of steel and concrete, their performance in fires can be relatively simple to predict and design for. As timber is a combustible material the situation becomes more complex, as the loss of wood section due to charring, the anisotropy of the material itself and the detailing of connections all serve to complicate the estimation of the fire resistance of timber floor systems.

The widespread use of timber as one of the main structural elements in tall buildings of the modern environment is inhibited as timber is a combustible material and commonly thought to behave poorly in fires. In order to facilitate the implementation of timber products into the New Zealand and Australian construction industries, these issues of fire resistance must be addressed. This research focuses specifically on the fire performance of different timber floor types used in multi-storey timber buildings.

1.2 Objectives

The main focus of this research is to characterise the performance of unprotected timber floor systems in a fire scenario. This is approached from different angles, involving the experimental, numerical and analytical analysis of different floor systems in fires. The major objectives of this research are:

- To investigate the fire resistance of timber floor systems. The major types of floors under consideration are composite joist floors, composite box floors and timber-concrete composite floors.
- To develop simplified design methods for predicting the fire resistance of timber floors.
- To predict the fire performance of timber floors in real buildings.

1.3 Methodology

In order to achieve the desired objectives, both numerical modelling and experimental testing are required to investigate the performance of different floor types exposed to fire. An analytical analysis is then pursued to tie the results of the experimental testing and the modelling together, which enables the performance of the floor systems to be estimated in a simple yet well-defined and validated manner.

The scope of this research extends to the characterisation of simply-supported timber floor assemblies which are unprotected and exposed to a fire from below. The specified floor geometries encompass a wide range of optimised designs currently used in the growing timber floor market, and have been chosen for their uniqueness and applicability with multi-storey floor applications. The fire curve used to illustrate the fire is the standard ISO 834 fire (1999). The floors are analysed in the following ways:

- Experimental furnace tests; four timber floors of varying load capacities and geometries heated with the standard ISO fire in a large furnace. The floors are loaded with two centralised point loads and simply-supported to simulate four-point bending.
- Finite element predictions using the software ABAQUS; modelling the floors in a sequential thermo-stress analysis and comparing the predictions with the experimental results.
- Analysing current design methodologies and developing a simplified method of estimating of the fire resistance of unprotected floor assemblies.
- Comparing the simplified method with both the experimental and numerical modelling results.

1.4 Outline of Thesis

The thesis is separated into chapters, each describing the major steps undertaken during the research. The literature review and experimental furnace testing are presented first, followed by the computational modelling and the analytical procedures. Other design considerations follow, with the thesis being concluded after this. The thesis is organised into the following chapters:

LITERATURE REVIEW – Chapter 2 provides a broad literature review on the background of fire safety in timber buildings, and the different types of timber products available. A comprehensive review of the macro properties of timber and the thermal and mechanical properties of the timber material follows. A general overview of timber floor systems is provided, with the focus

narrowing into the floors under consideration in this research. Chapter 2 is closed with some of the current code design methodologies followed around the world with regards to designing timber members for fire resistance.

EXPERIMENTAL FIRE TESTS OF TIMBER FLOORS – The experimental furnace testing is described in Chapter 3, with a detailed illustration of the testing facilities and tests methods used for the experiments. A comprehensive breakdown of the floor specimens tested is presented, followed by the test results section. This is split into results for each specimen, followed by comparisons and observations between each of the experimental furnace tests.

THERMAL FINITE ELEMENT MODELLING – Chapter 4 initially introduces the ABAQUS software, followed by the impetus and scope of the thermal modelling. Both one and two-dimensional thermal modelling is discussed, with particular reference to the material models used and the methods and test data used for validation of the modelling. This is followed by a sensitivity analysis considering mesh size, time-step size and a review using other software modelling packages. Comparisons are made with the experimental results presented in Chapter 3 for each relevant section.

STRUCTURAL FINITE ELEMENT MODELLING – The structural modelling is presented in Chapter 5, which describes a thermo-structural analysis of the timber floors under study. It begins with simplified models in which their development into a more appropriate but complex format is detailed. This covers one, two and three-dimensional modelling, their relevant inputs and issues with regards to the values and methods used, culminating in the sequential thermo-stress analysis of the floors from the experimental testing. These results are presented with comparisons to the experimental results. A sensitivity analysis is presented focussing on mesh sizes, loading arrangements, boundary conditions and material models. Studies on timber-concrete composite floors and post-tensioned members are presented as separate sections, with overall conclusions on the modelling methods to sum up the chapter.

MODELLING NON-STANDARD FIRES – Chapter 6 presents the modelling of non-standard fires using the thermal and structural models developed previously in Chapters 4 and 5. A discussion on the assumptions made and limitations of this type of modelling for timber is given. Results are then presented for the experimental floor designs tested in this research.

DESIGN METHODS – Chapter 7 covers the development and procedures chosen for the simplified design methods for estimating the fire resistance of timber floor assemblies. A

charring rate methodology is given, followed by worked examples and comparisons with the experimental and numerical results.

OTHER CONSIDERATIONS – Issues of concern which are not addressed in the main body of the thesis are covered in Chapter 8. This includes a discussion on design fire types, passive protection, active protection, penetrations and connections, exposed surfaces, tensile-membrane action of concrete topping slabs and construction site fires.

CONCLUSIONS AND RECOMMENDATIONS – The overall conclusions of the research and recommendations for further research are presented in Chapter 9.

2 LITERATURE REVIEW

2.1 Introduction

Fire safety is increasingly seen as an important aspect in both the design and construction of new structures in the modern building environment. With an increased awareness of the importance of fire safety comes a greater understanding and drive for research into how structures and their respective elements perform in fires.

In recent years engineered timber products have been used for many types of construction across many different countries. New and innovative methods are being developed to make use of this natural and abundant resource, and numerous tall buildings are now being constructed in large city centres for a huge number of different uses. These buildings range from being showcase buildings which generally have a lot of the timber exposed for aesthetic appeal, to a generic office building which has no timber members exposed to public view. Each type of building has its own unique challenges with regards to fire safety; however the most important factors are generally not the material but rather the intended use of the structure and the possible sources of fire. Any building will be unsafe to occupy no matter the building material if the fire safety strategy adopted is flawed.

This research investigates and discusses potential issues surrounding the use of timber as a primary construction material for multi-storey buildings, and is focussed on investigating the performance of timber floor assemblies in fires. It also endeavours to answer some of the most pertinent questions regarding the structural fire design of these floors, and covers much of the background knowledge important for an introduction to this field of study.

2.1.1 Structural Timber Innovation Company Initiative

At the University of Canterbury in New Zealand, research in timber engineering has been on-going in a variety of fields for many years. Some of the major subject areas studied in the past have been seismic design, composite floors, fire safety and sustainability. In 2008 the Structural Timber Innovation Company Ltd was established as a research consortium to implement structural timber solutions into the commercial sector of the construction industry, with a focus on large multi-storey timber buildings. Although much timber research has been undertaken in the past at the University, the establishment of STIC has provided a major opportunity for old

and new timber technologies to be combined and implemented in the modern commercial environment in the form of large multi-storey timber buildings.

STIC is co-funded by the New Zealand government, major companies in the construction industry and research organisations for the purpose of aiding in timber research and promoting the use of timber products in the commercial sector of the construction industry. Part of the overall vision of STIC is "the development of innovative large-span timber buildings for a wide range of uses in New Zealand, Australia and other export markets. Primary applications include commercial, educational, industrial, recreational and residential buildings" (STIC, 2009). Engineered timber components such as glulam (glue laminated timber) and LVL (laminated veneer lumber) form the backbone of the systems that these large-span buildings will consist of. The main objectives of STIC are:

- To create a step change in New Zealand's wood manufacturing and construction industries. It will enhance the international competitiveness of the wood manufacturing sector and will develop innovative solutions for construction of timber buildings world-wide.

- To target sustainable construction, developing new building solutions which greatly reduce environmental impacts. It will develop a wide range of new high-value structural products, and will add value to lower grade wood products that are part of the total construction package.

- To develop, commercialise and facilitate new structural timber solutions for New Zealand and Australia followed by the United States and other export markets.

- To produce comprehensive design guides for designers, regulators, manufacturers and builders. Delivery of the new building systems will be supported by strong relationships with fabricators and construction companies in local and international markets. Buildings will be constructed from prefabricated components, including beams, columns, frames, floors, walls, partition and cladding panels, manufactured from sawn timber, glulam, LVL, and wood-based panel products, sometimes in composite construction with steel and concrete components.

The major portion of financial support for this research has been provided by STIC.

2.2 Fire Safety in Timber Buildings

There is a general expectation of the public that they should be safe in their built environment from all types of internal hazards and the external environment with its associated hazards. This is not exclusive to the fire safety of the built environment, but broadly encompasses all forms of hazard which may threaten the safety of the public. The vast majority of occupants would not think about evacuating a building in their everyday working lives, however there is an inherent expectation that they will be able to safely evacuate when a fire occurs and that the building will not collapse in the event of a fire. Fire safety design is about ensuring these expectations are reasonably met, and this means finding an acceptable balance between the levels of safety and risk which are deemed acceptable in the environment in question.

When considering the fire performance of a building, there are many aspects to designing for fire safety. For the occupants of the building, early fire hazard warnings are paramount to allow occupants to exit the building safely without suffering injury or death. However life safety is only part of the overall fire strategy that must be considered when designing for large buildings. The structural integrity of the building must be considered in order to avoid a catastrophic collapse of all or part of the building, and to prevent the transmission of fire and smoke through the building.

2.2.1 Prescriptive versus Performance-Based Design

There are two major categories under which building codes are written, and many countries regulations around the world follow either of these approaches or a combination of the two.

Prescriptive codes generally give detailed guidance on a range of acceptable parameters and practices which can be implemented in the design of a building. For instance building geometries, material types and how the various building components should be assembled. These types of codes are usually based on easily quantifiable and well known properties and risks of various occupancies, and much of this knowledge comes from lessons learned from previous experiences and failures. Performance-based codes instead detail goals and objectives to be met, and establish criteria to determine if these objectives are reached. This is a relatively new concept, and is only recently enjoying widespread acceptance around the world (Cote and Grant, 2008). When considering fire design there is usually opportunity to partially or fully deviate from a prescriptive approach if the performance based parts are clearly identified and justified in the design.

As many of the new timber technologies which are becoming prevalent in our markets have not yet been properly implemented into design codes, it follows that much of the research

conducted in this thesis will aid in the implementation of these types of timber floor through performance-based design. With this in mind an objective and open approach has been taken in documenting this research to enable others to reproduce any part of it as required.

2.2.2 Active Protection

A number of active protection measures are readily used in practice to either reduce required regulatory criteria or to meet flame spread requirements for timber buildings. The most common form of active system used in multi-storey buildings is a sprinkler system, as these are reliable and well tested form of protection in fires, using a resource which is readily available in all developed countries.

The use of an automatic sprinkler system in a building may have a great impact on the design of exposed structural members. In many design codes when exposed timber is used concessions are allowed when using sprinklers, usually involving the reduction in the required level of fire resistance for the sprinkler protected firecell and any structural members in it.

An activated sprinkler serves to suppress the fire in question, while at the same time it also wets down the surrounding area and members hindering their respective ignition in the fire. Although sprinklers provide more time for occupants to evacuate from the building, and in some cases actually extinguish the fire, their major advantage is that of property protection.

Figure 2-1 shows an automatic sprinkler system installed in the Nelson Marlborough Institute of Technology Building (NMIT) in Nelson, New Zealand, during the construction phase. The building was one of the first post-tensioned timber structures erected in the country, and has fully exposed timber walls and floors throughout. Concessions were made on the allowable area of exposed timber due to the presence of the sprinklers for fire suppression.

Due to the response of sprinklers to suppressing a fire in its growth stage, the fire safety of a building can be considerably enhanced irrespective of the materials used in construction. This has been shown in historical large-scale tests by Fleischer (1960) in which the activation of the sprinkler system occurs in the earlier stages of the fire, thus nullifying the major issues of construction material or the occupancy of the building.

Figure 2-1: NMIT sprinkler system during building construction

2.3 Structural Fire Resistance

Generally the criteria that must be met to ensure an adequate level of fire resistance has been achieved by a building element are as follows:

- Stability – to prevent the structural collapse of the element.
- Integrity – to prevent the transmission of fire and smoke through the element.
- Insulation – to prevent an unacceptable level of heat being transmitted through the element.

Floor systems provide the means for directly supporting the primary service loads of a building. In terms of fire, floors also provide a separation between levels for compartmentalisation of fires. As the floor systems of a building are generally the least protected elements when compared with the rest of the supporting structure (primary beams, columns and walls), and due to the fact that a large fire in a building directly impinges on the underside of the floor system, floors are generally a critical element in designing for the structural fire resistance of a building.

2.3.1 Standard Design Fires

When considering the structural fire safety of a building as a whole, it is important that the fire resistance of a structural assembly is quantified in such a way that the relative effectiveness of different assemblies across a range of material types and structural forms can be appropriately assessed and compared. This allows for a multitude of assemblies to be used together in a building while still enabling a quantifiable level of the overall fire resistance of the system. In order to achieve this, standard test methods which specify a standard test design fire curve are most commonly used throughout the world. The most commonly used testing standards include the ISO 834 (1999) and ASTM E119 (1988) methods. The design fire curves for these two standards are very similar, and are shown in Figure 2-2.

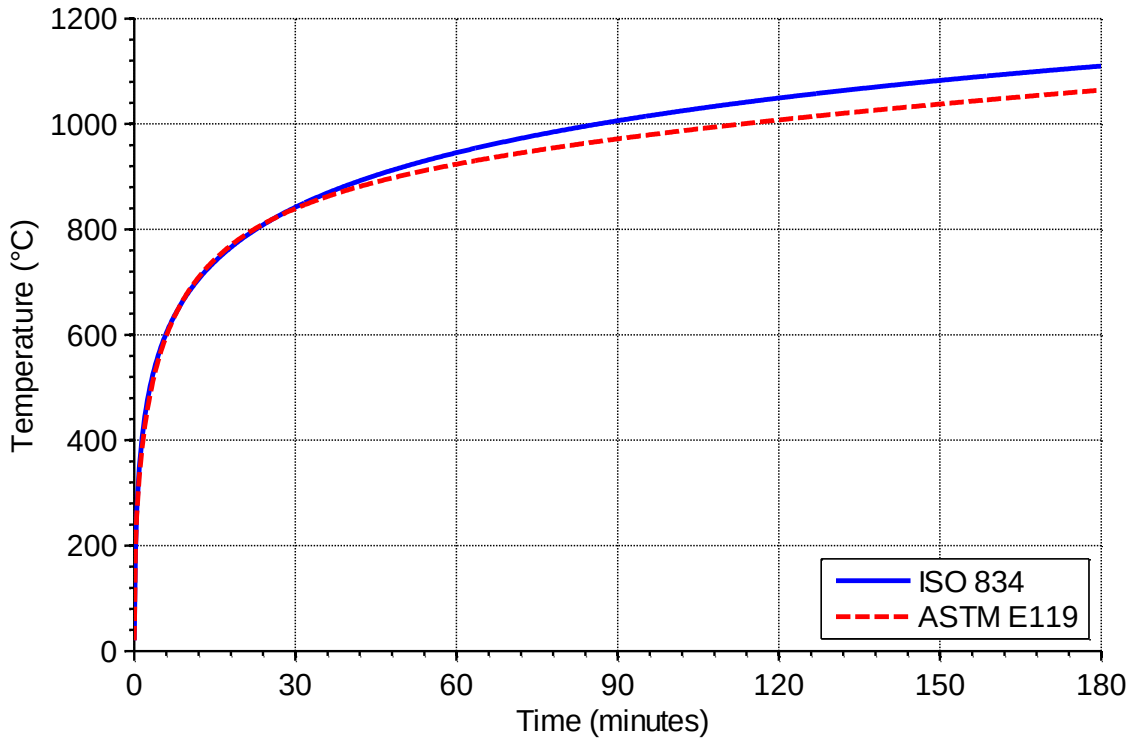

Figure 2-2: Standard test fire curves for ISO 834 and ASTM E119

Although these standard fire curves provide a good benchmark for comparison, they are not representative of real fires. Since they were developed, many improvements in understanding the science of fires and more appropriate fire curves representing modern fuel sources have been developed. Many modern furnishings contain large contents of foam which when burning will generally give a more rapid fire growth rate than the standard test curves. Despite this, the standard methods have been used so extensively in the past that a major step-change to a

different set of fire curves has not yet occurred. Standard test fires have been used in both the experimental and numerical portions of this research, however a more in-depth discussion on the different types of design fires and their respective applications is given in Section 2.4

When considering the design codes around the world with regards to the fire resistance of timber buildings, in particular for calculating the fire resistance of structural members, the procedures given in some of the available codes are briefly described below.

2.3.2 NZS 3603

Currently the fire design procedures for timber in New Zealand are given in NZS 3603 (1993), and consist of a simple charring rate calculation including corner rounding, using a rate of 0.65 mm/min. However this is only applicable to members with minimum dimensions of over 90 mm in any direction, and no further guidance is given for reduced properties under thermal loads or amendments for different product types or species of timber. This method also has no consideration of a zero strength layer in the timber, hence is generally much less conservative than other published methods.

2.3.3 Eurocode 5

The regulations covering the fire design of timber assemblies in Eurocode 5 (CEN, 2004) are comprehensive, encompassing a number of scenarios of protected and unprotected timber. Charring rates are given as both one-dimensional and notional rates (which incorporates corner rounding and fissures), and are specified for softwoods, hardwoods, LVL and panel products. For calculating the fire resistance of members under load two major procedures are proposed. The first is a reduced cross-section method which utilises an effective char depth calculated from the applicable charring rate and a zero strength layer, in this case specified as 7 mm. The second procedure is a reduced properties method which can only be used for specific cross-section geometries, where the strength and stiffness of members are reduced according to the area of timber exposed to the fire. Reductions are applied to a reduced cross-section calculated from a one-dimensional charring rate.

The Eurocode also has guidelines and specifications for advanced calculation methods, and many other types of timber assembly. A comprehensive summary of the state of European design requirements is given by Östmann (2010).

2.3.4 AS 1720.4

The building code of Australia specifies guidelines for designing timber members in AS 1720.4 (2006). The standard specifies a notional charring rate calculation based on the density of the timber at 12% moisture content, and also specifies a zero strength layer of 7.5 mm. This is applicable to all timber members for calculating a residual section and hence the load carrying capacity of that section.

2.3.5 AFPA Technical Report 10

Technical Report 10 (AFPA, 2003) produced by the American Wood Council details a comprehensive charring rate method similar to other codes. It consists of a notional charring rate with multiple guidelines on calculating section moduli and strength reduction factors. The charring rate calculation incorporates both corner rounding and a zero strength layer.

2.4 Structural Fire Design

The design fire is the key aspect in fire engineering which is usually specified by the practicing fire engineer, hence each fire scenario and the impact of that fire is different from one structure to the next. A design fire will be defined by the particular use of the structure, hence when trying to approximate a large range of possible fire scenarios with a standard fire, obvious issues of applicability will arise.

When considering design fires used for experimental testing, standard test methods and design fire curves have been developed for the purpose of continuity between all results obtained. This aids in comparing very different systems and defining benchmark performance with which can be specified for a building element. There are also some drawbacks to using standard design fire curves. When designing for fire safety a major factor is the occupancy or intended use of the building. This dictates the type of fires which are expected to occur in the building. Design fires can vary considerably in growth rates, peak heat release rates, decay rates and the by-products produced. This is largely dependent on the size and location of the ignition source, the type, quantity, orientation and surface area of the fuel, the geometry of the enclosure, the size and location of the compartment openings, and the material properties of the enclosure boundaries (Karlsson and Quintiere, 2000).

2.4.1 The Design Fire

As seen in Figure 2-2, both the ISO 834 and ASTM E119 standard fires have only a fully developed phase, however both the growth and decay phases are absent due to applicability of

the standard fires to a range of fire durations and conditions for testing. Lie (2002) presents an idealised fire curve which clearly shows these three major regions, as seen in Figure 2-3.

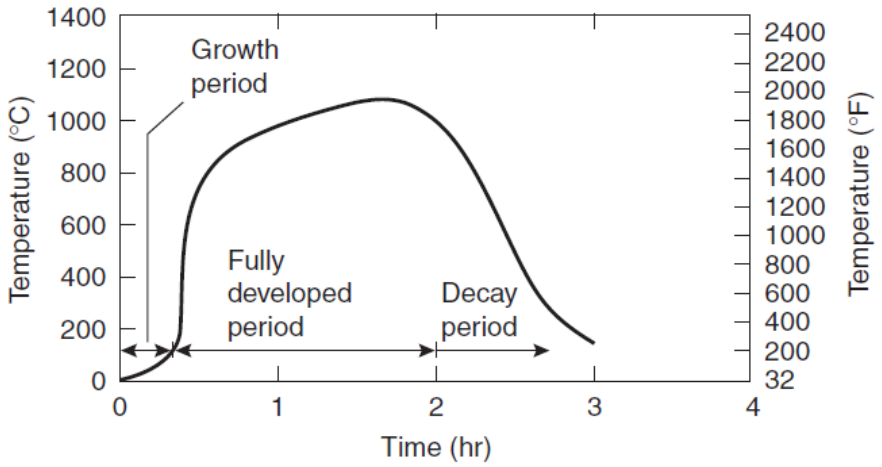

Figure 2-3: Idealised design fire curve (Lie, 2002)

The absence of this decay phase in the standard fires may not be an appropriate assumption to design for. It is reasonable to assume that the majority of fuel in a compartment to have been consumed after multiple hours of burning (for a standard building scenario), hence finite fire durations and decay phases should always be considered.

2.4.2 Growth Phase

It has been increasingly observed in recent years that new materials such as fabrics and foams used in buildings have much faster growth rates than materials which were commonplace when fires such as the standard ISO 834 fire was proposed. A wealth of literature can be found on the subject of characterising the burning rates of materials, an example of this is foam material which can significantly contribute to the fire load and burning rate of a firecell. Pau (2013) has conducted much research characterising the burning behaviour of different types of foam, and this research suggests that the growth rate of the standard fire may not be representative of a real fire in a modern furnished firecell.

Issues may arise with the applicability of the growth rate specified, as different fuel types and configurations can have massively different growth rates, and this can severely impact the performance of structural members exposed to the fire, especially those with low levels of expected fire resistance.

A parametric study conducted by Friquin et al. (2010) found significant differences in the charring rates of CLT panels when exposed to standard and parametric fires. The growth rate of the fire was found to be one of the major contributing factors to increased charring damage of timber members, along with the maximum temperature reached. This emphasises the importance of the selection of an appropriate growth rate for a fire in the design stages, and the impact it may have on the structural fire design of timber members.

2.4.3 Flashover

Flashover is the transition between the growth and fully developed phases, and is signified on Figure 2-3 by a steep increase in the temperature curve. It is usually defined as the transition from a localised fire to the combustion of all enclosed surfaces in a room (Buchanan, 2001). This leads to a rapid increase in both the temperature and the heat release rate of the compartment, and commonly signifies the transition from a fuel controlled to ventilation controlled fire.

2.4.4 Fully Developed Phase

The fully developed phase occurs when the firecell has reached flashover, and is generally characterised by temperatures in excess of 600 – 800°C which suggest all fuel items in the firecell have become fully involved in the fire. As previously mentioned, standard fire curves normally neglect a decay phase hence the fully developed phase comprises of the bulk of the fire curve. The major structural impact from the fire, especially to steel members, occurs during this period due to the high temperatures throughout the duration.

The duration of a fire in a compartment is dictated primarily by the total fuel load present and the ventilation conditions.

2.4.5 Decay Phase

When considering the ISO 834 (1999) standard fire used in this research, no decay phase is specified. For longer fire durations it would be likely that the fuel in a compartment would be exhausted and the temperature would decrease as the fire heat flux into the compartment decays. The standard fire gives a constantly growing and persistent fire temperature which may not be representative of the majority of real fires at longer durations. When considering the rate of decay of temperature the influence of the compartment linings must be taken into account.

2.4.6 Extinguishment

When considering timber in fires, a major point of contention is what happens to the timber members when the fire decays away but the timber still burns. Standard fire resistance tests are usually conducted to a set duration, and the possible effect of persistent burning after the set duration is not considered. This may be due to the reasoning that specific assembly must demonstrate its ability to meet its requirements only for that set period of time, after which it is assumed that fire service intervention occurs, otherwise a collapse may be inevitable.

However some furnace experiments on laminated timber assemblies have been conducted (Saito et al., 2007) with the members left to combust inside the furnace after shutoff. Burnt sections and char damage were measured after the entire experiment which consisted of one hour of standard fire exposure and three hours of resting in the furnace with no applied fire load. The air supply to the furnace was changed parametrically to determine the actual values required to ensure the timber members would continue to burn under their own volition. One experiment was conducted as a control by leaving it in the open air environment immediately after furnace shutoff. The findings were that the airflow to the furnace played a major role in determining the combustion of the timber after the fire, and a large amount of ventilation was needed to continue combustion on members. The fire died out in two of the four experiments, with continuing smouldering combustion in the specimen exposed to the largest airflow in the furnace and the open air control specimen. Figure 2-4 shows cross-sectional char damage results of the specimens tested.

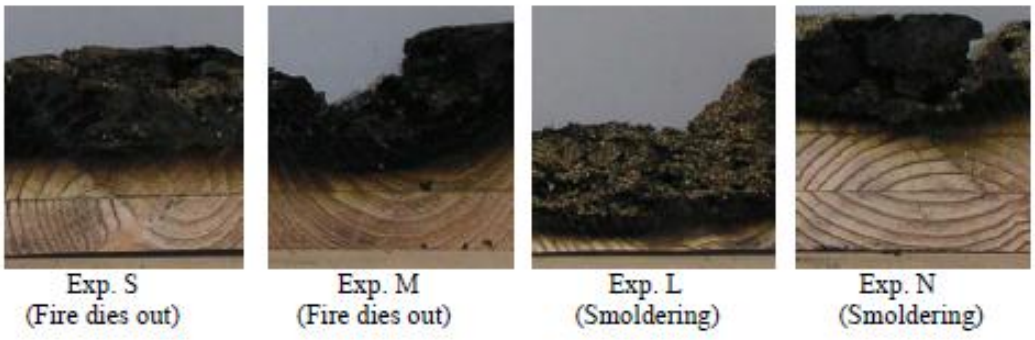

Figure 2-4: Char damage of the decay phase experiments (Saito et al., 2007)

This also calls the method of test into question, as the members immersed in the furnace were exposed to much higher temperatures than the control specimen in the open air environment as the furnace took over two hours to cool below 200°C after testing. Much of the reradiated heat from the inside of the furnace would be coming from the ceramic tile lining, which is not a good

approximation to real conditions in a firecell after burnout. The specimen left in the open air continued with smouldering combustion, however the char damage recorded was much less than the furnace specimen counterparts.

From these results it can be concluded that the ventilation conditions in the firecell after burnout have a significant influence on the burning behaviour of timber members in the decay phase. However, combustion of the timber will not occur in an open air environment without forced air convection and surrounding environmental temperatures lower than 200°C, and assemblies would likely resist loads until fire service intervention depending on the remaining level of redundancy in the timber assembly.

2.4.7 Eurocode Parametric Fires

Some alternatives to standard fire curves are parametric fires, which can encompass faster growing fires and more volatile materials and configurations. Annex A of Eurocode 1 (CEN, 2002) defines parametric fires accounting for the lining material of the enclosure, the densities of the combustible materials and the ventilation conditions present, as well as giving provision for a cooling (decay) phase.

The parametric fires are based on a maximum compartment size of 500m^2 with a completely enclosed roof for the duration of the fire, and it is assumed the fuel load in the compartment is completely burnt out.

Annex A of Eurocode 5 (CEN, 2004) gives charring rate modifications and strength reduction factors for timber exposed to the parametric fires. A commentary on these methods from a timber design perspective is given by Buchanan (2001) and König (2005). Further discussion of non-standard fires is given in Chapter 6.

2.4.8 Estimating a Design Fire

Inevitably, all aspects of the most likely fire scenario for a particular structure may not be adequately addressed by the simplified design fires specified in regulations. Therefore a performance based fire engineering approach can be very useful to appropriately design for an expected fire in a space.

A major factor dictating the choice of design fire will be the overall design objective. Generally, these objectives may be for the structural assembly to:

- Provide a fire resistance rating specified by a code or standard.
- Survive the burnout of a fire compartment.
- Survive until a level of fire brigade intervention or active suppression is incorporated after a period of time.

Any of these objectives will influence the different phases of design fire discussed above. It should be noted that a great degree of engineering judgement is relied upon at this stage of the process to determine the relevance and importance of each design objective. Thus, it is important that a conservative approach is taken in the assumptions made about the fire characteristics, in order to encompass a wide range of possible fire scenarios and to ensure the structure is not under designed.

Once the expected fuel load, ignition source, and ventilation conditions are specified, the design fire can be defined in terms of a heat release rate or a temperature versus time curve. The latter is generally more useful for structural applications, as temperature correlations are generally more important in assessing damage. Actual fire test data can also be used to determine likely fire characteristics, such as data for vehicle fires in a car parking space, however care must be taken to ensure the testing conditions are appropriate and acknowledged.

Some common simplifications when deciding on an appropriate design fire are as follows:

- Instantaneous growth and decay phases – commonly known as rectangular fire curves, these types of fires are ideal for situations in which a fuel load or maximum heat release is known, but growth and decay characteristics are not or deemed insignificant. These design fires are generally conservative as they can exaggerate the fire impact on structural members.
- Parametric growth phases – in order to account for faster growing fires or more volatile fuels, such as hydrocarbon pool fires. These generally grow to a maximum temperature at which a constant linear trend is followed until fire decay.
- Linear decay phase – in order to simplify the estimate of fire decay due to the limited data available in the literature on decay of different materials. Generally taken as a steady decrease from the maximum temperature to ambient, or the assumed compartment temperature immediately after burnout.
- Adequate ventilation conditions to reach flashover – it is normally assumed that compartment glazing breaks and there is adequate ventilation for the fire to grow to a maximum temperature or heat release rate and subsequent burnout.

As the above guidelines result in a multitude of potential design fires, it is not uncommon for the practicing engineer to specify a number of different fires which encompass differing conditions. For instance, in the case of a known heat release rate from a fire test, a rectangular design fire may be specified for a certain duration, and a different rectangular fire which does not reach a similar maximum temperature could be specified for a longer duration to account for the same total heat release over time. In this way the impact of the fire on the structure can be tested in a simple and justifiable fashion.

2.5 Timber in Fire: An Overview

2.5.1 Introduction

In order to model a material numerically, a detailed understanding of its properties and performance under the expected conditions is vital. When considering fires, timber is a complex material in that not only does the cross-sectional area of the timber reduce as it burns, the mechanical and thermal properties of the timber also change with respect to temperature. The insulative properties of timber are such that the penetration of the thermal wave into the virgin timber is relatively small in terms of expected beam and column member sizes in a multi-storey building; however this impact does increase as the section of the member in question reduces during a fire.

2.5.2 New Zealand Timber Species

In New Zealand the most prevalent species of timber used in construction is Radiata Pine, also known as Monterey Pine, coming from over 1.8 million hectares of sustainably managed planted forests (Buchanan, 2007). The climate in New Zealand is ideal for growing this species, and most forests mature and are usually harvested 25-35 years after planting. Radiata is a softwood which can be glued, nailed and machined easily making it ideal for a large range of uses and forming other engineered wood products.

2.5.3 Laminated Veneer Lumber

New Zealand laminated veneer lumber (LVL) consists of 3mm thick veneers of Radiata Pine glued together with a phenol-resorcinol formaldehyde adhesive. These layers have the grain orientation running in the same direction (as opposed to plywood changing grain orientation each layer) which gives the highest strength properties for bending and tension in one direction. This is ideal for most structural applications as members such as beams can resist much greater loads and hence span much longer distances when compared with traditional sawn

timber members. The manufacturing process of LVL also allows for greater dimensional accuracy, and additives such as fire retardants can also be implanted in the veneers depending on the desired performance. The layers are glued together in a staggered fashion such that any defect present in the timber will only be present in the LVL in a 3mm thick layer, so the effect of large knots in timber beams can be significantly mitigated and the expected strength can be reliably predicted when compared with sawn timber. A typical cut of LVL is illustrated in Figure 2-5 on the left.

Cross-banded laminated veneer lumber is LVL in which a number of veneers are oriented perpendicular to the primary span direction to increase panel stability and the strength in the perpendicular direction. This type of product is ideal for upper flanges in floors where a stronger floor diaphragm is required, and is shown in Figure 2-5 on the right. Note the two veneers of differing orientation in the figure at the third layer in from both extreme edges.

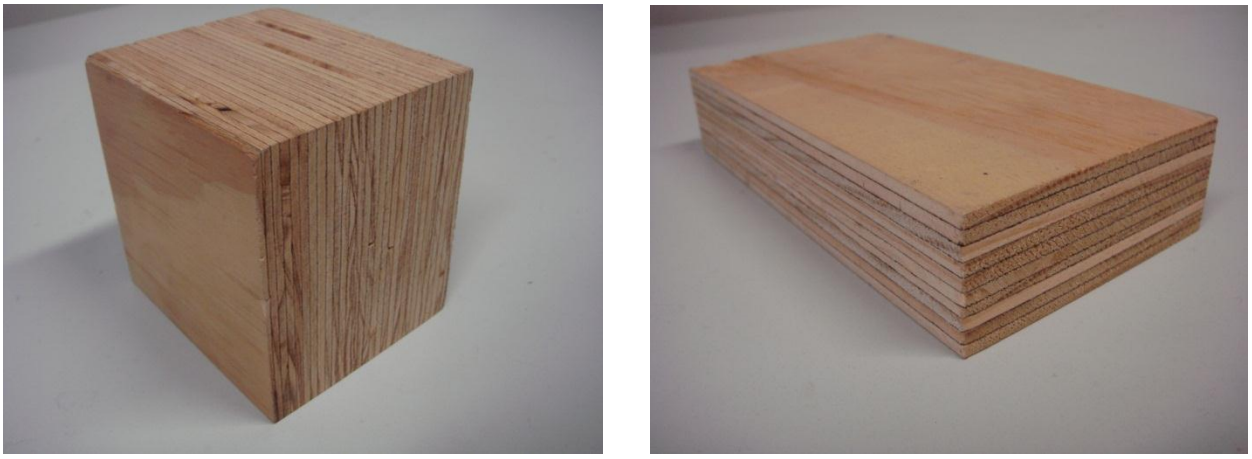

Figure 2-5: Examples of LVL and cross-banded LVL

The fire behaviour of sawn timber has been well documented in the past; however questions pertaining to the physical composition of LVL (layers of wood glued together), the charring behaviour and the load bearing properties of the material are all vital when the material is subjected to fire conditions. Recent research conducted by Lane (2005) has looked into the ignition, charring and structural performance of LVL. In terms of the glue lines in LVL affecting the charring rates, Lane found in a number of un-instrumented char tests that there was relatively no difference between charring for different grain orientations. These results show that the presence of the glue lines does not influence the burning behaviour of the material. Lane also conducted cone calorimeter tests on LVL samples, and furnace tests on LVL members. This furnace testing consisted of subjecting LVL members to the standard ISO 834 fire (1999) in

a pilot furnace, and also in a full-scale furnace under loaded conditions. From this research he was able to measure a charring rate for New Zealand manufactured Radiata Pine LVL of 0.72 mm/min. From the testing conducted there were no obvious defects found in the design of the LVL material that reduced the performance of the material in fire conditions. Further investigations conducted by Tsai et al. (2013) at the BRANZ facilities have drawn similar conclusions for the expected one-dimensional charring rates of LVL at 0.75 mm/min.

2.5.4 Glue-Laminated Timber

Glue-laminated timber (glulam) is an engineered wood product made by gluing a number of full length laminations together to form large solid sections of practically any size, shape and length. The laminations are staggered and finger jointed at each end, and many different types of glue can be used depending on the exposure of the end use of the member. This has the effect of reducing the impact of defects on the entire member, but to a lesser extent than LVL. Some of the unique advantages of glulam are that it can be easily shaped into curved members such as arches, and the finished product is very aesthetically pleasing. In many cases the decision to use glulam can be based solely on the aesthetic desired as opposed to its structural merits. New Zealand glulam is described in detail by Buchanan (2007), and is presented here as a viable alternative to LVL for members in high strength timber floors. Figure 2-6 depicts one of the uses of the material in a structure, a roof beam for a stadium in Calitri, where each beam section was over 2 metres deep with a span of over 25 metres.

Figure 2-6: Glulam beam fabricated at Holzbau Sud for use in a stadium in Calitri, Italy

2.5.5 Cross-Laminated Timber

Cross-laminated timber (CLT) is an engineered wood product similar to glulam except the layers of laminations are laid transverse to one another to form large panels which exhibit two-way action. They are primarily used as prefabricated wall and floor structures and, depending on the manufacturing process, massive CLT members can be produced suited for a range of purposes. Panels can range up to 5 metres wide, 18 metres long and 400mm thick. CLT was first developed in Austria and Germany, gaining widespread use throughout Europe in recent years (Östmann, 2010), and is now being implemented in Canada and the United States (Gagnon and Pirvu, 2011) as well as in other regions around the world. A sample of three ply CLT is shown in Figure 2-7.

Figure 2-7: Example of three ply CLT

As with glulam, a high quality finish is possible with CLT which makes it ideal for exposed wood structures from an aesthetic sense.

Some factors serve to complicate the analysis of CLT in fires. A major point of contention is that layer drop off has been observed in some furnace tests, where the layers oriented transverse to the major span direction tend to delaminate from the entire section. This results in a fresh layer of timber being exposed and greatly increased charring rates for the overall panel.

2.6 Material Structure and Burning Behaviour of Timber

As previously mentioned the impact of fire on timber causes a number of physical changes to occur in addition to the material properties changing with temperature. These changes serve to complicate any estimation of the behaviour of timber sections, and this is paramount to the application of timber building elements to understand the effects of a fire on the structure.

2.6.1 Timber Substructure

Timber is an organic material which grows and develops in a natural environment. This means that although it is easily cultivated and harvested, requiring little or no engineering influence to develop when compared to concrete or steel, it will have less consistent and reliably predictable properties in comparison. Environmental factors such as climate and the availability of water and sunshine have a large impact on the characteristics of the timber and the final product. Defects also play a large role in determining the characteristic properties of sawn timber, as their presence can significantly reduce the reliable strength of a member. The orthotropic nature of timber can also be problematic if is not properly accounted for. When being used on a large scale as an engineering material the potential issues that may arise due to these factors must be kept in mind to ensure timber is used appropriately and responsibly.

The microstructure of trees comprises of a complex biological structure, a composite of many chemistries and cell types acting together to serve the needs of a living plant. The main functions of a tree are that of conduction of water from the roots to the leaves, the storage of biochemicals, and the mechanical support of the plant body (Wiedenhoeft, 2010).

In order to explain the fundamental structure of timber as it relates to macroscopic properties (such as strength, density and hardness) the microstructure can be simplified down to cells and connective materials. An idealization of the cell structure in a typical softwood is comprised of tracheids which are very long and hollow tubes, grouped together all facing the same direction (also referred to as the grain). The cell walls provide the mechanical properties which manufactured timber is harvested for, however there are voids inside these cells called lumina. These voids provide a critical function for the tree to conduct water and nutrients from the roots to the extremities. Rays are collections of smaller storage cells which are oriented radially from the centre of the tree to the outer bark. The connective material between the outer cell walls is lignin, a brittle matrix material which binds the cells together. This is shown in Figure 2-8.

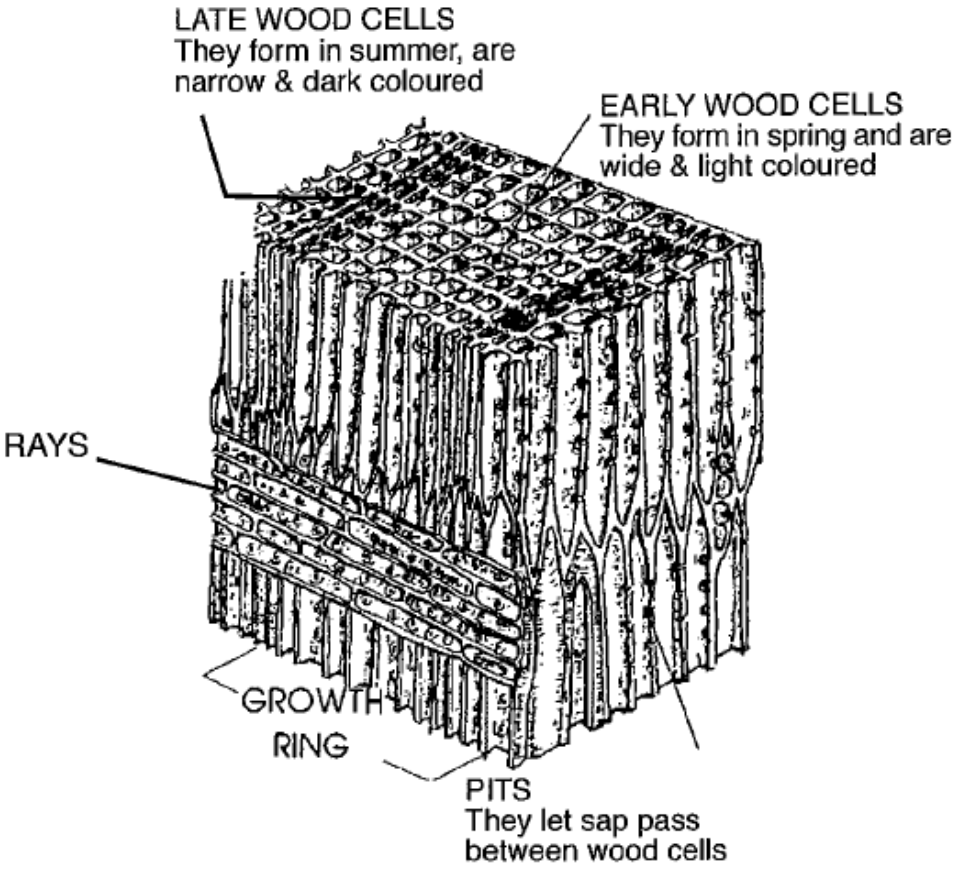

Figure 2-8: Cellular structure of softwood (Buchanan, 2007)

Due to the substructure of timber it is orthotropic in nature, in other words it possesses unique and independent mechanical properties in the directions of three mutually perpendicular axes. Generally, the longitudinal axis is taken as parallel to the grain, the radial axis is normal to the growth rings of the timber and perpendicular to the grain in the radial direction, and the tangential axis is perpendicular to the grain and tangent to the growth rings (Kretschmann, 2010). The strongest mechanical properties are exhibited parallel to the grain, while weaker properties are exhibited perpendicular to grain. This is especially true for compression perpendicular to the grain, as the tracheids are susceptible to crushing due to the voids collapsing.

2.6.2 Combustion of Timber

Many factors serve to complicate the analysis of timber structures in fire, none more important than the behaviour of the timber as it undergoes an increase in temperature from the ambient state to pyrolysis (thermally decomposing from a solid to a combustible gas in the case of

timber). As this process occurs, the physical, mechanical and thermal properties of the timber change with time. The timber loses stiffness and strength as it is initially heated, then undergoes an increase in stiffness and strength as it dries completely. Strength and stiffness reduce after the temperature increases beyond a certain threshold until the complete loss of stiffness and strength when the wood turns to char. An illustration of these zones is shown in Figure 2-9. The migration of moisture away from the heated zones affects the strength of the timber, but also serves to reduce burning rate with an increasing effect as the section size decreases. The formation of a layer of char acts to insulate the virgin timber from the fire, with an increasing effect as the char layer thickness increases.

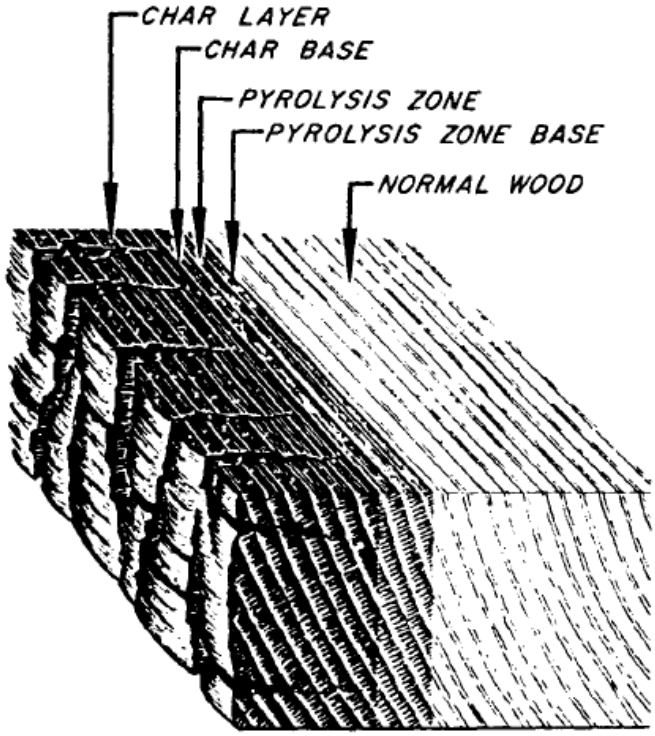

Figure 2-9: Degradation zones in a wood section (Schaffer, 1967)

Initially the charring rate of timber is fast as the fresh wood exposed to the fire undergoes pyrolysis and combusts. Once a layer of char has formed on the outside of the timber however this rate decreases to a relatively consistent value, dependent mainly on the design fire, the species and density of the timber, and if it is raw timber or an engineered wood product. Due to the excellent insulation characteristics of timber the thermal gradient is steep through the cross-section, with heat penetration commonly estimated at about 35mm thick under the char layer (Buchanan, 2001). The layer under this heated region remains at ambient temperature and is

referred to as the residual section. In the heated zone many processes are taking place. Moisture is migrating through the section and evaporating at 100°C, while the timber at about 200°C is thermally decomposing, giving off pyrolysis products which are ignited when reaching the oxygen and ignition source present outside the layer. The pyrolysed wood loses mass and discolours significantly, becoming charcoal at around 300°C. This layer of char generally stays connected to the timber section unless disturbed by an outside influence, and the extreme outer regions of the char are generally assumed to be at the fire temperature for modelling which holds true empirically. The char layer does shrink from the initial timber size however with the loss of mass and moisture, and cracks and ablations will form which can increase charring rates by exposing the fresh timber underneath. There are a number of other processes which the charcoal will undergo as it breaks down above 300°C, however these are of no concern from a structural fire engineering sense as charcoal has no significant mechanical properties and supports virtually no load. These different processes and their associated products are described in detail by White and Dietenberger (2010), with an in-depth review of previous historical literature on thermal degradation of timber covered by Beall and Eickner (1970).

As the design of heavy timber members traditionally is based on estimated charring rates, much work has been done in this field to quantify the rates at which timber burns and this is well documented in design codes and the literature, such as the research by White (1988), and more recent work by Friquin (2010). For the two-dimensional charring of LVL a value of 0.7mm/min is given in the Eurocode (CEN, 2004), and this agrees well with experimental observations of New Zealand LVL by Lane (2005) and O'Neill (2009). Post-fire investigations of actual buildings have found that without the presence of accelerants or specific design flaws such as large gaps in timber assemblies, charring rate values reported in the literature for fire resistance furnace tests are representative of real fires. Babrauskas (2004) concludes that charring rates between 0.5 – 0.8 mm/min are representative of severe post-flashover room fires.

When considering the thermal properties of heated timber from a structural engineering sense, the most important properties to affect the estimation of strength, stiffness and durability of timber members are the specific heat, thermal conductivity, density and moisture content. The effect of temperature on the properties of timber has been well researched in the past, most notably by Schaffer (1973), Hadvig (1981), Gerhards (1982), Östmann (1985), Glos and Henrici (1991) and König (2006). Much of this work has been incorporated into current design codes and methods of best practice around the world. As a basis for this research the Eurocode has been predominantly used for guidance as it is well regarded and grounded from this literature,

hence the following material property definitions refer to the Eurocode regularly. An excellent commentary on the derivation of the Eurocode guidance is given by König (2005).

2.6.3 Moisture Content

As will be discussed in detail during the modelling portions of this research, the moisture content in a timber member has a major influence on the mechanical and physical properties. Timber is a hygroscopic material; hence its moisture content is dictated by the humidity and surrounding temperature of its environment. As timber is heated the moisture in the heated outer layers will migrate via evaporation. Some of this moisture is forced into the cooler regions of timber and re-condenses, while some is driven out of the timber and lost to the surrounding environment. This can complicate the estimation of moisture content in timber sections during a fire, but for very large residual sections this is not a significant issue. However, as the section becomes smaller this has an increasing effect on the properties of the section and may need to be accounted for. The equilibrium moisture content based on temperature and relative humidity of the surrounding environment is shown in Figure 2-10.

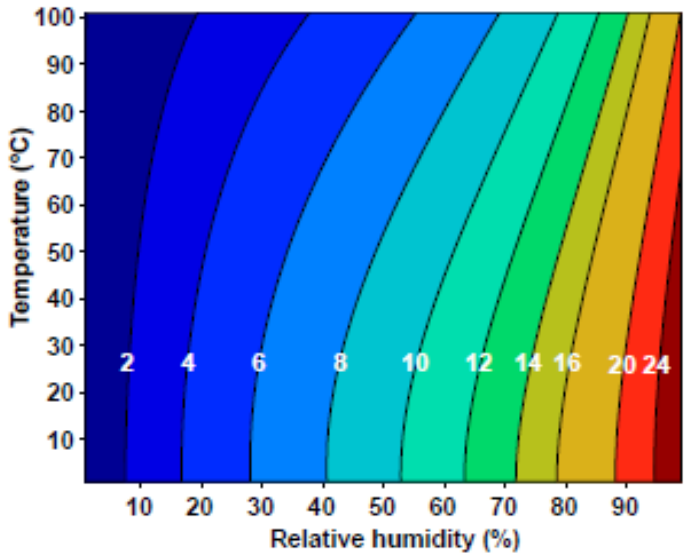

Figure 2-10: Equilibrium moisture content of timber relationship to temperature and relative humidity (Glass and Zelinka, 2010)

For the following sections and the purposes of the numerical modelling, the moisture content of the timber is assumed to be 12%. This is the equilibrium moisture content at an ambient temperature of 21°C with a relative humidity of 65%. 12% is used as the ambient temperature moisture content in many design codes and standards around the world, as this level of relative

humidity is generally assumed as a global average suitable for most countries, and for New Zealand timber it is a good approximation.

2.6.4 Density

The density of a material is the mass per unit volume. When considering the case for timber, this is complicated by the fact that both the mass and volume of timber is dependent on its respective moisture content, hence oven dry density is most commonly calculated for engineering purposes from tests of oven dried samples of timber.

Several different methods for calculating the density of timber and described in the Wood Handbook (2010) by Glass and Zelinka. Eurocode guidance on the effect of temperature on the density is given in Figure 2-11 (CEN, 2004).

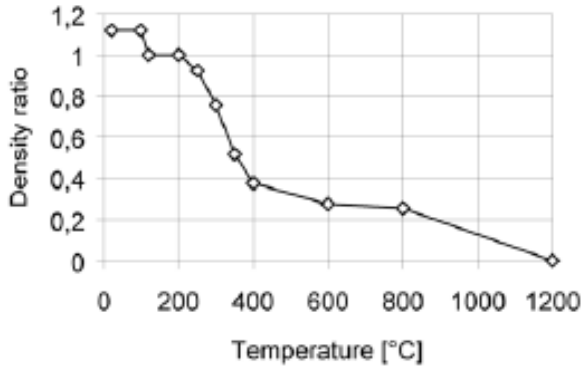

Figure 2-11: Temperature-density ratio relationship for softwood at 12% moisture content (CEN, 2004)

It can be seen in Figure 2-11 that the density ratio is plotted with respect to the oven dry density; hence below 100°C the ratio is 12% higher to account for the assumed 12% moisture content of the timber. For calculation of charring damage and other analyses the dry density of LVL in the Eurocode is specified at approximately 480 kg/m^3.

2.7 Thermal Properties

Timber, like many other structural materials, possesses a number of thermal properties which vary with respect to temperature. The thermal properties of timber have a significant impact on the mechanical properties, hence the structural performance of a timber assembly. It is of paramount importance for modelling fire scenarios that the thermal properties of a material and their relevant relationships to other properties are well characterised and accounted for. The

most significant thermal properties with regards to a structural engineering sense are discussed in this section.

2.7.1 Specific Heat

The specific heat of a material is the amount of energy required to increase one unit of mass by one unit in temperature. When considering timber the presence of moisture will change the specific heat curve, hence in standards it is usually defined for softwood timber at 12% moisture content. The Eurocode guidance for the variability of specific heat with temperature is shown in Figure 2-12.

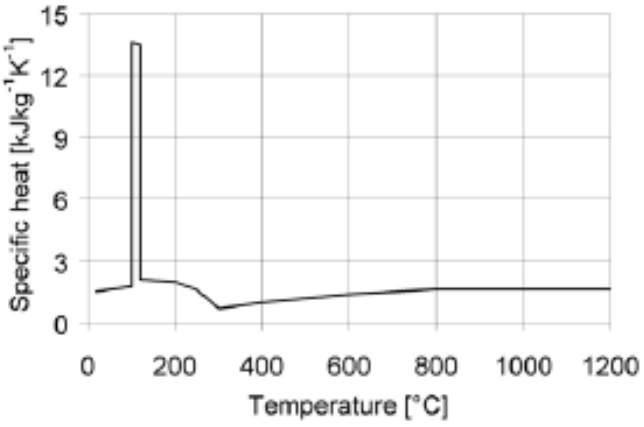

Figure 2-12: Temperature-specific heat relationship for softwood (CEN, 2004)

It can be seen from Figure 2-12 that the specific heat increases then decreases rapidly near to 100°C, this is to account for the increase in input energy required to vaporise the moisture present in the timber (facilitating the phase change from liquid to gas). For completely dry timber, this peak would not be present, however as structural timber in the built environment does not exist in a closed dry system, the standard specifies this relationship.

2.7.2 Thermal Expansion

The coefficient of thermal expansion is a measure of the relative change of dimension of a material due to a change in temperature. From a structural engineering sense this can have a drastic effect on the way an assembly performs not only in fires but in the regular heating/cooling phases of a building lifecycle, hence must be properly understood and quantified.

When dry, timber acts to expand when heated and shrink when cooled. Experiments on different species and grain orientations have quantified this behaviour and are discussed in more detail by Glass and Zelinka (2010). However, with the presence of moisture this behaviour is reversed. As moist wood is heated it expands due to normal thermal expansion but also shrinks due to the loss in moisture content, and this shrinkage generally becomes greater than the thermal expansion as more moisture is lost hence the net dimensional change of the timber is negative. Timber at a moisture content of 12% follows this trend, swelling initially then shrinking as moisture is driven off.

When timber burns these effects can be extremely difficult to gauge, as the properties of the charcoal are very different to the timber, and the char layer itself shrinks to a much greater degree than the timber. Therefore in actual fires the member sizes will tend to shrink from the onset of charring.

2.7.3 Thermal Conductivity

The thermal conductivity of a material is the rate of heat flow through that material when subjected to a unit temperature increase across a unit thickness. Timber is heavily influenced by properties such as moisture content, temperature and density, with a general trend of increasing thermal conductivity as the values of these respective properties increase. In order to characterise thermal conductivity in a general sense, the Eurocode defines a standard curve for softwood at 12% moisture content, shown in Figure 2-13.

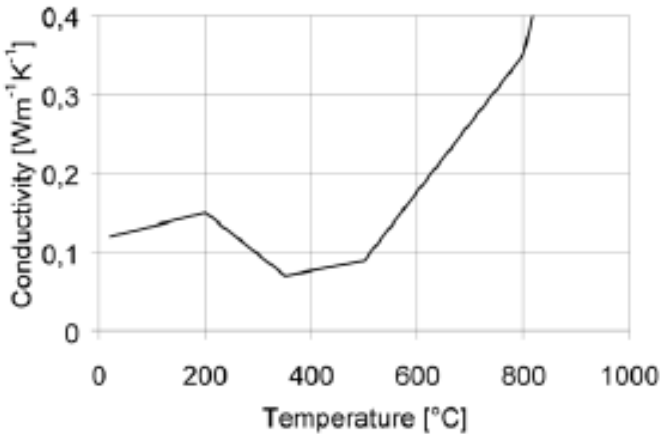

Figure 2-13: Temperature-thermal conductivity relationship for softwood (CEN, 2004)

The thermal conductivity of timber members will also be influenced by any deformities or knots through the cross-section, and the grain orientation of the timber. It has been found that the thermal conductivity along the grain is generally greater than conductivity across the grain by a factor of 1.5 – 2.8 (Glass and Zelinka, 2010).

2.7.4 Other Higher Order Effects

Mass transfer is the fundamental process underlying many of these thermal changes. However, modelling any type of mass transfer can become extremely difficult and time consuming; hence it is usually accounted for by taking effective values of other properties over a certain range. From a structural fire engineering sense this type of approximation is acceptable to the degree of calculating fire resistance of members spanning minutes to hours, and only requiring coarse material property approximations on a physical scale relative to the built environment.

A major form of mass transfer through timber in these conditions is moisture migration, as discussed in Section 2.6.3. However, the thermal decomposition of timber accounts for another large portion of the mass transfer in fires. As the material undergoes pyrolysis the chemical composition of the burned wood changes as by-products of the combustion process are released and the residual char layer forms. The density of charcoal is generally in the order of 200 kg/m^3, meaning that after moisture is driven off more than half of the original mass of the softwood will have been transformed into other products.

Increased heat transfer due to char cracking and drop off is also an issue. When a timber member burns and a char layer forms, this layer will contract longitudinally, transversely and radially. Cracks form when the longitudinal and transverse shrinkage stresses overcome the maximum tensile strength of the char (which incidentally is very low from a structural sense). These cracks aid in transferring heat into the residual section of the member and increase the charring rate of the timber, as well as providing a more efficient outlet for pyrolysed gases to leave the residual section.

A review of some of the numerous charring models which incorporate some or all of these effects is described by Janssens (2004), and his own model development is also discussed. Janssens highlights some of the difficulties and drawbacks of efforts in the past to model and predict charring behaviour by accounting for mass transfer, char oxidation, char contraction and modified properties. Although higher order effects such as these are important to understand, finding a method of reliably accounting for them without actually modelling the exact mechanisms taking place is difficult, and has been attempted in the past with limited success.

2.8 Mechanical Properties

Due to the presence of defects and the natural variation which occurs in timber in the environment, the mechanical properties of sawn timber can vary considerably more than other engineering materials. However the properties of engineered wood products such as LVL are much more consistent as a result of their respective manufacturing processes. The primary direction in which timber grows is the strongest (parallel to grain), and when structural members are constructed from timber materials this is generally known as the primary axis of the member. The secondary and tertiary axes are perpendicular to the grain and normal and tangential to the growth rings of the tree, as shown in Figure 2-14.

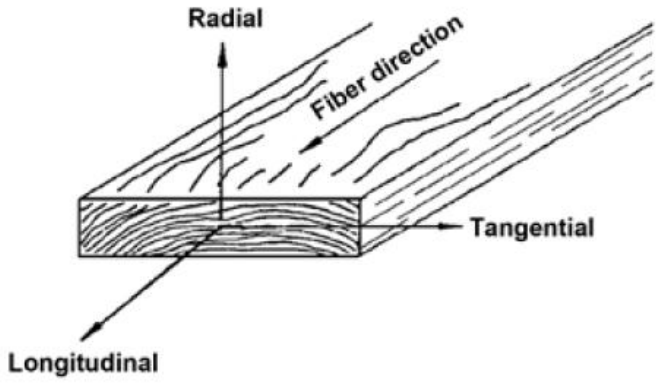

Figure 2-14: Principal axes of a timber member (Kretschmann, 2010)

For LVL, the primary axis is taken as the longitudinal direction as shown in Figure 2-14 parallel to the grain of the timber. The secondary axis is taken as parallel to the veneers but perpendicular to the grain (tangential in the figure), and the tertiary axis is perpendicular to the veneers and the grain (or the radial direction).

2.8.1 Modulus of Elasticity

The constant of proportionality of a material between the stress and the strain is called Young's modulus, or the modulus of elasticity. As one of the most important properties of a structural member it is a measure of the ability of the material to resist deformation, and is independent of the size and shape of the member (Williams and Todd, 2000).

When subjected to increasing temperature timber loses stiffness as a result of the thermal degradation of the cellular structure. This has an increasing effect with increasing temperature until the timber is turned into charcoal and all stiffness properties are assumed to be negligible.

Following Eurocode 5, the effect of temperature on the modulus of elasticity parallel to the grain is shown in Figure 2-15. Due to the anisotropy of timber, each grain direction has an independent modulus of elasticity.

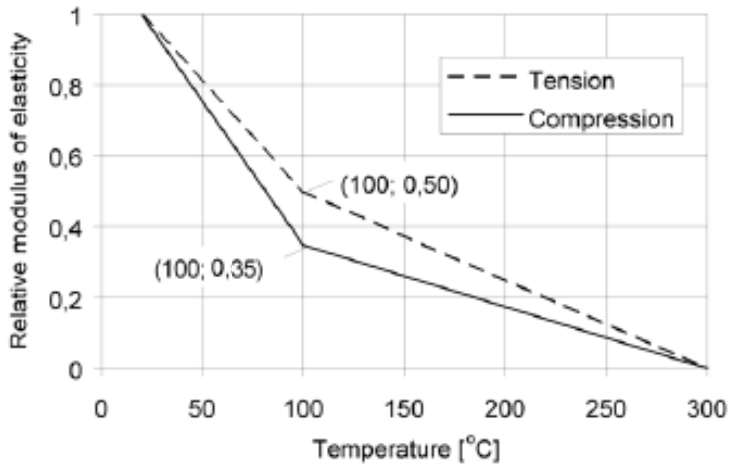

Figure 2-15: Effect of temperature on modulus of elasticity parallel to grain of softwood (CEN, 2004)

The modulus of elasticity varies with moisture content and also the density of timber hence can vary greatly between the different species harvested across the world. Generally the mechanical properties of a softwood species will be poorer than a hardwood species; however these properties are greatly improved by manufacturing the raw timber into an engineered material such as LVL.

2.8.2 Strength

Engineering strength properties for structural materials generally consist of evaluating tensile, compressive, bending, shear, hardness and rupture characteristics, dependent on the use of the material and its expected failure modes.

Timber exhibits its most desirable strength characteristics parallel to the grain direction, and structural members are always designed to utilise these properties by orienting the timber with the grain longitudinal to the primary span direction. Perpendicular to the grain direction, timber exhibits weaker characteristics hence absolute values of strength are significantly lower for this orientation. Eurocode 5 values for the effect of temperature on the behaviour of timber in compression, tension and shear are shown in Figure 2-16.

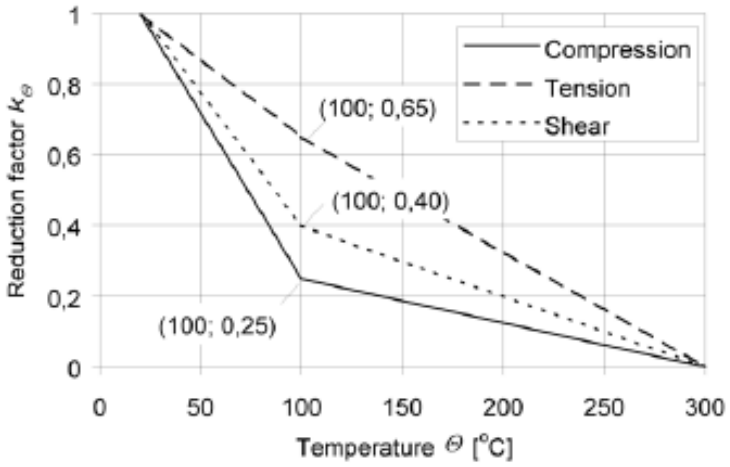

Figure 2-16: Reduction factor for strength parallel to grain of softwood (CEN, 2004)

For most modelling and design calculations of a structural member the tension, compression, bending and shear strength are generally critical in determining the failure mode.

There are a wide range of secondary strength properties such as toughness, torsion strength, fatigue, rolling shear strength and creep resistance which are not of major concern during a fire scenario for evaluating fire resistance, hence are not investigated in depth in this research. These are covered in detail by Kretschmann (2010).

2.8.3 Modulus of Rigidity

The modulus of rigidity of a material is a measure of its resistance to deformation caused by shear stresses. It is commonly referred to as the shear modulus, and as with the modulus of elasticity the modulus of rigidity is different for each grain direction of a timber member. Similarly the shear modulus is highly dependent on the moisture content and density of the timber.

2.8.4 Poisson's Ratio

When a specimen is loaded uniaxially it will deform longitudinally. As the length of the specimen changes under the load, so do its cross-sectional dimensions. The ratio of transverse to axial strain is known as Poisson's ratio. As timber is anisotropic, each different grain direction of a specimen of timber has a different Poisson's ratio.

2.9 Timber Floor Systems

The most common types of suspended timber floors are illustrated and discussed in this section with regards to fire safety. The major categories of floor are linear beam systems, composite systems, solid timber slab systems and timber concrete composite systems (of which there are both beam and slab types available). These are also described in detail by Kolb (2008), and some Australasian specific examples are covered by Grant (2010).

2.9.1 Linear Systems

Linear systems encompass most traditional timber flooring types where the main load bearing strength is provided by the joist elements of the system. These joist elements can range from solid timber sections to trusses, and support a structural sheathing that forms the base of the floor construction. Generic design methods such as those presented in Eurocode 5 (CEN, 2004) are based on these types of systems, where the assumption of reducing the structural floor strength based solely on fire damage to the joist element is sound practice. A typical linear system is shown in Figure 2-17. Although commonly used in residential and low-rise properties due to their simple design and construction, traditional linear systems are not generally suitable for larger multi-storey applications due to the large depths of the system required for longer spans. Due to the bulkiness of the traditional beam type linear systems, they exhibit good performance in fires as long as the joist members are not too slender.

Figure 2-17: Typical linear floor system

An alternative to a traditional solid timber beam is a timber I-beam similar to a steel I-beam. Timber I-beams utilise two flanges of any appropriate timber material (sawn timber, glulam or LVL) connected by a plywood web. This is an optimisation of the traditional beam from an engineering sense, and is commonly used in newer construction especially in the residential sector. Due to the relative slenderness of the components in the system, particularly the web, the fire resistance of these types of floors unprotected is minimal, sometimes only a matter of minutes. It is therefore paramount that these types of systems are fully protected from fires by a passive protection. A typical timber I-beam is shown in Figure 2-18.

Figure 2-18: Example of an LVL and plywood I-beam

2.9.2 Composite Systems

Timber composite systems such as cassette panel floors and hollow box floors are generally categorised as having a sheathing on one or both sides which acts as part of the structural system due to a fully rigid connection between the sheathing and the beam elements (commonly a glued and screwed connection along the beams). The composite action achieved

by the floor system must be accounted for to obtain a proper estimate of the fire resistance, however composite action is not considered in the simple design methods currently available.

An advantage of timber composite flooring is that it can be highly prefabricated into modular units, and these easily transported to and erected on-site due to their lightweight nature. Depending on the actual span and fabrication method employed, modular floors usually come in generic widths. Smaller spanning floors, under seven metres, are usually made in 1.2 metre widths, while larger spanning floors in the order of eight or nine metres are more commonly made in 2.4 metre widths.

The Potius floor system currently used in New Zealand falls under the composite system category. However due to the system being available in both joist and cassette type configurations where the bottom sheathing flange may or may not be present, separate issues need to be considered when it comes to estimating fire resistance. Although the connection is not the critical element to cause failure in this case, the other timber components of the system serve to complicate the analysis. A typical prefabricated composite cassette floor system is shown in Figure 2-19.

Figure 2-19: Typical composite cassette floor system

For the joist type floors, the direct impingement of heat flux onto the beam elements will degrade the integrity of the system at a faster rate than if a continuous bottom sheathing is added (in the case of the cassette type floors), as three sides of the beams are exposed to fire

as opposed to one side of sheathing which needs to burn through first. With the cassette type floors however the section will be shallower than the joist type floors due to the bottom sheathing acting as part of the structural system, and failure will be much faster after the bottom sheathing has burned through as the joist members will be more slender. The aspect of adding insulation materials to the inside of the sections can further increase the fire resistance of the floors, and consideration should be given to the integrity of the top sheathing for both types of floor during a fire scenario. Research has been conducted by Frangi et al. (2009) considering the aspect of bottom chord burn through, and a simplified calculation method was developed to account for this phenomenon which was verified by experiments.

There are many variations of composite floors using box beams or joists with added bottom flanges. Each may require a different protection strategy to be employed to achieve a consistent level of fire resistance, as the cross-sectional geometry may change drastically.

Composite floors are generally prefabricated due to the precise gluing procedures which must be adhered to in order to obtain a good bond between components. Many companies around the world provide guides with many variations on different floors available, one such example is Lignatur which create a number of cassette type stressed skin floors in their range of structural timber elements, an example of which is shown in Figure 2-20 to the left of the figure, and being installed on the right of the figure.

Figure 2-20: Lignatur prefabricated box floor product (Lignatur Product Guide, 2011)

2.9.3 Solid Timber Slab Systems

Solid timber systems such as CLT and slab panel systems are becoming more prevalent in the European market as more research is conducted to determine their performance and manufacturing processes are optimised. Due to the large amount of timber used in this type of system the timber can usually be of a lower quality. As timber is relatively expensive in New

Zealand it is for this reason that these systems have not been widely used in the past, however there is a growing interest in this area. Due to the geometry of most solid timber systems, the assumption of one-dimensional charring is generally valid hence the fire resistance can usually be calculated easily. Frangi et al. (2009) found that in cross-laminated timber the number and direction of layers influences the charring behaviour, and that layers can fall off in fire increasing the overall charring rate of the floor. Research on these panels is also being conducted in Sweden (König and Schmidt, 2007), and Italy (Menis et al., 2012). As there is much research of these systems currently on-going in Europe and due to their limited application in New Zealand and Australia currently, these slab type systems are not investigated in this research. A typical CLT flooring slab is shown in Figure 2-21.

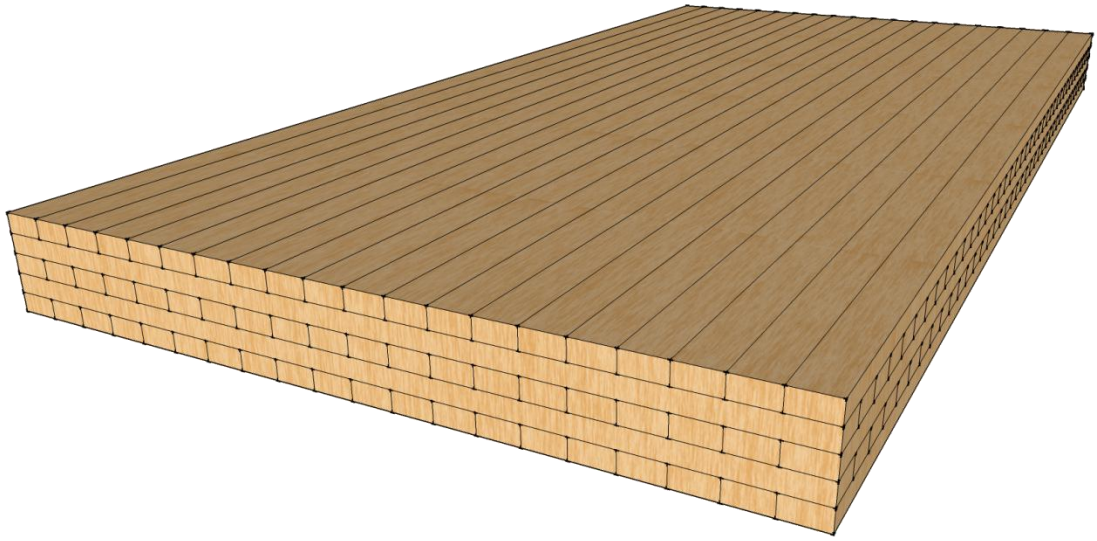

Figure 2-21: Typical CLT slab floor system

2.9.4 Timber-Concrete Composite Systems

The concept of timber-concrete composite systems arose in Europe as a method of strengthening existing timber floor systems with a concrete slab. A summary is given by Lukaszewska et al. (2007). This was then applied to the construction of new buildings, and has recently been under investigation in many parts of the world such as the United States (Fragiacomo et al., 2007), Italy (Ceccotti et al., 2006), Germany (Kuhlmann and Michelfelder, 2006, Bathon et al., 2006) and New Zealand (Buchanan, 2007, Buchanan et al., 2007). The performance of the flooring system depends mainly on the connection between the timber beams and the concrete slab, as a very stiff connection is required to ensure that sufficient

composite action is achieved, resulting in a higher ultimate strength and smaller deflections. Some connection types available are punched steel plates, shear studs or inclined screw connectors and in-filled concrete notches of varying shapes and depths, and these are shown in Figure 2-22.

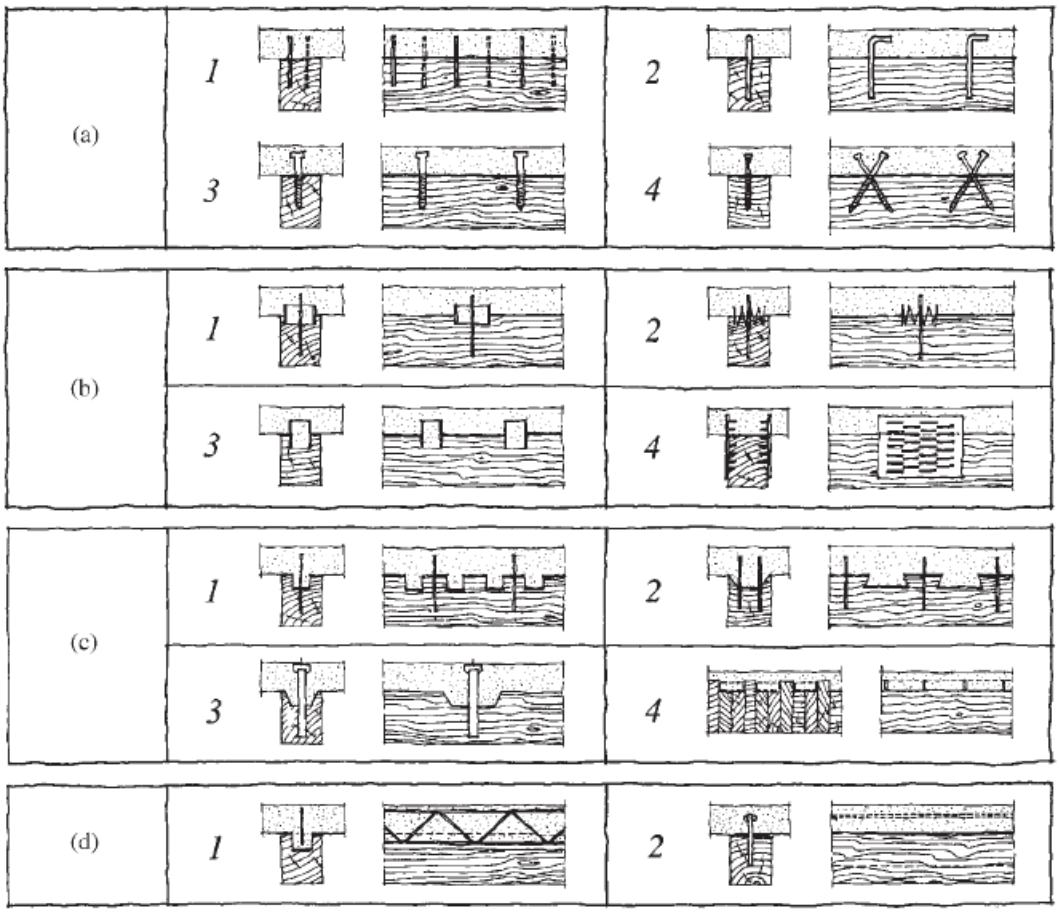

Figure 2-22: Examples of connections for timber-concrete composite floors (Ceccotti, 2002)

Considerable research has been conducted on determining the ambient temperature characteristics of these types of floor systems in recent years; however the behaviour of these systems under fire conditions has attracted less attention due to the specialisation of the field. The fire resistance of timber-concrete composite elements is mainly influenced by the timber and the connectors, and has been researched extensively by Frangi and Fontana (1998). Their study looked at two separate systems, firstly a solid timber decking composed of nailed planks or glue laminated beams, this had grooves cut into the top of the decking to act as the connection system with threaded bars glued into predrilled holes along these grooves, and a concrete layer cast on top. The second system was a sawn timber beam system consisting of

inclined self-drilling screws for the connection system implanted into a concrete slab cast on plywood sheathing. These systems are shown in Figure 2-23.

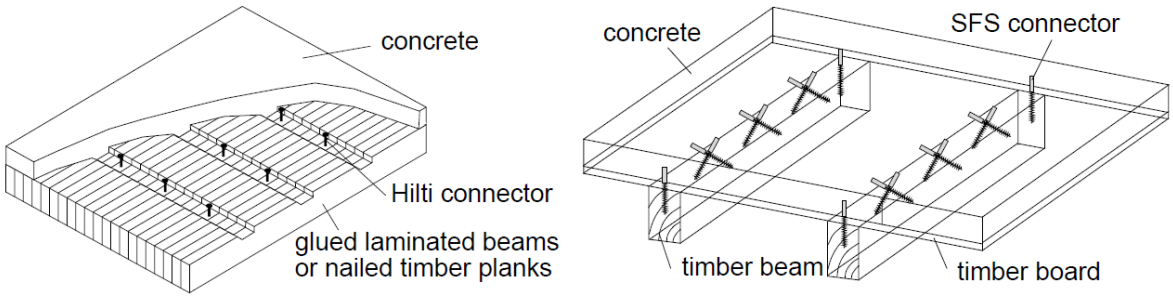

Figure 2-23: The timber-concrete composite systems studied by Frangi and Fontana (1998)

Two full-scale furnace tests were conducted and both systems exceeded 60 minutes of ISO fire exposure without structural collapse. Effects of the fire on the timber such as heating and reducing overall section size act to weaken both the timber section and the connection between timber and concrete. The form of connection is also important, as the integrity of the connection during the fire will be governed by its weakest element which can sometimes be difficult to predict. A simplified design method developed by Frangi and Fontana (2001) for timber-concrete composite floors based on the effective cross-section method from Eurocode 5 gave good results when compared with their large scale fire tests. Although these systems have some slight differences to the floors under investigation in this research, this method provides an insight into ways in which the fire resistance for these systems can be addressed.

Timber-concrete composite floors have been studied at the University of Canterbury in recent years (O'Neill, 2009) as a fore-runner to this study.

2.10 Floors Investigated in this Research

2.10.1 Composite Joist Floors

The composite joist floor under study consists of LVL beams ranging from 200mm to 600mm deep, fixed to a continuous LVL slab system as the primary supporting floor panel (top flange). A typical composite joist floor is shown in Figure 2-17 with fully rigid connection between the joists and slab components. Typically these floors range from 5 metres to 12 metres in length and are designed for normal service loads in office buildings and similar multi-storey applications.

A variation of this type of floor is under study at the University of Technology in Sydney with design procedures developed as a result (Crews and Shrestha, 2013). It is similar to the floor under study but with the addition of smaller bottom flanges, as shown in Figure 2-24. This configuration gives the added mechanical advantages of supporting greater loads at a higher level of lateral stability, hence resulting in the overall reduction of the floor member sizes after geometrical optimisation. However a larger area of timber is exposed to the fire in this regard, and due to the smaller member sizes the expected unprotected fire resistance of these floors will be lower under similar loading conditions and floor depths.

Figure 2-24: Typical composite joist floor with incorporated bottom flanges

Many protection measures are available to increase the expected fire resistance of these floors, and some are discussed in Section 8.2.

2.10.2 Composite Box Floors

The composite box floor is identical to the joist floor in all aspects but construction geometry. The bottom flanges of the joists are made continuous between each second pair and the spacing is modified, resulting in a box type system with every second panel missing on the bottom chord, allowing for services to be installed in the gaps. The advantage of a system such as this over the previous composite floor discussed is that the surface area of timber exposed to the fire is greatly decreased; hence the expected fire performance will be greater by a simple

change in geometry (for the same amount of timber per unit length of floor). A schematic of this type of floor is shown in Figure 2-25.

Figure 2-25: Typical composite box floor

Another type of configuration of this floor is a box section with a fully continuous bottom flange, which is used commonly around the world in many types of buildings. Due to the simplified methods in which the fire resistance of these floors can be calculated (as the initial face of timber is a slab subjected to one-dimensional charring), and the available literature present in the industry on this topic, they will not be further considered in this research.

2.10.3 Timber-Concrete Composite Joist Floors

The timber concrete composite joist floors under study have been researched previously at the University of Canterbury by Yeoh (2010) under ambient conditions. O'Neill (2009) concurrently conducted fire tests on these floor designs, and a full set of fire performance data is available for two full-scale tests which were undertaken as a result of the research.

The type of composite joist floor under study is a semi-prefabricated system comprising of "M" panels that are built with laminated veneer lumber beams and a thick plywood interlayer, which acts as a permanent formwork for the concrete. The plywood interlayer has holes cut into it to accommodate the form of connection being used between the beams and the concrete slab.

The connections tested were toothed metal plates projected into the topping slab, and concrete notches with a coach screw.

These panels are prefabricated off-site then transported to site and craned into position. The steel reinforcement can then be constructed and the concrete slab cast in-situ, the floor being propped if required. The concrete can also be precast atop the panels before transport to site. A sketch of a typical timber-concrete composite system such as this is shown in Figure 2-26.

Figure 2-26: Typical timber-concrete composite floor schematic

Design procedures for these types of timber-concrete composite floor systems are described in a design guide produced for the Australian and New Zealand markets (Gerber et al., 2012).

3 EXPERIMENTAL FIRE TESTS OF TIMBER FLOORS

3.1 Introduction

Experimental testing of any floor assembly is a key step in verifying its effectiveness in a fire scenario. Fires are by nature very dynamic and destructive forces from a structural engineering sense, and it can be extremely difficult to quantify the impact of a fire on a structural assembly by analytical and numerical methods alone. Experimental furnace testing is commonly used for the purpose of verifying the assumptions made about the performance of an assembly, and to collect more data on the "real world" behaviour of the assembly in a fire scenario. It provides a unique opportunity to discover any unforeseen effects or behaviours that may have been overlooked or not considered from the analytical viewpoint.

Experimental testing is of paramount importance for timber assemblies from a material sense not only to dispel the pre-conception of timber behaving poorly in fires, but also due to the general lack of test data in the field of timber engineering as it traditionally has not had widespread use when compared with its steel and concrete counterparts. Although fire testing on a large scale is very expensive, it can be a critical factor in determining whether a new assembly is commissioned for use in the construction market.

This section describes the experimental furnace testing conducted on four unprotected timber floor assemblies at the Building Research Association of New Zealand. The major objective is to investigate the behaviour of these floor systems subjected to load under fire conditions. Results and observations are presented, however comparisons with numerical modelling are given in Chapters 4 and 5.

3.1.1 Objectives

The objectives of the experimental furnace testing were:

- To investigate the behaviour of loaded timber floor assemblies subjected to fire conditions.
- To assess the performance of each timber component in resisting the fire, and determine the likely mode of failure for different floor geometries.
- To verify the thermal and structural numerical modelling by providing a base of reference with known inputs.
- To quantify the charring rates of the exposed components of the floor.

3.1.2 Scope

Four timber floor assemblies were tested in a full-scale furnace under controlled conditions. The floors were tested in one-way bending as strip beams, each measuring 1.2 metres wide and spanning the furnace interior of 4.0 metres. The floors were simply-supported at the ends and loaded at two central points, spread across the width of the floor panels as line loads. The loading regime was specified for normal office building loads, as described by AS/NZS 1170.1 (2002), and was held constant throughout the tests. The floors were subjected to the standard ISO 834 (1999) test fire for varying durations until runaway failure was observed and the floors were unloaded for damage assessment.

3.2 Testing Facilities

3.2.1 BRANZ

The Building Research Association of New Zealand (BRANZ) is a privately operated experimental testing facility which conducts experimental testing and data reporting for a wide range of products across many industries. In terms of fire testing facilities, BRANZ has both a large furnace for testing structural floors and walls, and a smaller pilot furnace for testing doors, windows, fittings and fixtures. BRANZ also has an ISO room and a cone calorimeter.

3.2.2 Furnace

The full-scale furnace at BRANZ has an opening of 4.0 by 3.0 metres and can accommodate varying depths of specimens depending on the number of steel loading frames used. The loading frames are craned on to the top of the furnace, allowing for multiple test specimens to be constructed and tested in quick succession if desired. This also enables the test specimen to be removed from the furnace whenever it is desired, which is vital to assessing damage to timber assemblies as they continue to char after the furnace has been shut off.

The furnace is fuelled by diesel injection burners and a gas extraction system to allow the pressure and temperature inside the furnace to be monitored and controlled to follow a specific regime. It is lined in ceramic fire bricks and has a number of thermocouples and pressure gauges on the interior to monitor the temperature and pressure inside the furnace. It should be noted that when testing combustible assemblies such as timber floors, additional fuel loads are introduced into the furnace which complicate the testing procedures when following a time-temperature regime. The furnace is manually controlled by technicians, hence a margin of error in the earlier stages of burning is expected and unavoidable.

The primary use of the furnace is for testing floors and walls, and due to the large 25 tonne crane housed in the warehouse the furnace can easily be rotated and inverted for either vertical or horizontal use. It can also be used to test structural elements, smoke vents and extraction fans, large doorways or glazed areas.

Due to the versatility provided by the crane and loading apparatus, unloaded or loaded tests are possible without any significant risk of damaging the equipment. The furnace is shown standing on its end (for wall testing) in Figure 3-1.

Figure 3-1: BRANZ full-scale furnace

As seen in Figure 3-1, 12 Type K (chromel-alumel) thermocouples are installed in an equidistant 3x4 array in the furnace interior to measure the fire temperature. These protrude in protective piping to approximately 250 mm below the top level of the steel loading frames, which in this case is also representative of the bottom chords of the floor specimens tested.

The extract ducts are located in the central region of the furnace interior on the floor, while the diesel and air injectors are located on the side walls (to the left and the right of Figure 3-1). This allows for an approximately uniform level of combustion to take place inside the furnace when lying flat, and the hot smoky gases are extracted from the bottom central region.

3.3 Specimen Details

3.3.1 Introduction

The motivation for deciding on the floor configurations was simple; it was desired that both a control type composite joist test and a more structurally optimal variation on a composite box floor system were to be compared. These were aimed at both the New Zealand and Australian markets which vary considerably in fire code regulations, with many Australian minimum design criteria being more than twice that found in New Zealand, hence both lightweight and heavyweight variants of the floor types were tested to assess products applicable to both markets. This also allowed for the testing of a broad range of fire endurances for better verification of the numerical modelling and analytical methods. Therefore a smaller floor size aimed at 30 minutes fire resistance, and a larger floor size aimed at 90 minutes fire resistance were chosen.

The geometries of the floors were sized to give these approximate resistances using the generic member sizes available from manufacturers (Nelson Pine LVL, 2012). Therefore both joist and box type floors were tested for 30 minute and 90 minute fire exposures, these are described in Table 3-1.

Table 3-1: Test specimen details

Test Name	Floor Beam Type	Fire Exposure Time (minutes)
A	Joist	30
B	Box	30
C	Joist	90
D	Box	90

One-way action is assumed for the floors as they are specifically designed for long span applications. The simply-supported end conditions are assumed as they are a common form of long-span floor construction used in practice (seating with a construction joint, no intermediate

supports). Fixed support conditions in most cases will reduce the maximum floor deflections due to continuity, however this is not as critical for timber as it might be for a concrete system, where steel curtailment in the tension zones is a major factor to consider in the floor design.

The practicalities of the experimental apparatus also play a role in these decisions. In order to simulate fixed conditions end restraints are required, ultimately the additional apparatus must be disassembled before the floor can be removed from the furnace and the fire extinguished. In order to gain meaningful charring measurements the disassembly process should ideally be as quick as possible, and fixed end conditions would severely hinder this.

3.3.2 Material Properties

The floors were constructed of LVL produced at Nelson Pine Industries in New Zealand. Some of the characteristic values for the recipe of Nelson Pine LVL 11 used in the testing are described in Table 3-2. The full specifications for the LVL used in the experiments are available in the manufacturer's specific engineering guide (Nelson Pine LVL, 2012).

Table 3-2: Nelson Pine LVL 11 characteristic values for limit states design (Nelson Pine LVL, 2012)

Characteristic Stresses (MPa)		
Bending	f'_b	38.0
Tension Parallel to Grain	f'_t	26.0
Compression Parallel to Grain	f'_c	38.0
Shear in Beams	f'_s	5.0
Compression Perpendicular to Grain	f'_p	10.0
Elastic Moduli (MPa)		
Modulus of Elasticity	E	11000
Modulus of Rigidity	G	550

It should be noted that these values are presented for a lower grade softwood LVL, and much higher characteristic values can be obtained when using higher grades or hardwood LVL.

The cross-banded LVL properties differ to a degree due to the changes in lamination orientation; hence values for F8 plywood are used in design for the standard cross-banded panels available (as per manufacturer guidance). The properties for this can be found in AS/NZS 2269.0 (2012), and are presented in Table 3-3.

Table 3-3: F8 plywood characteristic values for limit states design (Nelson Pine LVL, 2012)

Characteristic Stresses (MPa)		
Bending	f'_b	25.0
Tension	f'_t	15.0
Compression in the Plane of the Sheet	f'_c	20.0
Panel Shear	f'_s	4.2
Elastic Moduli (MPa)		
Modulus of Elasticity	E	9100
Modulus of Rigidity	G	455

3.3.3 Adhesives

The adhesive used in the process of manufacturing the LVL was in this case a phenolic adhesive applied in accordance with AS 2754.1 (2008), producing a Type A marine bond as tested to AS/NZS 2098.2 (2012). This adhesive performs well in fire conditions, and the presence of glue lines does not significantly impact the structural performance of the LVL at elevated temperatures. It is also rated as the highest and most durable form of bond which can be used for any external application.

The adhesive used by the fabricator is similar in nature, providing a fully rigid bond between timber components in ambient and elevated temperatures. A resorcinol adhesive was used which is also classed as a Type A marine bond, and was applied in accordance with AS/NZS 1328.1 (1998) and AS/NZS 1328.2 (1998).

3.3.4 Specimen A - Small Joist Floor

Specimen A consisted of two 400 mm deep x 45 mm wide LVL joists glued in a pair under a 36 mm thick x 1200 mm wide cross-banded LVL slab. The joists were fixed together in pairs to reduce the area of timber exposed to fire thus increasing the expected fire resistance of the assembly. A 3D view and cross-section are shown in Figure 3-2 and Figure 3-3 respectively.

Figure 3-2: 3D representation of Specimen A

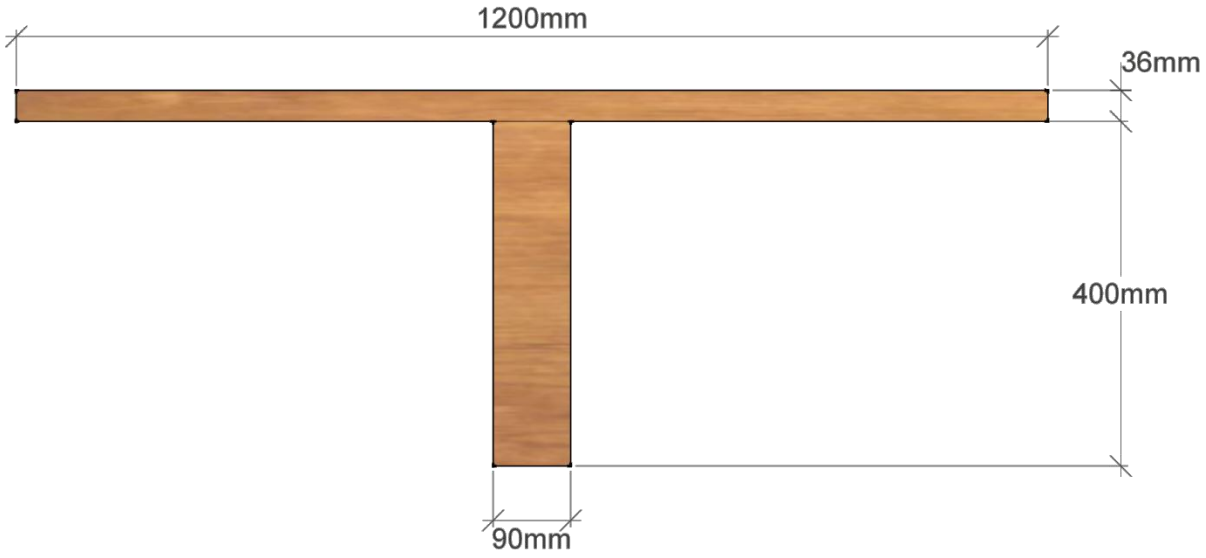

Figure 3-3: Section view of Specimen A

The plan view of Specimen A is shown in Figure 3-4, indicating the locations of all the thermocouples placed on the top of the timber slab. Six thermocouples were used in total, with three spaced evenly across the centreline and three similarly placed 700 mm in from one end of the specimen, protruding 500 mm into the furnace opening.

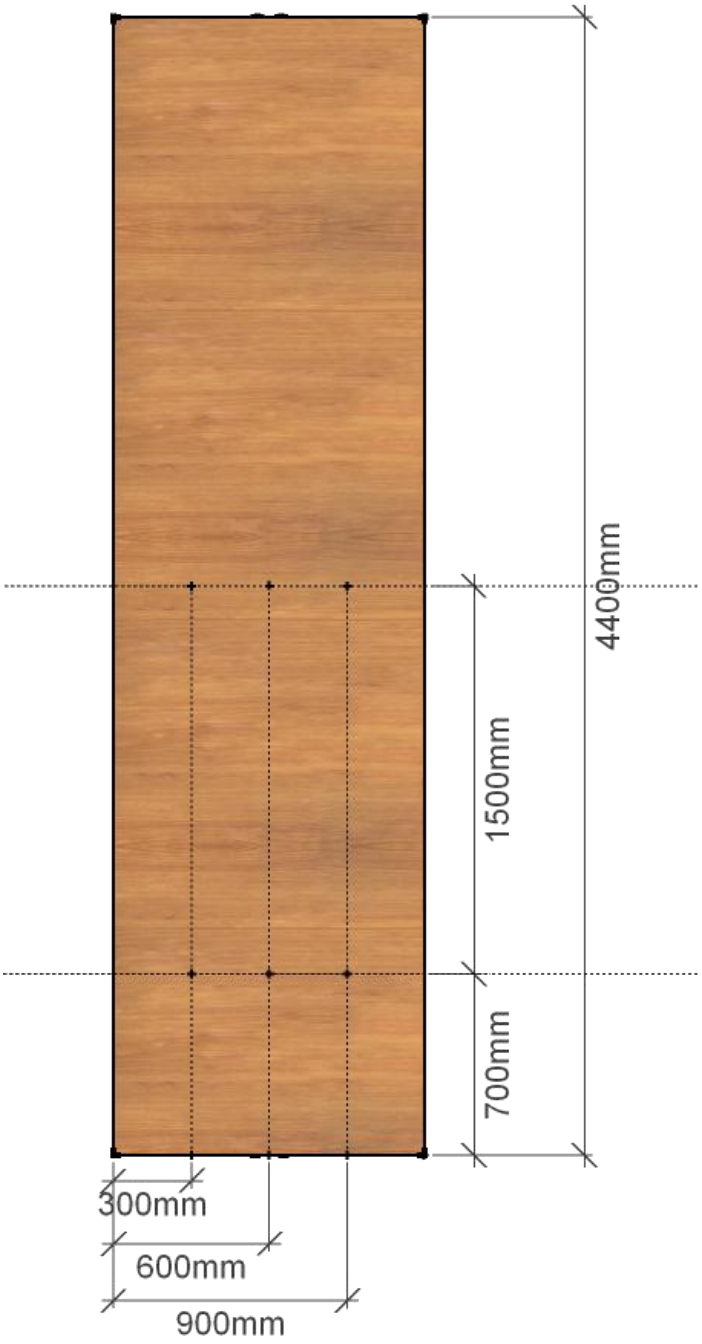

Figure 3-4: Plan view of Specimen A including thermocouple locations

3.3.5 Specimen B - Small Box Floor

Specimen B consisted of a box section formed from 360 mm deep x 45 mm wide LVL joists and a 45 mm thick x 300 mm wide LVL bottom flange. This box section was fully fixed to a 36 mm thick x 1200 mm wide cross-banded LVL slab as for Specimen A. The three-dimensional representation of this floor is given in Figure 3-5, with a sectional view shown in Figure 3-6.

Figure 3-5: 3D representation of Specimen B

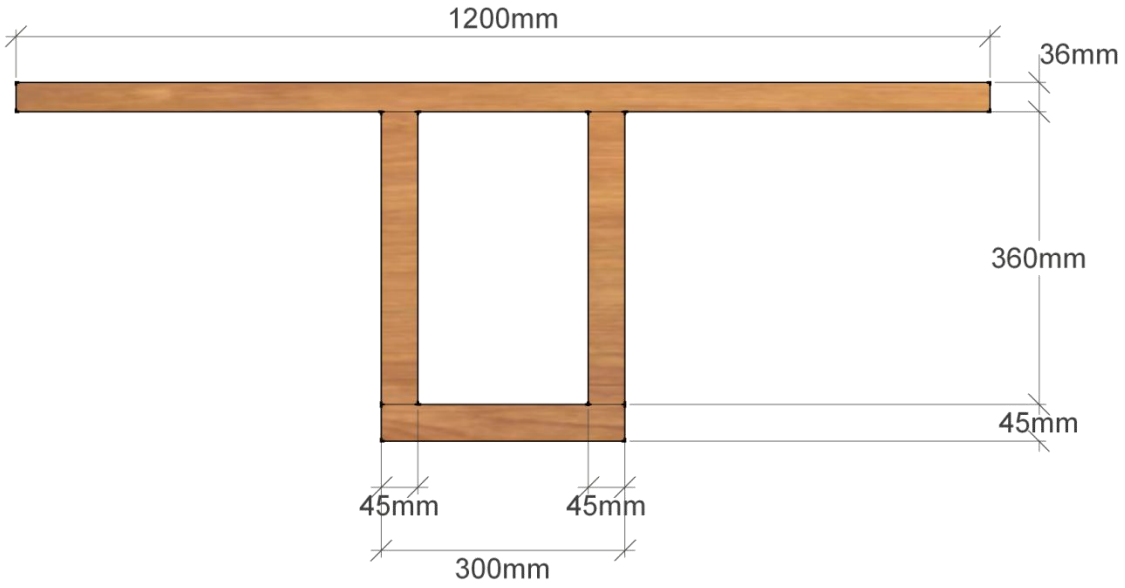

Figure 3-6: Section view of Specimen B

The plan view of Specimen B is given in Figure 3-7. Specimen B had two thermocouples placed inside the box cavity (on the bottom flange) situated approximately 800 mm into the furnace, and three more were placed over the mid-span at evenly spaced intervals across the width of the specimen. The thermocouple locations were laid out in a symmetrical pattern as shown.

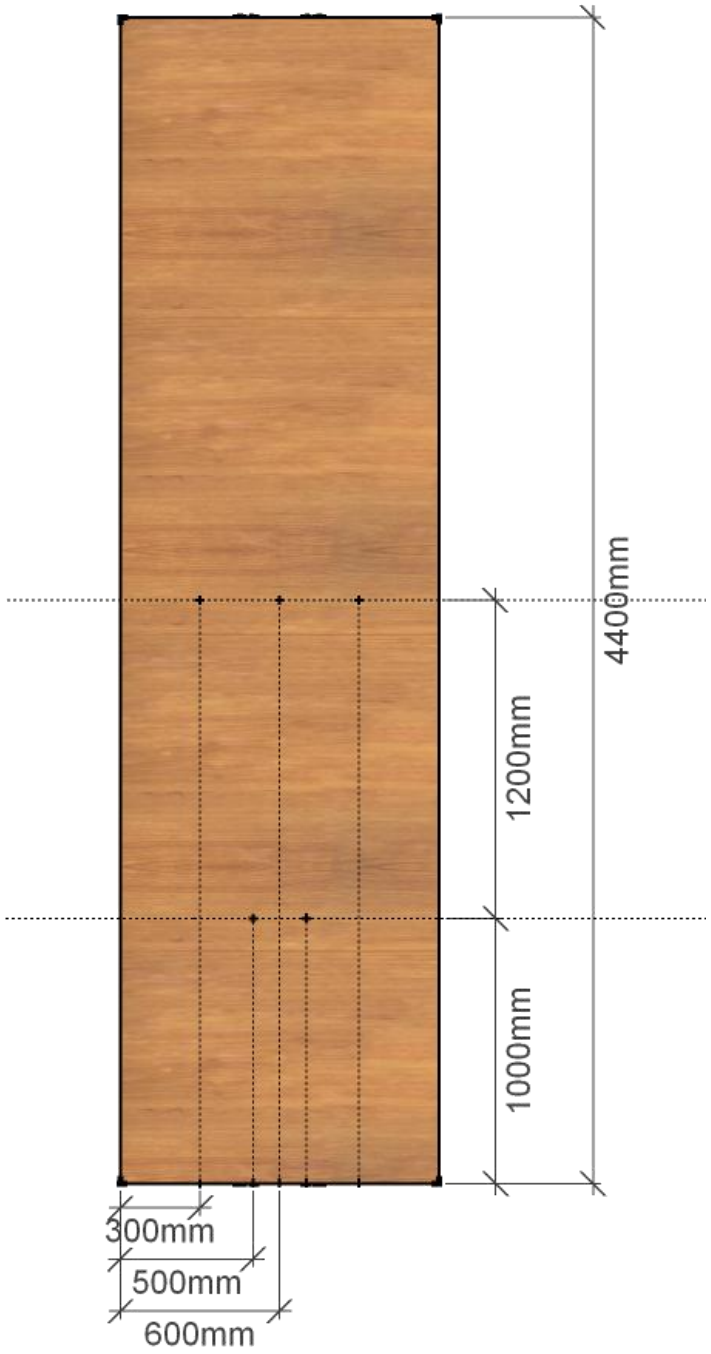

Figure 3-7: Plan view of Specimen B including thermocouple locations

3.3.6 Specimen C - Large Joist Floor

The design of the tests floors changed due to changes made from the first phase of testing; hence Specimen C consisted of three pairs of 450 mm deep x 90 mm wide LVL joists glued under a 108 mm thick x 1200 mm wide cross-banded LVL slab which was made up of 3 layers of 36 mm thick cross-banded LVL glued together. A three-dimensional depiction is shown in Figure 3-8, and cross-section shown in Figure 3-9.

Figure 3-8: 3D representation of Specimen C

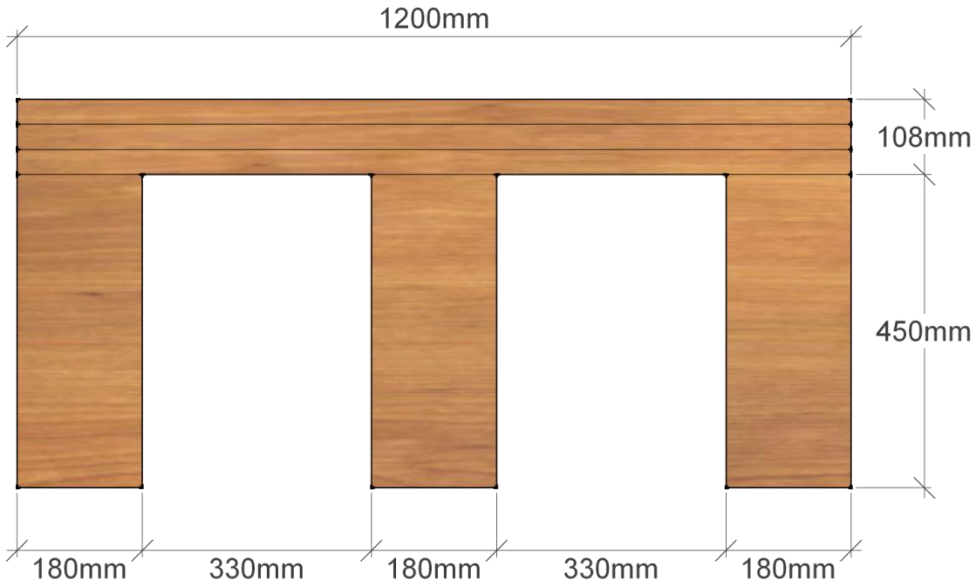

Figure 3-9: Section view of Specimen C

As seen from the plan view of Specimen C in Figure 3-10, two rows of three thermocouples were placed on the top of the slab at even 1100 mm intervals along the length of the floor, spaced equidistant between joist pairs. A single thermocouple was placed in the centre of the slab over the central joist pair at the mid-span.

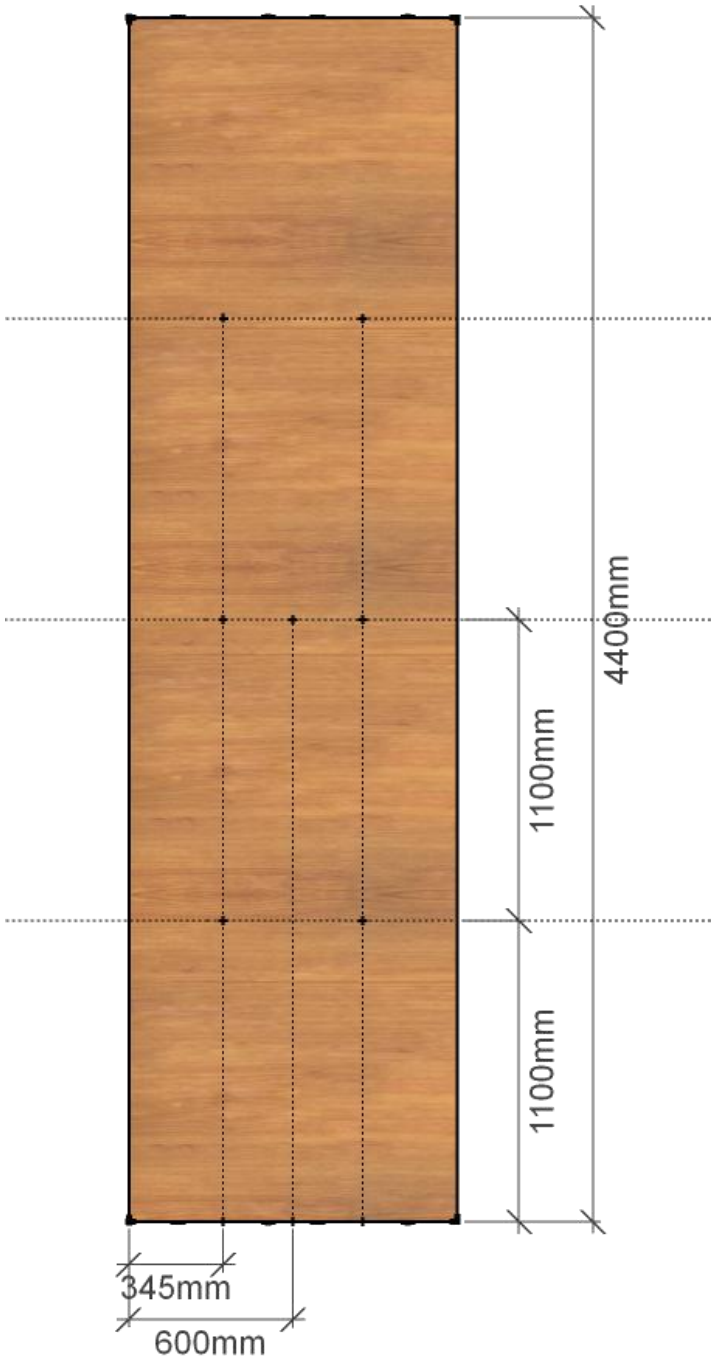

Figure 3-10: Plan view of Specimen C including thermocouple locations

3.3.7 Specimen D - Large Box Floor

Specimen D consisted of two box sections formed from 300 mm deep x 90 mm wide LVL joists and 90 mm thick x 400 mm wide LVL bottom flanges. The box sections were glued and screwed to a 108 mm thick x 1200 mm wide cross-banded LVL slab composed of three separate layers glued together as for Specimen C. The three-dimensional representation of this floor is given in Figure 3-11, with a sectional view shown in Figure 3-12.

Figure 3-11: 3D representation of Specimen D

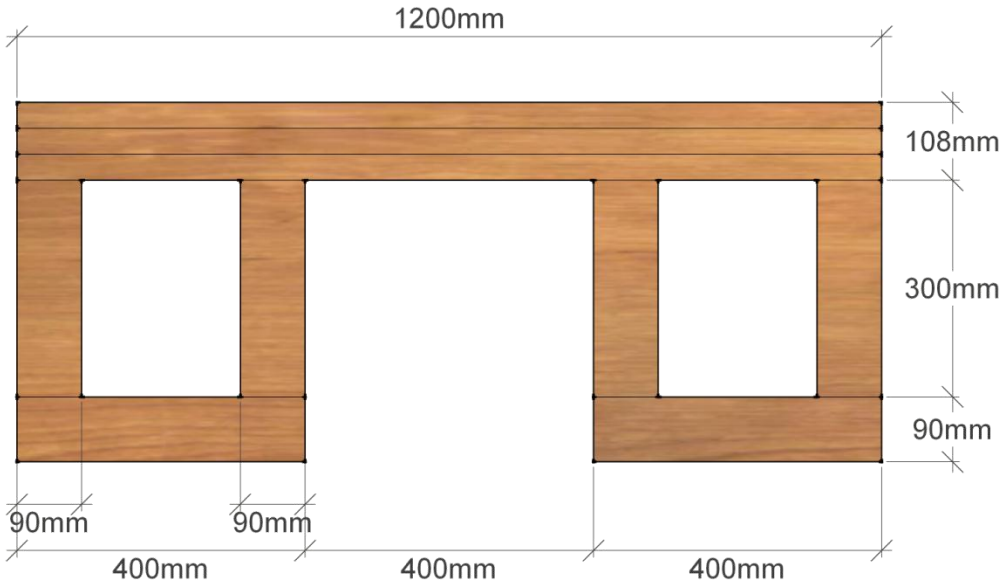

Figure 3-12: Section view of Specimen D

The plan view of Specimen D is given in Figure 3-13. Specimen D had two thermocouples placed inside each box cavity (on the bottom flanges) situated approximately 800 mm into the furnace, and five placed over the mid-span on the top slab at the spacing shown. The cavity thermocouple locations were laid out in a symmetrical pattern as shown.

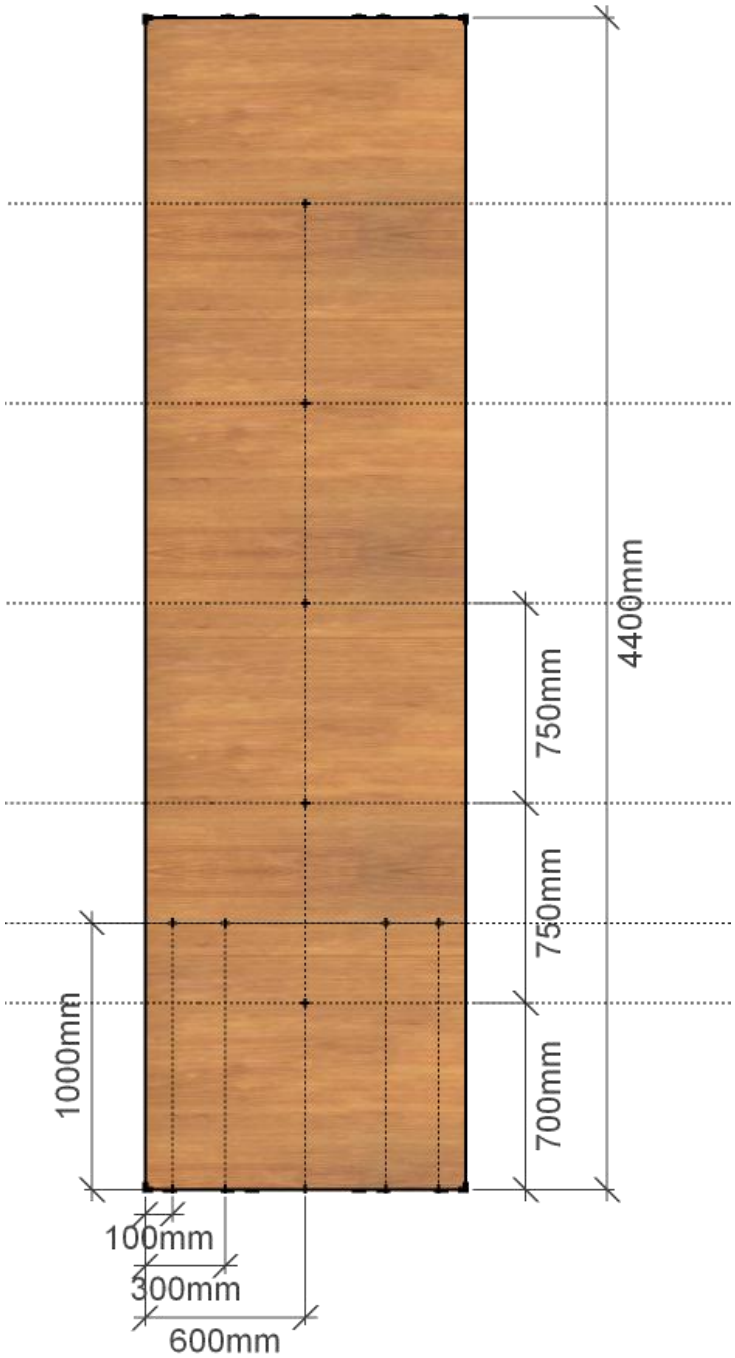

Figure 3-13: Plan view of Specimen D including thermocouple locations

3.3.8 Displacement Potentiometers

Due to the complexities involved in rigging up multiple potentiometers on the loading frame, two potentiometers were used in each test to measure mid-span deflections. The experiments were recorded on video to capture any unexpected displacement behaviour of the floors during testing, and to aid in the observations presented in the results section.

3.3.9 Thermocouples

Type K (chromel-alumel) thermocouples were used on the top of the specimens to allow for accurate measurements of the increase in temperature on the top of the floor assemblies. These were placed in locations to allow for a good average representation of the overall slab temperature. This was to assess possible insulation failures of the top slabs as they charred away during the tests. In the tests with box beams the cavities were also instrumented to measure the increase in cavity temperature for the duration of fire exposure. Specific thermocouple layouts are presented in Sections 0 to 3.3.7, while the temperature results are shown in Sections 3.6 to 3.9, relevant to the particular floor specimen described. The thermocouples placed on top of the slabs were covered with gypsum plasterboard to protect them from ambient temperature changes of the surrounding environment. The thermocouples in Figure 3-4 near the end of the furnace were left uncovered as shown in Figure 3-14. This was to determine how the ambient temperature outside the furnace would affect the readings given by the thermocouples. The results of this are presented in Section 3.6.4.

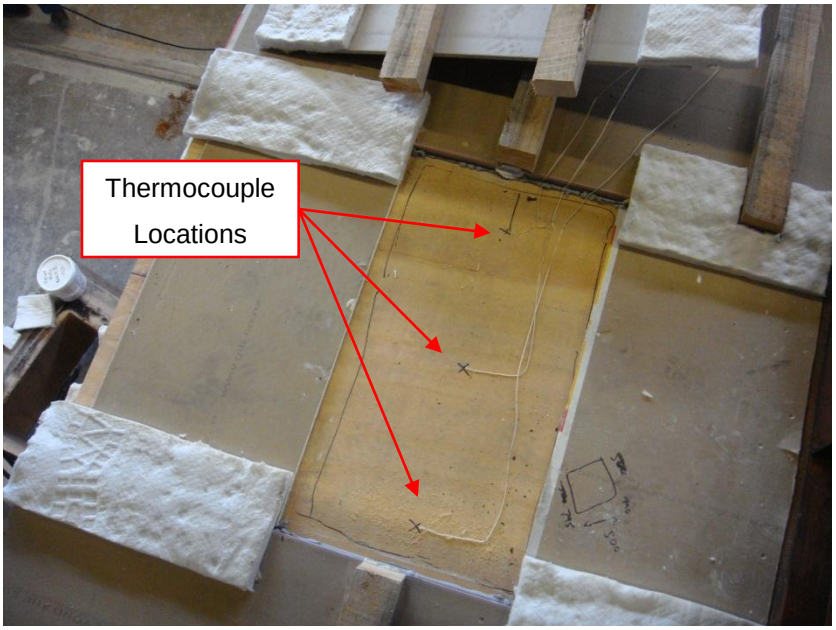

Figure 3-14: Uncovered thermocouple instrumentation for Specimen A

From previous tests conducted in the furnace (Spellman, 2012) it was considered likely that the implantation of a thermocouple tree through a central portion of a timber beam (by way of drilling a hole and inserting a wood plug) may have contributed to premature failure. To avoid this type of issue, and due to the fact that a large amount of research into the charring of the LVL used had already been conducted (Tsai, 2010), thermocouples were not implanted within the lower portions of the specimens, and only used on top of the slabs. Thermocouple positions on the slab were changed during each test to target areas most likely to suffer a burn through; hence a standard test method was not rigorously followed for positioning.

3.3.10 Construction

The LVL floor components were manufactured by Nelson Pine Industries and shipped to the fabricators for construction. In the initial testing phase both specimens A and B were constructed by McIntosh Timber Laminates, and for the second phase of testing specimens C and D were constructed by Hunter Laminates. During the fabrication process the gluing surfaces of the specimens were prepared and glued together, using both screws and clamping to allow the adhesive to bond and set. After this process the specimens were shipped to the BRANZ testing facility for preparation for the experimental testing. These are shown in Figure 3-15 and Figure 3-16.

Figure 3-15: Specimens A and B before furnace test preparation

As they were designed for smaller spans and lower resistance times, Specimens A and B are significantly more lightweight in comparison to Specimens C and D.

Figure 3-16: Specimens C (left) and D (right) before furnace test preparation

The specimens measured 4.4 metres in length, with a clear span of 4.2 metres exposed to the fire inside the furnace. After mounting on the steel loading frame, each floor was compartmentalised by constructing timber and plasterboard encasement to contain the fire within the furnace. This is illustrated in Figure 3-17.

Figure 3-17: Plasterboard enclosure for the furnace testing of Specimen A

This was very important for controlling the pressure and temperature inside the furnace to ensure the correct fire curve was maintained throughout the furnace testing. For the longer

duration tests concrete lids were used in place of the plasterboard encasement as they were more suitable for resisting the extended periods of fire exposure, as seen in Figure 3-18.

A lightweight concrete block wall was constructed around the boundary of the steel loading frame which housed the floor units. The reason the floors were laid atop the frame and not dropped into the furnace was due to the uncertainty surrounding what type of supporting connections to use and maintaining their integrity during the testing. Flange hung floors are commonplace in the industry however trying to incorporate this into the furnace tests would introduce another level of complexity and uncertainty to design for. Ultimately the purpose of the testing was to determine the structural performance of the floor system and not connections hence the specimens were simply-supported over the testing frames to avoid a premature connection failure.

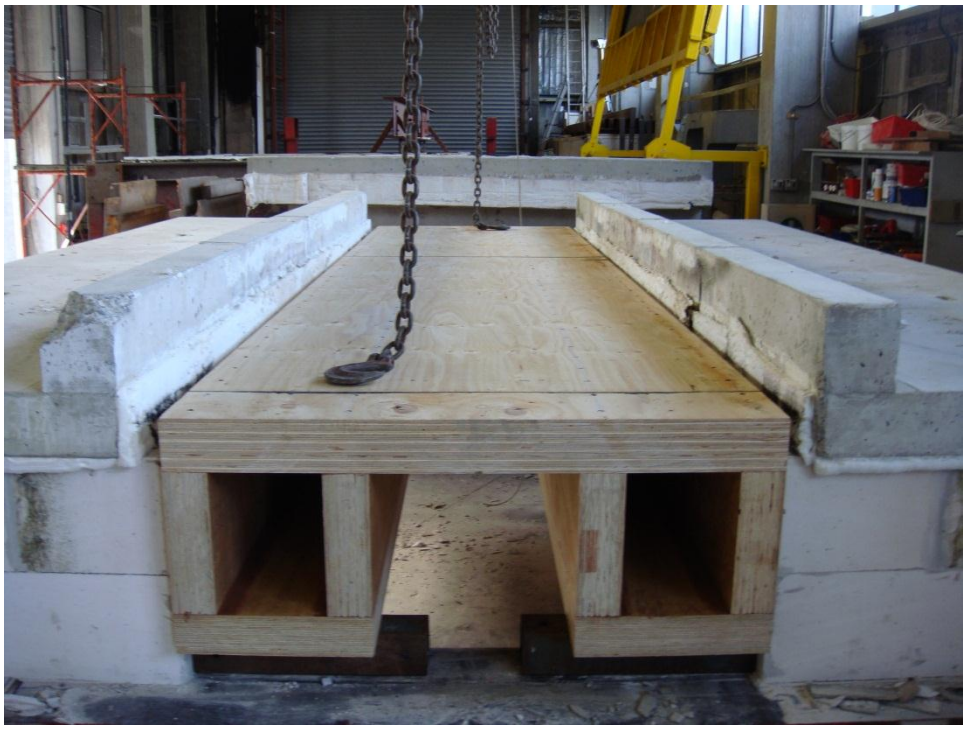

Figure 3-18: Concrete encasement for Specimen D

After mounting on the supports the remaining openings in the test floors were blocked up and packed with kaowool (a fire retardant ceramic blanket), and any gaps filled with an intumescent filler. This blocking up is shown on the left of Figure 3-19 from the inside of the furnace, while the kaowool sealing can be seen on the right from the exterior of the furnace before the plasterboard lid has been placed, (seen in the bottom of the figure).

Figure 3-19: Inner floor protection (left) and plasterboard cavity covers (right)

The kaowool has a maximum reliable service temperature of 1260°C so was ideal for protecting the steel supports and floor boundaries (Forman Building Systems, 2010). The underside of the fully prepared Specimen D before furnace testing is shown in Figure 3-20. This shows what was left completely exposed to the fire during the furnace testing.

Figure 3-20: Underside of Specimen D before furnace testing

At this stage the completed floor specimen and loading frame were craned onto the top of the furnace and the loading rig is installed atop the floor. The ends of the box beam cavities for

Specimens B and D were sealed with gypsum plasterboard (shown in Figure 3-19) and intumescent filler to simulate the real conditions of floor construction and obtain a higher, hence more conservative, estimate of cavity temperature.

3.3.11 Support Conditions

To achieve the simple pinned support condition of the floors, steel rollers and plates were used between the bottom chord at each end of the specimens and the loading frame. These were placed 100 mm inside the internal edge of the furnace opening, thus extending the actual span of the floors for all tests to 4.2 metres. Figure 3-21 shows a typical support fabricated on-site for the furnace testing. To reduce any interaction between the fire and the steel supports which may have influenced the results, the supports were heavily protected from the furnace interior via kaowool wrapping and lightweight concrete blocking where possible.

Figure 3-21: Pin roller support used in the furnace testing

3.4 Test Configuration

The furnace testing and specimen preparation were conducted following the guidance in AS 1530.4 (2005), Methods for Fire Tests on Building Materials, Components and Structures.

3.4.1 Loading Protocol

The loads applied to the specimens were held constant throughout each test until termination. In addition, the loads were applied to the specimens for 30 minutes prior to furnace testing in accordance with AS 1530.4 (2005) and ISO 834 (1999).

The loads were applied via a hydraulic ram over a spreader bar down to two point loads on the floor slab 1.3 metres from each support to achieve the desired level of force (spread across the width by steel plates). BRANZ alternatively has a barrel loading system for simulating uniformly distributed loads; however this system has its drawbacks in terms of the maximum level of load possible. Due to the higher levels of load required for the larger floor specimens, the ram option was used. The loading frame and spreader are shown in Figure 3-22 and Figure 3-23.

Figure 3-22: Loading frame and furnace setup for Specimen C

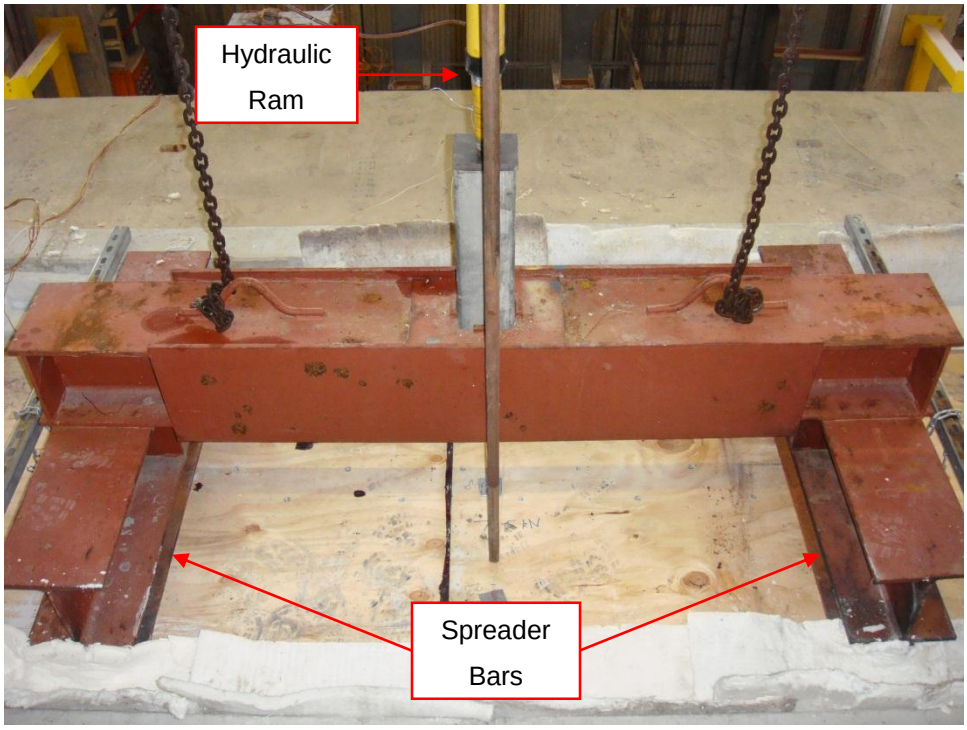

Figure 3-23: Loading ram and spreader configuration on top of floor slab

The time taken to dismantle and remove the loading apparatus from the furnace to then remove the loading frame and accompanying floor system was also a consideration during testing. Reducing this time is paramount to timber assembly testing in particular as the timber will continue to char after the furnace has been shut off, therefore, to obtain appropriate measurements of char damage this time must be minimised. During these tests the loading rig must be removed before the floor and loading frame could be lifted from the furnace, hence there was a delay (measured for each test) between shutting off the furnace and dousing the underside of the floors with water.

3.4.2 Applied Loading Calculations

The applied loads for the floor specimens were calculated based on normal office loading characteristics for a multi-storey building from AS/NZS 1170.1 (2002), with a live load of 3.0kPa and a superimposed dead load of 1.0kPa plus the self-weight of the floors. The resulting maximum bending moment at the mid-span from this was calculated for each specimen load case. However, the loading for the floors was calculated based on spans of 7 metres for Specimens A and B, and 8 metres for Specimens C and D. Therefore applied loads were increased (scaled) to account for the decrease in actual floor span to achieve the same maximum bending moment at the mid-span of each floor system specimen.

The total loading on the specimens was calculated using the loadings standard AS/NZS 1170.0 (2002) to check the cold design strength under ultimate limit state conditions:

$$E_d = 1.2G_l + 1.5Q_l$$ **Equation 3-1**

Where: E_d = Design load (kPa)
G_l = Dead load (kPa)
Q_l = Live load (kPa)

The situational fire load factor was then applied to this load case, reducing the coefficients as seen in Equation 3-2. This is to account for the reduced live and dead loads present in the case of a building fire, where an evacuation has taken place and the building is no longer in operational use.

$$E_{d,fire} = 1.0G_l + 0.4Q_l$$ **Equation 3-2**

Where: $E_{d,fire}$ = Fire design load (kPa)

The dead load includes both a superimposed deal load and the self-weight of the floor:

$$G_l = SDL + G_{self}$$ **Equation 3-3**

Where: SDL = Superimposed dead load (kPa)
G_{self} = Self-weight (kPa)

The uniformly distributed load applied to the floors is then calculated from the known tributary width of each specimen:

$$w_{fire} = W_t \times E_{d,fire}$$ **Equation 3-4**

Where: w_{fire} = Fire uniformly distributed load (kN/m)
W_t = Tributary width (m)

Once this load was calculated, for each particular specimen design length the bending moment at mid-span was obtained considering a simply-supported beam case:

$$M^*_{fire} = \frac{w_{fire} \times L^2}{8}$$ **Equation 3-5**

Where: M^*_{fire} = Moment demand for the fire design (kNm)

L = Span length (m)

Then a scaled load was derived for the shortened span to obtain an equivalent bending moment, considering a four point bending case as shown in Figure 3-24:

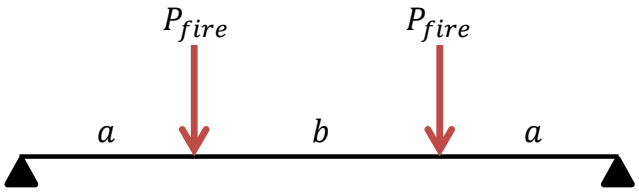

Figure 3-24: Four point bending configuration

$$P_{fire} = \frac{M^*_{fire}}{a}$$ **Equation 3-6**

Where: P_{fire} = Point load for the fire design (kN)

a = Distance between loading and support points, four point bending (m)

b = Distance between loading points, four point bending (m)

This scaling had the unfortunate effect of disproportionally increasing the shear force in the floors to a higher level than would normally be experienced, however hand calculation checks were made evaluating the shear strength of the section to ensure this would not dictate the failure mode of the floors under cold conditions and at the latter stages of testing with reduced cross-sections.

Table 3-4 summarises the loads and spans used for each floor specimen in both the initial design and the testing. The actual test span for all floors was 4.2 metres across the furnace to the centres of the supports, with the loading rig spanning 1.6 metres across the centre of the floor specimens.

Table 3-4: Design/test load and span summary for the floor specimens

Specimen	L_i	SDL	W_{self}	G_l	Q_l	W_t	w_{fire}	M^*_{fire}	a	b	P_{fire}
	(m)	(kPa)	(kPa)	(kPa)	(kPa)	(m)	(kN/m)	(kNm)	(m)	(m)	(kN)
A	7	1.0	0.3	1.3	3.0	1.2	3.0	18.5	1.3	1.6	14.2
B	7	1.0	0.3	1.4	3.0	1.2	3.1	18.8	1.3	1.6	14.5
C	8	1.0	1.2	2.2	3.0	1.8	6.1	49.0	1.3	1.6	37.7
D	8	1.0	1.2	2.2	3.0	1.6	5.4	43.5	1.3	1.6	33.5

3.4.3 Fire Testing Protocol

The ISO834 (1999) standard test fire curve was used to heat the underside of the floor specimens, as shown in Figure 2-2.

The furnace pressure was held constant at 12 Pa for each test inside the furnace, and the fire testing protocol followed for conducting the furnace testing was AS1530.4 (2005).

3.5 Experimental Results

3.5.1 Overview

In the following sections the results and observations of each individual test specimen will be described. Due to the loading apparatus used, the four floor specimens described were tested as strip beam tests consisting of a 1200 mm wide portion of slab and the corresponding beam members for that tributary width. For reasons discussed in the following sections the latter tests were designed with more members (and hence higher loads) to provide edge restraint and avoid premature failure of the tests.

3.5.2 Sign Convention

For all plots in the following sections of displacement versus time the downwards deflection of the floor specimen is reported as negative values of displacement, while upward deflection is reported as positive. Charring rates are calculated for the total duration of forced and uncontrolled burning, which is the time at which the furnace was shut off until the specimens were doused with water and combustion ended (both times are reported in the results).

3.6 Test Specimen A Results

The furnace testing of Specimen A was conducted on 20 March 2012. Specimen A was chosen as a standard joist floor option which is commonly found in many countries around the world, and was designed to withstand approximately 30 minutes of fire exposure under load.

3.6.1 Furnace Temperature

The average recorded furnace temperature of Test A, compared with the ISO 834 standard fire curve and its tolerances are shown in Figure 3-25.

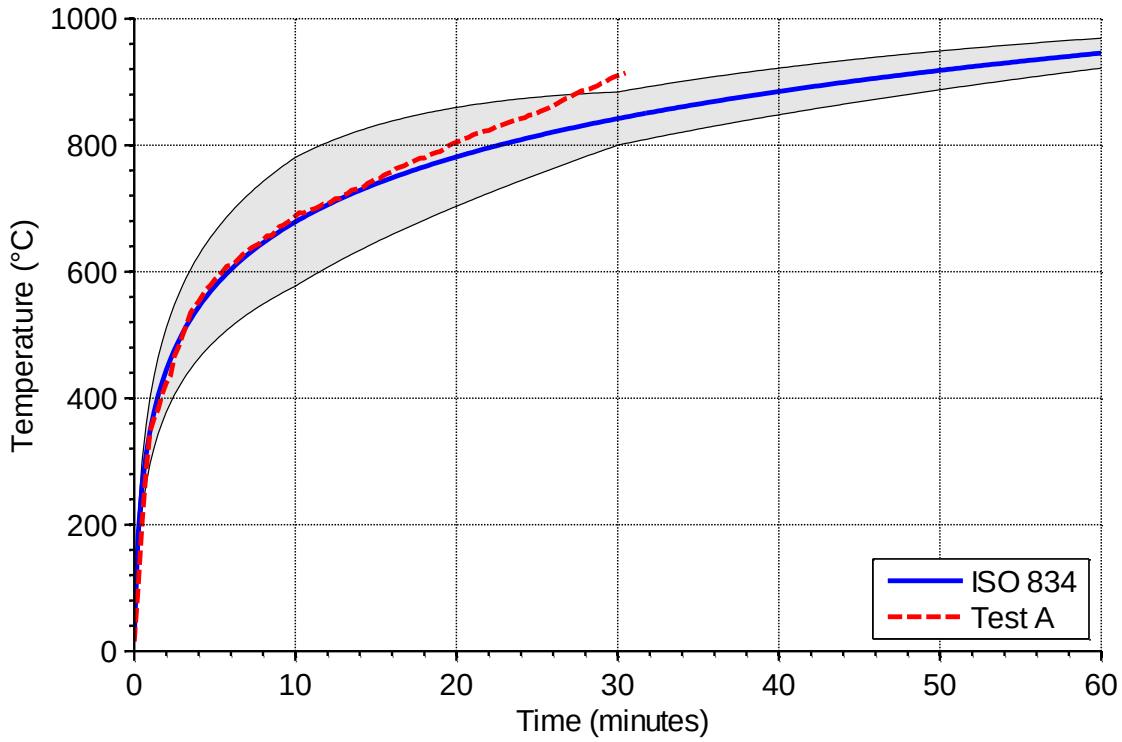

Figure 3-25: Furnace temperature for Test A

It can be seen that the furnace temperature followed the standard fire curve well until the very end of the test at which point the temperature increase did not slow at the same rate as was specified by the testing standard, which resulted in a more conservative approximation when considering resistance testing.

3.6.2 Observations

The first 10 minutes of testing was uneventful, with little smoke or gas escaping from the specimen enclosure and only small deflections recorded. As the test time approached 20

minutes a large amount of smoke was billowing from one corner of the loading plate sitting atop the floor slab, and the sides of the floor slab appeared to be deflecting down into the furnace, most notably on one side of the floor specimen. This region is shown in Figure 3-26. This indicated a downward bowing action of the sides of the floor slab, as there was not adequate edge restraint to support the sides of the panel. The downward bowing caused an opening in the test enclosure to the outside environment which resulted in increased burning through the opening at this spot. This eventually led to a burn through of the slab in this region of the specimen in approximately 30 minutes, and the test had to be stopped prematurely as the pressure and temperature in the furnace could no longer be controlled properly.

Figure 3-26: Floor burn through at the loading plate during Test A

Following these observations of the burn through of the slab, measures were taken to ensure the subsequent experiments would not incur this type of failure. Stiffening ribs were attached to the top of Specimen B (which had already been fabricated) to ensure this same edge deflection would not occur, and more continuous real world conditions could be simulated. Specimens C and D were designed in such a way that the supporting beam members were present on the edges of each slab, as can be seen in Section 3.3.6 and 3.3.7. Figure 3-27 shows the test of Specimen A shortly before termination at 30 minutes, and Figure 3-28 shows the test specimen and loading frame as it was lifted off the furnace immediately after testing.

Figure 3-27: Test Specimen A at 29 minutes

The burn through of the top slab can be seen in Figure 3-28 next to the burning beam at the top of the picture. It took approximately 6 minutes from the furnace shut off to unload the floor, remove the loading rig and douse the underside of the floor with water.

Figure 3-28: Specimen A immediately after furnace testing

3.6.3 Displacement

Figure 3-29 shows the displacement readings from the two mid-span potentiometers during the fire test of Specimen A. Only 2 mm of displacement was recorded during the first 10 minutes of testing. It can be seen from the readings that the floor began to deflect under the load at a relatively constant rate from 10 minutes to 25 minutes by approximately 10 mm. The rate of deflection began to increase at 25 minutes; however the test was ended prematurely before more measurements could be taken.

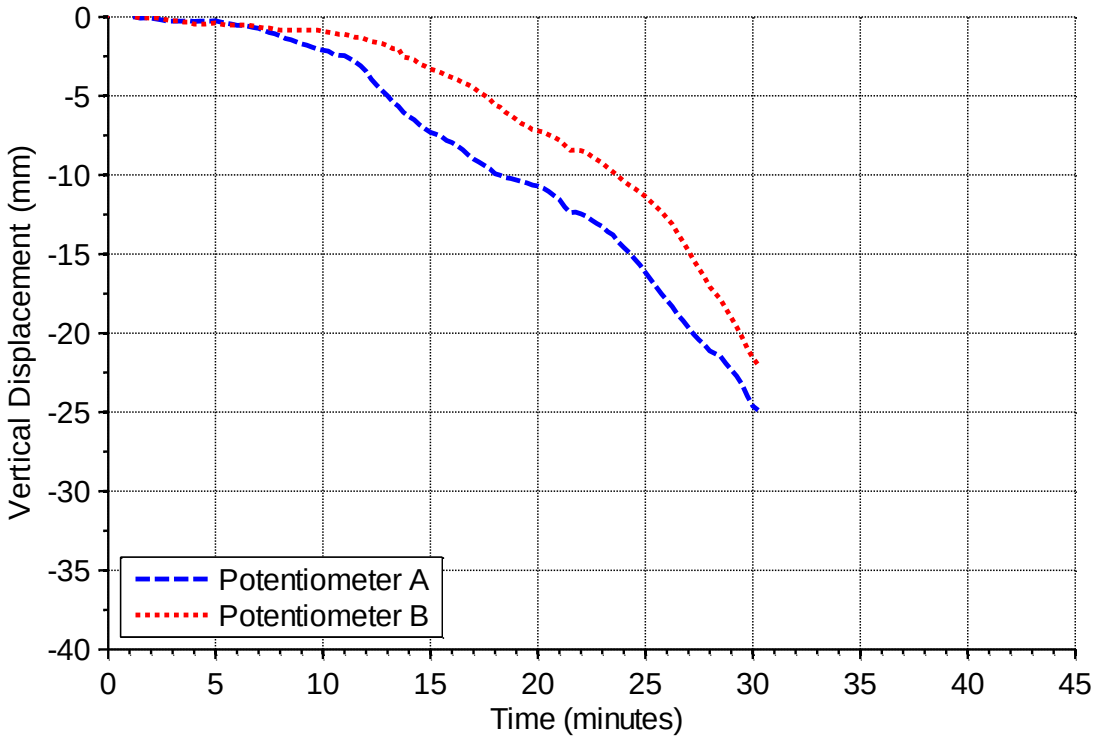

Figure 3-29: Mid-span vertical deflections of Test A

The side which displaced more and had the burn through can be clearly seen on the figure as Potentiometer A, which leads Potentiometer B by approximately 5 mm vertical deflection for the majority of the fire test. On inspection of the test data, the trend suggests that runaway failure would have occurred sometime near 33 – 37 minutes.

3.6.4 Slab Temperatures

Specimen A had six thermocouples installed on the top of the slab surface, three at the mid-span and three near one end of the furnace, all spaced at equal intervals across the width of the

specimen (refer to Figure 3-4). The temperature results recorded by these for Test A are shown in Figure 3-30.

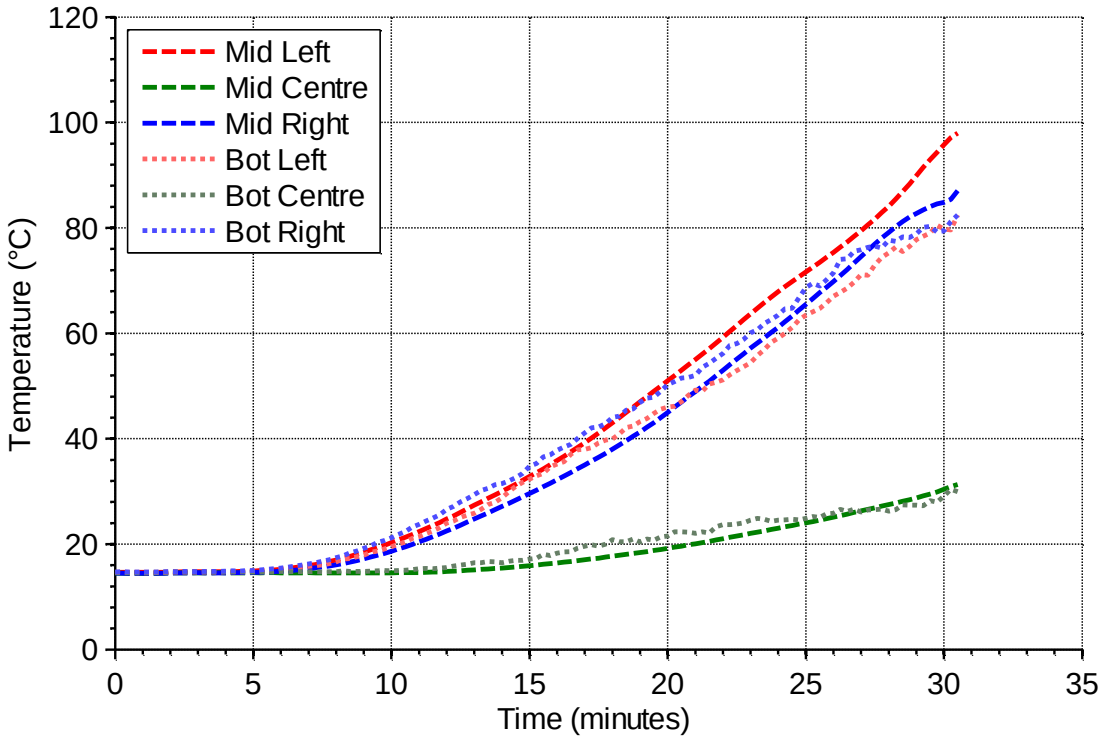

Figure 3-30: Slab surface temperatures of Test A

It can be seen from the figure that the left side thermocouples near the centre measured notably higher when compared with the other thermocouples, which reinforces what was observed in the test with the burn through. The thermocouples installed in the middle of the floor specimen were covered with gypsum plasterboard; hence the readings obtained from these are much more stable and exhibit less minor variance when compared with the thermocouples exposed to the open air. However, the presence of the plasterboard did not change the overall average result to a discernible level; hence using either setup for these environmental conditions was acceptable. This also indicates that the interior heat flux was relatively constant from the middle to the edges of the furnace along the span of the specimen.

As expected, the temperature readings from the top of the slab over the joist in the centre of the specimen were much lower than those over the slab panel alone. The maximum temperatures these central locations reached was approximately 30°C after 30 minutes testing, an increase of less than 15°C. The readings taken over the open slab sections showed a greater increase in

temperature, with an initial temperature increase recorded at approximately 8 minutes, steadily increasing to around 80 – 95°C by 30 minutes. In general to meet acceptable insulation requirements the cold side of the test specimen must not exceed an average increase of 140°C or 180°C at a point (Buchanan, 2001). From the results it can be seen that the average increase is less than 80°C hence by 30 minutes would meet these requirements.

3.6.5 Char Damage

The total charring damage caused to Specimen A was due to 30 minutes of exposure to the furnace design fire shown in Figure 3-25, and approximately 6 minutes of open air burning after the furnace was shut off. The charred section immediately after furnace testing is shown in Figure 3-31.

Figure 3-31: Underside of Specimen A after extinguishment

Measurements were taken at quarter points throughout the beam length (illustrated in Figure 3-32), and the actual char depth was found to be extremely uniform across the specimen. This was true for all specimens tested, and indicated an even level of combustion inside the furnace. The char depth measured along the beam section was found to be 25 mm on the sides of the beam, and 30 mm on the bottom chord. This left an approximate residual beam section of 370 mm deep x 50 mm wide, and is shown in Figure 3-32 after the removal of loose charcoal (the

overall depth including the unburned slab thickness above was 406 mm). The char depth on the underside of the timber slab was found to be 25 mm on average in the open region, leaving a residual thickness of 11 mm.

Figure 3-32: Residual section of Specimen A after furnace testing

3.7 Test Specimen B Results

The furnace testing of Specimen B was conducted on 22 March 2012. Modifications were made to the testing enclosure to remedy the issues raised when testing Specimen A to ensure a premature failure did not occur in a similar fashion. This resulted in timber stiffening ribs being installed on top of the floor transverse to the beam, as shown in Figure 3-33, which would aid in providing edge support for the slab but not interfere with the tests. Specimen B was similarly designed to Specimen A to resist 30 minutes of fire exposure.

Figure 3-33: Stiffening ribs and loading plates atop Specimen B before furnace testing

3.7.1 Furnace Temperature

The average recorded furnace temperature of Test B, compared with the ISO 834 standard fire curve and its tolerances are shown in Figure 3-34.

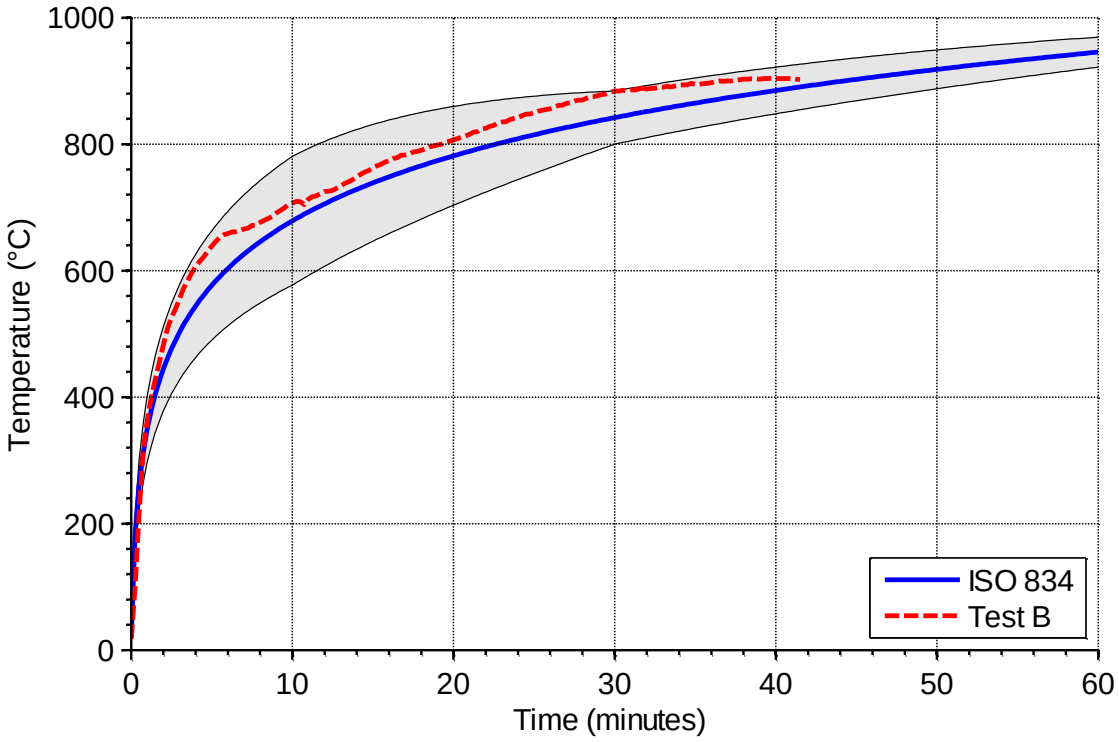

Figure 3-34: Furnace temperature for Test B

The fire curve followed in the test was once again slightly higher than that prescribed by the standard throughout the duration of testing, however was within the specified tolerance until the termination of the test.

3.7.2 Observations

During the first 30 minutes of Test B the amount of smoke seen escaping the specimen enclosure was significantly less than for Test A, and no premature insulation failure occurred as in that previous test. The first 35 minutes of the testing were relatively uneventful with a steady increase in the rate of displacement, and a photo of the entire furnace setup is shown in Figure 3-35 at that time. No other major issues of note arose during this time; minor patching efforts were made at several points around the enclosure and block wall to fill small holes and gaps with intumescent filler. After 38 minutes there was a significant increase in the amount of smoke coming from the top of the specimen enclosure, and the central floor displacement had become

apparent. The test was conducted for 41 minutes until runaway failure rapidly occurred. The floor specimen was immediately unloaded and approximately 1 minute after this the specimen collapsed into the furnace, shown in Figure 3-36.

Figure 3-35: Test Specimen B after 34 minutes of furnace testing

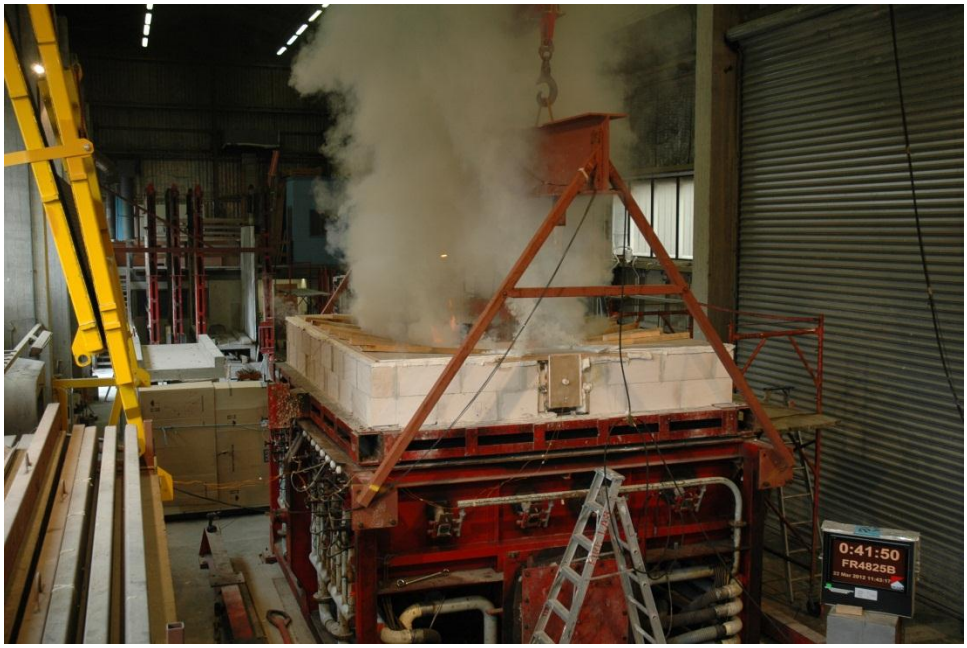

Figure 3-36: Test Specimen B at collapse (after unloading at 41 minutes)

An issue with fire testing of timber assemblies is that smaller timber specimens give much less time for removal from the furnace when compared with larger specimens due to the amount of residual strength and timber left after unloading. A larger floor may be tested at the same load level for a longer duration, hence the failure time is much easier to predict and when it is unloaded there is generally more time to save the specimen remains without suffering a complete collapse. This was the case for both series of testing for this research as the larger floor specimens were removed from the furnace intact.

3.7.3 Displacement

The results recorded by the two mid-span potentiometers are shown in Figure 3-37, and it can clearly be seen that they maintained good agreement throughout the test by both absolute value and trend followed. This indicates the top of the floor panel remained much more stable and level when compared with Test Specimen A.

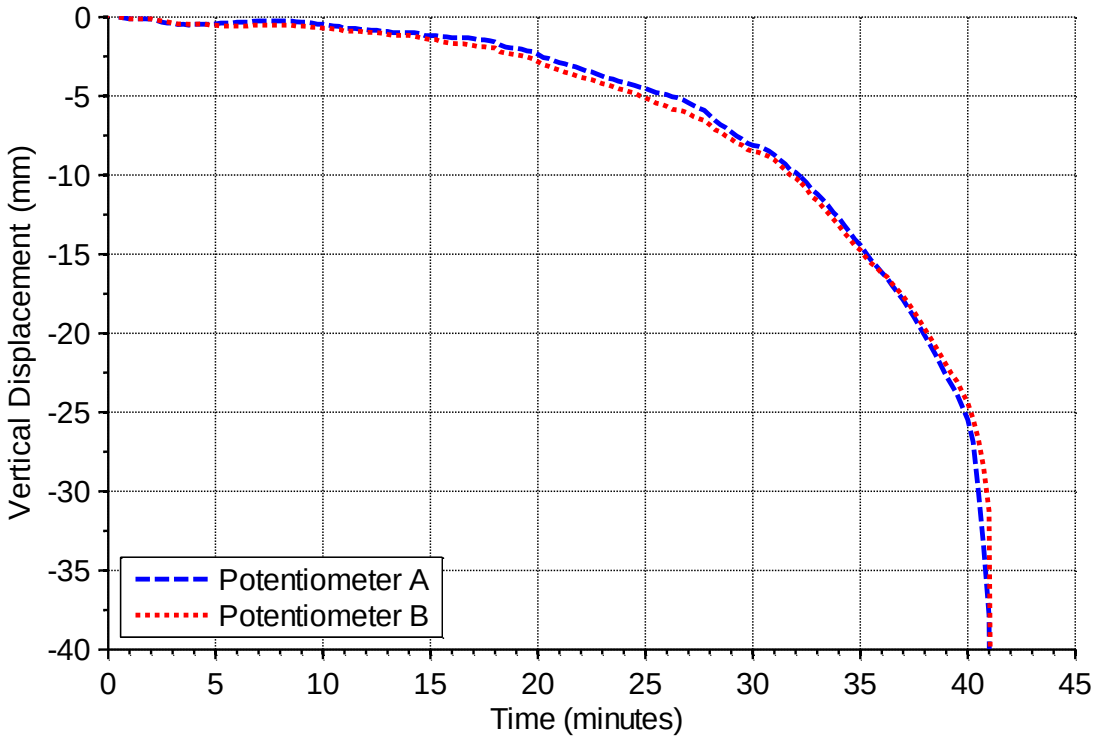

Figure 3-37: Mid-span vertical deflections of Test B

Very little vertical displacement was recorded for the first 10 minutes of testing, followed by linear downward deflecting trends to 4 mm at 18 minutes, then 8 mm at 30 minutes. At this stage the rate of deflection markedly increased dropping to 25 mm overall displacement by 40

minutes. Shortly after this point runaway failure occured, with deflections dropping off the testing scale at 41 minutes at which point the floor was unloaded.

3.7.4 Slab and Cavity Temperatures

Specimen B had five thermocouples installed in total, three on the top of the slab surface at the mid-span (concurrent with Specimen A), and two inside the box cavity inserted approximately 800 mm into the furnace along the span of the box beam. These results are presented in Figure 3-38.

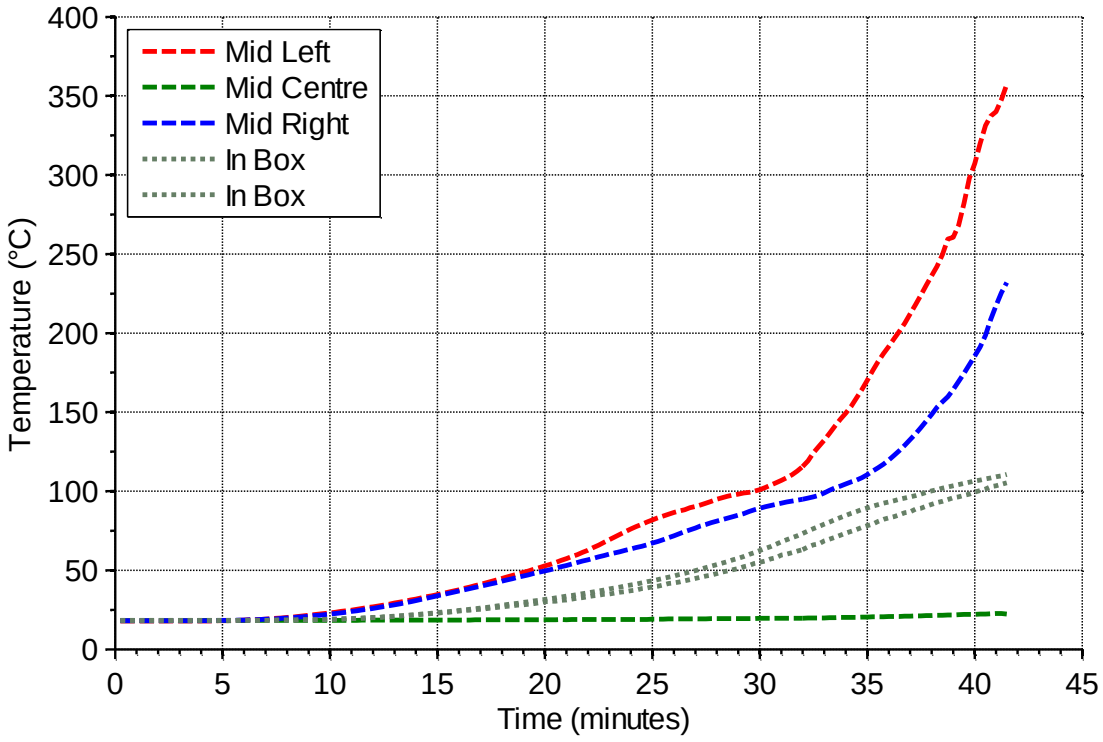

Figure 3-38: Slab surface and box cavity temperatures of Test B

The results show that the thermocouples on the top of the slab over the open section measure an increase in temperature to approximately 80 – 100°C by 30 minutes, similar to what was seen in Test A. The temperatures on the left side of the specimen also follow the same trend as seen in Figure 3-30 for Test A, being much higher at 30 minutes than for the right side of the furnace. This leads to the conclusion that the temperatures across the width of the furnace may not be uniform, with the left side of the furnace consistently showing a tendency to be hotter than on the right. This may also attribute to why the left side of Specimen A failed first during testing. An increase of 180°C was reached at approximately 37 minutes on one side of the floor

panel, hence left unprotected an insulation criterion would be exceeded at this time for this fire type. The average increase of 140°C was reached by both sides of the panel at 38 minutes. The temperatures measured over the top of the box beam showed virtually no increase for the duration of experimental testing. An almost complete burn through of the slab at 41 minutes was evident from data recorded on the left side, as the floor panel temperature reached 350°C at this time and was increasing rapidly.

Measurement of the cavity temperature is important for a multitude of reasons. The most prominent of these is that services or other structural elements may be installed in this cavity and serve a particular function; hence the temperature of the cavity and the behaviour of these elements must be known to provide adequate information for the fire performance of the floor assembly as a whole. For example a post-tensioned steel tendon may be installed in the cavity to aid in resisting loads imposed on the floors, and increases in temperature can result in losses of tensioning force which can have disastrous effects on these types of systems, as investigated by Spellman (2012).

The results obtained for the two thermocouples installed in the cavity show that it reached a temperature of approximately 100°C at 38 – 40 minutes after a steadily increasing trend from 15 minutes into testing, lower than for the top of the slab due to the thicker timber cover. For installations which are sensitive to these temperatures such as water piping or electrical cabling these temperatures may cause an issue during a fire event, however the system would likely be verging on structural collapse, so this becomes a moot issue. Note that these thermocouples were taped onto the surface of the inside of the timber beams, hence they were actually also directly measuring the temperature of the timber surface as opposed to the temperature of the air inside the cavity alone. It is therefore conservative to assume that the air inside the cavity is the same temperature as the timber surface; and in reality would likely be lower than this. For a cavity which had ventilation from the ends or from another protected source, these results shown are again a conservative estimate of cavity temperatures as fresh airflow would have a cooling effect inside the cavity. It was assumed that in the vast majority of constructed floors this would not be typical, and the floor ends would be sealed or blocked off in some manner.

3.7.5 Char Damage

During the removal of the loading rig the specimen collapsed into the furnace, approximately 2 minutes after termination of the testing and the furnace was shut off. The moment of failure is shown in Figure 3-39 on the left, and the failed specimen in the furnace on the right.

Figure 3-39: Failure of Test Specimen B

The collapse meant that no measurements of char depth could be made for the specimen as the burning remains could not be retrieved from the furnace interior. From the results inferred from the thermocouple and displacement readings, it was clear that at approximately 37 minutes there was an insulation failure in the slab, and simultaneously the rate of displacement began to increase to runaway failure at 41 minutes. Photos taken at 15 minutes into Test B through the portholes in the furnace show the char development.

Figure 3-40: Inside the furnace during Test B at 15 minutes (box beam on left, underside of slab on right)

From the figure it can be seen that both the underside of the box beam and slab exhibited char cracking and shrinkage, however the vertical sides of the box beam showed less cracking and discolouration earlier in the testing than the horizontal surfaces. This may have been due to the orientation of the timber faces resulting in slightly less charring for the initial stages of the testing due to some shadowing from the fire; however it was not apparent from 20 minutes onwards.

3.8 Test Specimen C Results

Specimen C was the larger variant of the joist design floors, and was tested on 23 August 2012. It was tested after Specimen D, however for continuity has been presented in the same order as the first series of tests. Specimen C was originally designed to resist approximately 90 minutes of fire exposure.

3.8.1 Furnace Temperature

The average recorded furnace temperature of Test C, compared with the ISO 834 standard fire curve and tolerances are shown in Figure 3-41.

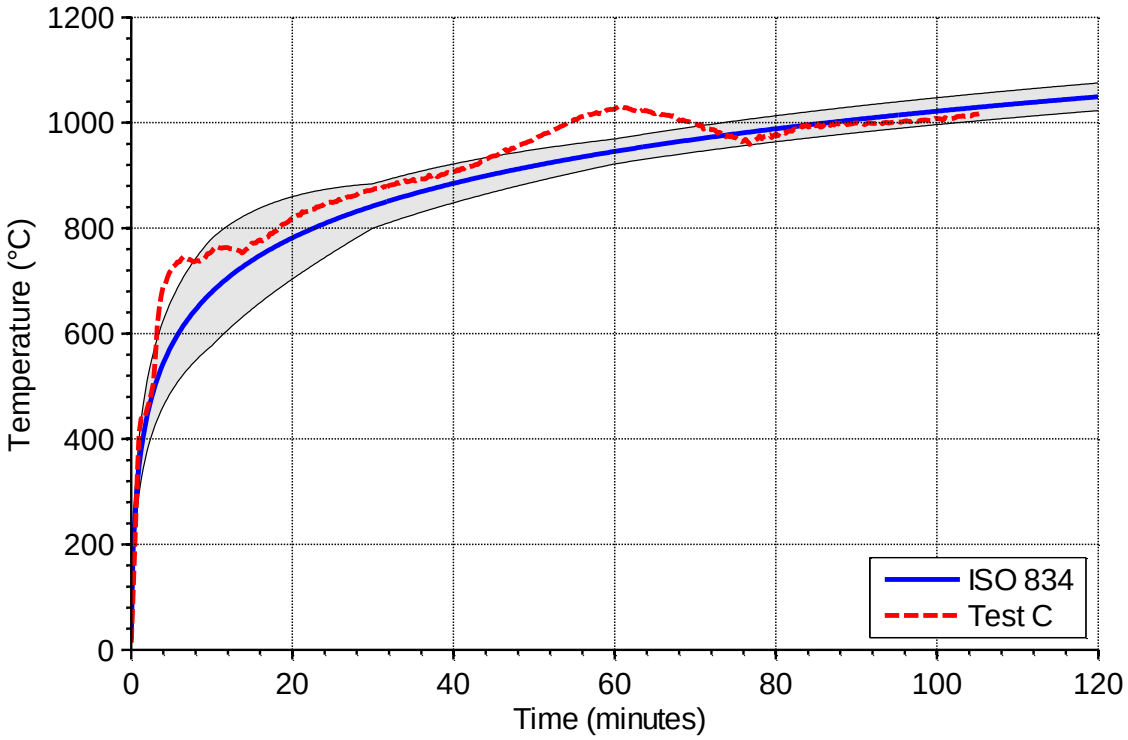

Figure 3-41: Furnace temperature for Test C

It can be seen from the plot that the actual fire curve measured in the test did not ideally follow the standard, and at two points it deviated above the tolerances. However the deviations were on the hotter conservative side of the standard curve, ensuring any assertions made about the assembly in comparison to other standard test results are still valid.

3.8.2 Observations

Due to the utilisation of concrete lids to enclose the furnace, only a small amount of hot smoky gases escaped from the enclosure for the duration of the test. As will be discussed in Section 3.8.3, the displacement of the specimen throughout the test was relatively low hence not notably visible from the outside of the furnace. Figure 3-42 shows Test C at 60 minutes, approximately halfway through the duration of the experiment.

Figure 3-42: Test Specimen C at 60 minutes

As the test showed a stable loadbearing resistance at 90 minutes with only small deflections, the experiment was left to run until a discernible level of failure could be seen in the displacement trend of the floor. Care was taken to ensure that the collapse of Test B was not repeated with Tests C and D, as an evaluation of the charred remains for these floors was desired. The final duration of testing was 105 minutes when the test was terminated and the furnace shut off.

The charring of the central beam is shown in Figure 3-43 at 40 minutes looking through a porthole in the furnace.

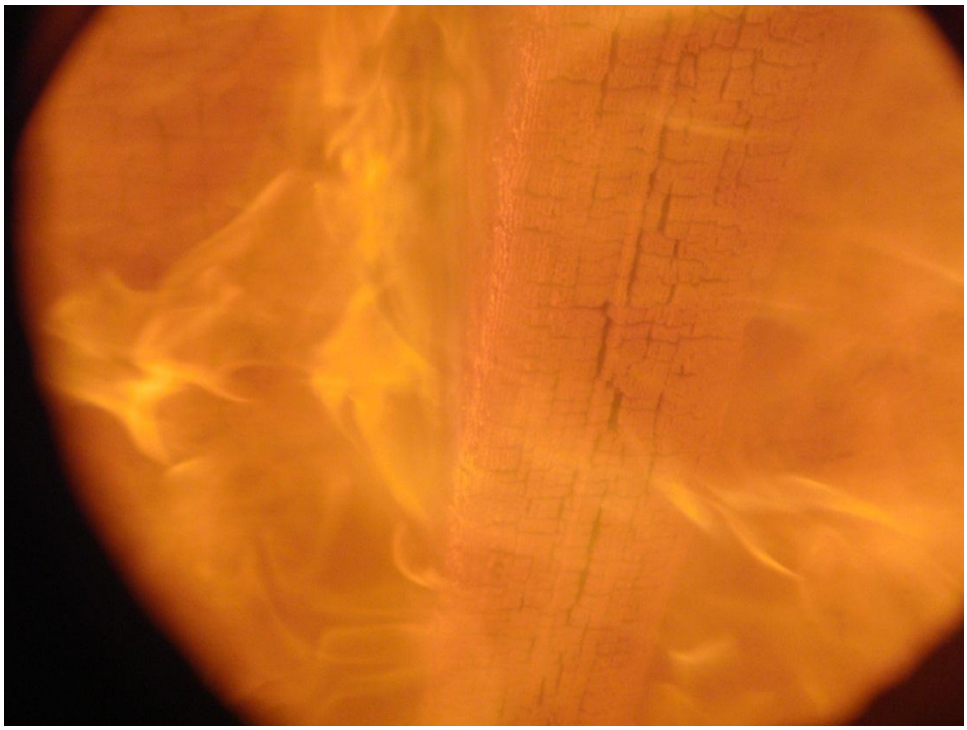

Figure 3-43: Inside the furnace during Test C at 40 minutes

After 60 minutes the beams began to seep an extremely viscous looking substance which was likely a combination of decomposed adhesive and cellulosic sap. As no physically distinguishable structural degradation occurred out of the ordinary at this stage, no adverse effects on the performance of the floor could be quantified from this phenomenon. The viscosity of the fluid was such that it was waving and moving with the flames in the furnace, occasionally dripping off the beam at points.

Figure 3-44 shows the same portion of beam at 90 minutes, where the brightly glowing fluid can be seen hanging off portions of the beam. The gap at the connection of the double beams is easily distinguishable in the figure; however no major gap opening took place throughout the testing. After approximately 80 minutes large chunks of char had dropped off in places along the bottom chord of the beams, however the underside of the slab suffered no char drop off. This can also be seen in the figure.

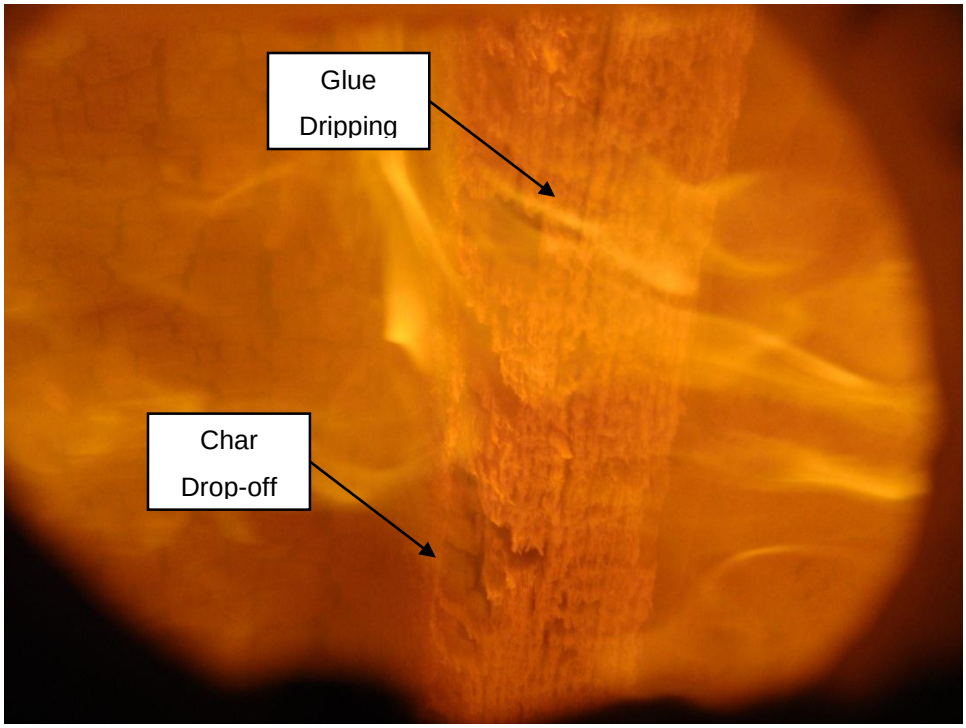

Figure 3-44: Inside the furnace during Test C at 90 minutes

When Specimen C was removed from the furnace the underside of the floor was well preserved (as seen in the left of Figure 3-45), and it took approximately 8 minutes from the furnace shut off to unload the floor, remove the loading rig and douse the underside of the floor with water to extinguish the fire. The specimen is shown after being dismantled placed on the ground in the right of Figure 3-45.

Figure 3-45: Specimen C immediately after extinguishment (left) and upside down on the ground (right)

3.8.3 Displacement

The mid-span potentiometer readouts for Test C are shown in Figure 3-46. The readings from both potentiometers followed a very similar trend, differing by less than 1 mm throughout the testing.

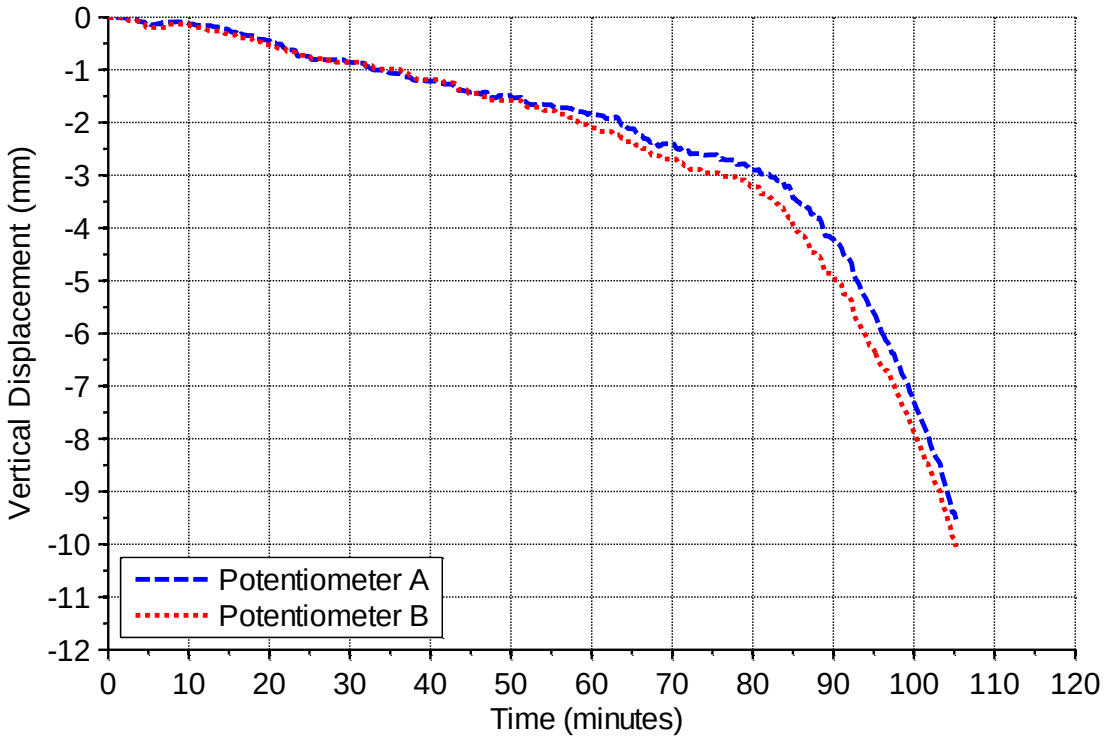

Figure 3-46: Mid-span vertical deflections of Test C

Due to the large redundancy in the floors which is inherent when designing unprotected timber members for longer durations that require thick sections of timber, the displacement response of the specimen was very stiff for the majority of the test. Specimen C had a relatively bi-linear displacement response, with the floor vertically deflecting 3.5 mm for 85 minutes of fire testing at a relatively constant rate. Following this stage the rate of displacement increases, with the floor deflecting to approximately 10 mm by 105 minutes. The test was terminated at this point as the residual section of the beams was previously calculated to be very small and imminent runaway failure was assumed to occur within the next 15 minutes. As seen from the plot, the trend suggests that this would be the case and an estimate of failure time for this specimen was approximately 120 – 125 minutes.

3.8.4 Slab Temperatures

The thermocouple layout for Specimen C is shown in Figure 3-10, with 7 thermocouples used in total. They were located in three rows spread across the slab surface at quarter points along the span, two per row over the open slab sections and one central thermocouple placed in the centre of the floor at the mid-span. The results from these for Test C are shown in Figure 3-47.

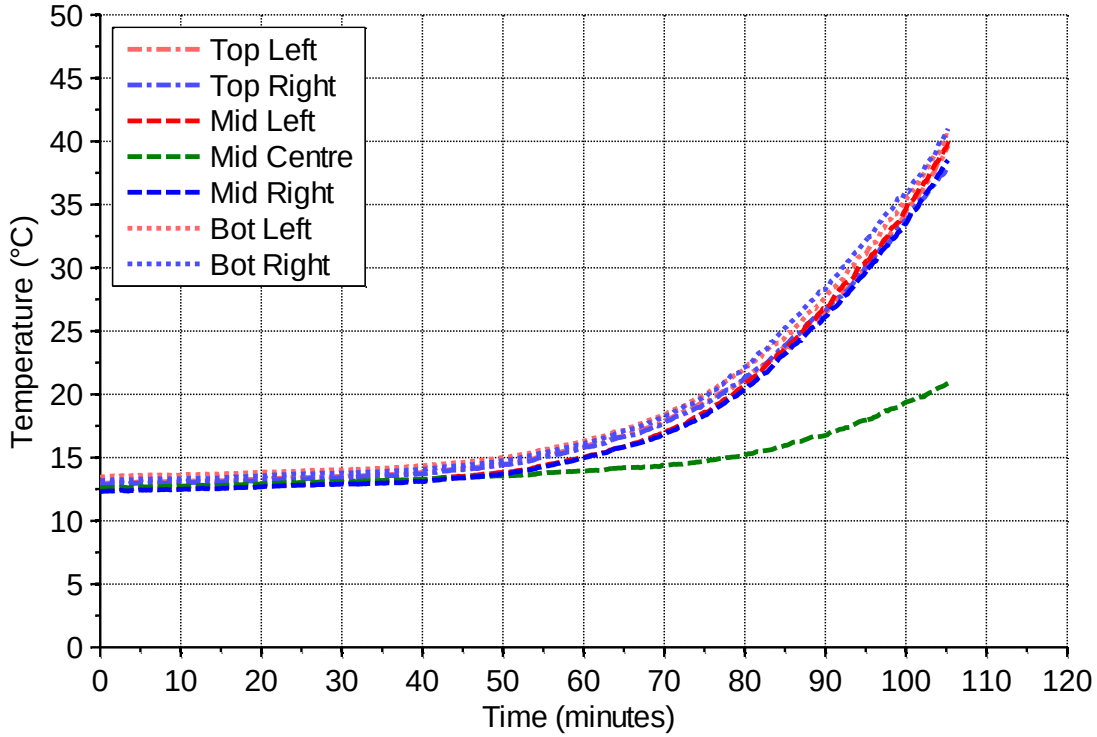

Figure 3-47: Slab surface temperatures of Test C

The results for the top of slab temperatures over the open sections of floor were extremely consistent. They showed a general increasing trend from near environmental ambient temperature at approximately 40 minutes to 40°C at the termination of the test, a total increase of 27°C. This was not unexpected as the 108 mm thick timber slab was designed to be relatively robust for these longer duration tests and suffer no insulation failures within two hours.

The central thermocouple was placed as a control to ensure the thermocouples were providing appropriate data. From its readout in the figure the temperature over the central beams had an increase of approximately 7°C due to the protection of the beam couple directly below it, which was expected due to the shielding provided by the beams.

3.8.5 Char Damage

Specimen C was tested in the furnace for 105 minutes, and then burned in the open air for approximately 8 minutes before extinguishment. This resulted in 113 minutes of total charring time, and was evaluated in a similar fashion to Specimen A to measure the char depth of the burnt specimen. This is shown for the mid-span of the floor in Figure 3-48.

Figure 3-48: Residual section at the mid-span of Specimen C following furnace testing

It can be seen from the charring pattern that the outer edges of the specimen did not char at the same rate as the inner portions of the specimen, most likely due to re-radiation from the inner beam increasing the rate of charring of the inner portions of the floor. The leftmost joist also shows slight cupping towards the inside of the specimen, indicating differential drying and a difference in charring damage, reinforcing this assertion. The measured depths of char on each beam were similar, ranging from 63 – 75 mm on the sides of each beam (bottom to top), and 90 mm on the bottom chords. This left an approximate residual beam section of 360 mm deep x 42 mm wide, and is shown in Figure 3-48 after the removal of loose charcoal (not including the unburned slab thickness above of 108 mm). The char depth on the underside of the timber slab was found to be 73 – 76 mm on average in the open region, leaving a residual thickness of 32 mm at the thinnest point under the thermocouples.

3.9 Test Specimen D Results

Specimen D, the larger variant of the composite box floor, was tested on 21 August 2012. As with Specimen C it was designed on an original 8 metre span to resist a minimum of 90 minutes unprotected in a standard fire.

3.9.1 Furnace Temperature

The average recorded furnace temperature of Test D, compared with the ISO 834 standard fire curve and its tolerances are shown in Figure 3-49.

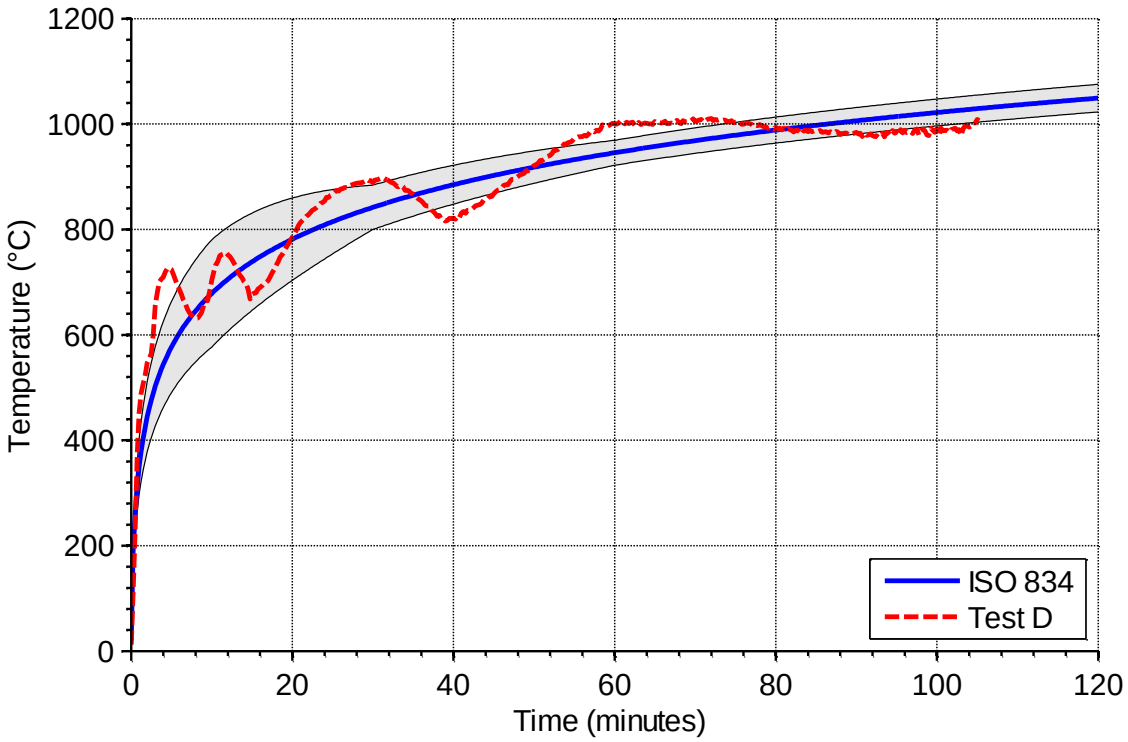

Figure 3-49: Furnace temperature for Test D

The actual fire curve measured in Test D deviated the most for any of the experiments, mainly within the tolerances but exceeding the maximum tolerances at two points in similar places to that shown for Test C, and going outside the minimum tolerance at one point during the middle stages of testing. Considering the trend in the figure and the area under the fire curve when compared with the standard, the actual fire curve used was still a reasonable approximation to the standard with respect to the duration of the test.

3.9.2 Observations

As with Test C, there was only a small amount of visible smoke escaping from the enclosure for the duration of the test. The measured displacements were also similar, which was testament to the accuracy of the design loadings calculated for the floors. The same regime was followed during testing after the 90 minute mark, resulting in the test being terminated at 105 minutes (the same time as Test C) and aiding in comparisons between the two specimens.

At approximately 70 minutes there was burn through of some of the sealing around the ends of the box beams. As seen in Figure 3-49 this was quickly attended to with intumescent sealant and kaowool stuffing. This was the only incidence of enclosure breach throughout Test D.

Figure 3-50: Burn through of beam ends during Test D

The same glue-dripping behaviour inside the furnace witnessed during Test C was seen again for Test D, this time to a greater extent as the bottom chord of the box beam was wider than the bottom of the joists.

At 50 minutes the bottom chord of the right box beam had suffered approximately 40 – 45 mm of char damage as a conservative calculation (0.8 – 0.9 mm/min), and is shown in Figure 3-51.

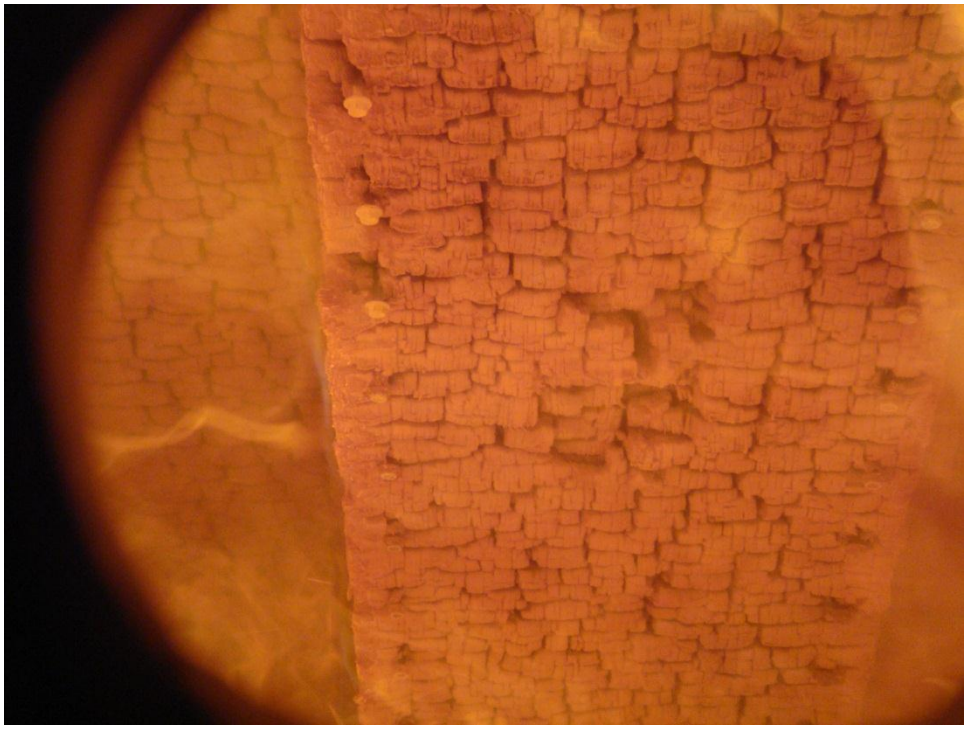

Figure 3-51: Inside the furnace during Test D at 50 minutes

Figure 3-52 shows the same floor section at 75 minutes into furnace testing.

Figure 3-52: Inside the furnace during Test D at 75 minutes

At 90 minutes the underside of the box beam had significantly degraded and the glue dripping behaviour is clearly shown in Figure 3-53. In addition to this, large pieces of char began to drop off from this point until the end of the test.

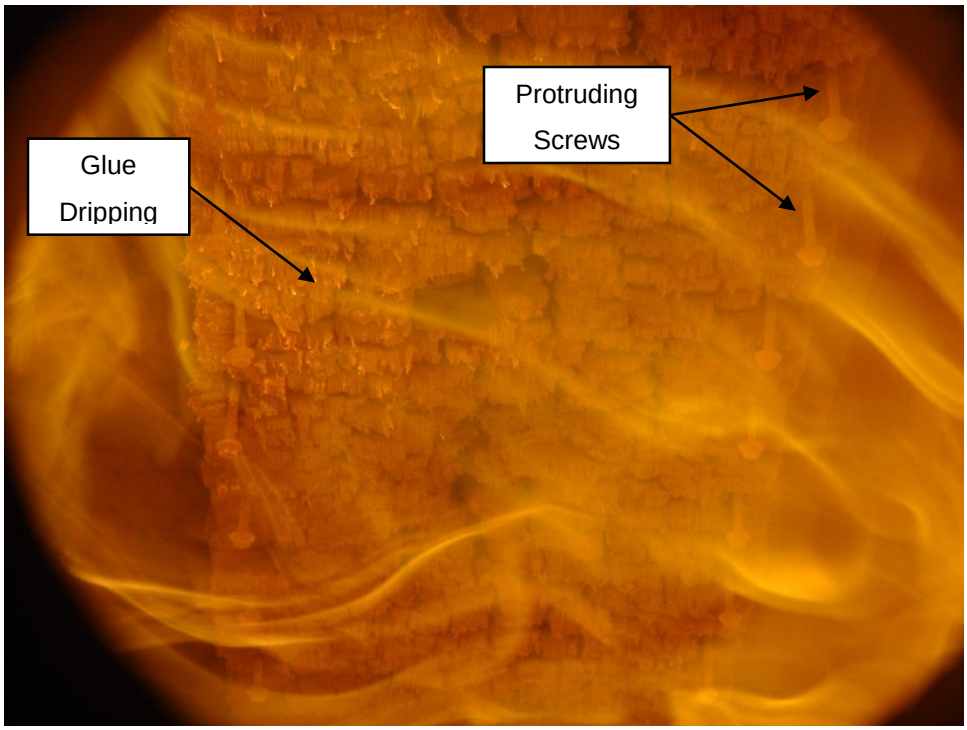

Figure 3-53: Inside the furnace during Test D at 90 minutes

The extent of the char shrinkage is clear from 50 to 90 minutes as seen in the figures by using the protruding screws as a benchmark. The screws were countersunk into the face of each member; hence the original position of the timber was level with the extreme edge of the screws shown in the figures.

When Specimen D was removed from the furnace the underside of the floor was well preserved as with its joist counterpart, and the screws which were used along the box sections in the fabrication process sat proud of the char as they had not moved from their original location but the timber had shrank and burned away. This is shown in Figure 3-54 as Specimen D was lifted from the furnace (after wetting down). After cooling the underside of the specimen down, the screws could be individually plucked from the underside of the beams. The screws had lost all purchase on the timber and were resting in the char, however there was no delamination during the testing; hence the glued connections were assumed to transfer the entire load throughout the specimen without the need for screws.

Figure 3-54: Specimen D after furnace testing

The inside of the cavities suffered discolouration and in both box beams there were small holes near the mid-span, shown in Figure 3-55. These has let small amounts of hot smoky gases into the cavities, however had not burned around their opening significantly, indicating that they had only burned through in the last minutes of the testing.

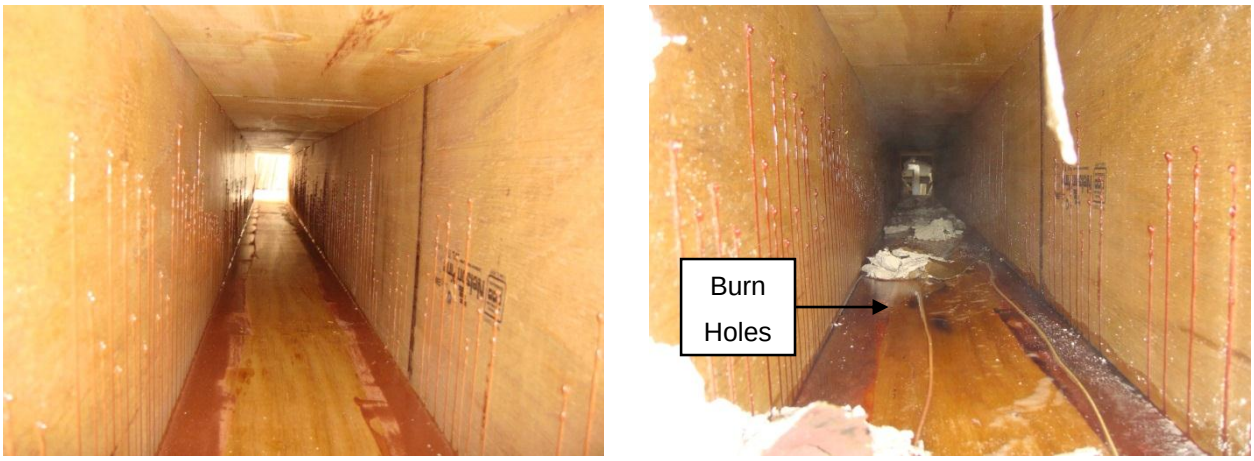

Figure 3-55: Inside of Specimen D box cavity before testing (left) and after testing (right)

3.9.3 Displacement

The mid-span potentiometer readouts for Test D are shown in Figure 3-56. The readings from both potentiometers followed an extremely similar trend, differing by less than 0.2 mm throughout the testing.

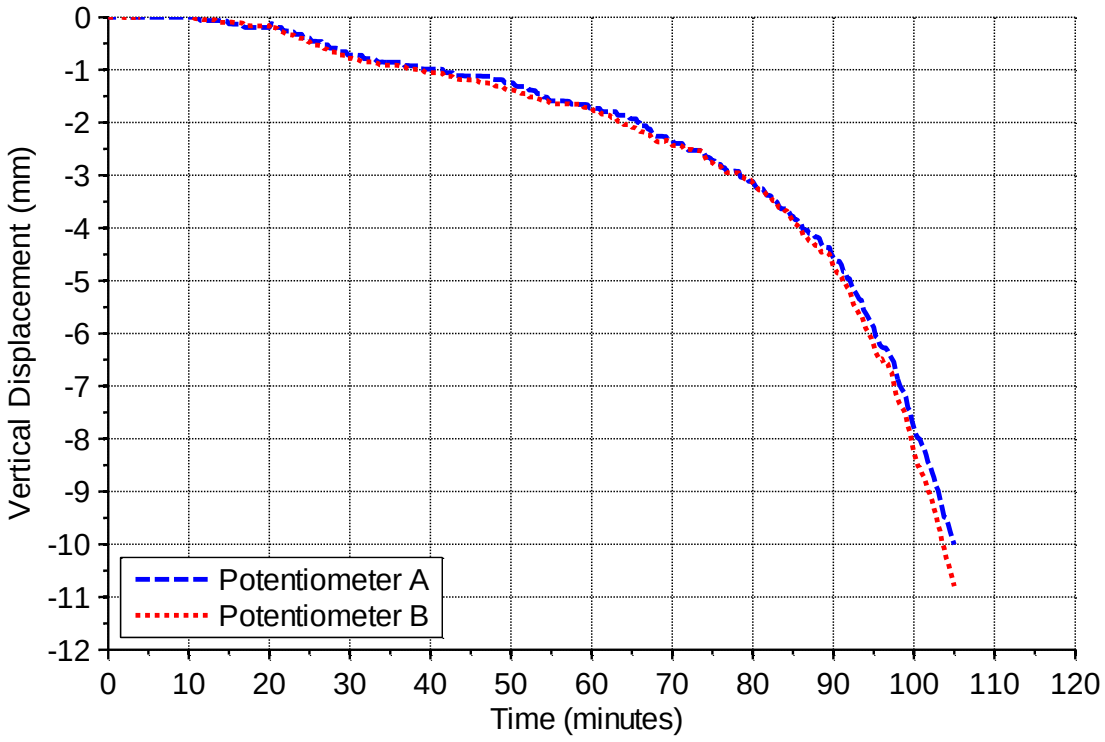

Figure 3-56: Mid-span vertical deflections of Test D

The bi-linear response seen during Test C is less visible in Test D, with a more tri-linear trend occurring from 0 – 20 minutes, 20 – 90 minutes and 90 – 105 minutes. The total displacement of the floor for these three phases was 0.2, 4.5 and over 10 mm, respectively. Similarly to the joist floor counterpart, the box beam floor was following a much steeper decline for vertical deflections after 90 minutes, heading towards likely runaway failure at approximately 120 – 125 minutes.

3.9.4 Slab and Cavity Temperatures

Specimen D had nine thermocouples installed in total, five on the top of the slab surface spaced directly down the centreline of the floor, and two inside each box beam cavity plunged approximately 800 mm into the furnace along the span of the box beam. These temperature results are presented in Figure 3-57 for these thermocouples.

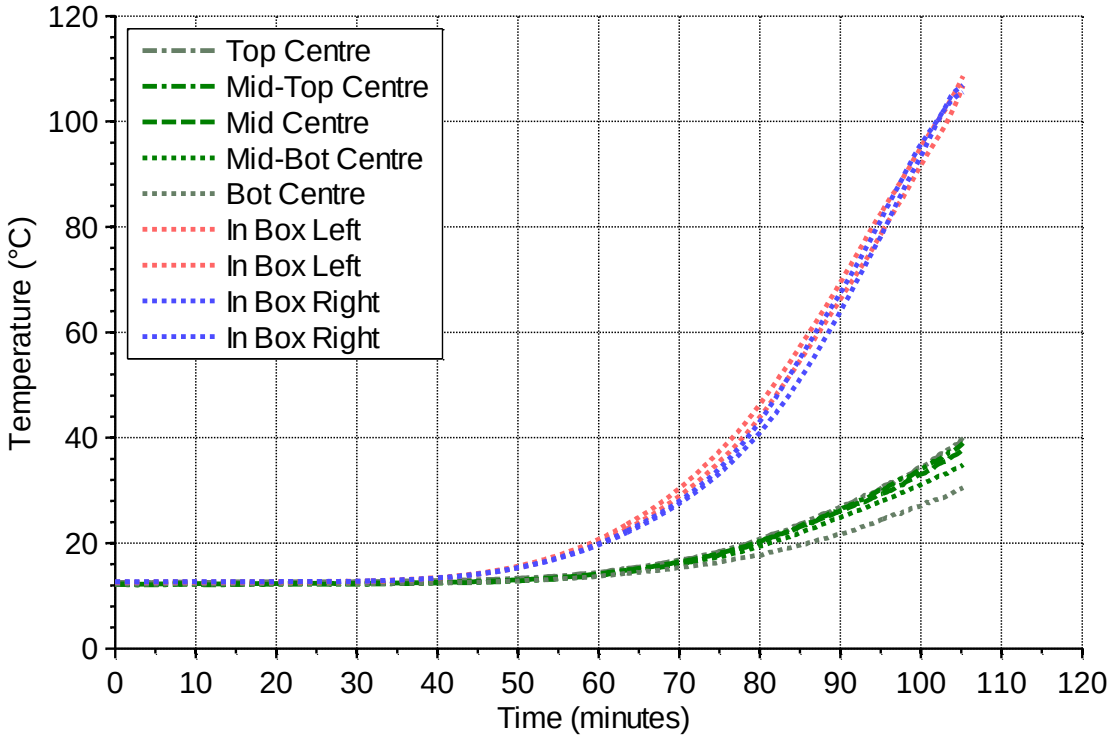

Figure 3-57: Slab surface and box cavity temperatures of Test D

The results for the temperatures of the top slab were very consistent with those from Test C with the slab surface reaching approximately 40°C, nowhere near the insulation failure criterion.

The temperatures measured in the box cavities were extremely consistent, measuring a notable increase from ambient temperature at 45 minutes to 80 minutes of approximately 42 – 45°C, and then increasing at a linear rate to 110°C at 105 minutes. As with Test B, the time at which the cavity temperatures reach unfavourable conditions for services and cabling is negated by the fact that the floor has almost reached structural failure by that time during a fire event.

3.9.5 Char Damage

Specimen D was tested in the furnace for 105 minutes, and then burned in the open air for approximately 8 minutes before extinguishment (similar to Specimen C). The floor was cut at the mid-span to determine the char depths as shown in Figure 3-58. Cupping effects on the separate members of the box beams were pronounced as these were subjected to one-sided exposure during the testing. As previously discussed there was very little fire damage to the inside of the box cavities, however small holes had begun to char around by the time water was doused inside the cavities.

Figure 3-58: Residual section of Specimen D after furnace testing, extinguishment and char removal

Once again the outer edges of the specimen did not char at the same rate as the inner portions of the specimen. The measured depths of char on both of the box beams were similar, ranging from 68 – 75 mm on the sides of each beam, and 75 mm on the bottom chords. This left a residual box thickness of approximately 18 mm around the section. The char depth on the underside of the timber slab was found to be 73 – 76 mm on average in the open region between the box beams, leaving a residual thickness of 32 mm at the thinnest point under the thermocouples, identical to the findings of Test C.

3.10 Test Comparisons

In order to better understand how simple joist and box beam systems perform, a comparison between these floor tests is made in the following section. This is divided into the respective designs for endurance ratings, hence Specimens A and B are compared for a lighter and lower fire resistance floor system, while Specimens C and D are compared for a heavier and higher resistance floor system. Tabulated values for the maximum slab and cavity temperatures, and the char depth across all floors are also presented.

3.10.1 Test A and B Displacements

The performance of the composite joist and box floor tests designed for approximately 30 minutes fire resistance are shown in Figure 3-59. The displacements of the potentiometers have been averaged for each test.

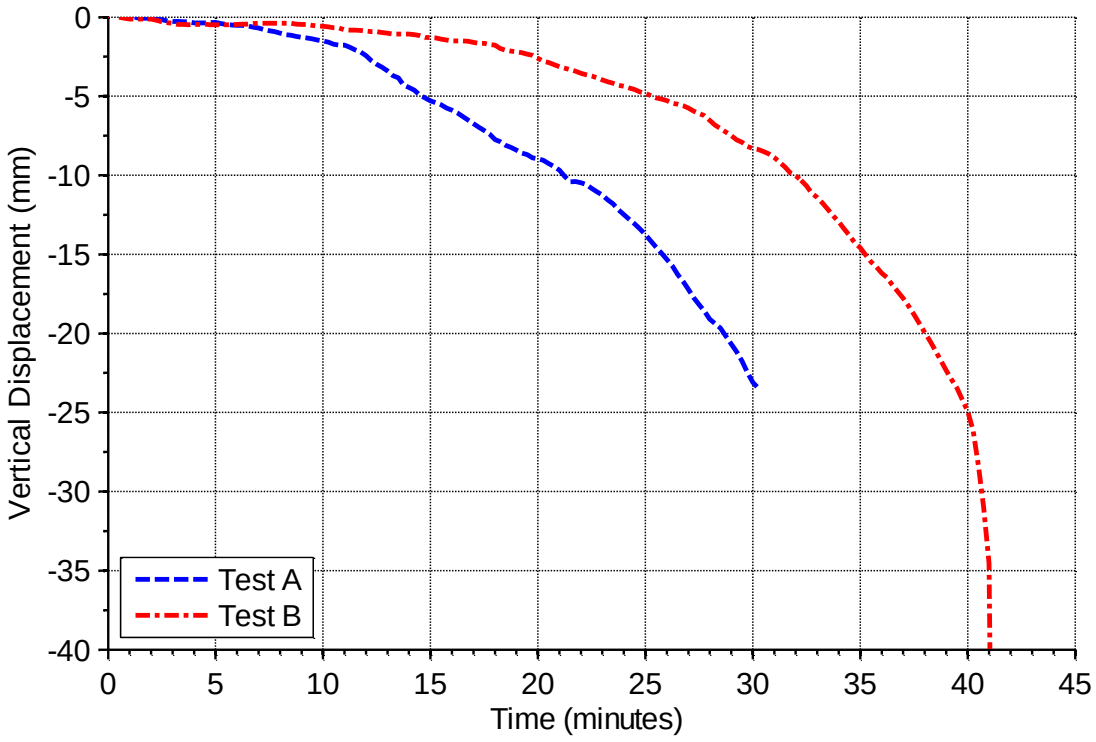

Figure 3-59: Comparison of averaged Test A and B mid-span deflections

On comparison of the two floors the deflection response of the box beam (which was slightly shallower than the joist floor but incorporated a bottom flange) had a much stiffer response for the duration of fire testing. This was expected due to the differing floor designs, with a much larger proportion of timber and loadbearing capacity in the composite box floor. Regarding the trend of the composite joist floor an estimated failure time would be in the range of 33 – 37 minutes, while the composite box floor failed at 41 minutes. Both floor types were shown to withstand a minimum of 30 minutes of standard fire exposure.

3.10.2 Test C and D Displacements

In contrast to the smaller 30 minute floors, the larger 90 minute floors were designed to be almost equivalent in terms of loadbearing capability after the results of the first set of testing.

This resulted in very similar levels of fire endurance and displacement behaviour, as seen in Figure 3-60 where the average displacements for each floor are plotted.

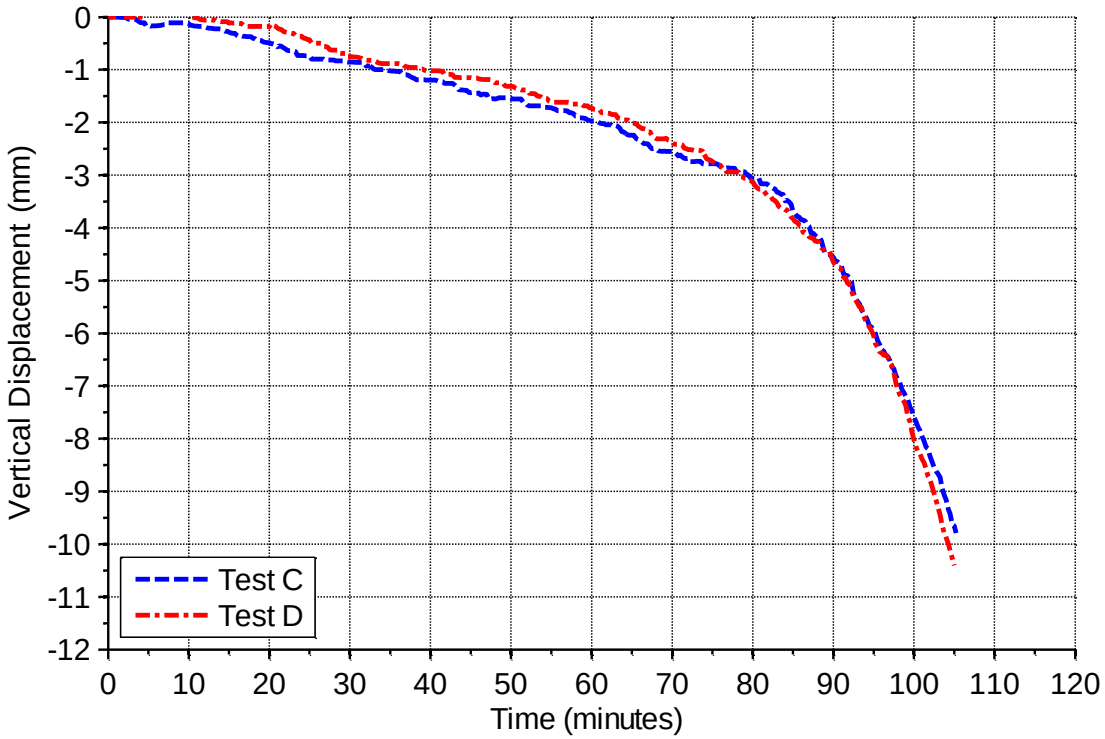

Figure 3-60: Comparison of averaged Test C and D mid-span deflections

The displacement response of both floors followed a distinct bi-linear trend, with subtle differences between the results. Figure 3-60 clearly shows the reduction in stiffness and strength of the floors over time due to the impact of the fire. The change in rate of deflection occurs at such a time when approximately two thirds of the original sections have charred away (about 60 mm of each exposed face), and the residual section has become so small that the stresses become concentrated in the remaining timber. This is because as the stresses are redistributed through the section during heating and charring, a limit is reached where the section is no longer of an adequate size to properly resist the applied loads and stress concentrations occur.

For the floors tested, as the fire damage is more localised around the bottom areas of the floor sections to the three sided exposure, the tension zone is the most affected region and structural failure occurs in this region. As the timber burns away and the neutral axis of the floor specimen begins to rise upwards, the thinning beam section has localised increases in stresses in the

tension zone and a brittle failure will occur once the stresses are too great for the section to resist. This behaviour was seen in Test B, where the floor specimen failed at the point of maximum moment in the span (between the loading plates) and the bottom chord of the beam failed in combined tension/bending, as seen in Figure 3-39.

The composite joist floor had higher deflections initially, and then followed a slightly lower rate of deflection during the latter stages of testing when compared to the composite box floor. However the actual measured differences in displacement were so low for much of the test that no real conclusions can be drawn from differences in the results, as they will be within the experimental error of the testing apparatus, and could also be attributed to the difference in actual fire curve followed in each test. Both floor types were shown to withstand a minimum of 105 minutes of standard fire exposure, with an estimated failure time for both floors to be approximately 120 – 125 minutes.

3.10.3 Slab and Cavity Temperatures

The maximum point and average surface temperatures are presented in Table 3-5, along with the maximum cavity temperatures reached for the composite box floor tests. These are reported for the time at which the furnace was shut off.

Table 3-5: Temperature comparisons for Tests A – D

Specimen	Furnace Time (min)	Temperature (°C)		
		Slab Surface Maximum	Slab Surface Average	Box Cavity Maximum
A	30	95	85	-
B	41	350	290	110
C	105	42	38	-
D	105	40	36	110

On comparison of the slab insulation failures for Tests A and B, the 36 mm thick panel failed to provide an insulating function at approximately 37 minutes. The maximum temperatures recorded over the 108 mm slabs for Tests C and D were very low, indicating that an insulation failure would not occur before the structural failure of the floors.

Comparing cavity temperatures, both box floors showed that by the end of testing the maximum cavity temperature was approximately 110°C. With regards to a steel tendon or other structural element, this increase may not be problematic in causing major losses in strength or stiffness. However for any temperature sensitive services and installations further protection measures may be warranted for installation in the cavities (such as a thermal blanket wrap or internal partitioning).

3.10.4 Char Damage

The average charring rates of each major surface of the floor specimens have been calculated in Table 3-6 with regards to the total burning duration of each specimen.

Table 3-6: Calculated charring rates for Tests A – D

Specimen	Burning Duration (min)	Charring Rate (mm/min)			
		Beam Sides	Beam Bottom	Slab	Average
A	36	0.69	0.83	0.69	0.74
B	43	-	-	-	-
C	113	0.66	0.86	0.84	0.79
D	113	0.68	0.71	0.84	0.74

At much longer durations the charring rates recorded become less variable, thus can be more reliably predicted. This is seen from the temperature results recorded through the slabs in Section 3.10.3, and from the table above where the charring rates for the 90 minute floors closely match. As Test B was conducted until destruction, no viable charring results could be obtained. The average values plotted in the fair right column are the averages of the three rates shown for beam sides, bottom and the slabs. This is presented to give an approximate estimate of the overall charring rate of each respective floor, and the charring rates for the major surface groups of the floors ranged from 0.66 – 0.86 mm/min across all specimens.

Charring rates for the vertical faces of the floors (sides of the beams) were all similar, ranging between 0.66 – 0.69 mm/min. For the bottom face of the box beams in Test D, the charring rate was similar being 0.71 mm/min.

Tests A and C had much higher charring rates on the bottom of the joists due to the corner rounding effect where in the latter stages of burning the radii of charring on each corner of the beam intersect, compounding the vertical rate of burning up the beam. This was observed in previous research on timber-concrete composite floors tested at BRANZ (O'Neill, 2009).

The charring rate of the smaller 36 mm thick timber slab was 0.69 mm/min in Test A, while the larger 108 mm thick slab charred at 0.84 mm/min for Tests C and D. This higher rate can be attributed to the longer duration of burning where the furnace temperatures are comparably higher at this time, being about 850°C at 30 minutes to reaching temperatures over 1000°C after 80 minutes duration of the standard fire.

3.11 Conclusions

Four furnace tests were conducted on unprotected timber floor systems in the full-scale furnace at the BRANZ facilities in New Zealand. The one-way strip floors had pinned support conditions and were exposed to the ISO 834 standard fire for varying durations of 30 – 105 minutes. The floors were loaded under standard office loading conditions of 3.0kPa live and 1.0kPa superimposed dead loading. From the four furnace tests it can be concluded that:

- The smaller floor designs based on 7 metre spans resisted 30 minutes of standard fire exposure under constant load without collapse.
- The larger floor designs based on 8 metre spans resisted 105 minutes of standard fire exposure under constant load without collapse.
- The insulation criterion for the 36 mm thick LVL slabs was exceeded at approximately 37 minutes of exposure, while the larger 108 mm slabs did not suffer any insulation failures up to 105 minutes of fire exposure.
- The charring rates of the timber members were found to range from 0.66 – 0.86 mm/min across all specimens.
- When designed to resist a similar load level both the composite joist and composite box floor types had a similar response to the fire loads, however the joist floors exhibited increased upward burning through the members in the latter stages of testing which may contribute to an earlier failure for smaller floor geometries.

4 THERMAL FINITE ELEMENT MODELLING

4.1 Introduction

Advanced numerical modelling is required when a problem is too complex to be solved by hand, and a greater understanding is required of the underlying principles and mechanisms involved in the analysis of the problem. This is usually preferable to the alternative, as experimental testing can be uneconomical, time and labour intensive, and only one particular set of circumstances can be investigated in each test. Furthermore when considering the modelling of floors, a numerical modelling approach allows for vast amounts of data to be calculated for many different types of floor geometry and loading conditions in an economical and efficient manner. This enables the user to obtain results directly proportional to the quality and quantity of the input into the software, and at a specified level of detail.

There are many advantages to numerical modelling, however it is of paramount importance that each step is clearly defined and understood in the process to avoid making fundamental errors in the analysis. Numerical models are essentially tools to aid in computing massive amounts of data simultaneously; however the inputs and outputs of the software and how they are interpreted must be considered under sound engineering judgement and principles. It is important that the analytical method used is not pushed beyond its limits of applicability (Cook, 1995).

In order to fully characterise and understand the heated behaviour of various elements and assemblies, thermal modelling can be used to analyse the problem and provide specified output to a level of detail defined by the user. As is common with any advanced numerical modelling, assumptions are of paramount importance to simplify a problem into a more manageable and easily defined form. When considering thermal modelling one of the major factors to which has a huge influence on the output obtained is the definition of the heating conditions. This can vary from simple conduction problems such as the surface of an element being exposed to a temperature gradient, to complex problems involving advanced fluid dynamics such as a growing fire in an open area interacting with many other objects and assemblies in the problem space.

With regards to this research, a sequentially coupled thermo-stress analysis is conducted to determine the effects of a fire on floor assemblies under load. Firstly a thermal analysis is performed to determine the temperature profile of the floor assemblies for the duration of

modelling, and then a stress analysis is performed using the temperature profile as an input into the structural model. This procedure is used as the stress profile of a timber member is influenced by its temperature profile, but the converse is not true, in other words the temperature is not affected by mechanical stresses and can be computed as a separate initial step.

The definition of the heating conditions is relatively simple in this case as loadbearing structural members are simulated as being exposed to a fire with the resulting temperature profiles of the members calculated. A standard fire curve is applied to the outer surfaces of the exposed elements and temperatures at any depth in the cross-section are obtained by solving a simple conduction problem. This type of thermal modelling can be undertaken in one, two or three dimensions depending on the element and geometry under scrutiny. With appropriately defined inputs almost any complex geometry and thermal exposure can be simulated, with the results exported to a structural model to determine the failure characteristics of the members. These results can then be compared with actual experimental test data to validate the modelling and any assumptions made.

4.2 ABAQUS

The general purpose finite element software ABAQUS 6.10 (2010) was used for the numerical simulations in this research. It is a suite of engineering simulation programmes based on the finite element method which is used to solve problems ranging from simple linear analyses to extremely complex nonlinear simulations. ABAQUS has been developed to solve an array of general purpose finite element tasks such as structural analyses, heat transfer, mass diffusion, coupled thermal-electrical analyses, acoustics, soil mechanics, piezoelectric analysis, and fluid dynamics. ABAQUS contains a large element archive which allows for modelling extremely complex geometries. It has an extensive list of material models that can simulate the behaviour of most typical engineering materials including metals, rubber, polymers, composites, reinforced concrete, crushable and resilient foams, and geotechnical materials such as soils and rock (ABAQUS, 2010).

ABAQUS/Standard is a general purpose finite element program which is used to solve a set of equations implicitly at specified time increments. ABAQUS/Explicit has the capability to solve dynamic tasks explicitly using a direct integration procedure, pursuing a desired solution through time without solving a coupled system of equations at each time increment. ABAQUS has both the traditional user input file method of building and running simulations, and also a graphic user

interface (CAE) which automates many of these processes and aids in the visualisation of a problem. In terms of heat transfer problems, ABAQUS can perform uncoupled heat transfer analyses, sequentially coupled thermal-stress analyses, fully coupled thermal-stress analyses and adiabatic analyses. The user can specify structural and thermal loading conditions and user specified regimes, all physical problem geometry including mesh sizes, element and material properties, boundary conditions and the solution method. The material properties input is both versatile and vast with a huge array of material types available, and in the CAE there are ready made functions to account for latent heat and many other thermal parameters paramount to both thermal and structural modelling. The range of inputs and outputs is huge; hence care must be taken in understanding how the inputs used will influence the results output from the software (ABAQUS, 2010).

4.3 Objectives

The primary objective of the thermal modelling was to approximate the thermal impact of a fire on unprotected timber members. This involved firstly investigating the given thermal properties for timber from the literature and comparing with experimental data in order to determine the acceptable range of effective properties to use in ABAQUS to appropriately model one-dimensional heat transfer through timber sections.

A secondary objective of this modelling was to compare what was observed in the experimental testing in terms of charred sections with two-dimensional thermal modelling of the experimental floors to verify the accuracy of the modelling, and confirm any observations noted during the experimental testing.

For greater confidence in the results obtained, three separate numerical software suites have been run in collaboration during this research focussing on defining acceptable material parameters and expected behaviour. The numerical software used in this research is ABAQUS however both ANSYS (2009) and SAFIR (2011) have been used to model the thermal impact of a fire on timber for other projects running simultaneously to this research. A tertiary objective of the modelling was to make comparisons between the results obtained from the three software suites for further validation of the thermal model. Once the thermal model had been validated the three-dimensional thermal profiles of any timber section could be calculated for a specified fire type and duration, allowing for a structural analysis of the timber system to be conducted.

4.4 Heat Transfer Model

The following differential equation describes the energy balance solved to calculate the conduction of heat through a solid anisotropic material:

$$\rho c_p \frac{\delta T}{\delta t} = \frac{\delta}{\delta x}\left(k_1 \frac{\delta T}{\delta x}\right) + \frac{\delta}{\delta y}\left(k_2 \frac{\delta T}{\delta y}\right) + \frac{\delta}{\delta z}\left(k_3 \frac{\delta T}{\delta z}\right) + \dot{Q}$$ **Equation 4-1**

Where:

ρ = Density (kg/m^3)

c_p = Specific heat (J/kgK)

δ = Differential operator

T = Temperature (K)

t = Time (s)

k = Thermal conductivity (W/mK)

x = Dimension in the x-direction (m)

y = Dimension in the y-direction (m)

z = Dimension in the z-direction (m)

$\dot{Q}$ = Rate of internal heat generation (W/m^3)

In this research the major forms of heat transmission considered are the convective and radiative heat transfer from the fire to the outer boundary of the timber specimen, and the conduction of heat through the specimen. Voids (such as those inside the box beams) introduce a much more complex scenario to model as convective and radiative processes occur between all surfaces inside the void, hence they are neglected in the analysis. Their influence on the overall floor performance is also minute until the latter stages of heating, as the insulative properties of the timber members prevent the inside surfaces of the voids from heating for the majority of the model run time. Void temperatures are conservatively assumed to be the temperature of the hottest inner surface of the void.

4.4.1 Initial Conditions

The ambient temperature of the nodes in the model were initially set to 20°C, and other key parameters such as the Stefan-Boltzmann constant were specified for the analysis.

4.4.2 Fire Input

The ISO 834 fire was used to aid in the reproducibility of the results obtained. The fire curve was calculated for the required simulation duration, and stored as a temperature amplitude

dataset in the software. This amplitude was then applied to each fire exposed surface of the members modelled. This was accomplished via surface film conditions, which are described as follows:

- The standard fire was applied to the exposed surface as radiative heat with an emissivity coefficient of 0.8 W/m^2K.
- The standard fire was also applied to the exposed surface as convective heat with a convective coefficient of 25 W/m^2K.
- The open air environment was modelled as a free convective surface with an assumed convective coefficient of 9 W/m^2K, to model both radiative and convective losses.

4.4.3 Element Type

The element type used in the one and two-dimensional heat transfer analyses were four node linear heat transfer quadrilaterals, while similarly for the three-dimensional analysis the element type was an eight node linear heat transfer brick. These elements have temperature degrees of freedom activated at each node and are ideally suited for these types of heat transfer analyses.

4.4.4 Time-step and Solver Technique

The choice of time-step is vital to calculating appropriate results in numerical analyses. The size of the time-step chosen is important to ensure that the solver technique will converge on a solution. This is highly dependent on the solver technique employed, as a low accuracy solver technique may require many more time-steps than a high accuracy solver technique, but may also be less computationally expensive and require less accurate initial estimates. The influence of any round-of errors must also be considered when choosing a solver technique, as these can compound and become significant over long simulations. Software such as ABAQUS has an automatic time-stepping procedure which can be used to avoid convergence issues that may be encountered setting manual time-steps.

In the thermal analysis the direct sparse solver technique in ABAQUS was used, using Newton's technique to solve the nonlinear equations with linear extrapolation. This is a simpler solver technique which is sensitive to large changes in calculated properties in the model, hence limits must be placed on values such as the maximum temperature and emissivity changes to ensure convergence. It was found on comparisons with the iterative linear solver that virtually no time savings were made; hence the default sparse solver was used. Automatic time-steps were also used to ensure numerical stability and for the ease of analysis.

4.5 Material Properties

Due to the computer power available and the general intention of the thermal modelling, higher order effects such as mass transfer and char contraction (as discussed in Section 2.7.4) cannot practically be modelled in the timeframe of the research. However, an in-depth study of thermal modelling alone would warrant further investigation into higher order effects. To account for these effects a set of effective values were determined for the timber material and these are described in detail below and compared with experimental data.

Two approaches were taken to modelling the material properties of the timber in ABAQUS. The first was a direct input method, consisting of defining the thermal properties of the material directly. The second was a slightly more efficient approach, accounting for higher order effects in the material properties in a less direct way to reduce the complexity of the computations required by the ABAQUS subroutines. These two methods are described in the following sub-sections, and the results of each method are compared in Section 4.10.1.

4.5.1 Thermal Inertia Material Model

The properties discussed in Section 2.7 from Annex B of the Eurocode (CEN, 2004) are used as baseline for configuring the material model of timber for heat transfer in ABAQUS. In particular these are the thermal conductivity, density and specific heat, as these properties have been found in the past to have the greatest influence on the transfer of heat through a material.

The product of the thermal conductivity, density and specific heat of a material is commonly known as the thermal inertia. It is a broad measure of the resistance of a material to temperature change. For instance, a material with a low thermal inertia will increase in temperature more rapidly than a material with a high thermal inertia when both materials are subjected to the same increase in temperature. This is the most intuitive and simplest method of inputting material properties into ABAQUS, and is referred to in this research as the thermal inertia material model.

4.5.2 Latent Heat Material Model

The latent heat material model uses the same inputs of thermal conductivity, density and specific heat, however it accounts for the peak in specific heat due to the vaporisation of water, shown in Figure 2-12, by substituting the extra energy required for this phase change into the energy balance equations separately. Therefore the rate of change of the specific heat property with temperature is significantly reduced, which aids in the computation of properties in the

elements at each step of the analysis as the change is smaller hence the time-steps can be larger. Although this is the only change made it will be referred to as the latent heat material model to avoid confusion with the thermal inertia material model.

The properties used in the thermal modelling are presented in Table 4-1. The bulk density of the LVL was taken as 480 kg/m^3 in ambient conditions with moisture content of 12%. Although both material models gave similar results, the thermal inertia model was much slower to run simulations hence the latent heat model was used to produce the bulk of the results, and comparisons between the models are made in the sensitivity analysis.

Table 4-1: Material properties used according to Eurocode 5 (CEN, 2004)

Temperature (°C)	Conductivity (W/mK)	Specific Heat (J/kgK)	Density Ratio (-)
20	0.12	1530	1.12
98.9	-	1770	1.12
99	-	13600	1.12
120	-	13500	1
120.1	-	2120	1
200	0.15	2000	1
250	-	1620	0.93
300	-	710	0.76
350	0.07	850	0.52
400	-	1000	0.38
500	0.09	-	-
600	-	1400	0.28
800	0.35	1650	0.26
1200	1.5	1650	0

4.6 Boundary Conditions

The boundary conditions are extremely important in heat transfer analysis, as they provide the major mechanisms for introducing temperature gradients across elements and dictating the bounds within which the problem will be solved. In this section the boundary conditions specified for the entirety of the thermal analysis are discussed with accompanying illustrations to better describe how the boundary conditions for each specific problem have been modelled.

4.6.1 One-sided Exposure

For the one-sided heat transfer described in Section 4.7, the timber members are best conceptualised as a slab of infinite thickness, thus completely reducing the heat transfer to a one-dimensional scenario. The boundary conditions for the semi-infinite sides of the model were implemented as adiabatic, as in the experimental testing layers of non-combustible gypsum plasterboard were used along these surfaces to minimise furnace interaction. The standard fire was applied to the exposed side of the specimen, and the unexposed side was modelled as a free convective surface, simulating an open air environment. A simplified illustration of this is shown in Figure 4-1, with the adiabatic surfaces shown in red.

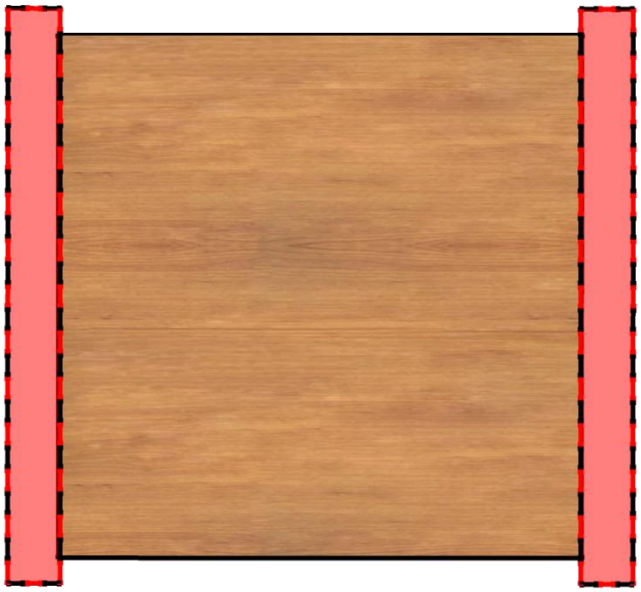

Figure 4-1: 1D thermal modelling boundary conditions

Note that the slab width is not critical as the heat flow is completely uniform across the section, hence to economise the computer resources available only small strips of timber are modelled.

4.6.2 Two-sided Exposure

The two-sided heat transfer described in Section 4.8 is modelled utilising the symmetry of a column subjected to four-sided fire exposure. In order to analyse two-dimensional behaviour the column section was divided into four quarters with only one quarter being modelled, as shown in Figure 4-2. The two adjacent outer sides were exposed to the fire conditions while the inner other two sides were modelled with adiabatic boundary conditions to simulate a reflective

boundary. This is shown in the figure with the reflective boundary cuts represented in blue and the three redundant quarters shaded in grey.

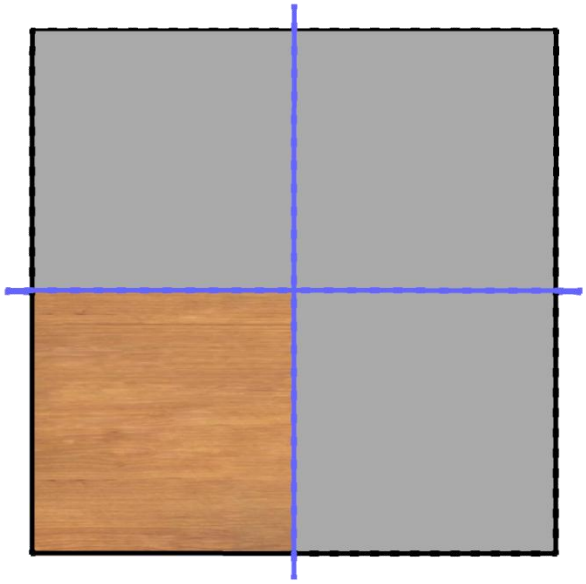

Figure 4-2: 2D thermal modelling boundary conditions

4.6.3 Three-sided Exposure

For modelling the actual test specimens discussed in Section 4.9, and for any other floors with fire exposure on the underside, three sided exposure was modelled as follows:

- The surfaces on the underside of the floors are completely exposed to the fire, and have the fire conditions applied to them.
- The cuts through the floor section simulate a continuous portion of floor; hence have an adiabatic boundary condition applied to simulate no heat transfer between floor strips but rather a reflective condition. As the fire is assumed to affect a larger area than the strip being modelled, this assumption is appropriate as no heat is lost over the boundary.
- The top of the floors are modelled as a free convective surface which simulate an exposed open air environment.

A depiction of these conditions is shown in Figure 4-3, considering a generic joist floor. The axes of symmetry for the floors allowed for two major cuts to be utilised in the modelling, being halfway through the cross-section vertically, and halfway along the span length.

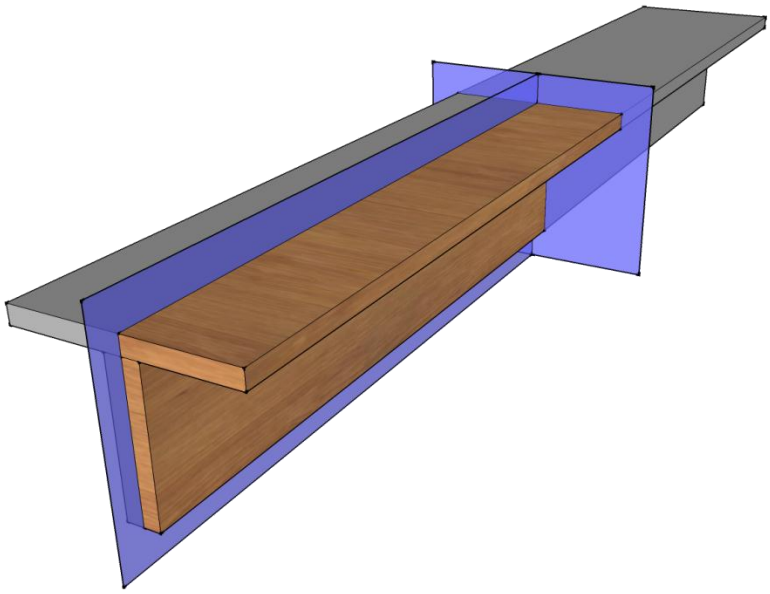

Figure 4-3: 3D thermal modelling boundary conditions

For the sequential modelling of the floors all node definitions must coincide in both the thermal and structural analyses, hence these same axes of symmetry were used in the structural modelling portion of this research.

4.7 1D Modelling

The majority of work presented in this chapter pertains to the efforts made in modelling heat transfer in ABAQUS. As previously mentioned, these heat transfer studies were also run in unison using ANSYS and SAFIR, and the results compared at key stages between each program. More detailed analysis of the results from ANSYS and SAFIR are discussed in detail by Werther et al. (2012), and only a brief comparison is presented here in Section 4.10.4.

4.7.1 König and Walleij's Experimental Analysis

In order to confirm the validity of the effective values used for modelling the heat transfer through timber, a stable set of reliable and well documented experiments is required for comparison. König and Walleij (1999) conducted a series of experiments on a semi-infinite timber slab (a slab with sufficient width such that the analysis could be considered as one-dimensional) exposed to standard and parametric fires. They measured the temperature increase at set points throughout the slab specimens, as shown in Figure 4-4, and compared the results to numerical simulations for a number of exposures.

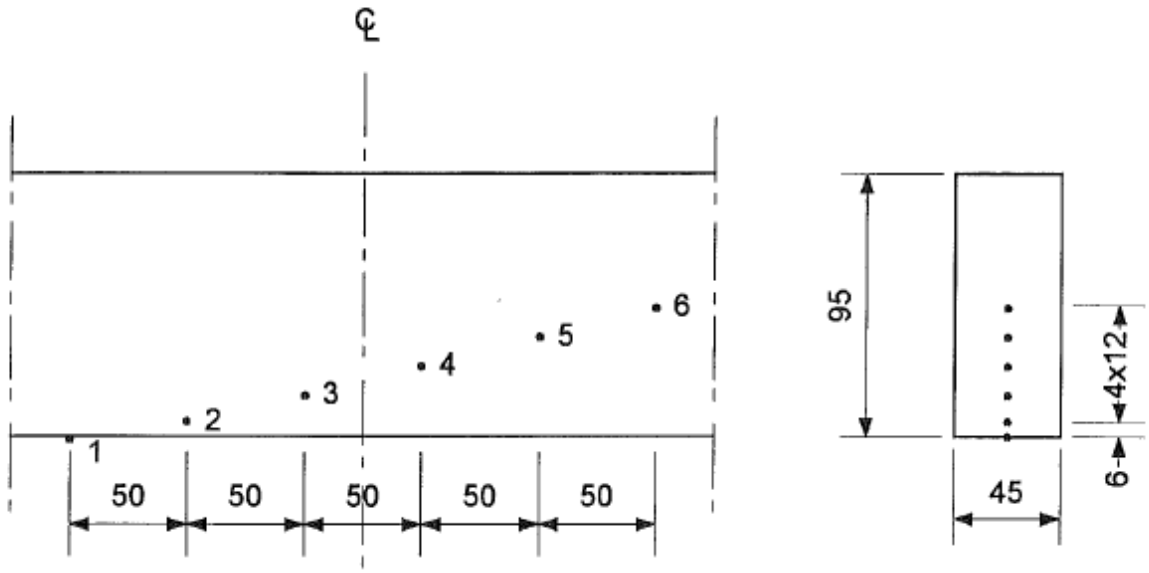

Figure 4-4: Location of thermocouples in König and Walleij's tests (1999)

Their results for effective properties have now been incorporated into the Eurocode (CEN, 2004), and were found to be valid for standard fire exposure. These results are revisited by König (2006) and reviewed modification factors proposed for a range of modelling parameters.

The experimental specimen was modelled as a 24 mm wide x 96 mm deep section (for ease of mesh divisions in the sensitivity study), with specific points of temperature recorded at 0, 6, 18, 30, 42 and 54 mm from the exposed fire surface. The simulations were run for 90 minutes to encapsulate the majority of meaningful temperature results found from the experiments at these depths, and a 1 mm mesh size was used.

4.7.2 Modelling Results

A comparison of the experimental results and the thermal modelling is shown in Figure 4-5 for the thermal inertia material model. The average recorded temperatures from the full series of experiments are depicted as solid black lines, with raw experimental data values shown in grey. The coloured lines depict the modelling output for each coinciding data measurement point.

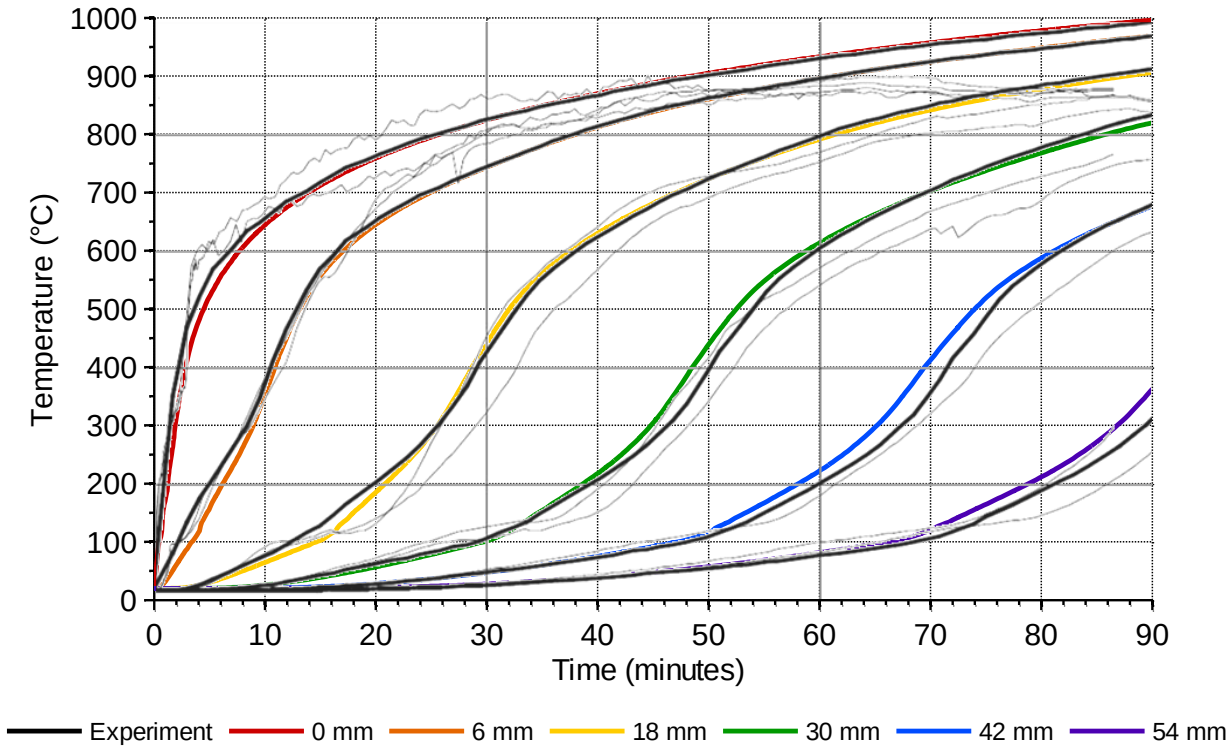

Figure 4-5: Comparison between experimental (König and Walleij, 1999) and 1D thermal inertia model

From the figure it can be seen that the thermal inertia model tends to over predict the temperatures in the zones of greatest rate of change of temperature. This effect becomes more pronounced with the depth of section analysed, as differences between the model assumptions and reality that cause this discrepancy are amplified as the number of element interactions is increased. The model however is more reliable at predicting the temperatures when the rate of change of temperature is low, and also when the data converges to a steady state solution as seen on the figure for all depths modelled.

Similarly, this comparison of the experimental results and the thermal modelling is shown in Figure 4-6 for the latent heat material model. The latent heat material model slightly under predicts temperatures in the latter stages, however is an overall better fit to the experimental results than the thermal inertia model. The most noticeable improvement is the temperature prediction at greater depths of timber, as the latent heat material model can better account for more rapid changes in the rate of temperature, and this is shown on the figure for the 30, 42 and 54 mm measurement points.

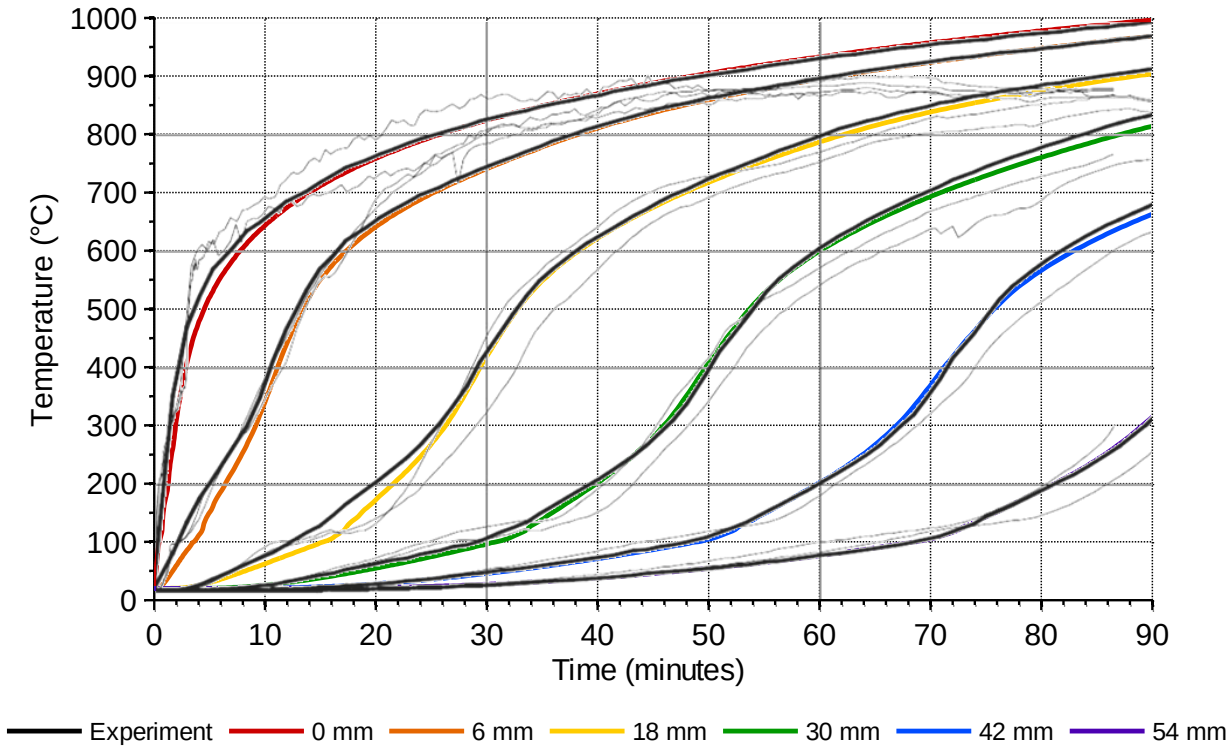

Figure 4-6: Comparison between experimental and 1D latent heat model

The steady state predictions are similar to the thermal inertia model and are seen to be approximated well. For both material models the initial increase in temperature up to 300°C for the 6 and 18 mm points in the timber is slightly under predicted by the modelling effort when compared with the experimental results. As explained previously, this is due to the great rate of change in temperature being difficult to approximate exactly by the modelling software with the current inputs, and this effect is more pronounced with a greater number of element interactions.

Due to the faster analysis time and noticeably more accurate output obtained when compared with the experimental results, the latent heat material model is used for the remaining two-dimensional and three-dimensional heat transfer analyses. Further comparisons between the results obtained for the different material models are presented in the sensitivity analysis.

4.8 2D Modelling

Due to the nature of problem being solved in the structural modelling, a two-dimensional thermal profile is the limit of what is required as an input. This is because the floor assemblies under consideration are assumed to be subjected to a thermal impact which is uniform along the

length of the assembly. In the case of a real fire this is a conservative assumption as it is expected that the hot upper layer would not be completely uniform in temperature, and areas of the floor further from the fire source may take longer to reach the maximum temperatures of those closer to the fire.

4.8.1 Column Modelling Setup

To investigate the interactions of thermal waves at corner junctions, the two-dimensional modelling of a simple square column cross-section is conducted. Experimental results from a column tested at MFPA Leipzig are used for validation, as discussed by Werther et al. (2012). The column dimensions in the model were 156 mm x 156 mm, and this was exposed to the standard ISO 834 fire on all sides for 90 minutes. In order to optimise the available computer power, the symmetry of the column was used to reduce the overall area modelled, as discussed in 4.6.2. The area modelled was discretised into square plate elements of a 1 mm mesh size.

Similar measurement points were used to the one-dimensional analysis for comparison, however some intermediate points differ to align with the experimental results used for validation. The measurement points were taken at 0, 6, 10, 20, 30, 42 and 54 mm, and these were located at 60 mm in from the edge of fire impact to determine the influence of the thermal wave interaction. A depiction of these points on the column edge is shown in Figure 4-7.

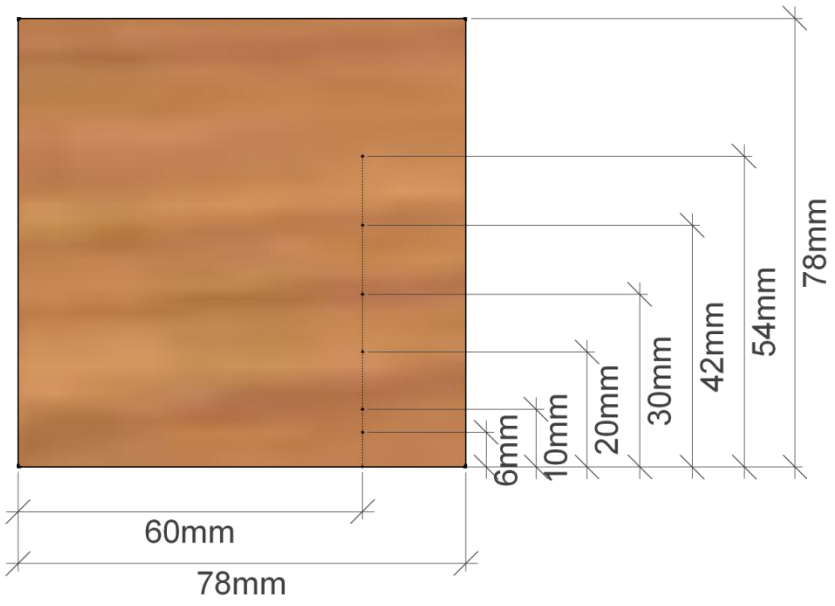

Figure 4-7: Setup of the 2D thermal modelling and experiments

4.8.2 Modelling Results

Figure 4-8 shows the comparison between experimental results and the thermal modelling effort. For this comparison, only aligning points of temperature measurement are shown for the modelling output.

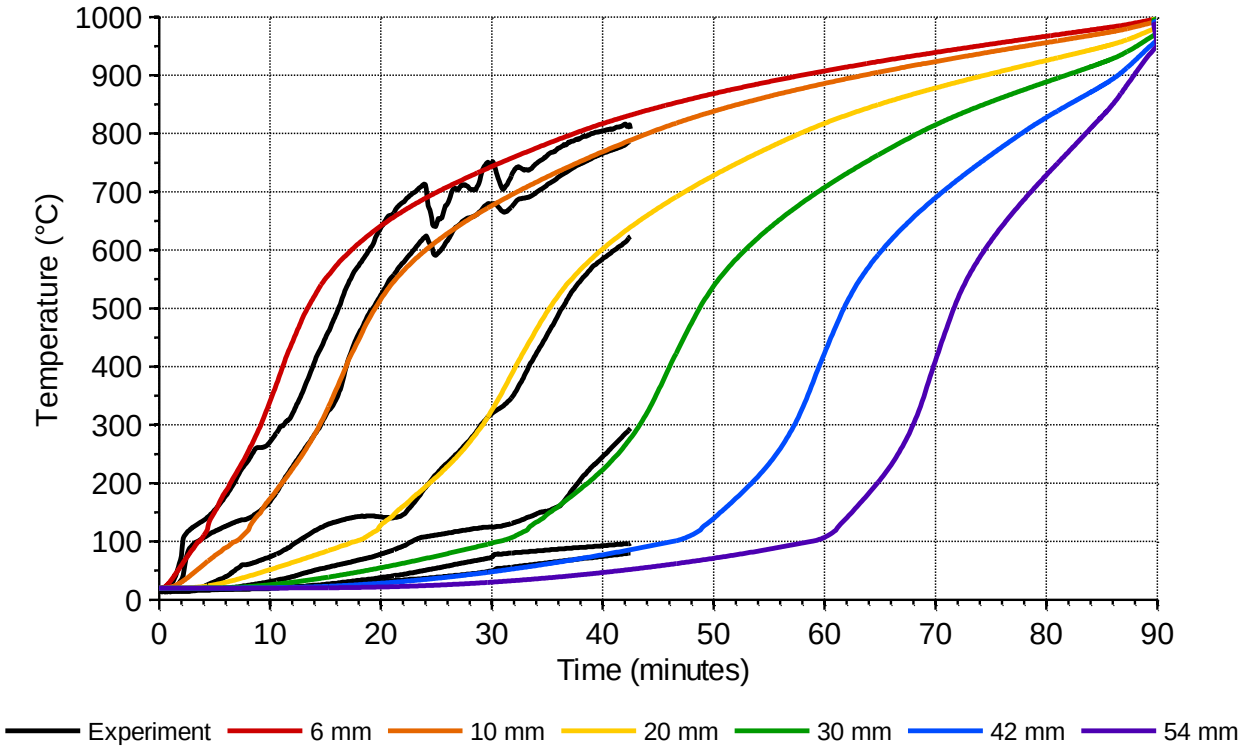

Figure 4-8: Comparison between experimental and 2D modelling

Due to the single set of experimental data for this two-dimensional case, the experimental results show a significant level of "noise" which reduces as the measurement points regress further into the timber column, the experimental values show a faster increase in temperature up to 150°C for all measurement points. Despite this, the modelling output does coincide relatively well with the experimental data, most notably at higher temperatures.

The experiment was terminated at approximately 43 minutes, but the modelling output is shown for 90 minutes as a comparison between the one and two-dimensional cases. It can be seen when comparing Figure 4-6 and Figure 4-8 that the influence of two-dimensional behaviour becomes apparent at different depths, however for this particular case with the temperature measurement points located 60 mm in from the heated surface the interaction has become apparent by 40 minutes. This is discussed further in Section 4.8.3.

4.8.3 1D Comparison

To determine whether a simple one-dimensional approximation is appropriate for use in thermal timber modelling checks must be made to ensure that the fire duration modelled will not incur significant isotherm interaction on the member in question. This is a function of the shape of the member, the relevant fire duration which determines the depth at which isotherms will interact, and the desired time to which the member is being designed for. In other words, the one-dimensional assumption is completely geometry and time dependent, and its use must be assessed on a case by case basis. Examples in which one-dimensional assumption would be appropriate are in the case of modelling slabs, sufficiently large beams or wide rectangular columns. Cases in which the members are more slender (including many different beam configurations) will most likely require the consideration of two or three-dimensional heating.

A comparison between the output for the one and two-dimensional modelling conducted is shown in Figure 4-9. For ease of comparison only the 6, 30 and 54 mm depths have been presented, with the one-dimensional results represented by solid lines and the two-dimensional results by dashed lines.

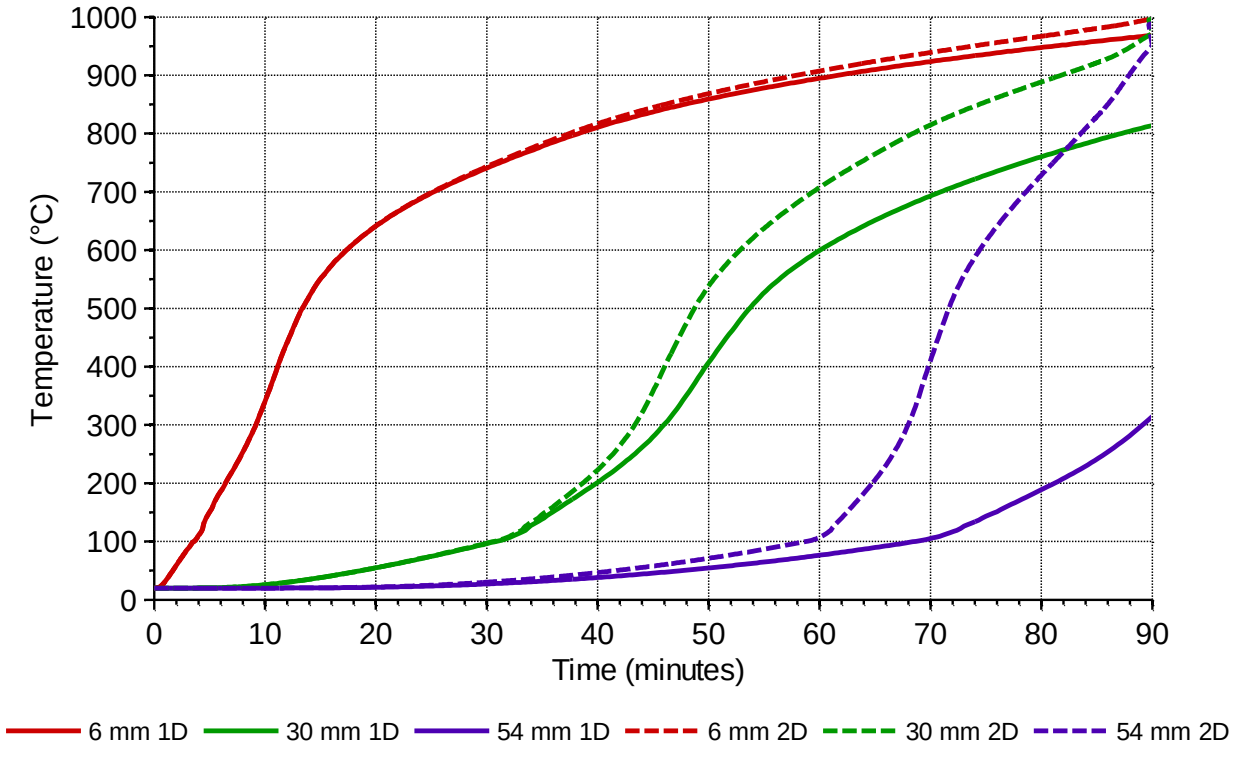

Figure 4-9: Comparison between 1D and 2D modelling

The graph shows that the interaction is apparent at about 40 minutes of fire exposure, and the influence of the two-dimensional behaviour has a significant impact on the thermal performance of the timber. This highlights the importance of checking whether one-dimensional behaviour assumptions are appropriate when modelling timber members to ensure fundamental errors are not made in design and analysis.

4.8.4 2D Interaction

A similar model was conducted for the column case changing the depth of measurement to determine the influence of the two-dimensional interaction with timber depth. Figure 4-10 shows a comparison between the original modelling results of the column experiment, and output where the distance from the heated surface is changed to 30 and 90 mm. These are shown for 6, 30 and 54 mm depths into the timber, represented as red, green and purple lines respectively. As the distance from the heated surface increases the lines are represented by dotted, dashed and solid lines.

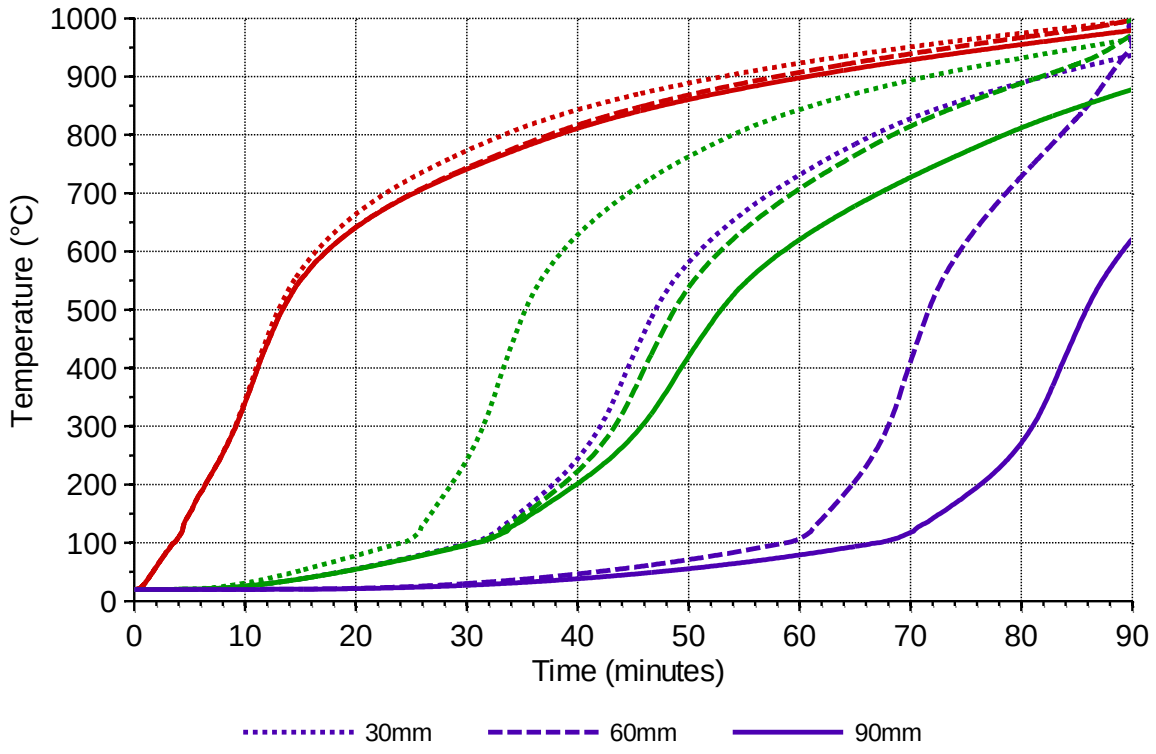

Figure 4-10: Comparison between depths of 2D modelling interaction

The measurement points spaced 30 mm from the heated surface record the most noticeable increases in temperature during the simulation, and the influence of the two-dimensional

thermal wave is evident for each point as the temperature increases rapidly at each respective stage of the simulation. For the 6 mm deep measurement point (red lines) this effect is almost instantaneous, occurring at about 10 minutes into the simulation. The 30 mm deep measurement point (green lines) spaced 30 mm from the hot surface records a greater initial growth to 100°C than the 60 and 90 mm deep points, with a large rate of change of temperature at approximately 25 minutes. The 54 mm deep measurement point (purple lines) spaced 30 mm from the hot surface measures the most notable difference to its 60 and 90 mm counterparts, with a temperature of over 300°C at 41 minutes. This is due to the increasing thermal interaction of the two-dimensional heat source, and this effect increases with the duration of burning as the interaction becomes more significant. This is seen from the figure as the spacing between the temperature curves for each measurement point becomes greater with the depth into the timber.

The 60 mm measurement points display similar trends to the 30 mm points, however with a lower rate of increase in temperature for the points closer to the surface. The 54 mm measurement point has a much greater rate of increase in temperature due to its physical location in the simulation which is almost equidistant from the two heated surfaces. This infers that by 60 minutes into the simulation the effect of the two-dimensional thermal wave interaction has become significant, and is greatest at this point. This measurement point is highlighted in Figure 4-11 in red, where the thermal contours are compared for both 30 and 60 minutes of simulation run time on the left and right of the figure respectively.

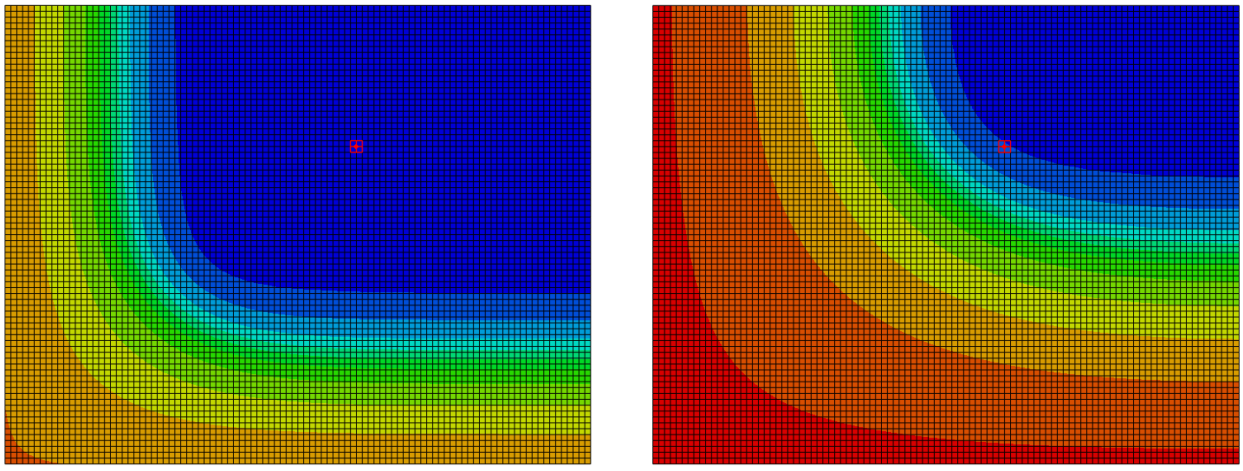

Figure 4-11: 2D column thermal contour at 30 minutes (left) and 60 minutes (right)

The contours vary linearly from blue representing 20°C ambient temperature, to red which signifies 1000°C. The level of the char layer is at the cyan to green boundary. The figure shows

the extent of amplification of the two-dimensional interaction over a 30 minute period, being much more significant at 60 minutes with a greater level of rounding of the thermal waves. It can be seen from Figure 4-10 that the temperature measurement at 90mm in is virtually identical to the one-dimensional case (Figure 4-6) for the first 70 minutes of exposure, with a noticeable influence of two-dimensional behaviour occurring at this stage of the simulation.

The major aspect which can be derived from Figure 4-10 is that the trends for each measurement depth are extremely consistent, showing that the two-dimensional behaviour of the timber can be predicted based on an estimated fire duration time. The analysis of the two-dimensional interaction above reinforces the requirement for the validity of a one-dimensional assumption for timber assemblies to be thoroughly checked. As previously iterated, this is highly dependent on the scope of the problem to be solved and should be considered on a case by case basis.

4.9 Experimental Comparisons

The validation of numerical studies is vital to ensure that any simplifications and assumptions made are appropriate within the scope of the problem being solved. This section presents the results obtained in the heat transfer analysis of the experimental tests described in Chapter 3. Comparisons between the simulations and the actual experimental results are made to ensure the adequacy of the thermal transfer model used as input into the structural analysis.

4.9.1 Test A

To take advantage of the symmetry of the floor geometry, only a quarter portion of a strip of the floor needs to be modelled as described in Section 4.6.3. To ensure the thermal model can be used as an input into the structural model in ABAQUS, all node definitions and positioning in the thermal model must correspond exactly to the structural model. This restricts the size of the mesh as the structural model geometry is large; hence a uniform density 5 mm square mesh is used in the plane of the cross-section of the floors, and a 300 mm long element length is used for the general modelling. A sensitivity study on this element length is given in Section 5.8.1.

To simplify the following thermal contour figures, the contours have been set to display the following thermal profiles which show all temperatures above 300°C as grey, assuming this timber is char. Ambient temperature timber at 20°C is represented as blue, and the temperature gradient is linear throughout the remaining colours between the ambient timber and the char.

Test A was terminated at 30 minutes, and the fire was extinguished approximately 6 minutes after this. The thermal profile of Specimen A at 36 minutes is shown in Figure 4-12. The full description of the results of Test A is described in Section 3.6.

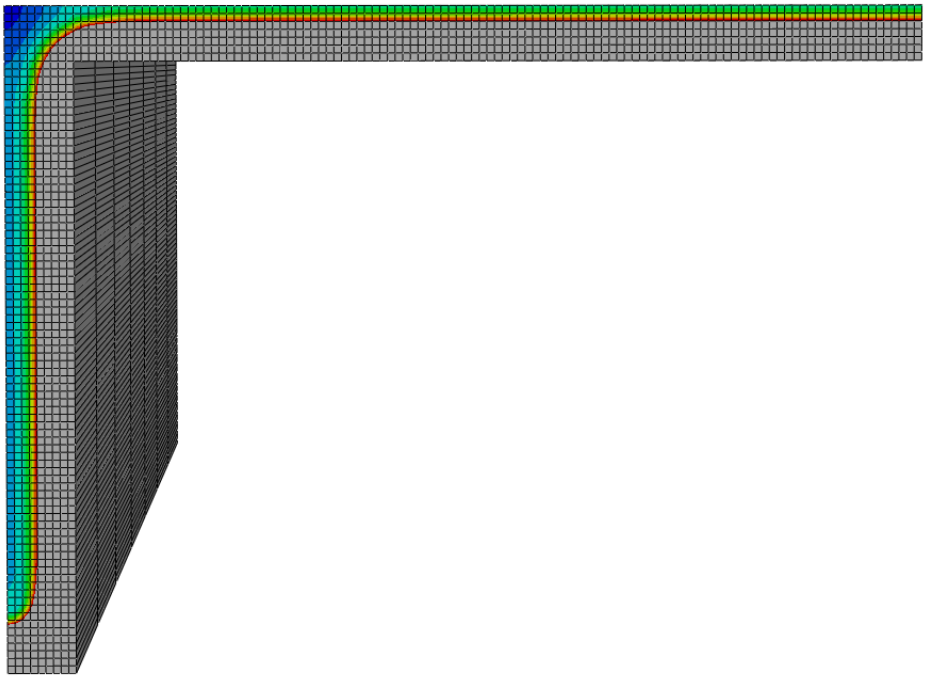

Figure 4-12: Thermal profile of Specimen A at 36 minutes

The thermal model of Specimen A at 36 minutes shows approximately 25 mm charring (readout of the 300°C isotherm) for the one-dimensional regions, and 32 mm for the two-dimensional zone at the bottom of the joist. These values agree well with the charred section measurements after testing, and the corresponding calculated charring rates as presented in Table 3-6, where the joist sides and slab also measured 25 mm char depth, and the measured bottom charring of the joist was 30 mm.

On comparison with Figure 3-32 the two-dimensional charring damage of the bottom section of the beam and the beam-slab connection correlate well with the remaining residual section of the floor specimen, reinforcing the adequacy of the two-dimensional thermal model for modelling this type of behaviour.

4.9.2 Test B

As the Specimen B was tested to destruction and no meaningful recovery of the floor section could be made, no viable char damage measurements have been recorded. Figure 4-13 shows

the thermal profile modelled for Test B at 41 minutes when the floor collapsed. The full description of the results of Test B is provided in Section 3.7.

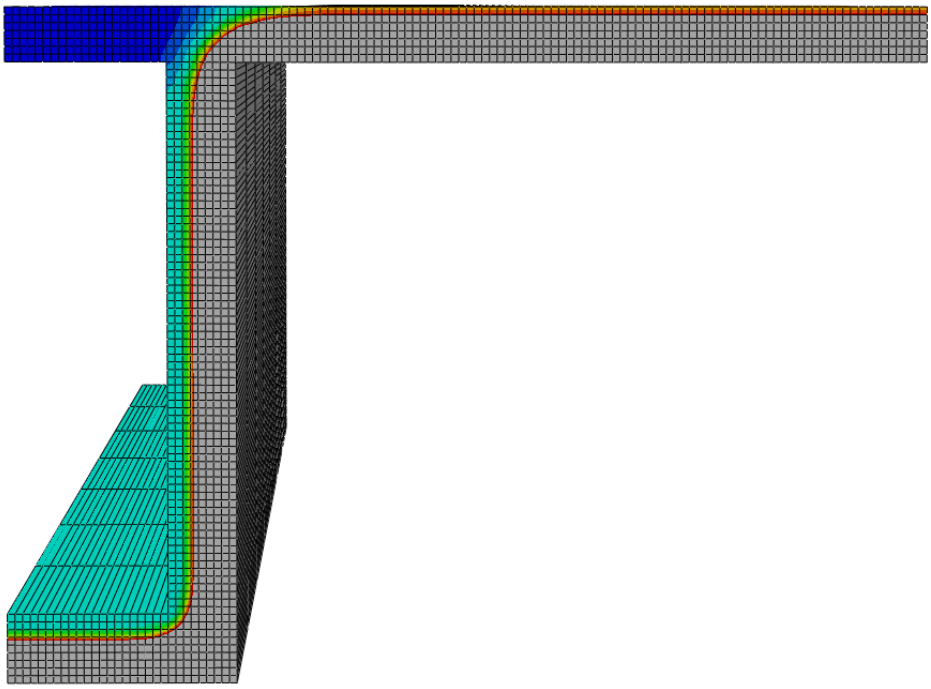

Figure 4-13: Thermal profile of Specimen B at 41 minutes

The figure shows the extent of the expected damage to the floor slab, with a uniform char layer of approximately 28 – 30 mm surrounding the majority of the floor specimen. From the observations during the furnace testing it was noted that at 38 minutes there was a large increase in the volume of smoke escaping through the top of the specimen enclosure, corresponding to a partial loss in the integrity of the top slab. The thermal modelling output for Specimen B at 41 minutes shows the top of the slab temperatures are in excess of 250°C. This corresponds well with the temperature results shown in Figure 3-38 where the slab was close to burn through at the time of collapse.

When considering the results of Test A the thermal modelling effort predicted the impact of a fire on charring for a 36 minute timeframe well, hence it is assumed to also be comparatively accurate for the Test B results at 41 minutes. Given this is the time of collapse, the residual section as shown in Figure 4-13 shows that for the given office loading level a composite box floor would exhibit structural collapse after approximately two thirds of its cross-sectional area has been burned away under three-sided fire exposure.

4.9.3 Test C

The thermal modelling output for Specimen C is shown in Figure 4-14 at 113 minutes of fire exposure time, corresponding to the time at which the specimen was removed from the furnace at 105 minutes and doused with water 8 minutes later. The full description of the results of Test C is described in Section 3.8.

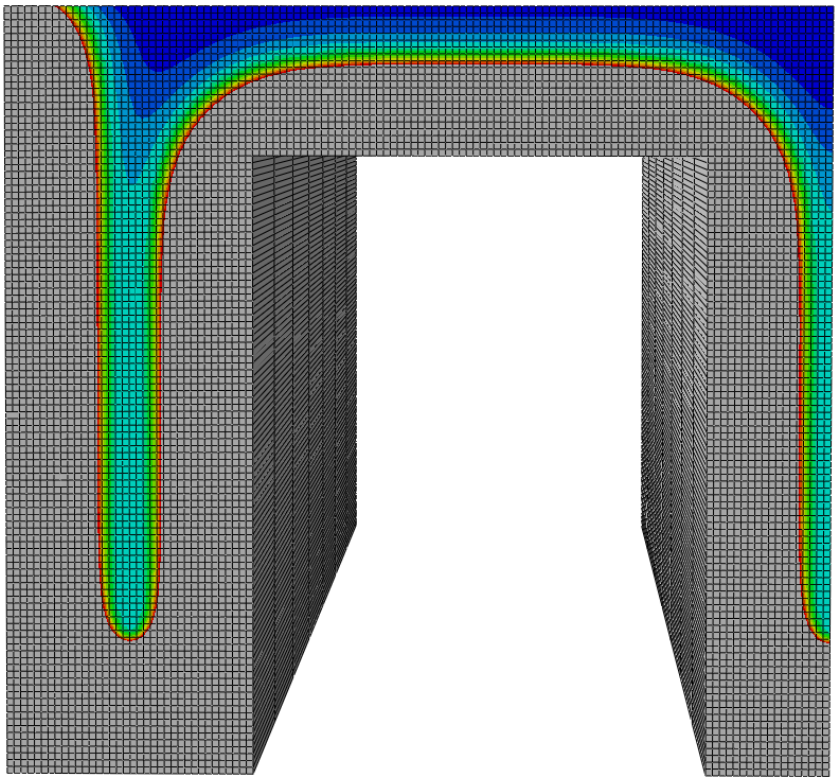

Figure 4-14: Thermal profile of Specimen C at 113 minutes

The thermal output produced a char layer depth of approximately 68 – 70 mm for the one-dimensional regions of the floor including the sides of the joists and the underside of the slab, and 98 – 100 mm for the two-dimensional zone at the bottom of the joists. On comparison with the experimental results the charring ranged from 63 – 75 mm on the sides of the joists, 90 mm on the bottom chords of the joists and 73 – 76 mm on the underside of the timber slab. This shows the thermal model still produces a good estimate of damage at 113 minutes, as most measurements correspond very well with the experimental results.

A higher level of charring was measured on the underside of the timber slab which was attributed to greater re-radiation on the inside portions of the floor specimen, as shown by the cupping which occurred on the joists and the different levels of charring from the inside to

outside edges of the specimen in Figure 3-48. Despite this, the thermal model still produces an estimate which is mere millimetres from the recorded damage after 113 minutes, hence would be appropriate for modelling applications of up to 120 minutes.

Due to the complexity of the mesh numbering system in ABAQUS and issues with creating partitions which were compatible with a structural model counterpart, the heating surface film conditions were applied to the entire edge surface as seen on the left of the figure. The section itself is small and its absence from the thermal model results in a more conservative thermal profile and thus structural results, hence it is not considered a major issue in the overall scheme of the modelling effort.

4.9.4 Test D

Similarly to Test C, Test D was terminated at 105 minutes and it took approximately 8 minutes to unload the furnace and extinguish the fire on the specimen. The thermal modelling of Specimen D is shown in Figure 4-15. The full description of the results of Test D is described in Section 3.9.

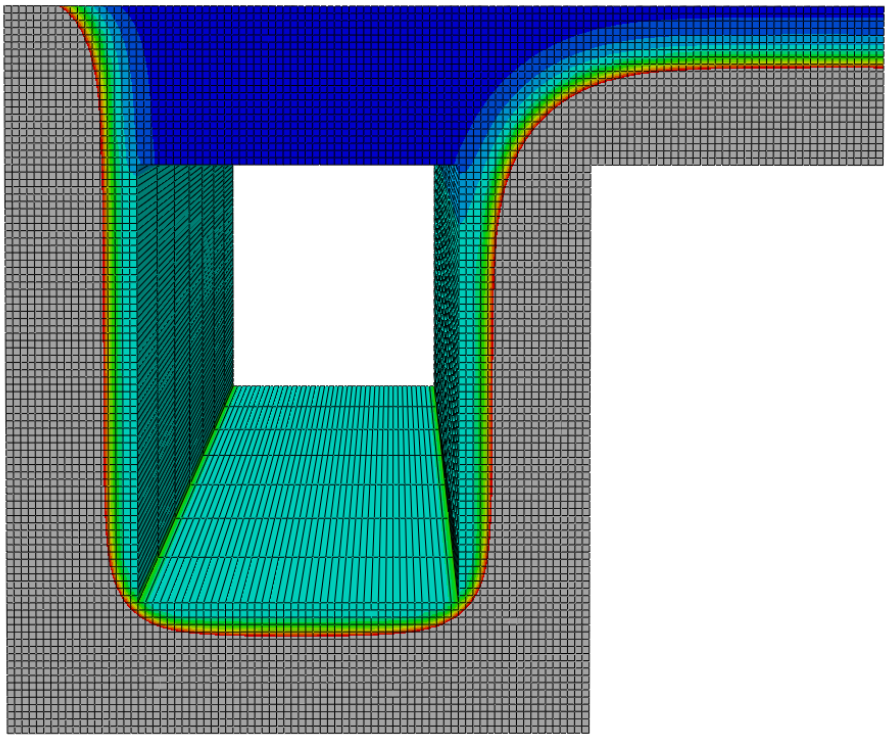

Figure 4-15: Thermal profile of Specimen D at 113 minutes

At 113 minutes the thermal modelling output gives the same results for charring as for Specimen C, with a one-dimensional char layer located at approximately 68 – 70 mm deep for the majority of the box beam and slab. This matches well with the recorded char depths of Specimen D which ranged from 68 – 75 mm on the sides of each beam, and 75 mm on the bottom chords. The char depth on the underside of the timber slab was once again found to be 73 – 76 mm as with Specimen C, and similarly the modelling output correlates well to the measured values from the experiment.

Cavity temperatures from the thermal modelling reach approximately 90°C at the location of the thermocouples, corresponding to a measured 40°C from the testing. This shows that taking this value to be the temperature of the cavity gases is a conservative assumption.

The above thermal studies reinforce the adequacy of the thermal model in solving this type of problem, and the inputs, boundary conditions, and other factors (such as the refinement of the mesh) are also appropriate for these purposes. The current thermal modelling setup is therefore adequate to conduct the sequential structural modelling described in Chapter 5.

4.10 Sensitivity Analysis

As discussed in detail by Chapra and Canale (2002), trade-offs are an extremely important part of the numerical modelling process. A certain degree of art, subjective judgement and compromise must be exercised to ensure their effective use in engineering practice. In many cases the accuracy of the modelling effort in question will undoubtedly be governed by its practical use and overall run-time, hence the computer power available and familiarity with the modelling software are paramount to producing comprehensive results. As with modelling any complex scenario such as the response of burning timber floors, assumptions are a key aspect which simplify the analysis but must always be made in the appropriate context.

A sensitivity analysis allows for the inputs into the model and some of the major structural characteristics of the model to be tested for their relevant impact on the outputs obtained. It also aids in validating some of the assumptions made, as they can be implemented and removed parametrically in the analysis to determine their overall applicability. This section gives a brief overview of the sensitivity analysis of some of the major variables which have a significant influence on both the accuracy and the computational run-time of the thermal modelling.

4.10.1 Material Model

The one-dimensional results obtained from the two material models used in the analysis are compared in Figure 4-16 for the 1 mm mesh size.

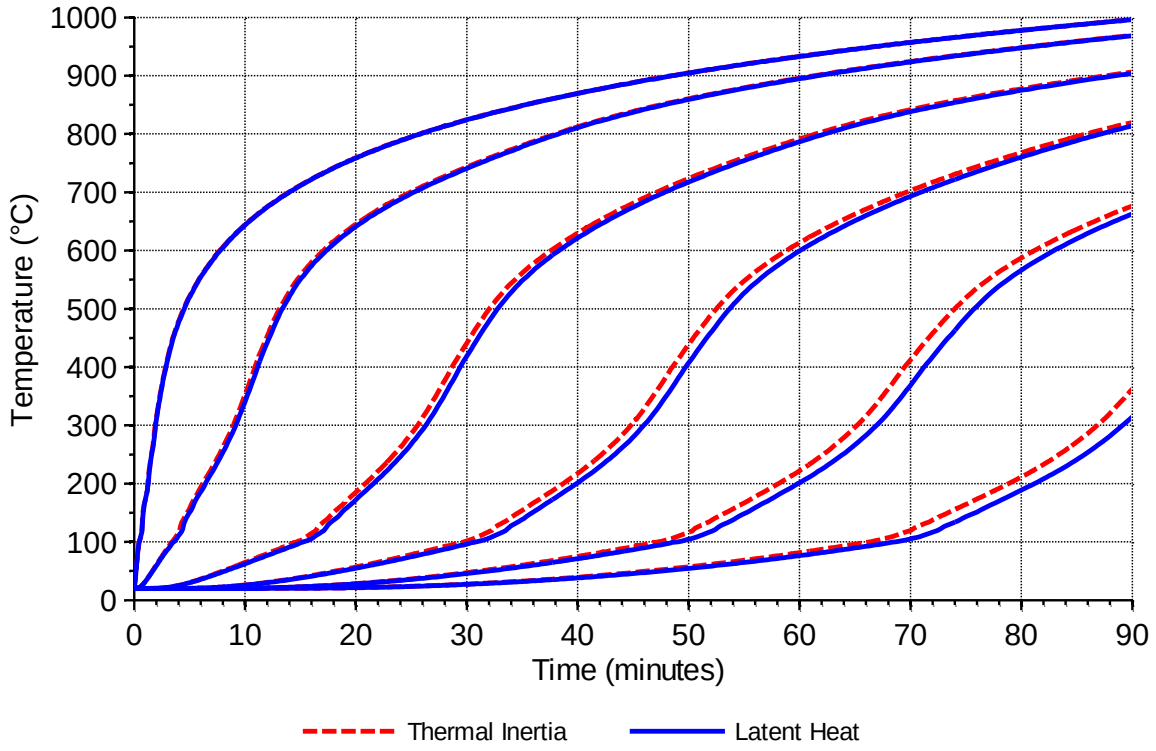

Figure 4-16: Comparison between material models for 1D thermal analysis

As discussed in Section 4.7, the thermal inertia material model tended to over predict the temperature of the timber section in the zones of greatest rate of change of temperature, while the latent heat model was a closer approximation to the experimental data. It can be seen that this issue is amplified with increasing depth into the timber; however the steady state solution is approximated well by both material models.

Due to the large property changes of the specific heat in the thermal inertia material model, the time-steps were required to be very small to ensure convergence. This caused some time delays during periods of extreme nodal temperature change, most notable at the start of the simulations. In contrast to this, the latent heat material model had much larger time-steps as the peak in the specific heat curve had been removed. This resulted in overall simulation times being significantly shorter than that of the thermal inertia material model for the same simulation conditions.

For these reasons the latent heat material model approach is recommended over the thermal inertia model approach as time savings and more appropriate results were experienced in this analysis.

4.10.2 Time-step

Considering the influence of time-step size on the one-dimensional latent heat model with a mesh size of 1 mm, automatic time-steps are used with a maximum of both 1 second and 120 second intervals for two simulations, as shown in Figure 4-17. This enables the simulations to converge, but also allows the parametric study to determine if larger time-steps can have a detrimental effect on the results obtained in the one-dimensional thermal analysis.

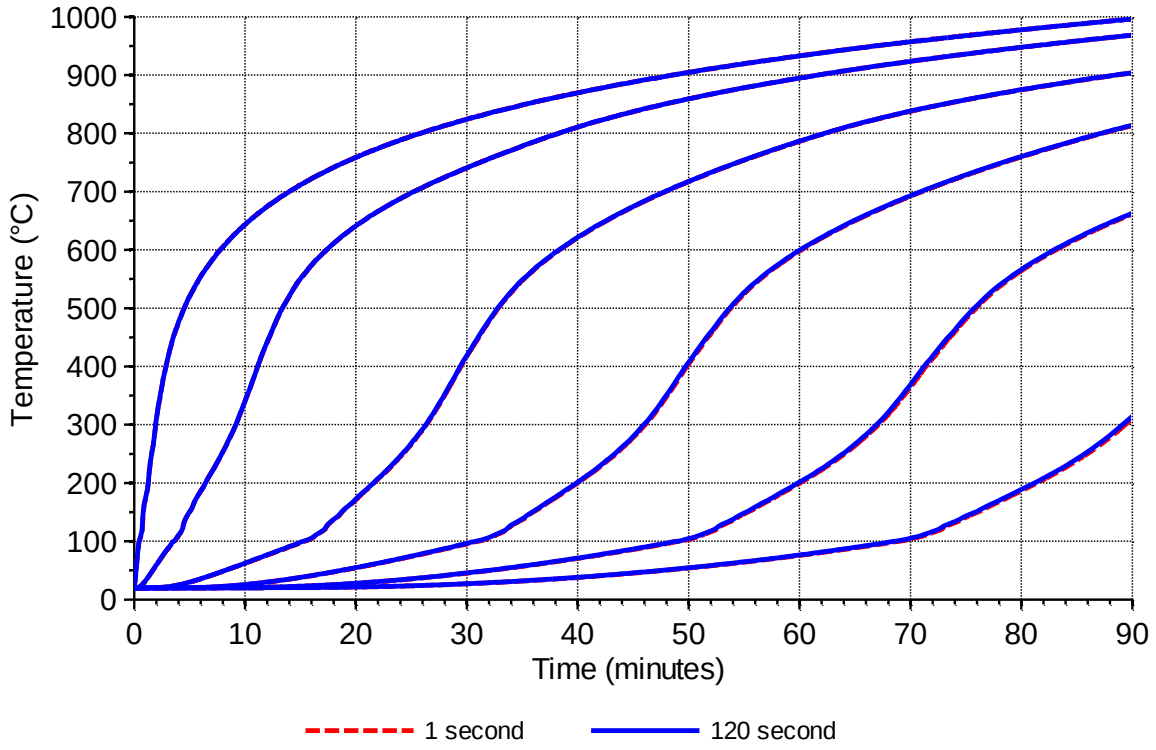

Figure 4-17: Comparison between time-step for 1D thermal analysis

As it can be seen from the figure, the results obtained for the time-step analysis are almost identical with each set of curves lying directly atop the other, showing that the maximum time-step has very little effect on the precision of the output obtained. It was also observed during the simulations that the automatic time-steps were large during periods of a lower change in the rate of temperature of the nodes. This emphasises the versatility of the latent heat model

approach, and the usefulness of numerical software with automatic time-stepping functions to allow for optimised analysis procedures.

4.10.3 Mesh Size

As with many forms of numerical modelling, the mesh size or refinement of the model has a major impact on the accuracy of the results and the run-time. It is important to reach a balance between these two factors to achieve meaningful results within a practical timeframe.

When comparing the influence of mesh size on the one-dimensional thermal model, the latent heat model was run with a 1, 3 and 6 mm square mesh size. Figure 4-18 shows the results of this analysis for the 6, 30 and 54 mm deep measurement points.

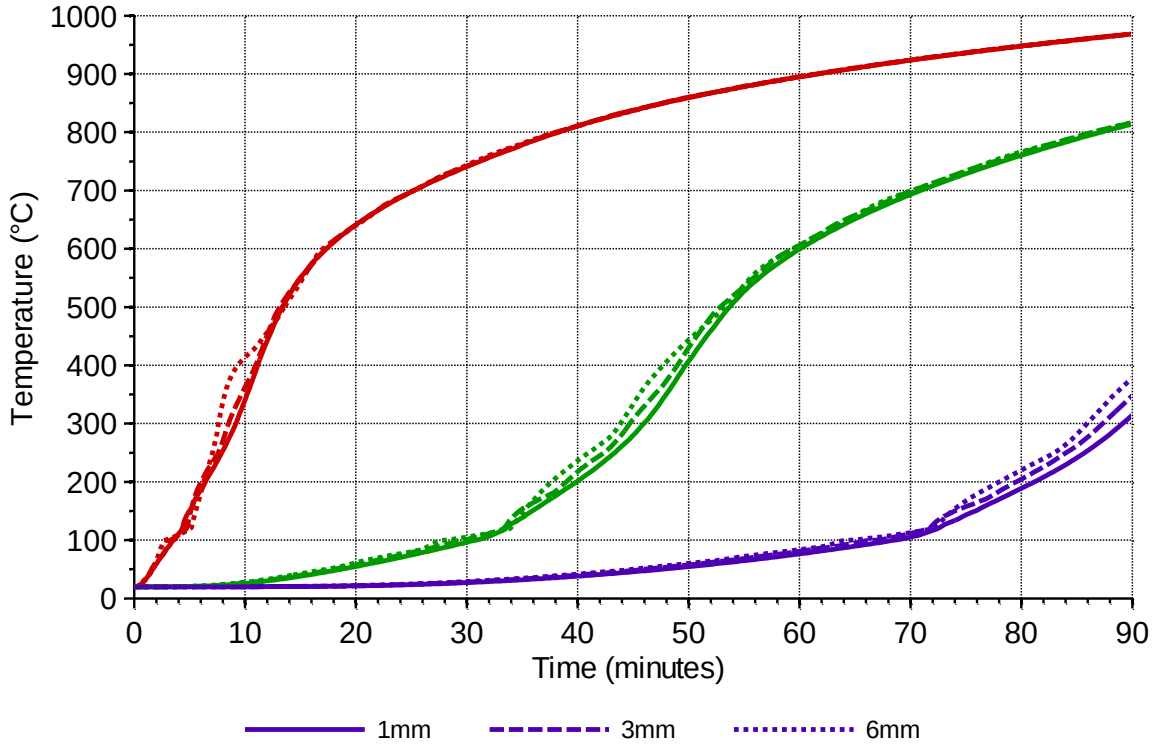

Figure 4-18: Comparison between mesh size for 1D thermal analysis

As it is already known that the 1 mm mesh size is a good approximation to the experimental results used for validation, it can be seen from the figure that the coarser mesh densities serve to over predict the temperature in the zones of the greatest rate of temperature change. From an engineering sense this means that the output obtained is more conservative, however with the addition of other safety factors applied during structural calculations this may result in compounding and unnecessary levels of conservatism. The coarser mesh output does however

converge back towards the steady state solution when the rate of change of temperature is low, and approximate this well.

An advantage of using a coarser mesh is that run times are greatly reduced; however an increasing level of output precision is lost. This type of trade-off may be appropriate depending on the scope of the problem being solved. For instance when considering the structural analysis of floors, small under or over predictions of a temperature band inside a large timber member will not influence the final results to any significant degree. However, when determining the heat transfer through a thin timber slab this type of trade-off may not be acceptable.

It can be seen from the results that a 3 mm square mesh provides a good approximation to the finer 1 mm mesh size and the experimental results with the added advantage of a much faster simulation run time. Depending on the problem being modelled, for most general heat transfer analyses in timber this mesh size would be a good starting value to use, with further studies to determine its suitability after the initial thermal analysis is complete.

In the context of this research, after a mesh sensitivity analysis was conducted for both the thermal and structural models, a uniform mesh size of 5 mm x 5 mm was chosen for the cross-sections of the test floors, with the span dimension of the elements being 300 mm long. This was chosen as a compromise between the reasonable accuracy obtained with both models at that refinement, and the run-times achieved. A further sensitivity study on the structural mesh refinement in the span direction of the floors is given in Section 5.8.1.

4.10.4 Modelling Software

A comparison between three numerical software suites was conducted to investigate any differences between the respective programs. The results shown from ANSYS and SAFIR were obtained by other researchers conducting a parallel study on the thermal modelling of timber. The majority of sensitivity analysis is discussed by Werther et al. (2012), hence only a portion of the work conducted is shown below.

Figure 4-19 shows the results for the 1 mm mesh size using a latent heat material model, while Figure 4-20 is for a 6 mm mesh size. As with the previous comparisons, the output shown is with regards to the 6, 30 and 54 mm deep measurement points in the one-dimensional analysis.

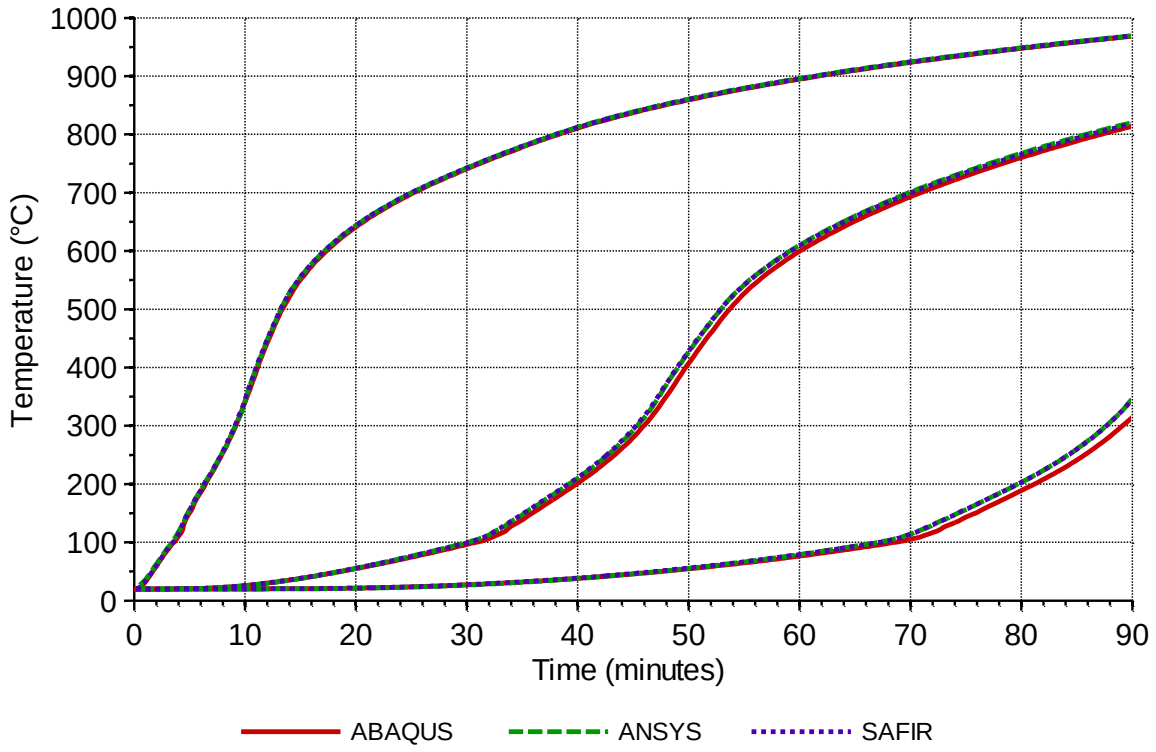

Figure 4-19: 1D thermal analysis comparison between software suites for 1 mm mesh size

From Figure 4-19 it can be concluded that for a 1 mm mesh size all three software suites provide very similar and accurate output when compared with the experimental results. As the ABAQUS output was almost coincident with the experimental results for the 54 mm measurement point, both SAFIR and ANSYS give slightly more conservative temperatures which can be seen to be amplified as the depth of the timber increases.

The results are slightly more dispersed for the coarser 6 mm mesh size shown in Figure 4-20, with both SAFIR and ANSYS under predicting the ABAQUS results, which incidentally has become more conservative compared with the finer mesh. The results of SAFIR have exhibited the least amount of deviation from the corresponding finer mesh, while the ANSYS results are less conservative than the modelling with a finer mesh size.

Despite what might be construed as a relatively large difference between the ABAQUS and ANSYS results in the zones of greatest rate of temperature change, all of the programs still give output which is identical through the zones of a low rate of temperature change, and hence converge on the same steady state solution at approximately 500°C. This level of crudeness may be acceptable for many different structural applications, and the choice of mesh size is

highly dependent on the level of precision of output required within the context of the problem being solved.

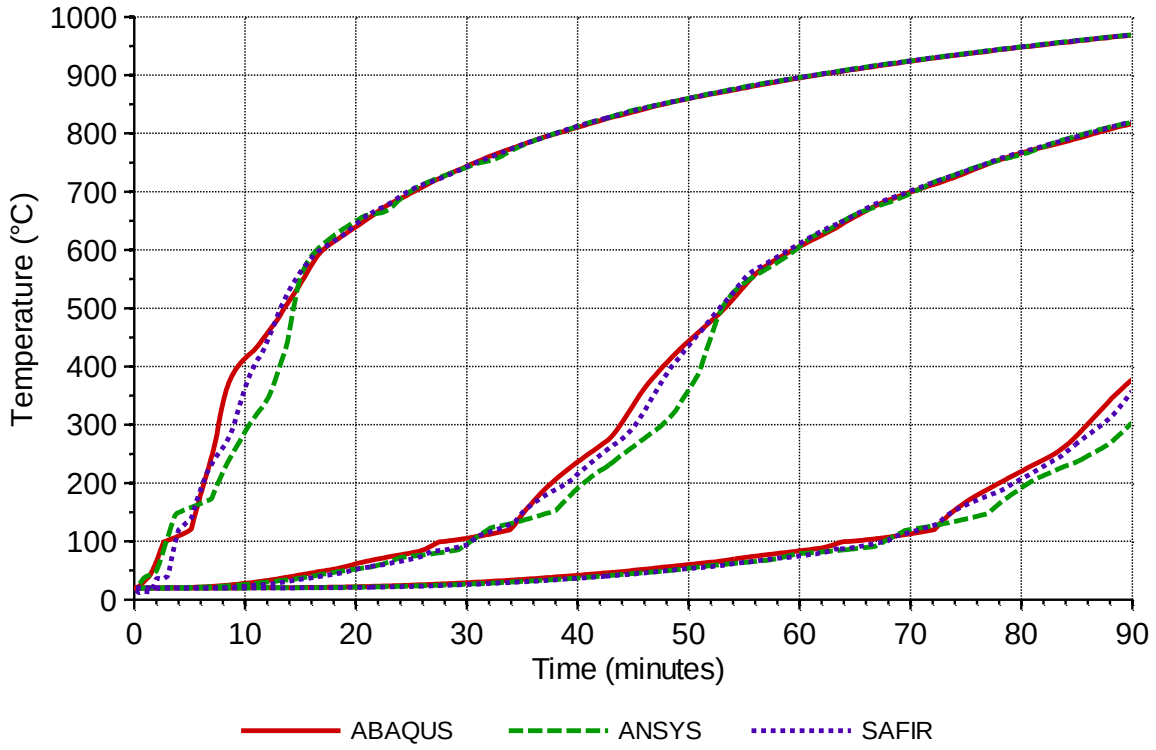

Figure 4-20: 1D thermal analysis comparison between software suites for 6 mm mesh size

These results emphasise the fact that although each modelling software had identical inputs and was run in the most similar fashion practically possible, subroutines and calculation processes between each type of software differ. This has resulted in different output with coarser mesh sizes in this specific case, but these differences may be compounded with an increasingly complex heat transfer problem.

Although a sensitivity study such as this may be time consuming due to the level of expertise required to run separate software programs, for any major heat transfer analysis project there is merit in ensuring that the output obtained from one particular program will correspond to others available. This is not only useful as a solution checking procedure, but to aid in making comparisons with what other research has been conducted in the field.

4.11 Conclusions

In conclusion, the modelling of heat transfer through timber members is complex due to the many internal processes which take place through the section and the thermal and physical changes that occur. This includes mass transfer and the movement of moisture, as well as the physical degradation of the timber member and the property changes through the heated sections of timber. In order to model the heat transfer of timber in fires, assumptions must be made to simplify these processes as long as they are made within the appropriate context and applied in an appropriate fashion.

This study focussed on both the one and two-dimensional behaviour of timber under thermal loads. A proposed set of effective values has been used to account for the mass transfer processes occurring in the timber and as such, it has been shown that these values are adequate for design purposes as long as a number of guidelines are adhered to. The furnace experiments conducted by König and Walleij (1999) were used to validate the one-dimensional modelling, while unpublished column testing experiments from MFPA Leipzig were used for validation of the two-dimensional modelling, as discussed by Werther et al. (2012).

A sensitivity study was conducted comparing different mesh sizes, time step sizes, material model approaches and software suites to determine any shortfalls which may be encountered in the analysis. It was found that a material model adopting a latent heat approach was the most adequate for modelling timber in fires using these effective values, and mesh sizes of up to 6 mm produced relatively precise results. Automatic time-stepping was ideal in reducing computational run times, however this was not vital to the precision of the analysis. Three numerical software suites were run in unison and it was found that the output obtained was relatively consistent between the software packages throughout the analysis.

The floor assemblies which were experimentally tested in this research were thermally modelled to validate the adequacy of the thermal parameters used for structurally modelling timber floors in fire. It was found that the thermal modelling effort predicted the charring damage of the floors to within a few millimetres of precision, and the simplified assumptions made in relation to fire inputs, boundary conditions, mesh refinement and effective material parameters were accurate to the required level of precision desired. These findings reinforced that the thermal model developed is appropriate for the sequential structural modelling conducted in this research, considering fire durations of up to 120 minutes.

For general heat transfer analyses considering structural timber members and assemblies it is recommended that:

- An initial square mesh size of 3 mm is used, with further refinement following a mesh sensitivity analysis.
- A material model adopting the latent heat approach is used.
- Simplified boundary conditions should be used describing radiative and convective heat fluxes on surfaces simulating fire conditions and convective losses on surfaces simulating an open air environment. Adiabatic surfaces should be used to simulate voids and cavities initially, with this revisited depending on the purpose of the void.
- All axes of symmetry should be utilised for applying boundary conditions, and an automatic time-stepping function should be specified if available.
- Checks are made to ensure where two-dimensional heat transfer behaviour will become significant through cross-sections, and whether this needs to be incorporated into the analysis.

5 STRUCTURAL FINITE ELEMENT MODELLING

5.1 Introduction

This chapter describes analytical models of simply-supported timber floors subjected to constant mechanical load and fire conditions using the finite element software ABAQUS. It is aimed at predicting the expected fire resistance of a range of timber floors subjected to similar environmental conditions. The structural modelling is a stepwise approach, gradually introducing levels of detail into both thermal and structural analyses. The models are constantly compared with test results, where applicable, to ensure that reasonable output is being achieved at each step of the analysis, and also to the previous models used to ensure accuracy. The ultimate endpoint is to use the results of the two-dimensional thermal analyses in Chapter 4 as input into a three-dimensional structural model to attain practically usable results.

5.2 State of the Art

There has been a broad range of research conducted on the performance of different types of timber under varying load conditions in fire. As structural modelling of timber systems in fire generally requires a degree of thermal modelling to be conducted in parallel, complex studies on timber systems can be time consuming and hence are not as common. The state of the art review given here covers thermal and structural modelling, adhesives and design methods.

5.2.1 Thermal Modelling

A number of authors have investigated the properties of timber under fire conditions without venturing into advanced numerical modelling of three-dimensional behaviour. Peng (2010) has looked at bolted connections in timber members, and conducted thermal modelling in ABAQUS and validated this against experimental results. The structural modelling was limited to the calculation of embedding strengths and comparison with experimental data. However, Peng also developed simplified methods for predicting the fire resistance of heavy timber connections based on the thermal analysis and the empirical data obtained. Although only looking at fasteners, the methods used by Peng (2010) are fundamentally similar to those which are used in the current research and provide a valuable point of comparison for such work.

A comprehensive analysis of the thermal impact of a fire on LVL members has been conducted by Fragiacomo et al. (2010) in which a number of LVL specimens were burned in small-scale furnace tests. Two-dimensional thermal modelling of the sections was conducted in ABAQUS,

and proposals were made for modifications to the guidelines on some thermo-physical parameters specified in literature, including those from the fire part of Eurocode 5 (CEN, 2004). The LVL material and modelling software used by Fragiacomo et al. (2010) is identical to that used in this particular research thesis; hence many comparisons can easily be made between the results. Although the modelling effort does propose changes to some thermo-physical parameters for thermal modelling, it has been decided for the current research that the guidance from the Eurocode is followed due to its wide acceptance in the field and the validations made in Chapter 4.

5.2.2 Adhesives

Research conducted by Craft et al. (2008) investigated the performance of a range of adhesives in loaded specimens of finger-jointed timber when exposed to elevated temperatures. A range of testing procedures were analysed, and from this a small-scale testing method was developed for this purpose. A large number of adhesives were tested under load at 200°C, and it was found that the phenol-resorcinol formaldehyde (PRF) and melamine formaldehyde (MF) adhesives performed extremely well during testing, with no adhesive failures. This result is encouraging as the PRF adhesive in these tests is the same as the adhesive used in all the LVL investigated in this research, further reinforcing the idea that an adhesive failure can be safely ignored in this research. Seven polyurethane adhesives and one polyvinyl acetate (PVA) with a phenolic compound were also tested, with failure occurring very quickly during testing, many not lasting five minutes under load. The results were found to be conclusive as the test specimens failed with no failure in the timber, as shown in Figure 5-1.

Figure 5-1: Failed polyurethane adhesive test specimens (Craft et al., 2008)

Klippel et al. (2011) attempted to model the influence of adhesives on the load carrying capacity of glulam members in fire, which involved a sequential thermal-stress analysis and some

experimental testing of glued joints. ABAQUS was used for the two-dimensional thermal analysis, and the program CSTFire (Schmid et al., 2010) was used for the mechanical analysis. The software allows for the ductile behaviour of timber at elevated temperatures, and the shear forces between glued lamellas are calculated to determine failure. It was found from the modelling, and on comparison with experimental results, that the fire resistance of glulam is governed by the bending resistance of the beam and not by the shear resistance. Although the effects of adhesives are not considered in detail in this research, the results from the numerical modelling provide an insight into the expected failure behaviour of glued timber assemblies.

5.2.3 Structural Modelling

Sequential modelling has been conducted on timber members and systems in the past. However, it very commonly only considers members in either tension or compression. This is because modelling bending with timber is more complex than pure compression or tension, as it requires deflections to be calculated in two separate directions, as well as the method of failure being properly defined and modelled. The anisotropy of the material and the selection of suitable elements further complicate the numerical modelling process, as deciding when and where failures occur and how these happen is difficult with so many degrees of freedom. As opposed to ambient conditions where a beam in bending will fail at the extreme chord in a brittle manner, numerical modelling must account for the redistribution of stresses to the inner parts of the beam under fire conditions. To obtain sensible results it is important to ensure that what others in the field have done can be modelled alongside the current research at each stage of development, so a final three-dimensional model incorporating the properties described above can be achieved with a reasonable level of certainty in the results.

One such study involving sequential modelling is that of Fragiacomo et al. (2010) which involved the experimental testing of LVL in tension in a small-scale furnace, and the efforts to numerically model the tests. The tests were conducted on rectangular sections of LVL, half immersed in a furnace and loaded under a constant tension force. A sequential thermal-stress analysis was then carried out in ABAQUS concentrating on modelling the experimental testing by first building a thermal profile of the timber section, then inputting this into the three-dimensional structural model considering axial forces only. Failure was considered to occur when the elements were no longer able to properly redistribute stresses to cooler regions, hence the solution was seen as diverging and failure time was taken as the last increment in the model. The results of the numerical model slightly under predicted the temperature in the timber when compared with the experiment, but overall it was a good approximation of the thermal behaviour. The work

provides an insight into ways in which ABAQUS can be used to model simple structural behaviour under fire conditions.

A comprehensive investigation into the performance of timber I-joists in fire was conducted by Tabaddor (2011), which focussed on the sequential thermo-stress analysis of the timber beams. For instance, effective thermal material properties were used in the thermal analysis, the heat source was modelled with simple boundary conditions, and the structural modelling was coupled with the thermal analysis in a similar fashion. ANSYS was used for the numerical modelling portion, which is a physics-based software very similar to ABAQUS. Simulation times for the numerical models were low due to the slenderness of the members being modelled, this resulted in very short failure times in the fire (less than 20 minutes). The major findings of the research were that the thermal input has a significant impact on the deflection response of timber assemblies and conducting actual furnace tests aid greatly in validating numerical models. It was also found that simplified boundary conditions describing the fire, loading and supports can produce meaningful results.

Work to develop an integrated model for predicting the fire resistance of timber floor assemblies has been undertaken by Takeda (2010). A heat transfer study was conducted for traditional joist floors, followed by a simplified elastic structural analysis. The effects of joist re-radiation, protective membranes and gap openings were included in the heat transfer analysis; however the structural analysis did not consider plastic behaviour. The results showed a relatively good correlation to the experimental data.

Due to a preference for prefabricated processes in the construction industry the CLT market in Europe is vast, relatively optimised and competitive. From this has spawned a wealth of research investigating potential issues with the CLT system. Although this is only covered briefly here, a large database of literature on the subject is available on the internet. Research conducted by Fragiacomo et al. (2012) provides a good background on much of the current work looking at CLT systems in fire in Europe. In their study a number of large CLT slabs were tested in a full-scale furnace at the Ivalsa Trees and Timber Institute in Italy. Four point bending tests were conducted on eight 5-layer, 150 mm deep CLT panels spanning 5 metres across the furnace. A sequential thermo-stress analysis was conducted using ABAQUS following Eurocode guidance. The concrete damaged plasticity model was used to fully characterise the stress-strain relationships of timber in tension and compression, and due to computational limitations only a small block of CLT was modelled. The thermal modelling effort gave comparable results

to that measured during the experiments, and the structural modelling effort predicted the results of the experimental testing to within 2% using Eurocode 5 (CEN, 2004) degradation laws for the mechanical properties of timber.

Other modelling software has also been used to analyse CLT in fire, as described by Schmid et al. (2010) in which the SAFIR and CSTFire programs were used for the respective thermal and structural analyses. Small-scale furnace tests were also performed on protected and unprotected CLT specimens, and a simplified model developed for the design of CLT assemblies for fire resistance. Some major findings of this work were that the current Eurocode guidance on zero strength layers may not be adequate with regards to CLT, and proposals were made for a more adequate range of zero strength layers for design. What is apparent from much of the research is that due to the relatively recent development of CLT there is a definite need for more research on its behaviour to effectively influence current code guidance to ensure structures are designed adequately for fire resistance.

5.2.4 Design Method Development

As with the previously discussed literature, Bobacz (2006) also investigated axially loaded timber members not only considering them tension but also in compression. A large portion of this research was geared towards defining an appropriate charring model based on earlier existing literature. The model was broadly based on investigating compartment fires. Then a generic thermal model was developed from this to adequately predict the temperature profile throughout a cross-section of timber. This member was then mechanically simulated under fire conditions in ANSYS. In terms of assessing failure, Bobacz only considered cross-section analyses in which a displacement controlled strain was applied until the ultimate strength was reached, and then the ultimate load at this point was derived from the integration of the stresses over this cross-section. From this he proposed a stochastic method to sizing members for fire based on inputs of the three major modelling sections above. At each major step the modelling was checked against the simplified methods available in the literature (CEN, 2004), and validated against experimental testing where possible. This research was comprehensive in both defining timber properties in fires and simplified ways of thermally and structurally modelling timber, and provided good results for comparison with other numerical models.

Some less recent research conducted by Thomas (1996) gives a comprehensive analysis of the fire resistance of light framed walls and floors undertaking compartmental, thermal and structural modelling. For the modelling effort effective values were developed and used to more

accurately represent the real behaviour of the timber systems. Some of the major findings by Thomas with regards to timber assemblies were that simplified time equivalence formulae were not entirely appropriate for the estimation of the performance of timber assemblies in fire. Structural modelling was validated by tests conducted by König (1995) on timber joists exposed to fire. Guidance was given on appropriate means of using time equivalence formulae, and alternative design methods were proposed for calculating the expected fire resistance of timber assemblies within a building. A conservative temperature based failure criterion for structural performance was derived. However its applicability to much larger timber members such as those used in this research is limited due to the relative sizes, and hence fire impact on the respective assemblies.

5.3 1D Modelling

5.3.1 Introduction

A common first step in modelling structural assemblies is the one-dimensional idealisation of the structure and its interaction with the environment. One-dimensional modelling can be limited in the scope of inputs possible and the subsequent levels of output detail. However, it is also a powerful tool in understanding simplified system behaviour, and can be used to verify many basic initial assumptions in the modelling process.

In this research the limitations and capabilities of one-dimensional structural analysis are investigated with regards to timber floor assemblies in fire.

5.3.2 Objectives

The objective of the one-dimensional structural modelling was to enable the competent modelling of different loading conditions on timber such as tension, compression and bending, and to compare with experimental results.

A secondary objective was to determine whether further levels of complexity are required, and if one-dimensional modelling can adequately model the floors in question to a required degree of precision. This involved an investigation into the element types and thermal inputs possible for one-dimensional members, and their application to complex real problems. Hence one-dimensional modelling was used as an entry point to fully understanding how to use the software appropriately for the tasks required.

5.3.3 Boundary and Loading Conditions

Pinned roller support conditions were specified at the ends of the effective span length of the floors, restricting movement and rotations out of plane.

Loading conditions are simulated as point loads in the model. This is applied to the nodes corresponding to loading points. For example when simulating the floors tested in the furnace the point loads are applied to nodes corresponding to the line loads on top of the specimen.

A simplified depiction of these conditions are illustrated in Figure 5-2.

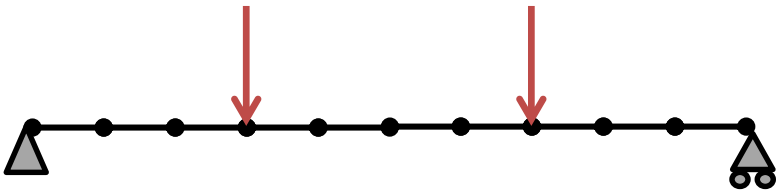

Figure 5-2: Boundary and loading conditions of the 1D structural modelling

5.3.4 Time-step and Solver Technique

In the structural analysis the direct sparse solver technique in ABAQUS was used, using Newton's technique to solve the nonlinear equations with linear extrapolation. Automatic time-stepping procedures were specified to ensure numerical stability in the solution convergence.

5.3.5 Element Type

Standard 2 node linear beam elements were used to perform the tasks required. The entire floor length is modelled, connected by a number of beam elements in a line. For the following analysis 30 beam elements are used to model the experimental floor, each element having a length of approximately 140 mm.

5.3.6 Thermal Input

As the element type does not allow sequential input of temperature profiles during the analysis, the only method of inputting temperature gradients through the beam is by direct specification defined over a specified number of steps. This is implemented via geometry profiles in the software, and generic shapes such as t-beams and box beams are used for the purposes of this research as an approximation to the floor geometries tested. Issues arise with this method in that temperature values are only integrated through these profiles at a set number of points,

hence a very inaccurate temperature profile can be specified for the section. Figure 5-3 shows examples of these for an I-beam and a box beam in space.

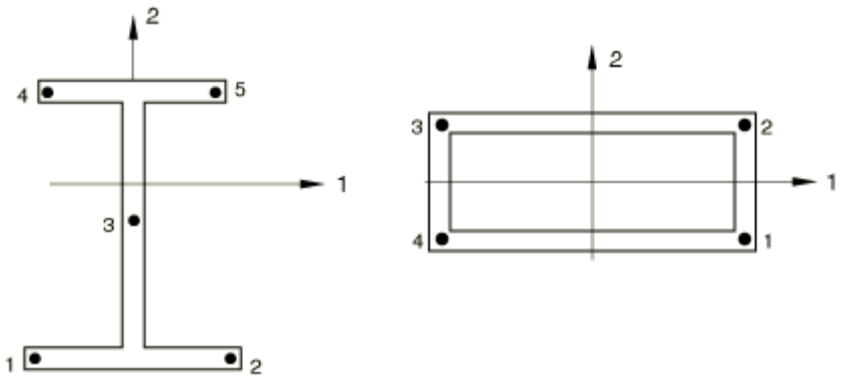

Figure 5-3: Temperature input points for beam elements (ABAQUS, 2010)

This may be adequate for lumped mass heating methods when dealing with steel members; however temperature approximations must be made for timber to produce meaningful results.

5.3.7 Material Model

The material model used is the concrete damaged plasticity model. A more detailed discussion on the inputs used in this model and its development is described in Section 5.6.

5.3.8 Test A

The heated analysis is run over 10 steps in which at each step a thermal input is specified for the integration points for a T-beam (as shown for an I-beam in Figure 5-3 with no bottom flange). A lumped mass approach must be taken, thus values to characterise the temperature of the timber joist at these points are taken from Figure 4-8 for the 10, 20 and 30 mm depths as a sensitivity study. This is an approximation of the average temperature of the section for a 90 mm thick joist under two-sided exposure. The same three depths are also used for the 36 mm thick slab under one-sided exposure. Although the heat penetration through the timber is not linear, these are used as an approximation of the average temperature of the section at that point. The mid-span displacement for the analysis of Test A with the three different temperature profile inputs is shown in Figure 5-4.

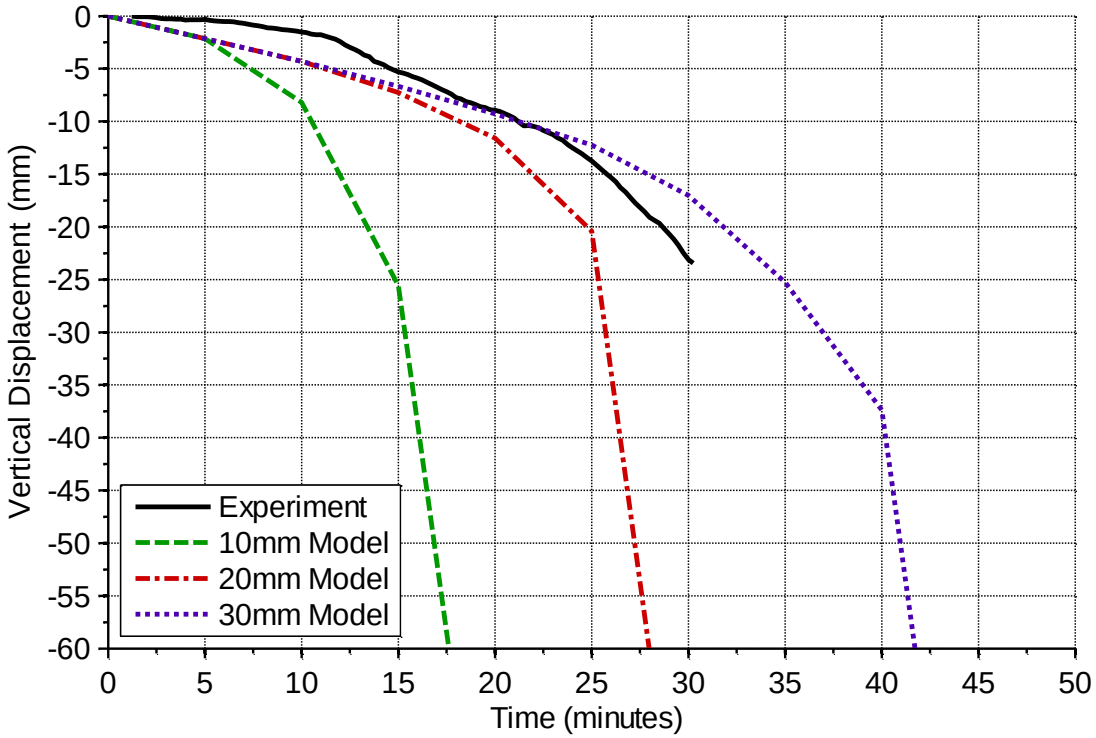

Figure 5-4: One-dimensional structural modelling of Test A

The purpose of this study is to gain a relative insight into the feasibility of the one-dimensional method, and the results are expected to be equally as coarse as the inputs. It is clear from the plot that the results are highly dependent on the temperature profile input, and using the temperature records for the 10, 20 and 30 mm depths gave a large range of results.

Figure 5-4 shows that the results are purely speculative and highly dependent on the temperature inputs, which are not well known in this case. Hence further experimental comparisons are not conducted here as the level of input complexity is not great enough to warrant further analysis when considering timber assemblies under fire loads.

One-dimensional modelling of timber floor assemblies in this manner is not recommended unless an in-depth understanding of a lumped mass average temperature for the section geometry is known.

5.4 2D Modelling

5.4.1 Introduction

Two-dimensional modelling at first glance may seem to be the logical next step to progress from one-dimensional modelling; however there are serious limitations which must be considered when attempting to simulate the behaviour of a heated material. The question of thermal inputs is again raised as to how they are implemented in this format, as three-dimensional behaviour is desirable across the entire floor assembly.

Due to the nature of two-dimensional modelling, the global behaviour of a floor cannot be properly considered as the finite thickness of the elements must be specified. Hence it is best described as only a "slice" of a floor can be investigated for a given time, and global floor behaviour cannot be modelled in this way. If a three-dimensional model is constructed from two-dimensional shell elements, limitations on the degrees of freedom in the elements and the method of thermal gradients applied through sections becomes a major issue. As elements such as these can only transmit heat in two directions, the three-dimensional impact of a fire on the underside of a floor assembly can only be crudely modelled in this manner, and major application issues are raised on the functionality of this modelling with regards to different three-dimensional floor geometries. An example of this is shown in Figure 5-5, where a concept of the heat transfer conditions required is shown on the left, and a possible two-dimensional configuration of the heat transfer of the floor using shell elements is shown on the right. The arrows signify the planes in which heat transfer is required (left) and possible (right) for a fire on the underside of the floor systems.

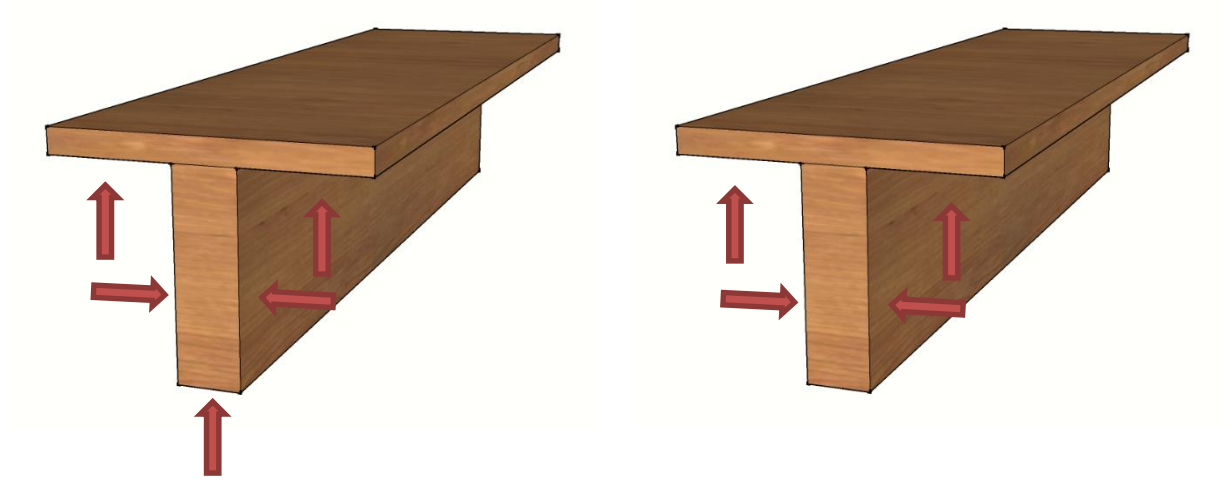

Figure 5-5: Heat transfer concept required (left) and a possible floor configuration using 2D elements (right)

Figure 5-6 shows generic shell elements for stress analysis where the temperature can only be varied through the thickness of the elements, between sides numbered 1-3 and 4-6 (left) or 1-4 and 5-8 (right).

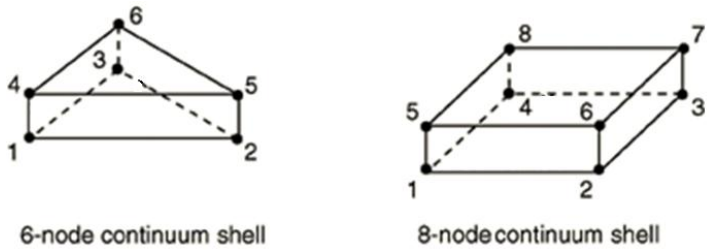

Figure 5-6: Solid continuum 2D shell elements

In this regard, two perpendicular directions of heat flow through the same element cannot be modelled, and this is required for modelling the floor assemblies described in this research.

5.4.2 Concluding Remarks

Although two-dimensional modelling has a vast range of applications, for this particular type of problem it may be more difficult to implement with less obvious gains than can be foreseen from using a three-dimensional model. Due to the above difficulties, it was decided that progression to a three-dimensional model would be attempted as this type of modelling is able to capture global behaviour, and complex thermal profiles can be used as inputs as has been shown by similar research in the field which has also tended to use three-dimensional modelling.

5.5 3D Modelling

5.5.1 Introduction

In order to fully encompass complex thermal profiles for timber sections, three-dimensional modelling is a critical step in evaluating the fire resistance of unprotected timber floor assemblies.

A number of complexities arise with the graduation from one to three-dimensional structural modelling, such as element behaviour, loading and boundary conditions, failure modes and stress analysis. Although the method and scope of inputs become more complex and can be applied to a wider range of situations, this does not automatically imply that the output from the model will be a better approximation of reality than a one-dimensional model. Rather, a more in-depth analysis can be conducted for a certain situation and more detailed results relevant to that

problem can be calculated, which is what is required in this research with regards to timber floors in fire.

5.5.2 Objectives

The primary objective of the three-dimensional structural modelling was to fully investigate and predict the performance of structural timber floor assemblies exposed to fire conditions. This was achieved via a sequentially coupled thermo-stress analysis, utilising the thermal model developed in Chapter 4. The bulk of this investigation involved building on and developing the procedures investigated in the one-dimensional structural modelling of floor systems, and comparisons are made with the experimental furnace results obtained in Chapter 3 for validation purposes.

A secondary objective was to run a sensitivity analysis on the different facets of the modelling procedure to assess the range of inputs used and their influence on the results obtained.

5.5.3 Initial Conditions

For these types of analyses the major initial conditions set are the predefined fields for temperature, set at an ambient value of 20°C. Due to the input of the thermal profile during the heating steps, this is only important for an ambient displacement check on the structure before heating, and as a reference temperature (for thermal expansion).

5.5.4 Loading Conditions

The loading arrangement simulated in the numerical model follows the experimental setup. The loads are assumed to be applied on a rigid steel plate. The plate was not included in the thermal analysis, and it was considered to be at room temperature for the duration of the simulations. The load was applied to the top surface of the steel plate as a pressure. The applied forces were transferred to the timber surface through rigid ties between the plate and the slab surface.

The load is applied gradually during the initial stage of the analysis. This is implemented in a number of separate steps in ABAQUS for the simulations shown in this chapter. The final step is the heating step where the results of the transient thermal analysis are used as input for the fire duration modelled.

5.5.5 Boundary Conditions

In order to avoid element distortion and stress concentrations at the support points of the beam, the bearing area of the pinned roller supports was spread over two rows of nodes at the ends of

the floor beams. The simulated span of the beam was adjusted to accommodate this so that the interior nodes were considered to be at the location of the pinned base connection.

The axes of symmetry shown in Figure 4-3 were maintained in the structural modelling. At these planes of symmetry the rotation and translation was fixed to ensure that a full floor was simulated in the model. For example, a plane of symmetry cutting through the length of the floor simulates fixed translational motion transverse to the span direction (the reaction force), and fixed rotation in both directions of that plane (the reaction moments). Hence the floor is ideally simulating a mirror image of each boundary.

5.5.6 Time-step and Solver Technique

In the structural analysis the direct sparse solver technique in ABAQUS was used, using Newton's technique to solve the nonlinear equations with linear extrapolation. The model allowed for geometric nonlinearity. This is important for analyses where relatively large displacements in one plane may affect stresses in a perpendicular plane. Automatic time-steps were used to optimise the modelling procedure, and to ensure numerical stability in solution convergence.

5.5.7 Element Type

The element type used in the three-dimensional structural analysis is an eight node solid continuum linear brick with reduced integration and hourglass control. These elements have temperature and displacement degrees of freedom activated at each node which allow for the thermal input to be modified over a specified step time while conducting a stress analysis.

A study by Fragiacomo et al. (2010) found that for sequentially coupled thermo-stress analyses modelling timber in tension, the twenty node linear brick elements showed no noticeable improvement in results obtained with a significant increase in computational time required to run simulations. Due to the similarities between that study and the current research, the eight node linear brick element has been specified to economise the available resources. Figure 5-7 shows both the linear and quadratic solid continuum elements for stress analysis.

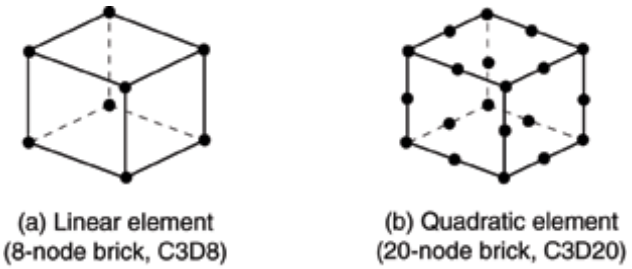

Figure 5-7: Solid continuum 3D elements

In ABAQUS reduced integration is used to economise run time by using a lower-order integration to form the element stiffness matrix. This results in reduced run times, and usually provides more accurate results in three-dimensions as long as element distortion is limited. Reduced integration also avoids issues with shear and volumetric locking.

Hourglass control is required with first-order reduced integration elements as the elements can distort in such a way that strain calculations at the integration points are zero, leading to further mesh distortion and instability. This is known as hourglassing, referring to the shape of the distorted elements.

5.5.8 Material Model

The concrete damaged plasticity model was used due to its functionality in allowing for different strength curves to be defined in tension and compression, which is a key aspect required for timber modelling. Further information on the material model and a detailed description of the model development is given in Section 5.6.

5.5.9 Thermal Expansion

Thermal expansion is extremely important to consider in structural analyses, as when the structure is restrained a change in temperature will cause a change in the stress state of the elements. In the case of modelling a floor in three dimensions, restraining the floor in any direction results in an increase in the stresses with an increase in temperature, hence proper definition of support conditions are paramount to ensure appropriate analysis.

Although the floor assemblies under study are simply-supported and free to move at one end, any additional expansion or contraction effects will influence the vertical displacement of the floor assemblies. The coefficient of thermal expansion is highly dependent on the moisture content, grain direction and temperature of the timber. Common values for softwoods parallel to the grain range from $3.0 - 4.5 \times 10^{-6}$ m/mK (Glass and Zelinka, 2010; Weatherwax and

Stamm, 1956), with both radial and transverse directions being approximately 8 and 13 times greater than the parallel to grain value respectively. Due to the lack of available data to determine the actual variation of the coefficient of thermal expansion for LVL, a set value of 3.5×10^{-6} m/mK was specified in the analysis. A parametric study into the effect of the thermal expansion coefficient is presented in Section 5.8.4.

As discussed in Section 2.7.2, the char which forms on the outside of timber as it burns tends to shrink, while a normally moist timber member exposed to a thermal gradient will also expand initially but would tend to shrink at higher temperatures as the moisture is driven off. In terms of a large timber member exposed to fire, some moisture is driven off while some is driven deeper into the section increasing the remaining moisture content of that section, and it is important to appropriately quantify how the entire member will behave and whether to incorporate thermal expansion effects. As the heated section of the timber is very small compared with the residual section for the majority of any fire duration, the effects of thermal expansion are likely to be relatively small on the global system when compared with a material such as steel.

For a timber floor assembly, the uneven expansion of the floor in the cross-section will be crucial in the concentration of stresses on that cross-section. This effect will increase as the heated portion of the floor increases, in other words during the latter stages of burning. However, both radially and transversely the effects of thermal expansion will also be nullified by the presence of the shrinking char layer as the fire progresses. Hence for the following analyses an isotropic coefficient of thermal expansion of 3.5×10^{-6} m/mK is specified.

5.6 Material Model Development

The material model used in the analysis has the most significant impact on the output due to its influence on structural behaviour. A major aspect of the numerical model development has always been to achieve a consistent level of crudeness in each input.

Although many other factors can be modified in the structural analysis with regards to ensuring a closer fit to the experimental results, this is completely dependent on the model setup, the floor geometry, and most importantly the thermal input. The method adopted in this research is to build a numerical model which uses inputs as published values from the literature, and to investigate simple means of modification to factors to some proposed guidelines as opposed to well defined and reported properties.

The primary material model used in the development of the structural model is the concrete damaged plasticity model. Although other material models were also used in unison with this material model, the output and capabilities of the concrete damaged plasticity model were found to be the most adequate for modelling timber floors in ABAQUS. A sensitivity study on some of the major material models used in the structural analysis is shown in Section 5.8.3.

When adapting existing material models to perform in a specific manner, as is the case in this research, it is important that the limitations of the material model are known and that any modifications made do not simulate unrealistic behaviour. When adapting the concrete damaged plasticity model for timber, a number of the features of the model are useful while some have a detrimental impact on the output. The major features of the model and some modifications to this are discussed in this section.

5.6.1 Moduli of Elasticity and Rigidity

The modulus of elasticity is defined over a range of temperatures congruent with the guidance from the literature, discussed in Section 2.8.1, and presented again in Figure 5-8.

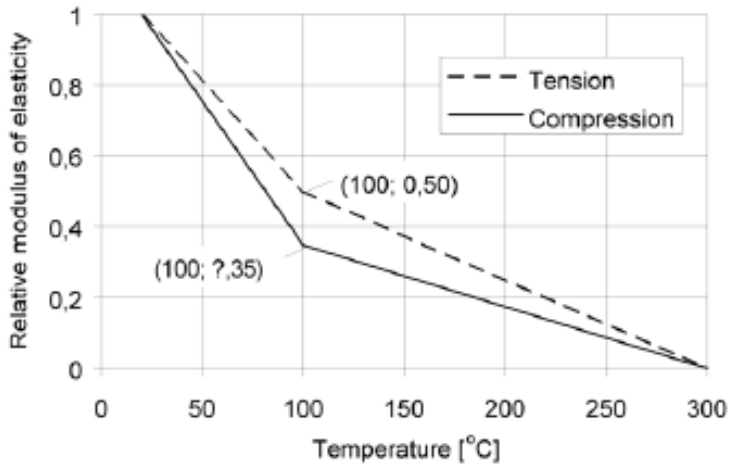

Figure 5-8: Effect of temperature on modulus of elasticity parallel to grain of softwood (CEN, 2004)

The definition of the linear elastic properties over the range of temperatures specified by the guidance requires the assumption of elastic isotropy for the material. Because of this assumption, the reduction factors for compression are used for the elevated temperatures for both compression and tension, as these values are larger in magnitude than those specified for tension (hence more conservative). As the modulus of elasticity in the primary (strongest)

direction is defined for the isotropic material, the influence of the secondary and tertiary directions on the loadbearing resistance of the one way system is not able to be modelled.

Issues arise with the definition of the modulus of rigidity, in that the linear elastic model is used for implementing these values; hence the modulus of rigidity is calculated via the following relation:

$$G = \frac{E}{2(1+\upsilon)}$$ **Equation 5-1**

Where: G = Modulus of rigidity (MPa)
E = Modulus of elasticity (MPa)
υ = Poisson's ratio

Traditionally with timber the following relation is used for a rough estimate of the modulus of rigidity (Bodig and Jayne, 1982):

$$G = \frac{E}{16}$$ **Equation 5-2**

As with clear specimens of timber, this approximation generally holds true for LVL. Thus the relation described in Equation 5-1 defines a relatively inappropriate modulus of rigidity for the timber being approximately five to seven times greater than what would normally be defined as an appropriate range for LVL, however this cannot be avoided using the model. The effect of this is to model a stronger section, hence giving a stiffer displacement response as shear deformations are lower.

5.6.2 Poisson's Ratio

A value of 0.3 is specified for the Poisson's ratio in accordance with measured data for pine softwood parallel to the grain (Kretschmann, 2010). Due to the physical limitations on Poisson's ratio which are implemented in ABAQUS, attempting to modify the calculated modulus of rigidity by varying the value of Poisson's ratio was not feasible.

5.6.3 Strength

Under uniaxial tension the model allows for definition of a linear elastic stress-strain relationship until a yield stress is reached, at which point a softening stress-strain response follows to simulate to onset of micro-cracking. This model idealises the mechanisms in timber as well, as

the plastic response can be modified to simulate very brittle behaviour such as would occur in the tension failure of a timber member.

Under uniaxial compression the model gives a linear elastic response until a yield stress limit, at which point stress hardening occurs and strain softening follows, after the ultimate stress is reached. This is also very applicable to the behaviour of timber during plastic deformation, and can be easily modified to represent this behaviour. These curves can be modified to encapsulate the behaviour of the material at elevated temperatures; hence a number of curves can be defined for both tension and compression over a wide range of temperatures. The addition of plasticity is vital for modelling timber in fires, as timber has been found to become more plastic at higher temperatures with the migration of moisture through the section. An in depth analysis of plastic and elastic models is given in Section 5.8.3. Reductions in strength for both compression and tension are taken from the guidance found in the literature and discussed in Section 2.8.2.

The model values for the plastic strains were taken from small-scale testing conducted on LVL at the University of Canterbury, summarised by van Beerschoten (2013). These were from ambient temperature tests. In order to achieve similar stress-strain behaviour shown in the profiles by König and Walleij (2000) and Buchanan (2001) at elevated temperatures, arbitrary values were specified an order of magnitude higher than those found from the tests for the plastic strains. A representation of these curves is shown in Figure 5-9.

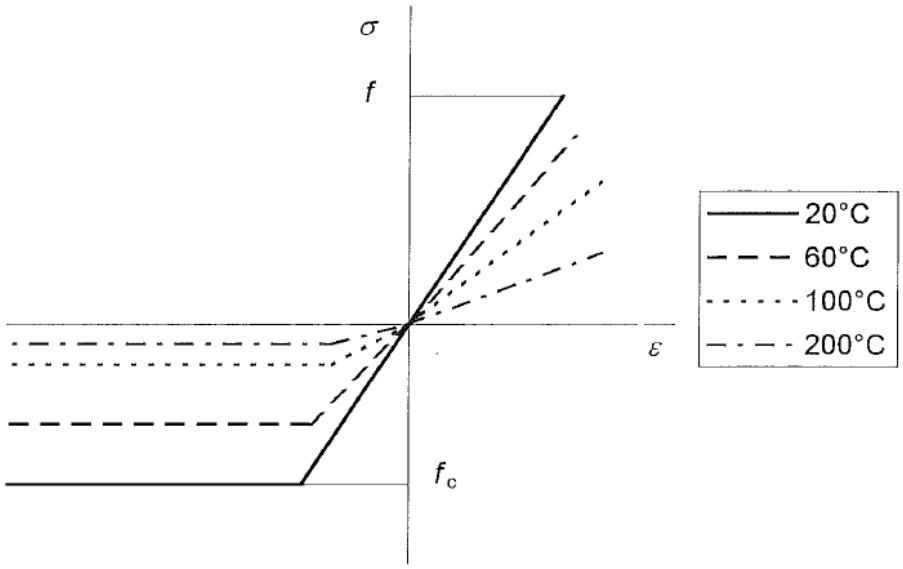

Figure 5-9: Temperature dependent stress-strain relationships (König and Walleij, 2000)

It was assumed that a greater degree of plastic behaviour would occur at higher temperatures and specifying higher strain values at lower stress limits would achieve this. A parametric study was conducted on the effects of changing these values, the results of which concluded that for modelling these types of timber assemblies the values specified here had only a small impact on the response of the assemblies. This was due to higher levels of stress and hence more plastic flow occurring at elevated temperatures, thus a higher sensitivity to the values characterising this plasticity.

5.6.4 Damage

The damage function is implemented in ABAQUS as a function of cracking or crushing strain, and the absolute damage value defined corresponds to a reduction in the stiffness during that step. For example when a value of 0.1 is specified, this results in a 10% reduction in the stiffness at this point and the next step must either be increasing or stay constant with this level of damage. This has the effect of simulating damaged concrete behaviour in such a manner that numerical instability will occur during the simulation, and this point corresponds to a critical failure when the loads can no longer be supported by the assembly.

Although it has been shown to work as expected for predicting the failure time of a timber assembly by tension, material properties data available in the literature for measured strain at elevated temperatures is severely limited. This is due to the costs of testing in furnace conditions, the difficulty in measuring strain values accurately and absence of appropriate standardised test methods for very specific purposes. This lack of information makes it difficult to properly characterise the stress-strain curves for timber at elevated temperatures, hence a parametric study was conducted to assess the impact of each factor on the analysis.

It was found that the choice of cracking strain was crucial in determining the failure time of the floor assembly, and due to the lack of available data for this at elevated temperatures it was decided that the damage function would not be implemented into the structural model at this stage of the research.

Care must be taken when adapting material models developed for other materials to force specified behaviour such as in this research. As a greater level of complexity is implemented by the model, a similar level of understanding and modification must be made to the model in order for it to function as desired. Ideally if a full set of tested values for strain at elevated temperatures was available for the LVL in question and time restrictions on the research were not so stringent, the effects of damage for this application could be considered in more detail.

A comprehensive description of some of the caveats of modelling damage is discussed by Kmiecik and Kaminski (2011) with regards to reinforced concrete, however the principles remain the same when applied to timber.

5.7 Experimental Comparisons

In order to gain an insight into the adequacy of the steps taken during the construction of both the thermal and structural models, experimental test data is used as a validation measure. The experimental furnace tests in Chapter 3 provide an excellent set of base data to make comparisons with. Hence each of the four timber composite floors tested is simulated in this section in a sequential thermo-stress analysis. The results of the thermal analyses of these experimental floors from Chapter 4 are used as an input into the structural models.

5.7.1 Test A

The structural modelling effort for Test A is shown in Figure 5-10, with the solid black line representing the experimental results and the dashed red line representing the modelling effort.

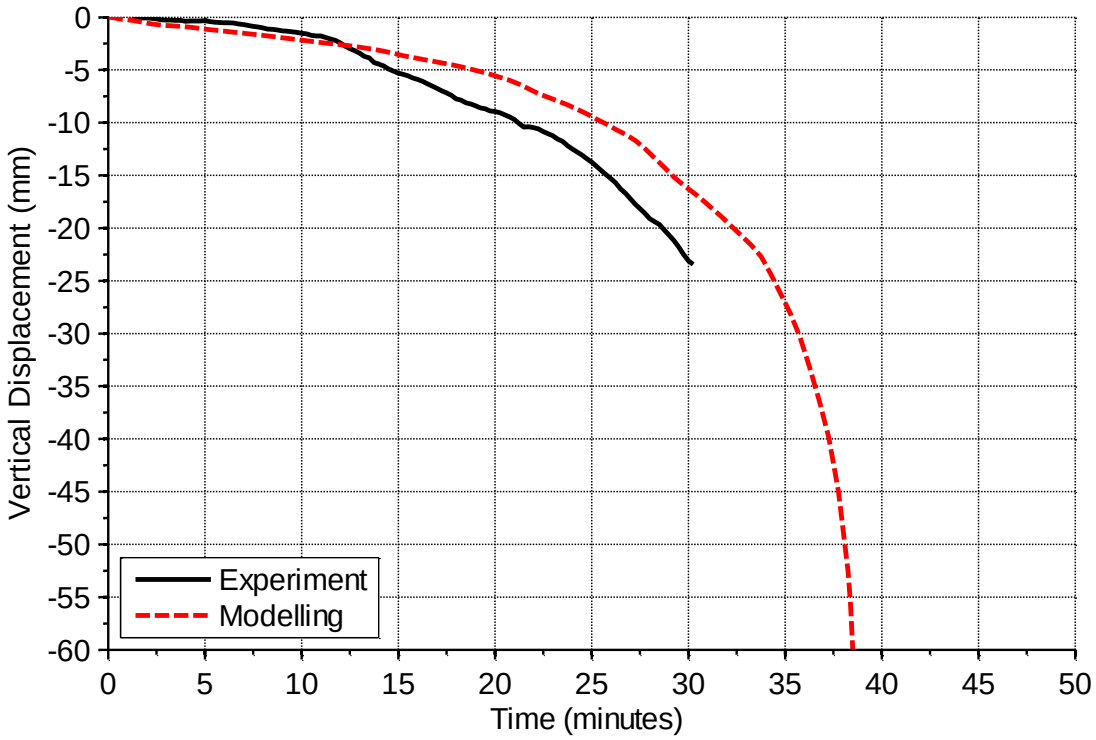

Figure 5-10: Structural modelling of Test A

As the data set for Test A terminates at 30 minutes it is relatively incomplete, hence the failure time of the floor can be speculated on by considering the displacement response of the floor up to 30 minutes and with comparisons to Test B. With this in mind, the modelling effort predicts the displacement response of the experimental results to within a margin of 20% for the entirety of the test, with the discrepancy between the results from approximately 12 minutes due to uneven floor displacement as shown on the potentiometer readings in Figure 3-29. Failure is predicted by the model at 38 minutes, which is clearly near a reasonable expected failure time of Specimen A during the furnace testing.

An artefact of this form of modelling is that the elements assumed to be char still carry some load at temperatures above 300°C. This is due to the limitations of the strength reduction factors built into the modelling software, in an effort to avoid numerical instability. In ABAQUS the strength and stiffness values can only be reduced to one percent of the maximum defined value, resulting in a weak outer section which still carries load but should ideally simulate zero load carrying capacity. Hence the plasticity inherent in the material model used and this phantom residual strength results in large runaway displacements in the modelling. However failure is relatively easy to predict as the point at which the displacement response increases rapidly, as observed here at approximately 37 minutes.

This behaviour is seen to a much larger and more noticeable degree in the work by Tabaddor (2011), in which the timber beams modelled were much more slender, hence a greater proportion of the residual section became char over a much shorter period of time in comparison to the floors described in Chapter 3.

It should be noted that the purpose of these comparisons is to assess the validity of the model for predicting the response of timber assemblies in fire. As such, the aim is not to calibrate the model but rather explore the limits and capabilities of the finite element software, and identify areas where further study is required.

5.7.2 Test B

The structural modelling effort for Test B is shown in Figure 5-11.

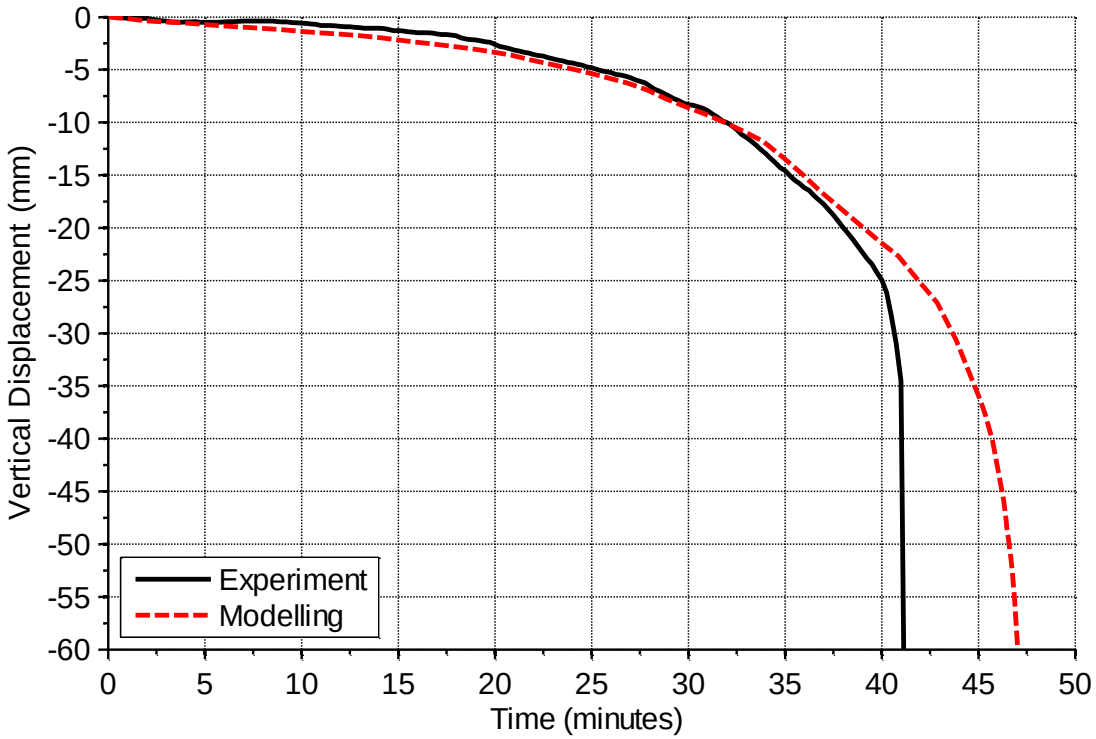

Figure 5-11: Structural modelling of Test B

Similar to the modelling results of Test A, the model predicts the displacement response of the experimental results for Test B accurately for most of the test duration. The model predicts failure at 47 minutes.

It can be seen from the latter stages of the test that the displacement response tends to be over predicted by the numerical model, while the floor displacement throughout the duration of the test (until approximately 38 minutes) is well predicted by the model. This reinforces the choices made with regards to the elastic material properties, boundary conditions and the coefficient of thermal expansion; however as seen in the figures, the strength properties of the model in these conditions do not predict the failure time of the floor conservatively.

5.7.3 Test C

A comparison of the deflections from Test C and the structural model is shown in Figure 5-12.

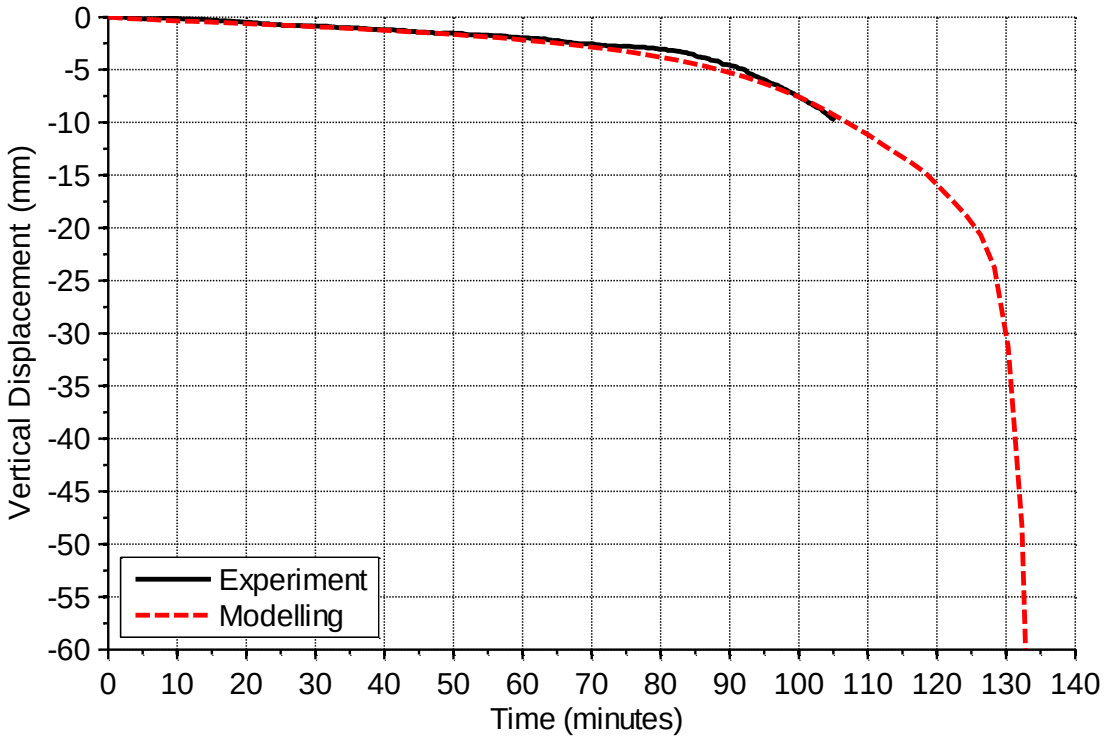

Figure 5-12: Structural modelling of Test C

Similar results are reproduced for Test C, with a better prediction of the stiffness of the floor for the duration of the test. The failure time of the actual test floor was predicted to be around 120 – 125 minutes, while the model gives 133 minutes.

The artefact of the modelling in which the char layer still carries some load is exacerbated for the larger floor sections due to the larger proportion of char elements remaining near failure. This has the effect of over exaggerating the remaining stiffness, hence reducing the gradient of the displacement curve and giving higher expected failure times. However in both cases (Tests C and D), the floor tests terminated with low levels of overall vertical displacement. Hence it is difficult to draw definitive conclusions on the exact failure behaviour of the floors.

5.7.4 Test D

The structural modelling result for Test D is shown in Figure 5-13.

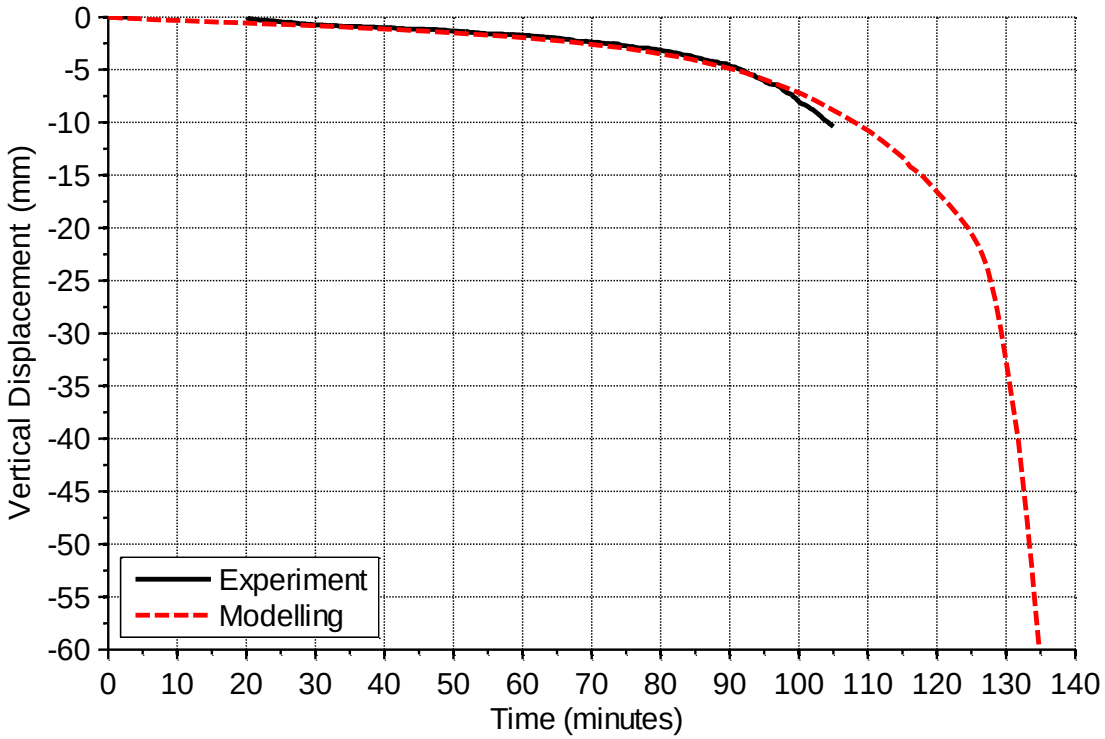

Figure 5-13: Structural modelling of Test D

The numerical model for Test D is also a good approximation for the displacement of the floor system until 105 minutes when the test was terminated, as some deviation between the model and experimental results could be seen at that stage. From the figure it can be seen that the expected failure time is predicted to be approximately 135 minutes. The predicted failure time was 120 – 125 minutes.

Despite this over prediction of failure time, much of the displacement behaviour is very accurately predicted by the model. This indicates a good correlation between the model inputs and what was measured in the experiment.

5.8 Sensitivity Analysis

In this section a sensitivity analysis on some of the major inputs into the structural model his conducted. The results from Test B are used for two main reasons. Firstly, the test data is complete as the floor was tested until destruction. Secondly, the computational intensity is much lower than for the larger floor Tests C and D, as the duration of the test is shorter and the number of elements is reduced due to the physical size of the floor being smaller. The majority of work was conducted for Test B, but checks are made against the other data sets to ensure the validity of the conclusions. The modified material model is used for all parametric studies as it is the closest approximation to the experimental results.

5.8.1 Mesh Size

As previously described in Section 4.10.3 the mesh refinement for the cross-section of the floors has been specified as a square 5 mm x 5 mm density. This current sensitivity analysis focusses on the mesh refinement along the length of the floors.

The following analyses simulate the displacement response of Specimen B for 100, 300 and 500 mm mesh lengths. The results are shown in Figure 5-14.

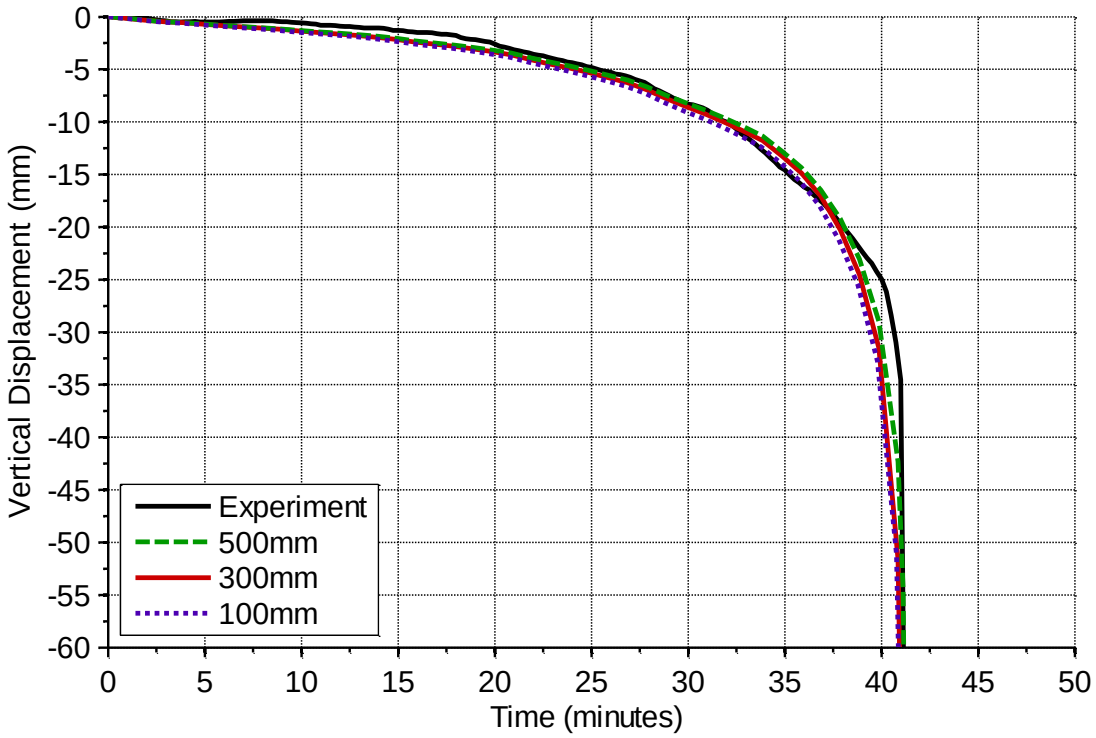

Figure 5-14: Comparison between mesh lengths for 3D structural analysis

It can be seen from the comparison that the largest mesh length results in a slower rate of change of displacement, and a very slightly higher predicted failure time of the floor in question. However these differences are very small between the tested parameter, with very little deviation between 100 mm to 300 mm mesh lengths. Hence it can be inferred that refining the mesh past 100 mm for this type of floor analysis results in very small gains in precision.

The key issue is determining an acceptable length which will achieve reasonable run times, without sacrificing a desired level of precision of the results. It is of paramount importance that the elements still act in an appropriate manner for their intended use, and must not be poorly shaped to ensure convergence to a solution. A comparison of the computational run times are given in Table 5-1 for each mesh length, with a ratio of the total run time when compared with the standard 300 mm mesh length used for the bulk of the numerical analyses.

Table 5-1: Comparison of mesh length refinement to model run time for Specimen B

Mesh Length (mm)	100	300	500
Run time (minutes)	29.0	17.5	6.5

It can be seen from comparing Figure 5-14 and Table 5-1 that only small discernible gains in output precision are made once the mesh length is refined past 500 mm. For general analysis of floors from 5 – 10 metres in span, a general guideline of approximately 250 – 500 mm is suggested for the mesh refinement along the span. This obviously can be reduced for floors with a less dense cross-sectional mesh, smaller cross-sectional areas, or if computational run time is not a major issue when running the simulations.

5.8.2 Loading Arrangement

To appropriately investigate structural modelling requires that the loading method is scrutinised to ensure different methods of applying a load give the results expected. This also enables any unforeseen model behaviour to be checked, such as element distortion and stress concentrations under concentrated loads.

The first method of applying loads was through steel plates designed to be identical to those used in the experiments, as discussed in Section 5.5.4. A separate method of applying a uniformly distributed load across the entire surface of the timber slab was used as a check to ensure any unreasonable element distortion did not occur in the steel plates or timber slab, and the contact pairs worked properly. This was simulated as a pressure across the entire upper

surface, calculated to achieve the same bending moment as the point loads in the test conditions. In this way comparisons could be made between the results, as the displacement response should be relatively similar for these conditions, but not identical. The displacement response for Test B is shown in Figure 5-15 for both loading types.

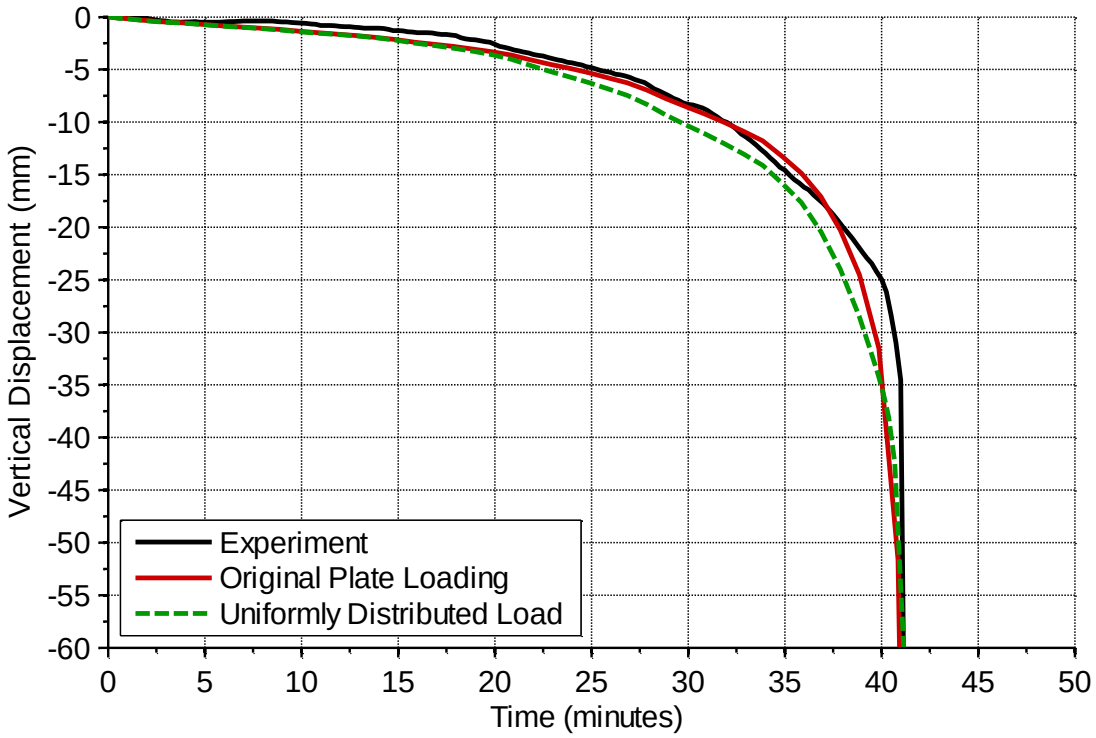

Figure 5-15: Comparison between loading arrangement for 3D structural analysis

It can be seen from the figure that changing the loading arrangement had a small impact on the results. A greater displacement response is seen through much of the test duration, with almost identical failure times predicted for both loading arrangements. Considering the moment demand through the span of the floor and hence the deflected shape, this behaviour is as expected for comparisons between uniformly distributed loading and four point loading scenarios.

This proves that for this type of analysis a simplification of the loading arrangement to be a pressure across the entire top slab is therefore appropriate as the differences in displacement response are small.

5.8.3 Material Models

During the course of the structural modelling, a number of material models in ABAQUS were used and compared to determine which was the most appropriate for defining the mechanical properties of timber. As there are no predefined properties pertaining to timber as a material, and the creation of separate subroutines to do this requires an advanced programming knowledge of ABAQUS, the material models available were adapted to suit this purpose. This provides a unique challenge in that each material model has been derived for separate purposes, and applying these to timber in the fire state requires that many assumptions need to be made to adapt their use to timber appropriately. The different mechanisms of each of these material models need to be understood, adjusted for and in some cases manipulated to produce the behaviour desired.

The major material models investigated and described in this section are:

- Engineering constants – elastic.
- Engineering constants – plastic.
- Steel – elastic.
- Steel – plastic.
- Concrete damaged plasticity.

The engineering constants material model is the most versatile of the models available for modelling in ambient conditions, and is primarily used for homogenous materials. The model allows for the definition of the moduli of elasticity and rigidity, and a Poisson's ratio for three separate directions, hence orthotropic behaviour can be easily implemented, and a vast number of materials can be simulated using this model in ambient conditions. Once the thermal loads are introduced however, the model has no appropriate method of implementing plasticity but for defining a yield stress and a corresponding plastic strain. The stress-strain curve in this material model is used for both tension and compression which in turn limits its applicability to thermal problems in timber, or any material which exhibits significantly different tension and compression behaviour.

The steel model, as the name suggests, is primarily designed for use in modelling steel materials. The definition of linear elastic properties requires the assumption of elastic isotropy for the material. The model only allows for the definition of a modulus of elasticity and a Poisson's ratio, and the modulus of rigidity is calculated from this using the generic relation

shown in Equation 5-1. Hence as with the concrete damaged plasticity model, the calculated modulus of rigidity is much larger than is preferable for timber which impacts on the results.

Figure 5-16 shows the results of the four models plotted together with the original concrete damaged plasticity model. Results have been plotted for 100 mm displacement to show the complete record of behaviour. The original concrete damaged plasticity model is plotted as a solid red line, while the other plastic models are represented by dashed lines and the elastic models represented by dotted lines. The steel models are illustrated in green and the engineering constants models are purple.

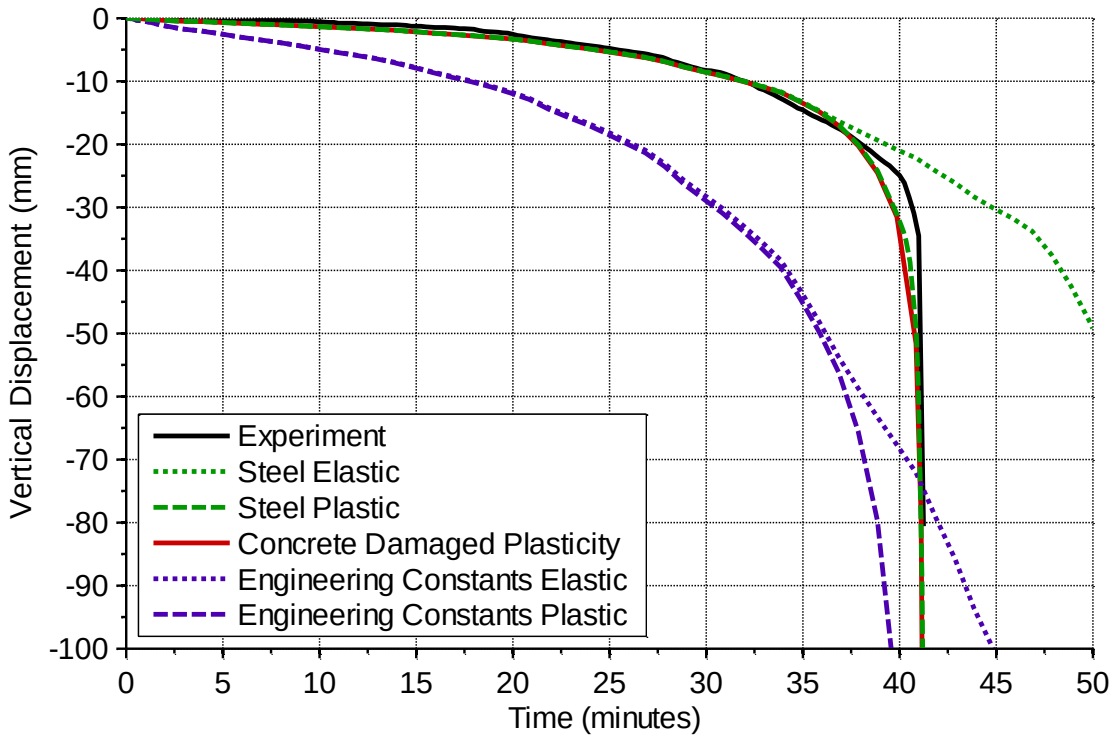

Figure 5-16: Comparison between material models for 3D structural analysis

It can be seen from Figure 5-16 that the variation in results for the material models is large. Considering the elastic engineering constants analysis, the model shows a constant large over-prediction of displacement response throughout the test, and does not give meaningful results when identifying failure behaviour. Focussing on the plastic analysis, the improvement of the engineering constants model is questionable. The modelled displacement response became greater, hence this could be argued as worse as it was now further away from the experimental

results. However a failure trend is now more discernible, and is seen from the figure to be very near to the concrete damaged plasticity model output.

The elastic steel model provides a much better approximation to the concrete damaged plasticity model output, with an over-prediction of stiffness occurring at approximately 37 minutes. It is clear that the elastic analyses cannot capture any failure behaviour, and the displacement results do not runaway at any stage.

Incorporating plasticity into the steel model has improved it from the elastic analysis, and is identical to the concrete damaged plasticity record with the exception of a very small deviation at 40 minutes. This is completely expected, as both the elastic and plastic inputs used are identical, although implemented in a slightly different manner. The downfall of the steel plasticity model is apparent when a larger range of analyses are conducted, as only a compression or tension stress-strain curve can be defined for general plasticity. Hence when a structure is analysed which fails in compression, with these inputs defined only for tension, unrealistic behaviour may result.

As previously discussed, a complete record of strain behaviour is required in order to properly characterise the behaviour of timber as a material. Inputs of properties such as strain can differ between material models, so much so that careful consideration of the model mechanics must be undertaken before simple analysis in order to obtain meaningful results.

The wide spread of results reinforces the importance in choosing an appropriate material model which can incorporate the desired behaviour of a real assembly. For any research considering timber assemblies, it is highly recommended that the concrete damaged plasticity model is used as a starting point, moving to other material models depending on the model behaviour desired.

5.8.4 Thermal Expansion

To determine the influence of the coefficient of thermal expansion on modelling, a parametric study is conducted varying the value of the coefficient parallel to the grain direction of the timber. Values of 0, 3.5 and 7.0×10^{-6} m/mK are compared in Figure 5-17 for Test B, where the value used in the numerical model is represented by a solid red line.

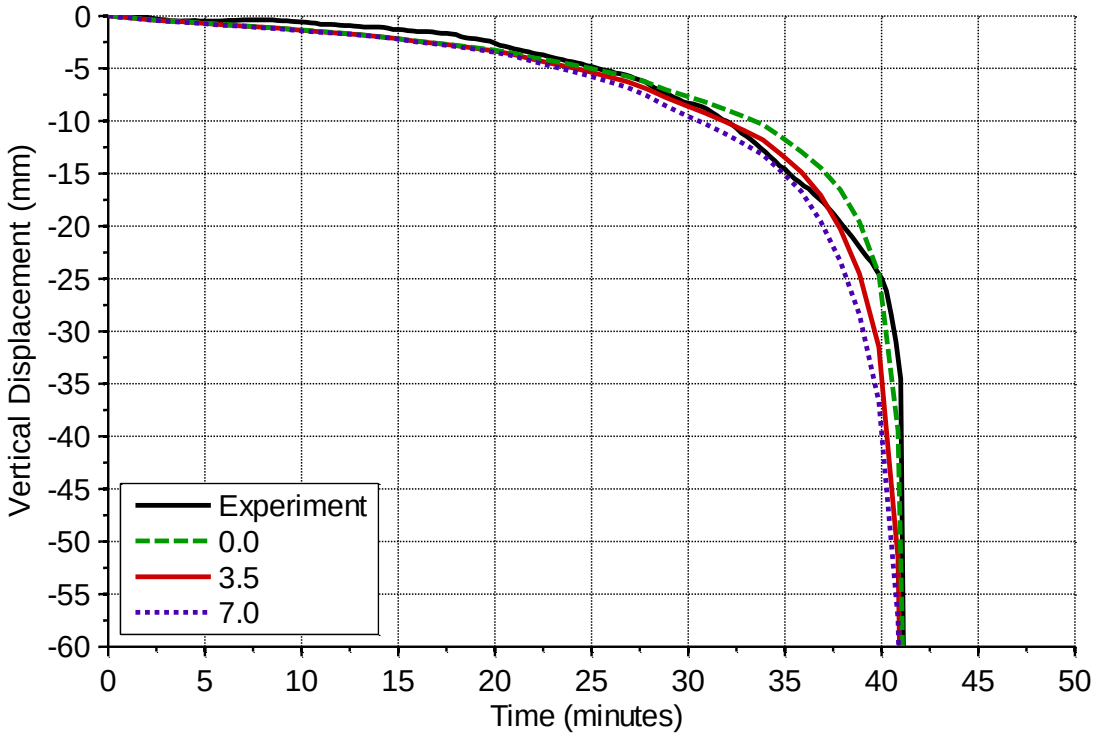

Figure 5-17: Comparison between thermal expansion coefficient for 3D structural analysis

As the elements expand they tend to cause a build-up of stresses throughout the section, due to the uneven nature of the heating profile. This in turn causes the displacement response to be adversely affected from a structural sense as the section cannot support the same stresses it could if the thermal expansion was not present. It can be seen from the figure that the variation in displacement response is relatively low for the range of parameters modelled, with a higher coefficient of thermal expansion corresponding to a greater level of displacement throughout much of the test duration. The major impact of this parameter is seen during the latter stages of the simulation, where a larger proportion of the cross-sectional area of the floor is heated.

Ignoring the coefficient of thermal expansion completely results in a stiffer deflection response and a less conservative model. As a product of the modelling process the failure time predicted by the model is very similar regardless of what coefficient is specified (within a reasonable range as shown here). When the floor undergoes large displacements the effect of thermal expansion through the section becomes almost negligible due to the scale of the strains caused by the thermal expansion being nullified by the very large strains due to load displacement.

5.9 Material Model Modifications

It is apparent from the modelling effort that although the displacement behaviour of the floors across the range of experiments has been simulated well, the failure behaviour is less well predicted due to a number of factors. Of the major parameters controlling the failure behaviour, one of the most significant inputs is the tension strength of the floor. Focussing on this parameter alone, the literature cites a wide range of values from the spread of test data for tension strength at elevated temperatures. Eurocode guidance was followed, hence a starting point for the improvement of the model lies with changing the least known parameter.

As a modification to the original material model described above, the strength reduction factor for timber in tension is changed from the value prescribed by the literature (CEN, 2004) of 65% at 100°C to 25%, the value used for compression strength at 100°C. The large scatter of experimental data available on the influence of elevated temperatures on the tension strength of timber emphasised the importance of varying this value from the one prescribed in the modelling. These test values are commonly derived from small scale tests considering clear specimens in pure tension. A major issue with regards to timber floors in fire is that throughout the floor section a combination of compression, shear, tension, and bending stresses act, and this is further complicated by the redistribution effects and a constantly changing stress profile due to mass loss. It is likely that the combination of stresses have a greater impact on the floor section integrity, and this tension strength reduction factor is a method for accounting for the extra unknown stresses which are not present in the small scale testing from which the data is derived from.

The results of this simple modification to the strength reduction factor are shown for the test floors and compared with the original modelling results in the following sections.

5.9.1 Test A

Applying the material model modifications to the structural model and re-simulating the case of Test A, the output for both the modified and original models are shown in Figure 5-18 compared with the experimental results. The original modelling effort is represented by a red dashed line, while the modified model is represented by a blue dashed dotted line.

It can be seen from the results that the revised failure time is approximately 35 minutes as opposed to 38 minutes, which compares closely with the experimental result.

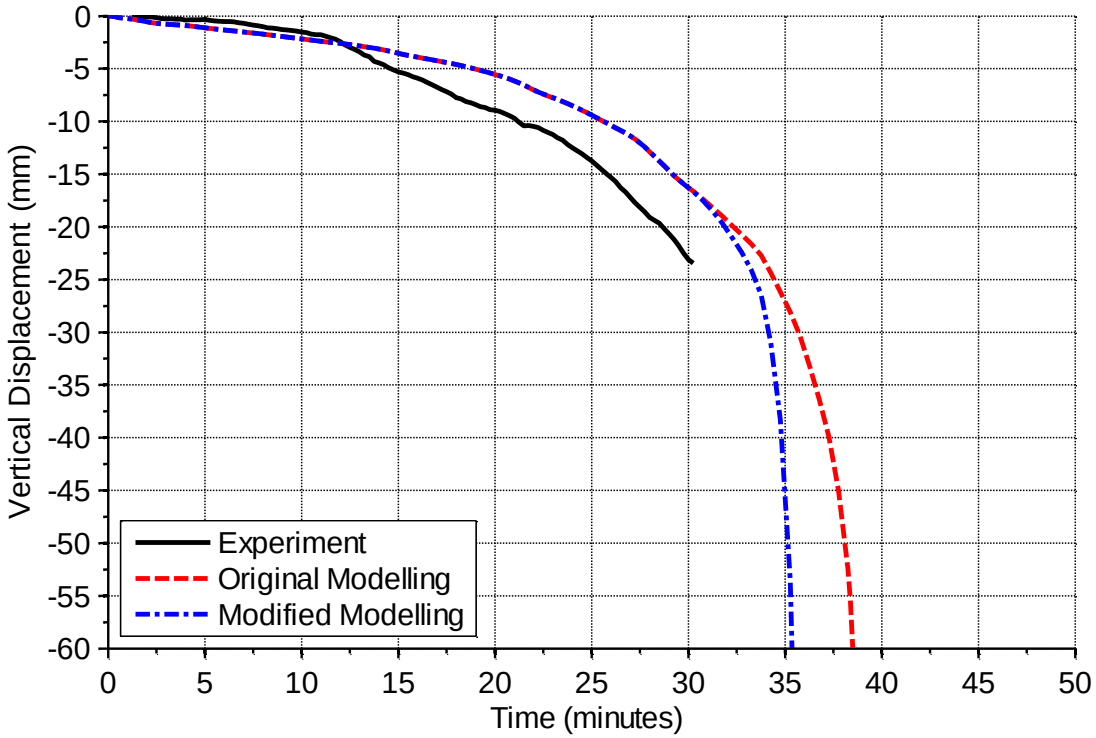

Figure 5-18: Modified structural modelling of Test A

The major physical processes that take place which are being approximated by the numerical model are mass loss primarily from the bottom of the section as the floor burns away in the fire. As the top of the slab is protected from the fire this results in the neutral axis of the section rising over the duration of the fire exposure. As the bottom elements of the floor become more slender (due to charring), the tension zone becomes the critical region in which failure will occur, and tension and bending stresses are redistributed throughout the heated bottom portion of the floor. Failure occurs when the bottom elements can no longer redistribute these stresses and the floor begins to displace at an accelerated rate, simulating runaway failure where the ultimate capacity of the timber has been reached in the remaining bottom chord. The physics of these processes implies that the critical region is the tension zone, as it is most highly impacted by the fire. This emphasises the influence of strength reduction factors, especially for tension strength under the three-sided exposure of timber floors, and their importance in determining failure in the simulations.

5.9.2 Test B

The modified modelling effort for Test B is shown in Figure 5-19.

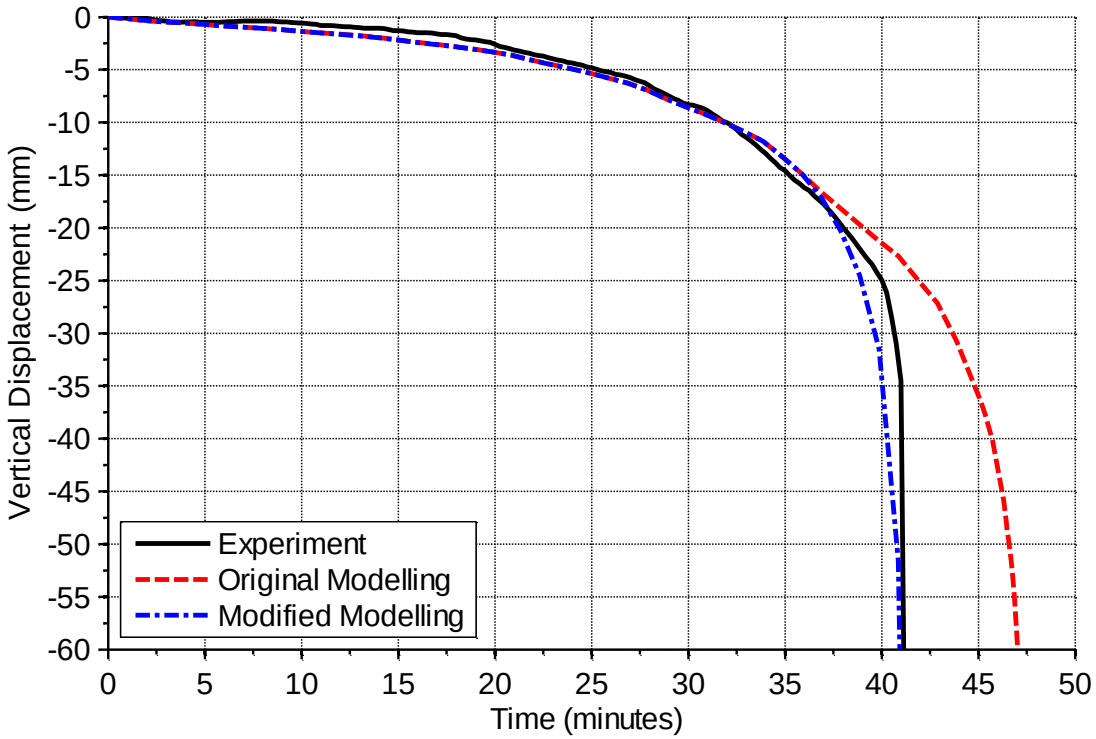

Figure 5-19: Modified structural modelling of Test B

From the figure it can be seen that the original numerical model slightly over-predicts the displacement response of the experimental floors, and failure is predicted at approximately 47 minutes. The modified model improves greatly on predicting the displacement behaviour of the test, resulting in a very close approximation for the entire duration of the test until failure at 41 minutes. The stiffness of the experimental results is very well predicted for the duration of the simulation; more so than for Test A for which a less complete dataset of displacement was recorded in the experiment.

On comparison with Test A the modification has a larger impact on the modelling difference, being an 8% reduction for the Test A and a 13% reduction for Test B. This is due to the presence of the bottom flange in the composite box floor. The heated properties are more prominent in determining failure in the composite box floor scenario, as more timber is lost from the tension zone in a more rapid manner in proportion to the entire residual section of the floor.

5.9.3 Test C

The modified modelling effort for the larger joist floor, Test C, is shown in Figure 5-20.

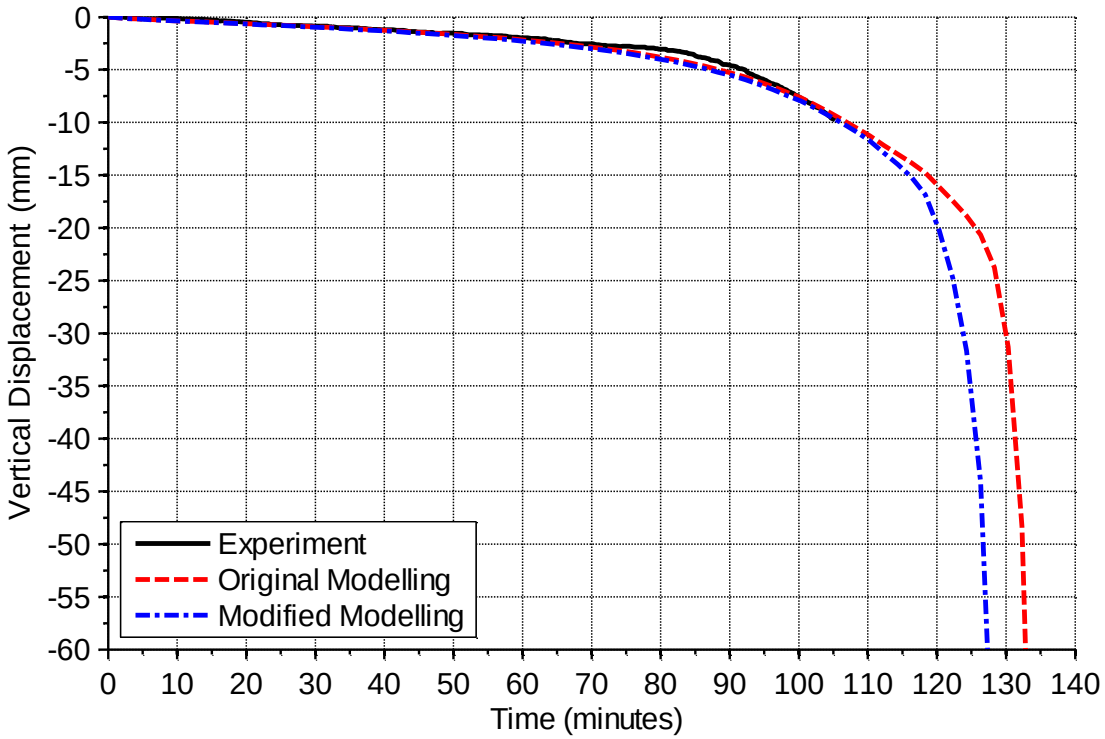

Figure 5-20: Modified structural modelling of Test C

From the experimental observations it was estimated that the floors would fail at approximately 120 – 125 minutes. The numerical prediction of floor failure is approximately 133 minutes using the original model, and 127 minutes with the modified model. The modified model results are much more conservative than its counterpart, as was seen previously with the smaller floors, and are a better approximation to the experimental results.

Due to the larger section sizes (and hence smaller ratio of heated to ambient temperature timber throughout the section), the effect of the reduced tension strength at elevated temperatures is not as pronounced as with the smaller floors, and is not seen until the final stages of the simulation. Also, as the duration is longer for this experiment the adequacy of the thermal model is tested to a much greater extent, as any error in the overall approximation is amplified by the duration of the simulation, as was seen with the thermal modelling.

Similar to the smaller floors, the stiffness of the larger joist floor is also predicted well by the modified model throughout the duration of the fire, with the predictions becoming slightly more

conservative with an increasing effect in the latter stages of the simulation. As previously iterated about the charred elements still carrying load, due to the larger sections involved with Tests C and D the impact of the strength reduction on the modelling output is reduced. This result is also exacerbated by the higher load levels causing the section to fail at a time where a smaller proportion of total cross-sectional floor area is heated compared with the smaller floors. Hence the modified method produces a smaller difference in the overall predicted displacement response for the larger floors.

5.9.4 Test D

The modified modelling effort for the larger composite box floor, Test D, is shown in Figure 5-21.

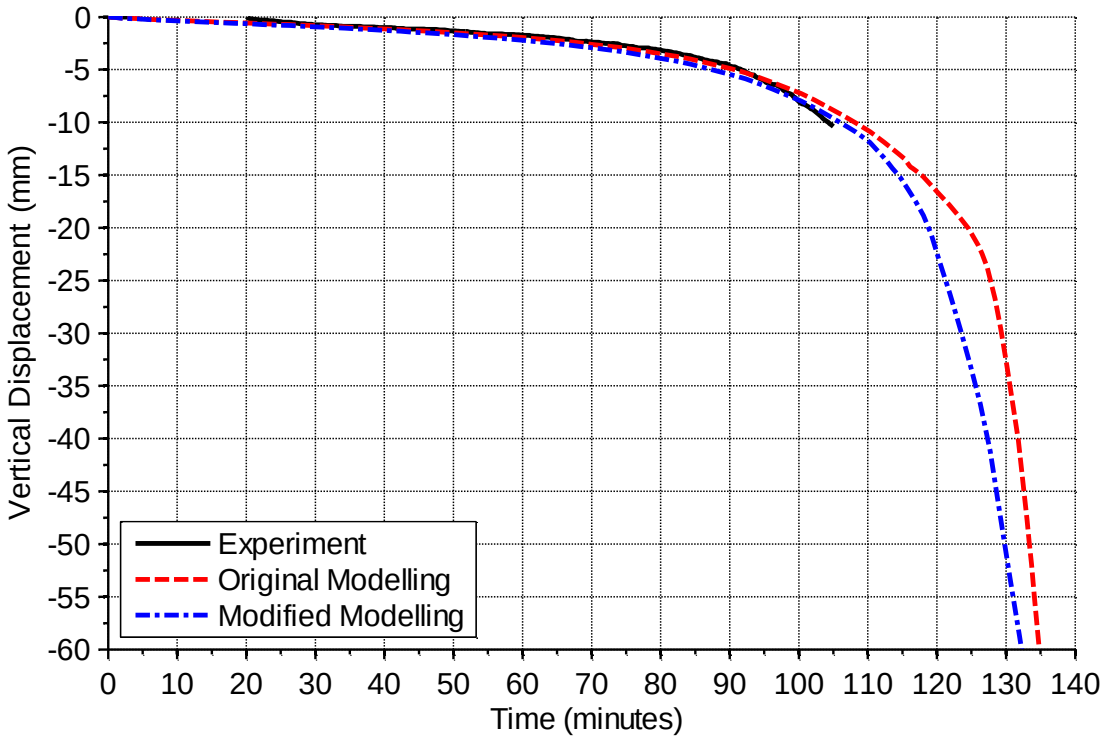

Figure 5-21: Modified structural modelling of Test D

As with Test C, experimental observations suggested that the floors would fail at approximately 120 – 125 minutes. The numerical prediction of floor failure is approximately 135 minutes using the original model, and 132 minutes for the modified model. The modified model simulation results are only slightly more conservative than its counterpart, as was seen previously with the smaller floors to a greater extent, and are a better approximation to the experimental results.

A different effect is seen in comparison between Tests C and D than was seen for the smaller floors. In this case the joist floor has a wider spread of modelling results, while the composite box floor had only a smaller range. This is again attributed to section geometry, as seen from the thermal profiles shown in Section 4.9, the two-dimensional heat interaction has developed to such an extent that no part of the residual section of the joist is at ambient. In these conditions, the heat penetration and thus the charring rate upwards through the joist greatly increases and collapse occurs quickly. This behaviour was observed in the tests conducted by O'Neill (2009) on timber-concrete composite floors made from similar LVL and tested in the BRANZ furnace to destruction. This behaviour is not seen to such an extent in Test A as the residual section of the more slender joist cannot support the applied loads at a much earlier stage of the test, hence the heat penetration has not developed to such an extent as in the longer experiments.

5.9.5 Other Modifications

Although the only modification made here was the tension strength reduction for elevated temperatures, many other factors have varying influences on the failure results obtained and may produce similar results when changed. Some of these factors are investigated in the following sensitivity analysis.

As testing timber in its multiple failure modes and achieving reproducible results is difficult, especially at elevated temperatures, many proposed reduction factors have been derived from simple laboratory tests. These tests usually are testing clear specimens in pure shear, tension or compression. A major issue with regards to modelling floors in fire is that throughout the floor section a combination of these stresses act, and this is further complicated by the redistribution effects and a constantly changing stress profile due to mass loss.

Considering floor slabs, it is likely that the combination of stresses above and the bending stresses induced from the loading have a greater impact on the floor section integrity; hence the results for increasing the strength reduction at elevated temperatures were shown to be a closer match to the experimental results. Therefore it is suggested that further research into the impact of elevated temperatures on timber properties is conducted, especially with regards to combined actions on members.

5.10 Timber-Concrete Composite Floors

5.10.1 Introduction

To investigate the validity of the numerical modelling across a wider range of floor options and material types, the next logical step is to consider timber-concrete composite floors. This section focusses on the addition of a concrete slab to the top of a traditional timber joist floor. The reason for this is that timber-concrete composite floors generally have a very thin formwork sheathing applied to the top of the joist members for the purpose of holding the concrete slab until it has set, or no sheathing layer if the floors are highly prefabricated, hence the influence of extra timber layers under the concrete is not considered in this analysis.

Previous full-scale experiments on timber-concrete composite floors were conducted at the BRANZ facilities (O'Neill, 2009); a brief description is given in this section while a more detailed overview of these tests can be found in the relevant literature. The structural model in ABAQUS (O'Neill, 2012) and further developments are discussed in this section, along with comparisons to the timber systems discussed earlier and any deviations made from modelling timber only floors. The model considers a timber joist with a fully rigid connection to a concrete slab as a generic timber-concrete composite floor case.

5.10.2 Background

Recent research on the short term behaviour of timber-concrete composite floors has been conducted by Khorsandnia et al. (2012, 2013) in which both experimental tests and subsequent finite element modelling in ABAQUS have resulted in a numerical technique and analytical model for predicting the loaded behaviour of the floors. A comprehensive review of the available literature is also given, which delves into much more detail than outlined in this Section. The long term behaviour of timber-concrete composite floors is also investigated by Khorsandnia et al. (2012), in which the most recent research is examined and future work proposed. Although the entirety of this work is conducted under ambient temperature conditions, insights are made into the numerical approach and possible modelling techniques which may aid in the development of a detailed numerical method for predicting the fire performance of timber-concrete composite floors.

Comparisons between the recent literature and the current research will be beneficial to aid in accounting for more detailed slip behaviour between the major floor components (concrete and timber). The characterisation of the connection behaviour is vital to the loadbearing capacity and

thus failure behaviour of the floors, hence is of paramount importance in future work. As the modelling of timber-concrete composite floors is conducted as a side study, a fully rigid connection is assumed as a simplification to the modelling process.

5.10.3 Furnace Tests

The primary objective of the full scale tests were to investigate the failure behaviour of timber-concrete composite floors when exposed to fire, which encompassed a wide range of information that was required to be collected from different parts of the floor systems. Specifically, the failure mode of the floors was an important part of this as it would identify the critical component of the floor system that governs the design for fire safety, whether it was failure in the beams, the concrete slab or the connections between the two. Other important areas of interest were the charring behaviour of the timber beams, the spalling behaviour of the concrete, the fire damage about the connections and the performance of the plywood sheathing. The test fire specified was the ISO 834 standard test fire (ISO, 1999).

The design loads of the test specimens were based on a live load of 2.5 kPa and a dead load of the self-weight of the floor only, with no additional dead load. The first floor specimen tested was a 126 mm wide x 300 mm deep beam floor, which was tested to destruction. The concrete slab was made of 30 MPa standard concrete, of a 65 mm thickness. Below this, 17 mm thick plywood sheathing comprised the formwork for the floors, and rigid notched connections were used between the joists and the concrete slab. Failure occurred at 75 minutes under the ISO 834 design fire and applied design load.

The second floor was identical to the first apart from the 400 mm deep joists. The test was stopped after 60 minutes to assess the damage at that time and to provide insight into how the beams were charring before complete destruction.

5.10.4 Thermal Modelling

Two major cases are considered for thermal modelling, the first being three-sided standard fire exposure to the timber joist only, while the second case includes the concrete slab. Identical methods to those presented in Chapter 4 have been used to model the timber beam; hence will not be discussed in further detail here. A square mesh size of 5 mm is used throughout the cross-section. To model the concrete guidance from Eurocode 2 (CEN, 2004) was followed with regards to defining the thermo physical properties of the material, notably the conductivity, density and the specific heat.

5.10.5 Structural Modelling

Similar to the thermal modelling, the structural modelling is conducted with identical parameters to those described in this chapter for the timber only floor models. The modified concrete damaged plasticity model is used to model the timber joist and the concrete damaged plasticity model is also used to model the concrete slab as an isotropic material. A mesh length of 300 mm is defined along the span for the floor systems, and as previously iterated the connection between the joist and the concrete slab is modelled as fully rigid.

5.10.6 Results

The displacement response of the 300 mm deep joist floor tested in the furnace is shown in Figure 5-22 represented as a solid black line. The modelling effort for this floor is illustrated by the dashed and dash dotted lines, with the blue and red lines representing the cold and hot concrete analyses respectively.

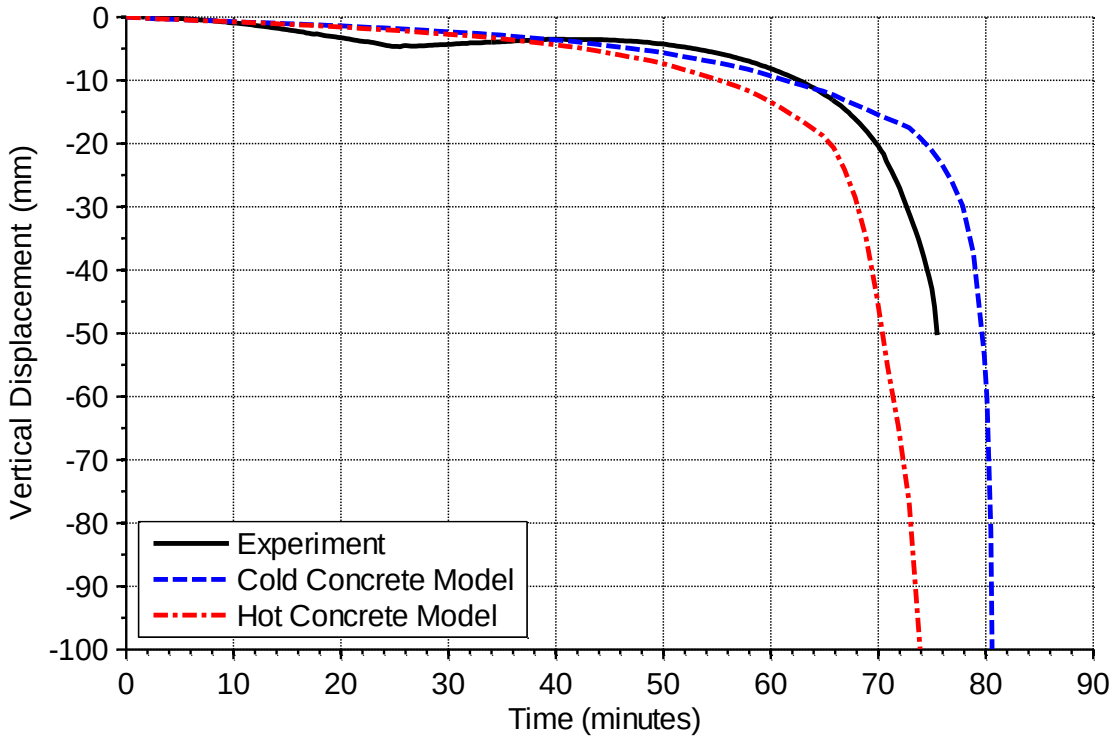

Figure 5-22: Structural modelling of 300 mm deep joist TCC floor

The runaway failure of the floor was recorded at 75 minutes, and from the figure it can be seen that this is predicted well by the hot concrete model which specifies a failure of approximately 74 minutes. The cold concrete model overestimates the capacity of the floor, giving a failure time of

approximately 81 minutes. The displacement behaviour in itself is not as well represented as for the timber only floors; however both models are a reasonable approximation to the experimental results shown.

In the experiment a thermal bowing action was observed in both tests which can clearly be seen on the figure. Initially the floor joists char which in turn reduces the floor capacity to resist the applied loads and the floor deflects downwards. However, as the underside of the concrete slab was heated the stiff connectors to the joist restrained its expansion, thus causing the entire floor to bow upwards, aiding in resisting the applied loads. Once the joists have burned down to such a degree that their relative capacity is less than what can resist the applied loads and the thermal expansion of the concrete, the floor begins to deflect below the rest position, as seen here at approximately 40 minutes. Unfortunately this behaviour is not captured in the model, but rather the tied elements distorted at the connection point. An in-depth analysis providing a more suitable method of contact would aid in predicting this behaviour.

The displacement response of the 400 mm deep joist floor tested in the furnace is shown in Figure 5-23 compared with the modelling effort.

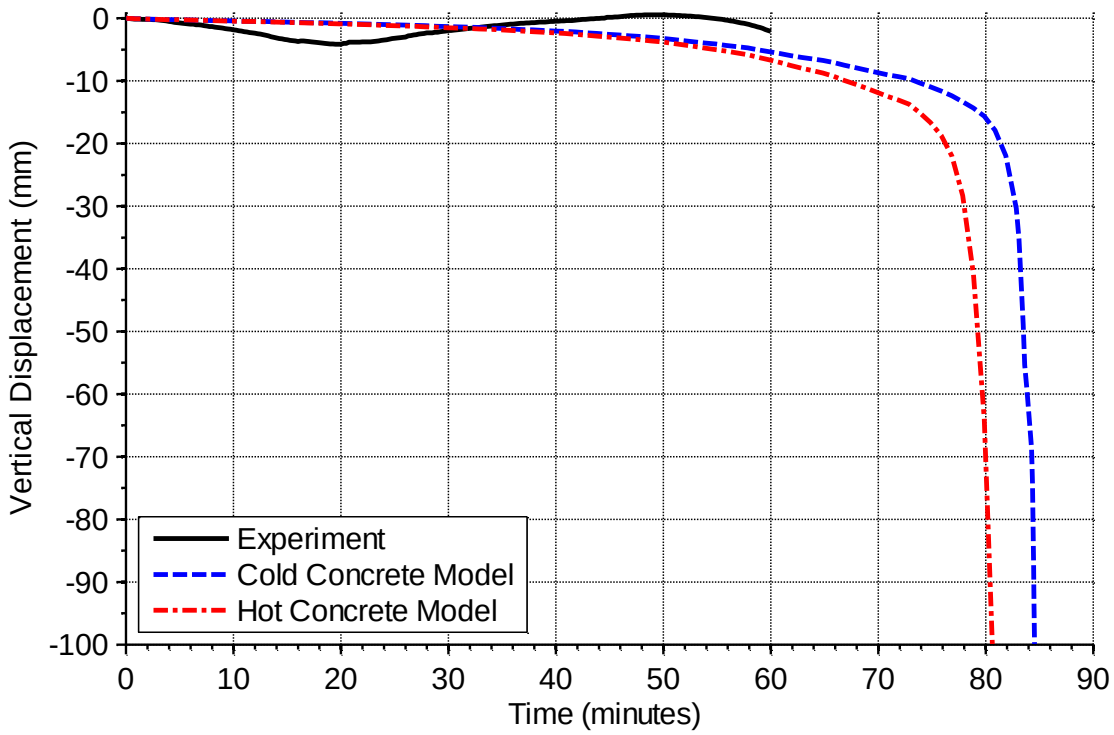

Figure 5-23: Structural modelling of 400 mm deep joist TCC floor

As with the 300 mm deep joist floor tested, a similar result can be assumed for the 400 mm deep joist floor and both modelling curves follow a similar trend as before (Figure 5-22). In comparison to the smaller joist floor, it can be seen from the simulation results that the response is much stiffer for the deeper joist floors, as expected. The cold concrete model predicts failure at approximately 85 minutes, while the hot concrete model is slightly more conservative predicting failure at 81 minutes.

As the floor joists were larger this thermal bowing action observed in the test was more pronounced for the 400 mm deep joist floor as seen from the figure, and the second trend of downward deflection does not occur until approximately 50 minutes.

In conclusion, the modelling approach adopted for timber only floors also predicts the failure time of timber-concrete composite floors to a relatively precise degree. Further refinement into the connection between the timber and concrete components of the floor is warranted to enable greater confidence in the results.

The incorporation of heated effects into the concrete aids in refining the results obtained when compared with the experimental data. Failure times predicted become more conservative when heated effects are considered and a simplistic approach to modelling isotropic concrete does provide reasonable results.

5.11 Conclusions

In conclusion, the sequential thermo-stress analysis of timber floor systems is difficult for many different reasons. The thermal, physical and material inputs into the model are very important in dictating the type of behaviour which is output, none more important than the material property definitions. In order to appropriately model the behaviour of timber floor assemblies in fires, a detailed understanding of the underlying processes involved and the modelling software used is paramount.

In this research both one and three-dimensional structural analyses are conducted on timber floor assemblies, with varying degrees of input complexity, in order to adequately model behaviour observed in experimental tests. The one-dimensional modelling utilised simplified wire elements to model the structural response of floors under mechanical and thermal loads. The thermal loads were input at specific points in a section profile which severely limited the applicability of the method. As the results are purely speculative and highly dependent on the temperature inputs, which are not well known, the level of input complexity is not great enough

to warrant further analysis when considering timber assemblies under fire loads. A one-dimensional approach for modelling the structural behaviour of timber floor assemblies in fire is not recommended.

The three-dimensional modelling utilised solid continuum brick elements and used the thermal profiles calculated in Chapter 4 to sequentially model the structural response of floors under mechanical loads subjected to a standard fire. It was found that the structural modelling effort predicted the displacement response and failure times of the floors very well, and the simplified assumptions made in relation to fire inputs, boundary conditions, mesh refinement and effective material parameters were accurate to the required level of precision desired. A modification to the reduction in tension strength at elevated temperatures was proposed which refined the modelling results closer to the results of the experiments conducted in this research, and investigated the impact of that parameter on the overall modelling effort.

Sensitivity studies were conducted on the three-dimensional structural modelling, and for the sequential analysis of timber assemblies the following recommendations are made:

- For general analysis of floors from 5 – 10 metres in span, a general guideline of approximately 250 – 500 mm is appropriate for the mesh refinement along the span. This obviously can be reduced for floors with a less dense cross-sectional mesh, smaller cross-sectional areas, or if computational run time is not a major issue when running the simulations.
- An initial square cross-sectional mesh of 3 mm is used. A square mesh size of 5 mm was found to be adequate for this research hence further parametric studies on the mesh size are important to optimise the modelling process.
- Simplified boundary conditions such as pins and ties can be used for all major surface interactions, and all available axes of symmetry should be used to the fullest advantage. In order to avoid element distortion and stress concentrations at any support points, the bearing area of the supports should be spread across an appropriate number of nodes.
- Loads can be modelled as simple uniformly distributed loads across the top surface of the floors, although modelling exact loading conditions will give more precise results.
- The material model definition plays a vital role in the output of the modelling. For any simplified research considering timber assemblies in ABAQUS, the steel material model may be suitable for use as a starting point, however for implementing plasticity and

more complex analyses the concrete damaged plasticity model is strongly recommended for input flexibility.

- Other parameters such as the thermal expansion coefficient can impact on the output to varying degrees. It is crucial that a parametric study on all major inputs is run for any in-depth analysis to provide confidence in the results obtained.
- When modelling timber-concrete composite floors, accounting for the slip behaviour of the timber to concrete connection is paramount for confidence in the results obtained, however a simplified approach to modelling isotropic concrete can give reasonable results.

6 MODELLING NON-STANDARD FIRES

6.1 Introduction

Although standard fire exposure of timber floors and validation with experimental testing was studied in Chapter 5, the question of non-standard fire exposure and its impact on a timber floor assembly remains. In many regards, this is the predominant question for all modern buildings as the collective understanding of the complexities of fire dynamics progresses around the world. The floor designs tested and previously modelled are investigated further with regards to non-standard fire exposure in this chapter.

6.1.1 Important Limitations

Historically, parametric or non-standard fire exposure of timber structures has not been attempted in the past with simplified models as the more complex physical phenomena occurring during fires cannot appropriately be accounted for. This is also true for the effective properties developed in Chapter 4. The reasoning behind why the effective values for thermal properties are only suitable for standard fire exposure is aptly described by König (2006) and reiterated by Mikkola (2010). When considering the underlying combustion processes occurring with timber pyrolysis, König states that "Due to convective cooling caused by the reverse flow of pyrolysis gases, the heat flux through the char layer into the wood is delayed. Since this delay is dependent on the rate of charring, the effective conductivity is a function of the charring rate; thus it is also a function of the rate of increase or decrease of temperature". This means that for faster heating than the standard fire the effective conductivity is over-predicted, and conversely for slower heating it is under-predicted. It is stated that these limitations can be overcome by deriving thermal properties from analytical models that take into account more complex physical phenomena, or from an extensive series of fire tests.

These limitations are understood by the author, however as more complex phenomena are still difficult to account for with numerical models and fire test results of full-scale timber assemblies are sparse, this chapter endeavours to provide a starting point from which further study and research can take place on this subject. It may be that the results presented here are only indicative of possible behaviour for non-standard fire exposure, however they provide a point of reference from which further modelling and testing can be conducted in future.

For this reason, the effective thermal properties developed for standard fire exposure will remain unchanged and be used for the modelling presented herein, and further refinements can be made by others in the future when the changes of thermal properties are better known and characterised for non-standard fire exposure. This will provide at the very least a comparison to the modelling of response to standard fire exposure.

6.2 Parametric Design Fires

As discussed in Section 2.4, non-standard fires differ from standard fire curves by incorporating both a specified duration and a decay phase, and having a growth phase and maximum temperature specific to the environment and fuel stored within the compartment.

In this chapter the equations to calculate parametric design fires presented in Annex A of Eurocode 1 (CEN, 2002) are used as the fire input into the thermal model developed in Chapter 4. This is then applied to the structural model for each experimental floor described in Chapter 3 and modelled in Chapter 5. The base equation for calculating the temperature-time curve in the heating phase is as follows:

$$\theta_g = 20 + 1325(1 - 0.324e^{-0.2t^*} - 0.204e^{-1.7t^*} - 0.472e^{-19t^*}) \quad \textbf{Equation 6-1}$$

Where:

θ_g = The gas temperature in the compartment (°C)

t^* = Fictitious time (hours)

Modifications can be made to incorporate the influence of different compartment linings, multiple layers of linings and fire growth rates. The equation for calculating the decay phase is:

$$\theta_g = \theta_{max} - 625(t^* - t^*_{max} \times x_1) \quad \text{for } t^*_{max} \leq 0.5 \quad \textbf{Equation 6-2}$$

$$\theta_g = \theta_{max} - 250(3 - t^*_{max})(t^* - t^*_{max} \times x_1) \quad \text{for } 0.5 < t^*_{max} < 2$$

$$\theta_g = \theta_{max} - 250(t^* - t^*_{max} \times x_1) \quad \text{for } t^*_{max} \geq 2$$

Where:

θ_{max} = The maximum gas temperature (°C)

t^*_{max} = Time for maximum gas temperature (hours)

x_1 = Time modification factor

6.2.1 Design Fire Scenario

The design fires were based on a room generic to multi-storey office buildings. The room was specified as 10 metres wide by 15 metres long, with an internal height of 3.6 metres. This typical room was specified to be within the range of applicability of the parametric fire equations, being under a total floor area of 500 m^2 and a height of 4 metres, without any roof openings. The interior lining of the walls in the room was assumed to be gypsum plasterboard, with the ceiling assumed to be exposed timber, and a medium growth rate was used for all design fires.

6.2.2 Opening Factor

In order to correlate the fire types chosen with real fires and what is found in the literature, three opening factors were chosen which encompass a range of temperature conditions outside of the generic standard fire (ISO, 1999) for a compartment in an average office building. These opening factors were 0.02, 0.04 and 0.08, and were considered to be representative of a wide range of ventilation conditions for a generic office building compartment. A comparison of the opening factors with the standard fire curve is given in Section 6.2.4. In this research the opening factor is defined as:

$$F_v = \frac{A_v\sqrt{H_v}}{A_t}$$ **Equation 6-3**

Where:

F_v = Opening factor ($m^{1/2}$)

A_v = Area of vertical openings (m^2)

H_v = Height of vertical openings (m)

A_t = Total internal area of compartment surfaces (m^2)

6.2.3 Fuel Load Energy Density

In order to determine the duration of each design fire, three specific fuel load energy densities (FLEDs) were also specified to incorporate a range of loading conditions in the space. The three FLEDs defined by total floor area were 400, 800 and 1200 MJ/m^2 of floor area. Typical FLED values for some occupancies are given in Eurocode 1 (CEN, 2002), and are reproduced below with 80% fractile values in MJ/m^2 of floor area:

Table 6-1: Fuel load energy densities for common occupancies (CEN, 2002)

Occupancy	Average	80% Fractile
Dwelling	780	948
Hospital (room)	230	280
Hotel (room)	310	377
Library	1500	1824
Office	420	511
Classroom of a school	285	347
Shopping centre	600	730
Theatre (cinema)	300	365
Transport (public space)	100	122

6.2.4 Design Fires

The combined fuel loads and opening factors resulted in a total of nine design fires, which are shown in Figure 6-1, Figure 6-2 and Figure 6-3 for opening factors of 0.02, 0.04 and 0.08 respectively.

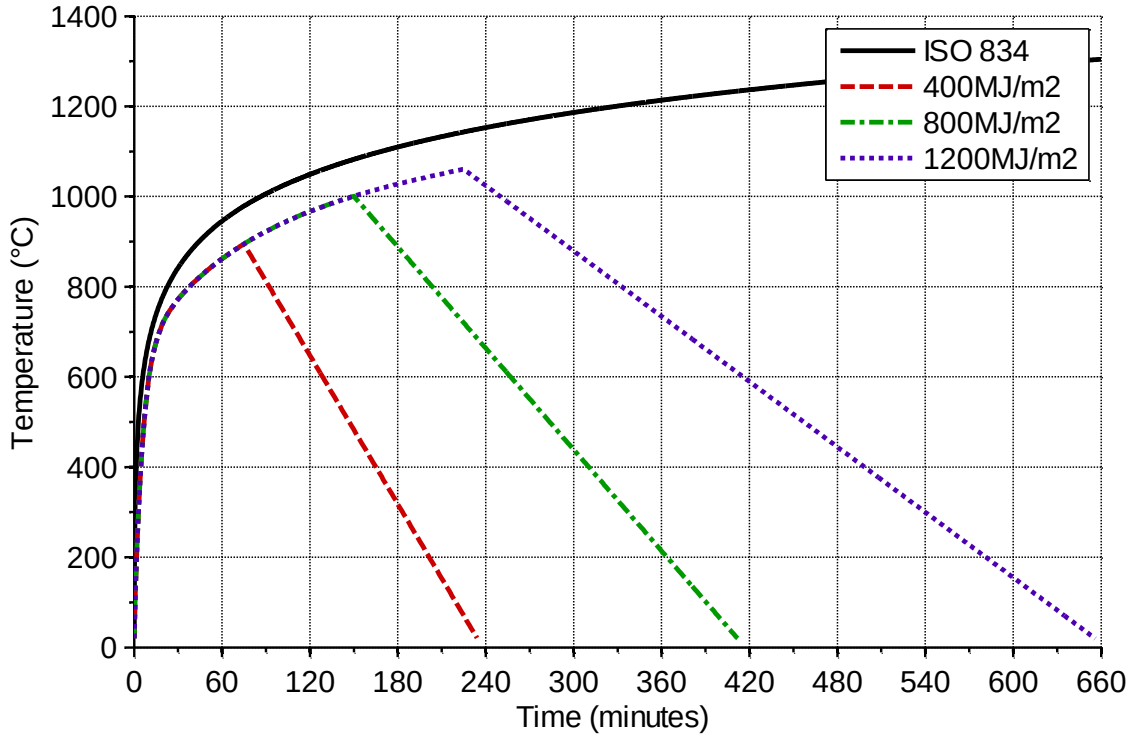

Figure 6-1: Parametric fire curves for an opening factor of 0.02

It can be seen from Figure 6-1 that very small openings in the compartment push the extreme limits of applicability of the parametric method, and it is unreasonable to expect plasterboard linings to still be intact after six or more hours in the case of a high fuel load of 1200 MJ/m^2 as shown above. This is due to the combination of surface lining interaction, low openings and high fuel loads which serve to disproportionately increase the expected burning duration.

Despite these obvious drawbacks for these conditions, the more applicable zone of within the first three hours shows that the above compartment conditions with a ventilation factor of 0.02 correlate closely with the standard fire curve, having slightly lower temperatures throughout the duration of the design fire.

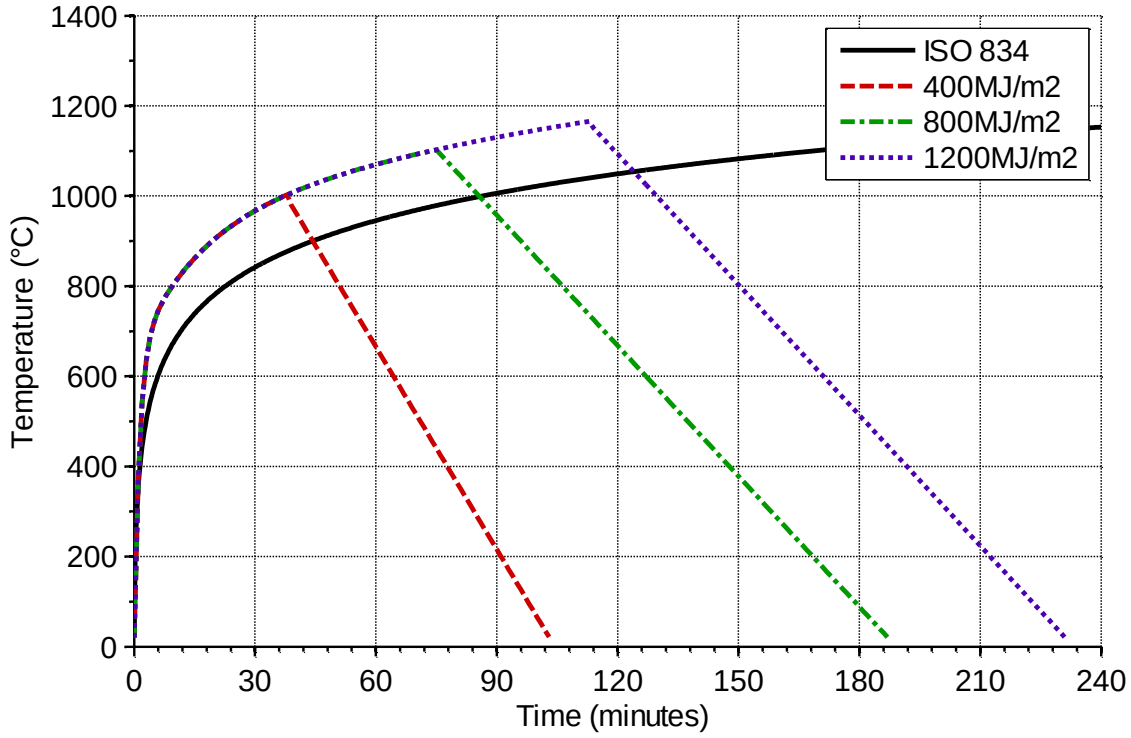

Figure 6-2: Parametric fire curves for an opening factor of 0.04

It can be seen from Figure 6-2 that an opening factor of 0.04 has a moderately higher temperature impact compared to the standard fire curve. The difference in fuel load energy density of 400 to 1200 MJ/m^2 has a significant impact on the overall design fire temperatures and duration for this compartment.

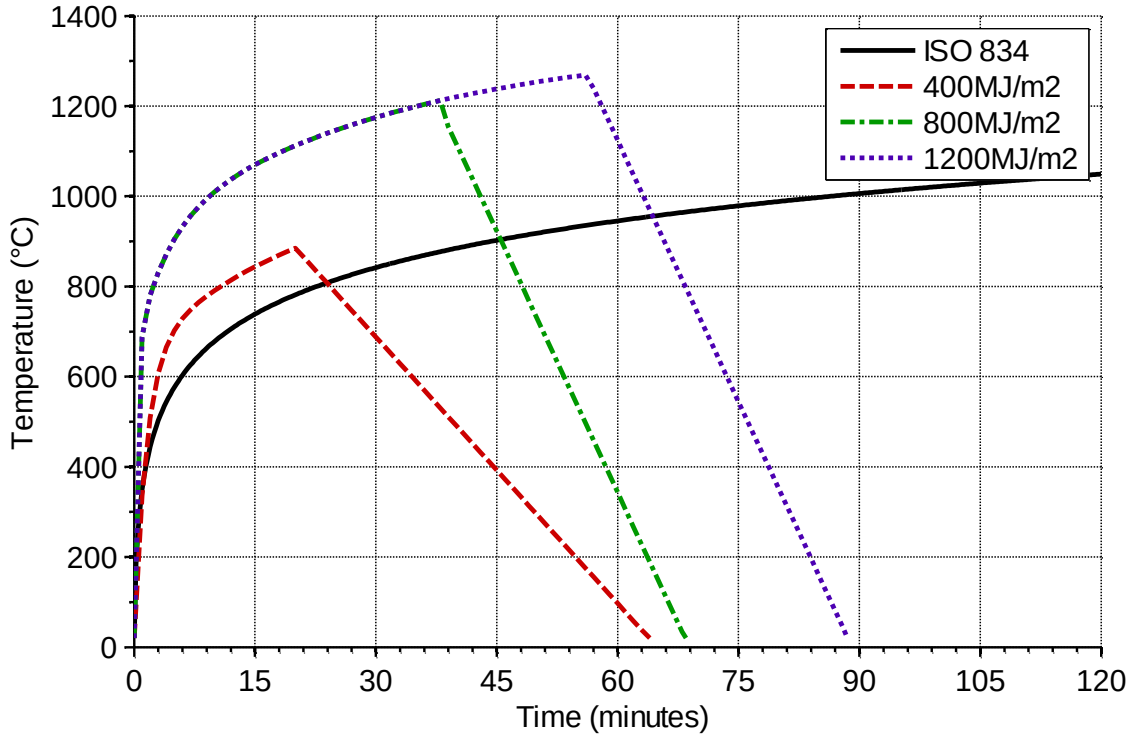

Figure 6-3: Parametric fire curves for an opening factor of 0.08

In contrast to the design fires with lower ventilation factors, once the factor increases beyond 0.08 it can be seen in Figure 6-3 that the design fires quickly reach high temperatures in comparison to the standard fire curve. In a well-ventilated office with a high fuel load, the figure shows that the expected temperature of a parametric fire may be much greater than the standard fire curve.

The ratio of fuel to openings is low enough for the 400 MJ/m^2 case such that the fire is no longer ventilation controlled and does not follow the steeper temperature curve of the higher fuel load scenarios.

6.3 Modelling Comparisons

In this section comparisons are made between the experimental results of Chapter 3 and the numerical model developed in Chapters 4 and 5 in which the above design fires are input.

6.3.1 Test A

Figure 6-4 shows the modelling results for Test A considering all opening factors at a FLED of 400 MJ/m^2.

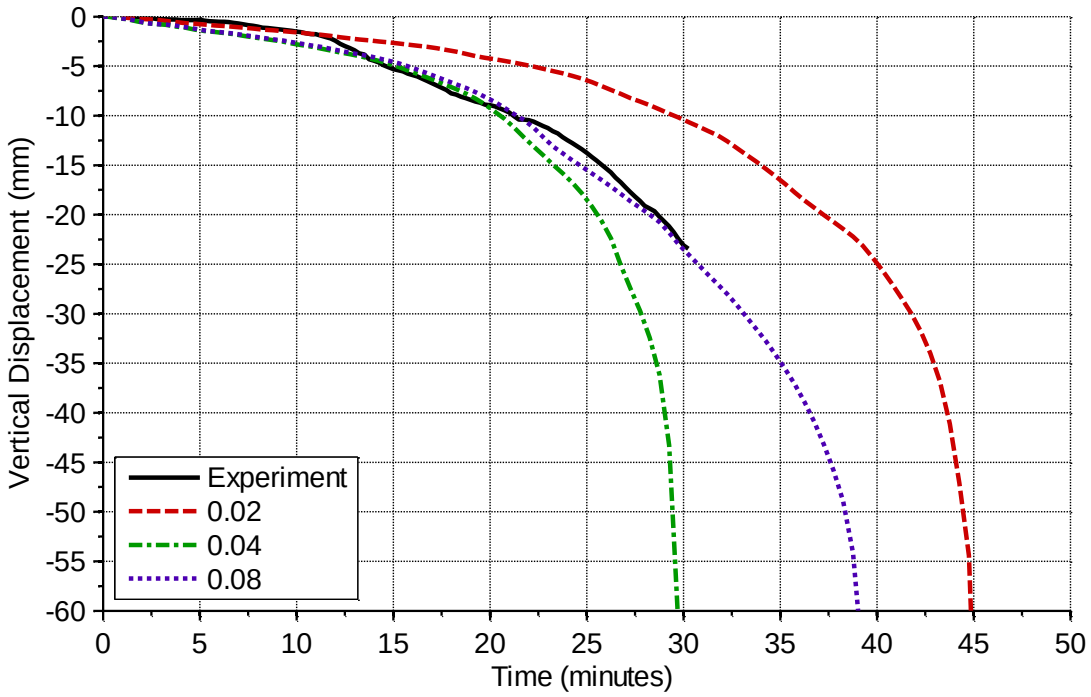

Figure 6-4: Modelling results for all opening factors and a FLED of 400 MJ/m^2 for Test A

From the results it can clearly be seen that there is an important correlation between maximum fire temperature and displacement. For example, as seen from Figure 6-1 and Figure 6-2 the temperature results for the respective 400 MJ/m^2 design fires show that the curve with an opening factor of 0.04 reached a higher temperature much faster than for an opening factor of 0.02. The impact on the displacement of the floor can clearly be seen to be much more significant for the hotter fire, with failure predicted at 30 minutes for an opening factor of 0.04 compared with 45 minutes for an opening factor of 0.02. This was expected as the failure occurred in the growth phases of both fires.

However, for an opening factor of 0.08 the maximum temperature is reached at approximately 17 minutes. Decay begins, and reaches ambient temperatures at approximately 65 minutes. The displacement results of the floor reflect this drop in temperature, with a slower increase in the rate of deflection from approximately 20 minutes and floor failure predicted at 39 minutes.

The thermal model does not account for any continued combustion of the exposed timber members in the room and is directly dependent on the external heat flux input, hence additional assumptions would be required to model this behaviour and the structural response would be more adversely affected by this than is shown by the numerical model above. Phenomena such as continued burning can be included in a rudimental fashion by tailoring the temperature input, however the lack of available resources on this topic inhibits further modelling.

Figure 6-5 shows the modelling results for Test A considering all opening factors at a FLED of 800 MJ/m^2.

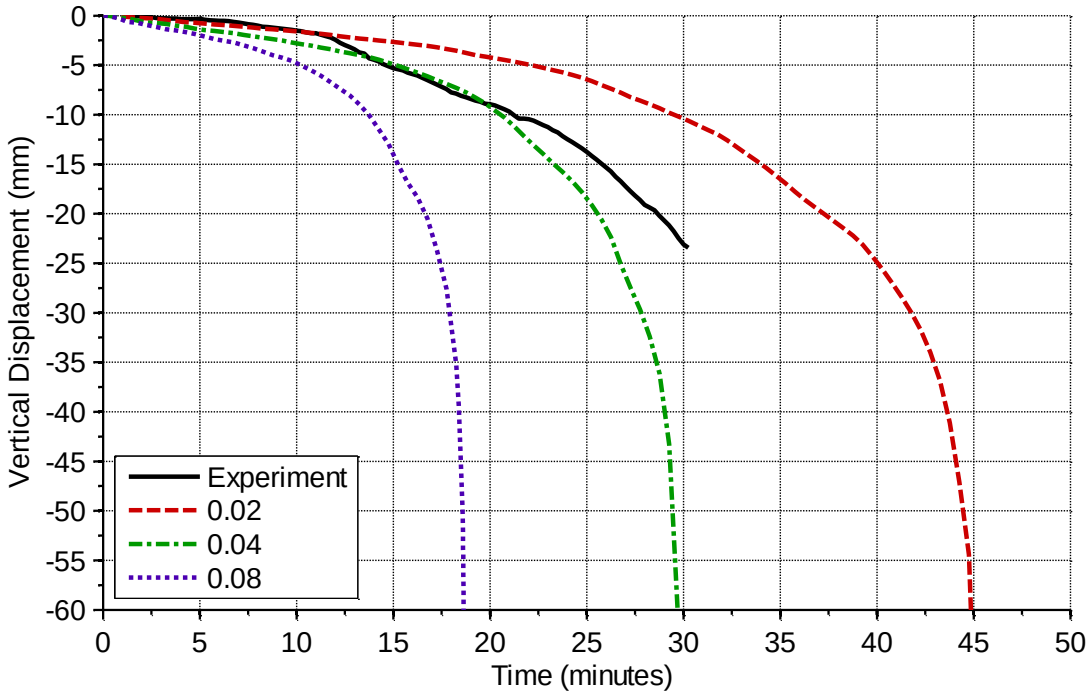

Figure 6-5: Modelling results for all opening factors and a FLED of 800 MJ/m^2 for Test A

The higher fuel load results in increased design fire durations and temperatures, and the severity of each fire directly correlates to the results seen in Figure 6-5 with failure occurring sooner for a larger opening factor.

It is evident that the duration of fire exposure plays a crucial role in determining the overall thermal, and thus structural, impact on the timber floor assembly modelled. The results for the 800 and 1200 MJ/m^2 fuel loads are similar due to the floor failing before the decay phase is reached for the design fire curves. For this reason results have not been presented for a FLED of 1200 MJ/m^2 as the modelling output was identical.

6.3.2 Test B

Figure 6-6 shows the modelling results for Test B considering all opening factors at a FLED of 400 MJ/m^2.

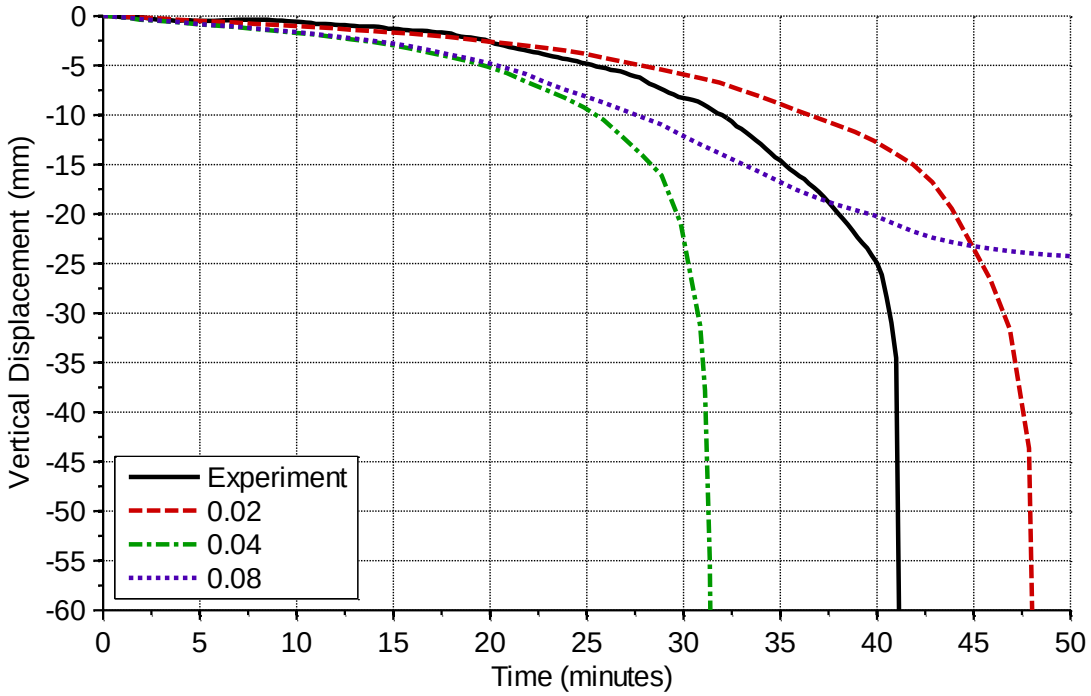

Figure 6-6: Modelling results for all opening factors and a FLED of 400 MJ/m^2 for Test B

The results reinforce what was seen for Test A, with failure predicted at 32 minutes for an opening factor of 0.04 compared with 48 minutes for an opening factor of 0.02. This was again expected as the failure occurred in the growth phases of both fires.

For an opening factor of 0.08 the drop in temperature has a significant influence on the model results, with a reduction in the rate of displacement and an eventual plateau at approximately 50 minutes. This emphasises the importance of the fire duration specified, as the low severity of this fire results in the floor withstanding a complete burnout, with the residual section able to continue to carry load after the fire has gone out.

Figure 6-7 shows the modelling results for Test B considering all opening factors at a FLED of 800 MJ/m^2.

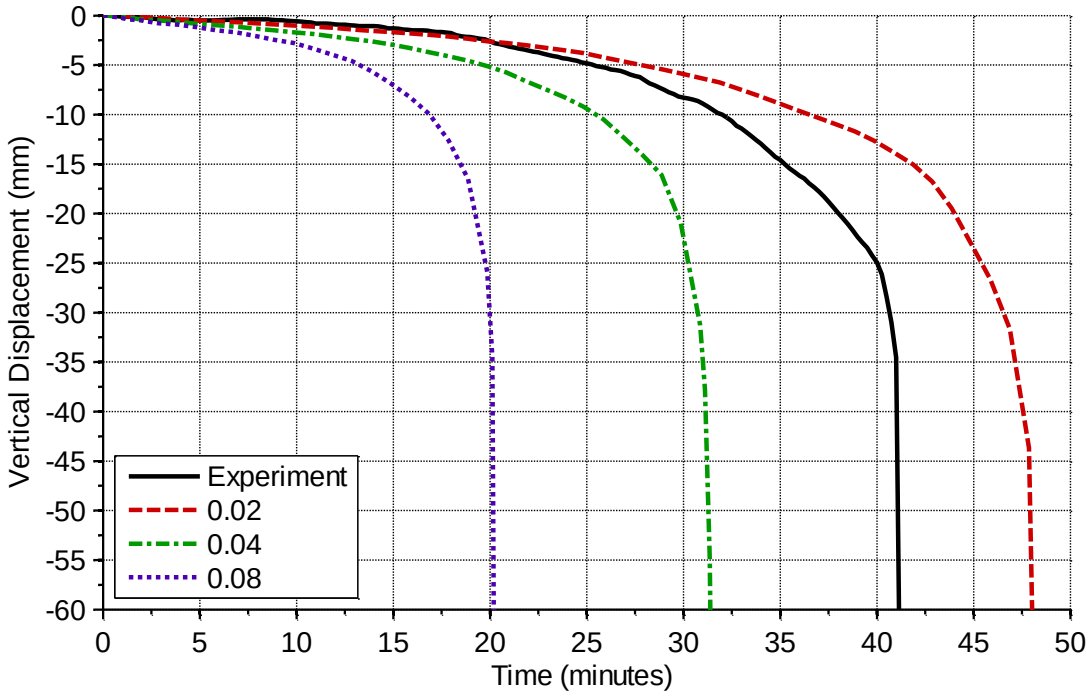

Figure 6-7: Modelling results for all opening factors and a FLED of 800 MJ/m^2 for Test B

Figure 6-7 gives an approximate illustration of the level of impact each design fire has on the floor assembly when compared with the standard fire test result. This is due to the design fires not reaching a decay phase before failure, hence the temperature of each fire increases until floor failure. For opening factors of 0.02, 0.04 and 0.08 the failure times were predicted to be 48, 32 and 20 minutes respectively.

As with Test A, the results have not been presented for a FLED of 1200 MJ/m^2 as the modelling output was identical to the 800 MJ/m^2 results. It can be seen that this was also the case for opening factors of 0.02 and 0.04 between FLEDs of 400 and 800 MJ/m^2.

6.3.3 Test C

Figure 6-8 shows the modelling results for Test C considering all opening factors at a FLED of 400 MJ/m^2.

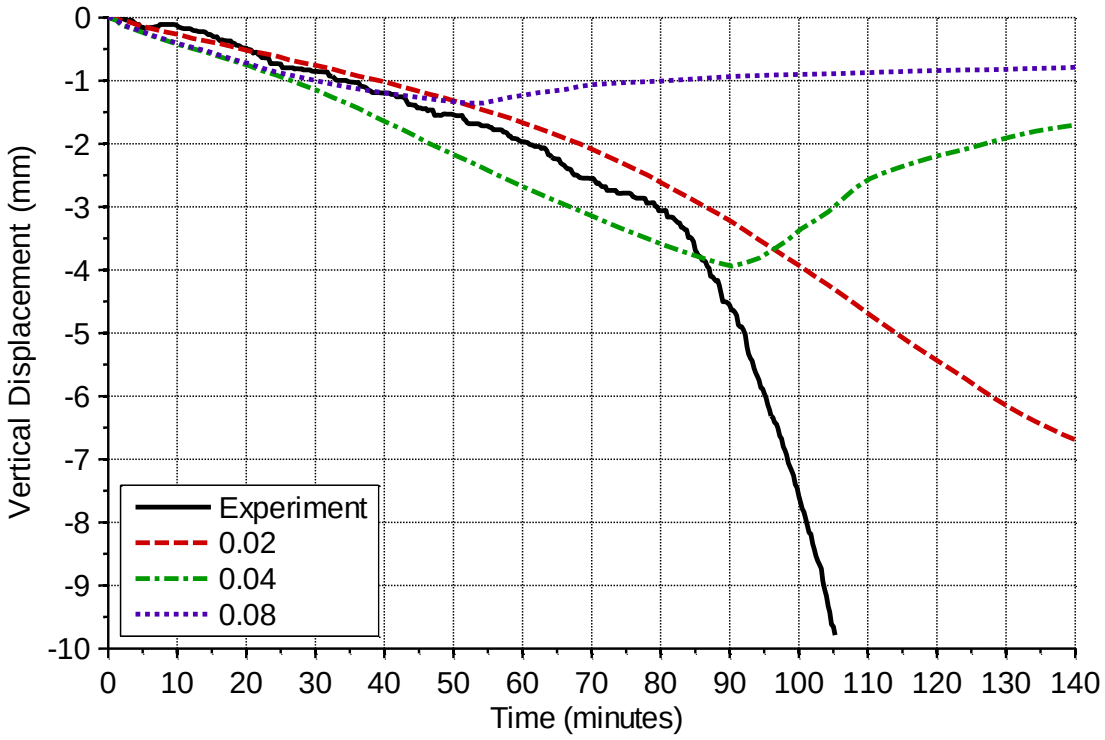

Figure 6-8: Modelling results for all opening factors and a FLED of 400 MJ/m^2 for Test C

Due to the higher resistance achieved by the larger floors, the 400 MJ/m^2 design fires all reach their decay phases, and in the case of the well ventilated fires with opening factors greater than 0.02 the compartment temperatures return to ambient in under 120 minutes.

It can be seen clearly from Figure 6-8 that for opening factors of 0.04 and 0.08 the vertical deformation trend of the floors reaches a maximum once the fire has almost burned out. This effect increases with fire duration, such that a longer duration fire will result in displacement recovery sooner as the elements in the model cool. This is because lower maximum temperatures are reached in the longer duration fires, hence the heat penetration is less significant in these cases. This behaviour is also seen to a lesser degree with an opening factor of 0.02, however the trend is much slower due to the longer duration and slower decay rate of the fire.

Residual plastic deformation has occurred, hence the total vertical displacement is not entirely recovered when the floors cool down from the higher temperatures. Despite the permanent plastic deformations, the elastic deformations are recovered as the elements cool down to ambient temperature. This is an artefact of the modelling process in that as the elements in the model are not physically removed when they exceed temperatures of 200°C (as the timber turns to char), hence when the elements cool they will recover strength and stiffness which would not occur in reality.

Other finite element programs such as SAFIR do facilitate the ablation of elements in the analysis, however this process may not be specifically designed for timber modelling hence further investigation into its effect is warranted. Furthermore, the drawbacks of using other analysis software may present in the form of limitations in material inputs or element types, and a wide degree of flexibility with regards to these aspects is required for modelling timber in fires.

Figure 6-9 shows the modelling results for Test C considering all opening factors at a FLED of 800 MJ/m^2.

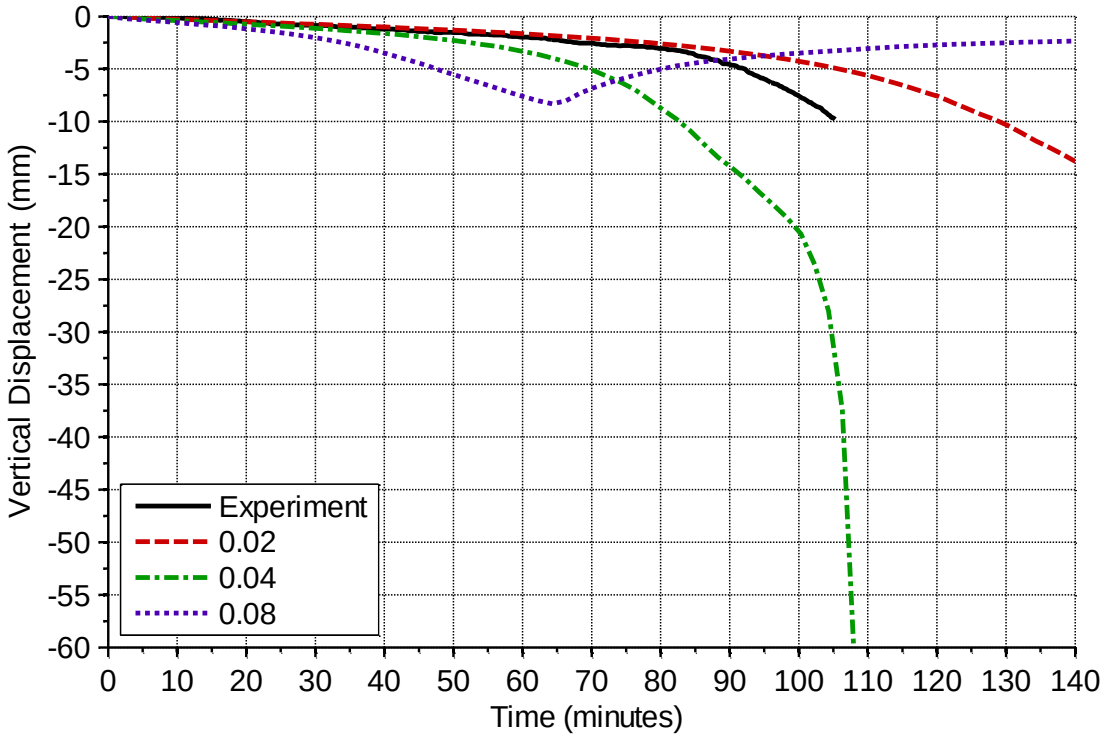

Figure 6-9: Modelling results for all opening factors and a FLED of 800 MJ/m^2 for Test C

The higher FLED of 800 MJ/m^2 exacerbates the issues seen previously for an opening factor of 0.08, in which the total vertical deformation reached is approximately 8 mm, and the residual vertical displacement reached is about 2.5 mm. The opening factor of 0.04 results in a failure prediction of 108 minutes, while the opening factor of 0.02 does not fail within a plausible timeframe.

Figure 6-10 shows the modelling results for Test C considering all opening factors at a FLED of 1200 MJ/m^2.

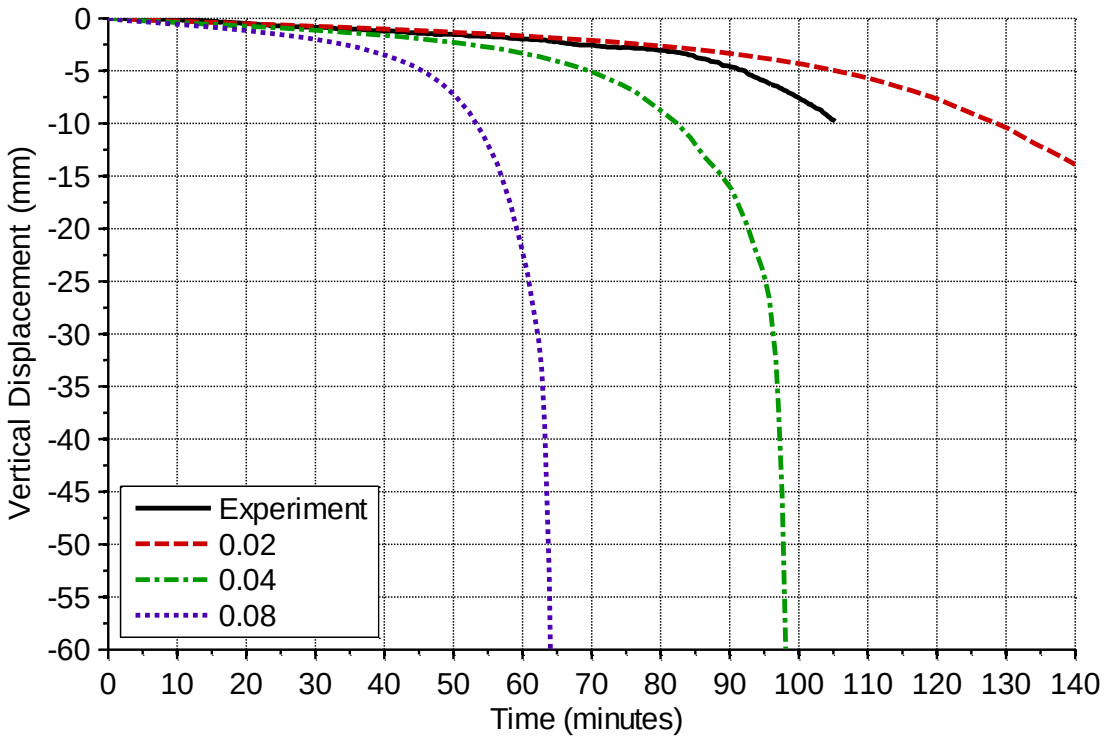

Figure 6-10: Modelling results for all opening factors and a FLED of 1200 MJ/m^2 for Test C

The predictions shown in Figure 6-10 for failure time are very similar to the results seen in Figure 6-5 and Figure 6-7, in which definitive failure times are seen for the larger opening factors, being 98 and 64 minutes for opening factors of 0.04 and 0.08 respectively. As with Figure 6-9, the design fire resulting from an opening factor of 0.02 has a much lower deflection response on the floor due to the lower temperatures of the fire.

6.3.4 Test D

Figure 6-11 shows the modelling results for Test D considering all opening factors at a FLED of 400 MJ/m^2, and Figure 6-12 shows the modelling results at a FLED of 800 MJ/m^2.

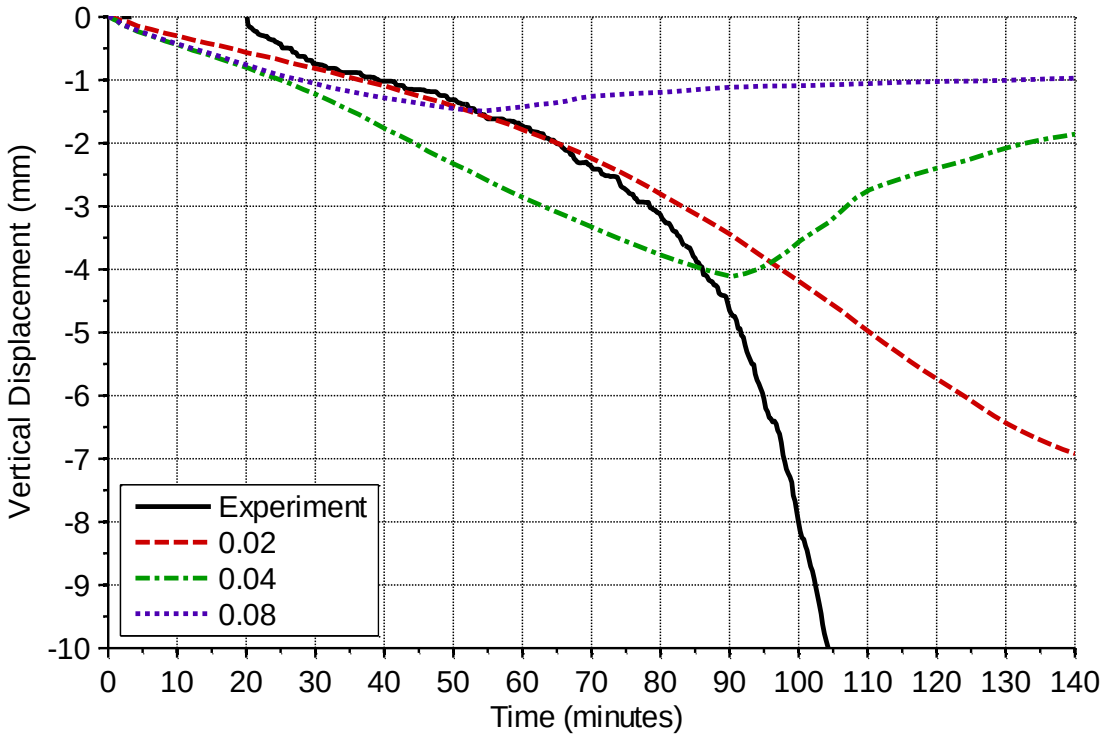

Figure 6-11: Modelling results for all opening factors and a FLED of 400 MJ/m^2 for Test D

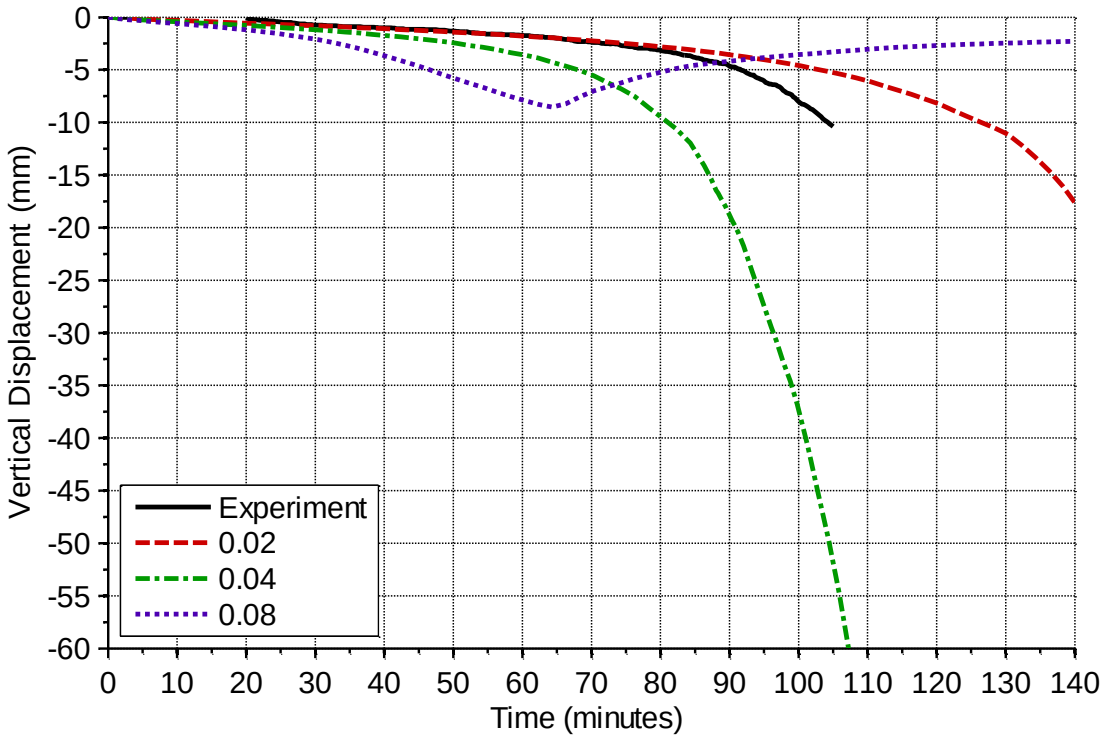

Figure 6-12: Modelling results for all opening factors and a FLED of 800 MJ/m^2 for Test D

Similar trends as Test C are seen for Test D. Figure 6-13 shows the modelling results for Test D considering all opening factors at a fuel load energy density of 1200 MJ/m^2.

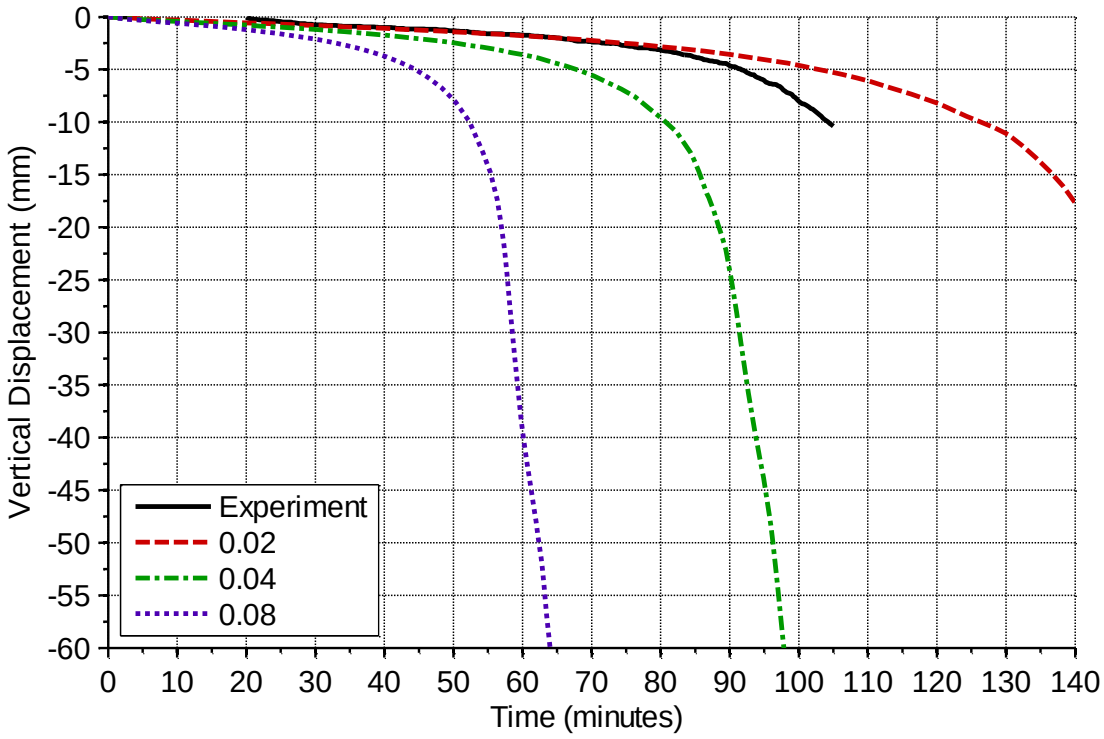

Figure 6-13: Modelling results for all opening factors and a FLED of 1200 MJ/m^2 for Test D

6.4 Conclusions

In conclusion, non-standard fire exposure is a useful tool which will likely play a much larger role in structural fire engineering in the future. It enables the investigation of other scenarios not currently captured by the standard fire curves, such as differing growth rates and fire decay.

It is important to reiterate that this form of modelling is not ideal. The modelling presented here is purely speculative and suffers from some severe limitations, the least of which is that the material model used may not be adequate to assess timber floor assemblies in its current state. With these limitations in mind, the study conducted in this chapter allowed for an investigation into some of the more unknown phenomenon, such as decay rates and fire durations, which are prominent questions when using performance based design methods.

It is important that an objective view is taken to model practical real fires. Although the current model does not include a facility for modelling continual burning of timber, some of the other

assumptions of fuel load and ventilation may also be quite conservative for many possible multi-storey applications. Phenomena such as continued burning can be included in a rudimental fashion by tailoring the temperature input, however the lack of available resources on this topic inhibits further modelling.

The major conclusions drawn from the numerical modelling were:

- The maximum temperature and growth rate of a fire has a large impact on the overall displacement response of a timber floor.
- The fire duration and decay characteristics also have a significant impact on the displacement response of the floors, and failure may be avoided provided there is adequate residual strength left in the floor once cooled.
- The modelling of continued burning of timber is important to obtain a true assessment of structural performance. Models that do not account for element removal may not give adequate results during the decay phase of a fire.

7 DESIGN METHODS

7.1 Introduction

Simplified design methods are the backbone of current engineering practices in the modern environment. Although each structure and its expected hazards may be unique, a simplified approach and its supporting design methods allow the majority of these structures to be designed by engineers of varying skill levels while still attaining a minimum acceptable standard.

The purpose of this Chapter is twofold. Firstly to postulate a general method for calculating the fire resistance of timber members suitable for use in the New Zealand and Australian markets. Secondly, this method will be extended to evaluate a range of timber floor options with comparisons to the experiments and modelling conducted.

As discussed in Section 2.3, there are a large range of methods and approaches taken to estimate the fire resistance of timber members. The major questions posed by the approach taken can dictate the validity of the method and if it is ultimately accepted or applicable in a given regulatory environment. For instance, when using a reduced properties method the definition of material properties (and their degradation under a thermal gradient) are required to be comprehensive, otherwise the method may become too conservative and therefore not optimal. As has been shown in the literature review the estimation of timber properties at elevated temperatures is challenging due to difficulties in testing methods, and the results can vary significantly. When considering a reduced cross-section approach the determination of an acceptable charring rate is paramount, and although these are well documented they vary considerably between different species and products available. Also the issue of whether to incorporate corner-rounding and what the corresponding charring rate can be reduced to can convolute what is expected to be a simplified analysis.

It is vital that a consistent level of crudeness is achieved with the major inputs into a simplified design method, and the limitations of the method must be clearly identified to avoid the method being used for anything other than its intended purpose. Despite this, it must be relatively simple to implement and also efficient in its estimation of fire resistance. Furthermore it must be applicable to a broad range of scenarios and types of structure to ensure its usefulness.

7.2 Reduced Cross-Section Method

The simplified method developed in this research is based on a reduced cross-section method that does not incorporate corner rounding of timber members. This is because corner rounding often complicates what should in essence be simple hand calculations, and the impact of corner rounding is highly dependent on the exposure duration. This degrades down to a single nominal charring rate calculation for both glulam and LVL, incorporating a zero-strength layer for heated timber, and is shown in Equation 7-1. This method is suggested as it is simple to apply, and the approach taken is clearly detailed and understandable to those without a fire engineering background.

$$d_{char} = \beta \times t + k_0 \times d_{zero} \qquad \textbf{Equation 7-1}$$

Where:

d_{char} = Charring depth (mm)

β = Nominal charring rate (mm/min)

t = Time (min)

k_0 = Zero strength layer modification factor

d_{zero} = Zero strength layer (mm)

Where the nominal charring rate is defined as 0.7 mm/min and the zero strength layer is defined as 7 mm. These values were chosen as a good approximation to the experimental results in this research, and are also representative of a wide range of currently accepted codes such as AS 1720.4 (2006) and Eurocode 5 (CEN, 2004) which specify similar values of nominal charring rate and zero strength layers for LVL. The zero strength layer modification factor is the same as specified in Eurocode 5 (CEN, 2004), and defined as follows:

$$k_0 = t \div 20 \quad \text{for } t < 20 \qquad \textbf{Equation 7-2}$$
$$k_0 = 1.0 \quad \text{for } t \geq 20$$

The measured charring rates of the sections presented in Table 3-6 give an overall rate of approximately 0.74 – 0.79 mm/min. With the inclusion of the zero strength layer, the proposed formulation gives results consistent with the experimental values in this research for a range of fire durations. For instance, considering Test C and Test D which had average recorded charring rates of 0.79 and 0.74 mm/min respectively for the 113 minute duration, the proposed formulation gives:

$$d_{char} = 113\,\text{minutes} \times 0.7\ mm/\,\text{min} + 7\ mm = 86.1\ mm$$

$$\beta_{overall} = \frac{86.1\ mm}{113\ minutes} = 0.76\ mm/min$$

Where: $\beta_{overall}$ = Calculated overall charring rate (mm/min)

The overall charring rate of 0.76 mm/min is a good approximation to the experimental values. The incorporation of a zero strength layer allows for an extra level of safety to be built into the method, and its effect is most prominent at lower levels of charring depth. This ensures that the method is not abused when designing for very slender members and low fire resistance times.

7.3 Failure Criteria

When considering the fire resistance of a floor assembly, it is paramount to consider not only the structural stability of the system, but also its integrity and insulation to resisting the effects of the fire. These factors can be critical when designing fully timber systems as burn-through of timber slabs can dictate the failure mode. This is highly dependent on the cross-sectional geometry of the floor, and whether a concrete slab has been incorporated in the structural design.

The major design factors for assessing the failure of timber floor systems are:

- Bending failure.
- Shear failure.
- Bearing failure.
- Insulation/integrity failure of the slab membrane.

As fires are intermittent events and of very short duration when considering the operation processes of a building, failure criteria only apply to ultimate limit state conditions and serviceability limit states do not apply. These design checks can be made using simple composite beam theory.

The insulation and integrity criteria for the slab membrane are closely linked failure modes, however to fully check the insulation criteria a heat transfer analysis must be conducted. Depending on the method used this may not be time efficient. A more conservative approach is to only consider the integrity criterion of the slab with a minimum thickness remaining, thus ensuring the top surface does not greatly increase in temperature. This makes the requirement

for heat transfer analyses redundant as the zero strength layer and a minimum thickness of slab will ensure that the top surface of the slab is still at a low temperature with regards to the failure criteria.

As a general guideline the thickness over which a heat gradient affects timber under the char layer is approximately 35 mm (reported in Section 2.6.2), hence considering the addition of the zero strength layer and the steepness of the temperature gradient through the timber section, values ranging from 15 – 35 mm would be appropriate to use for the design checks. For the purposes of this research and the following design examples, an arbitrary value of 15 mm is specified as a conservative estimate based off what was observed during furnace testing. It should be noted that the temperature gradient of timber is extremely steep due to the insulative properties of the material, hence although 35mm below the timber there may be a slight increase in temperature, it is not significant from a fire resistance perspective until the temperature reached is over 100°C.

Although this value is quite conservative for smaller slab thicknesses due to the zero-strength layer in Equation 7-1, this choice is purely a reflection of the uncertainty and variability of the fire impact over longer durations. As the uncertainty of char depth increases with the duration of a fire, so does the assumption of a “safe” thickness for the insulation criterion.

7.4 Floor Design Methodology

The basic methodology behind the design of composite floors described in this thesis is to sum the contribution of each component of the floor system to the structural resistance. This involves a number of assumptions, the most significant being that the connections between the components are fully rigid. This assumption is true for most timber components that have been glued together; however other types of connection such as nailed or bolted members may need additional consideration due to the slip between the floor components under load. The purpose of this approach is to ensure the process is a simple as possible, thus allowing the addition of further modifications or factors at a later stage much easier.

7.4.1 Loading Arrangement

The design of timber-only floor systems is similar to a generic beam design, hence the specific guidelines presented in NZS 3603 (1993) are used in the following examples to demonstrate a simple calculation method utilising the proposed nominal charring rate formulation. Initially, both the effective span and loading conditions must be known, for the following examples the normal

office loading characteristics for a multi-storey building from AS/NZS 1170.1 (2002) will be used which are a live load of 3.0kPa and a superimposed dead load of 1.0kPa plus the self-weight of the floors. The effective span is defined as the clear span of the floor between support points, taken from the centre of each bearing area for simply-supported floor assemblies or the extreme edge of a top flange for flange hung floor assemblies.

7.4.2 Cold Design

After determining the appropriate loadings on the floor the next step is to calculate the expected cold design checks for both ultimate and serviceability limit states. Generally a cold floor design consists of taking a strip of the floor encompassing one beam element and a uniform width of slab for all design checks, and this is normally dictated by the beam element spacing. As the fire design considers only the ultimate limit state conditions, these checks will be shown here while the serviceability limit state conditions should be investigated as part of a more detailed floor analysis. Some equations shown in the chapter are reproduced from Section 3.4.2, however are presented here for completeness of the method.

For the ultimate limit state criteria the loading conditions are prescribed by the loadings standard AS/NZS 1170.0 which is:

$$E_d = 1.2G_l + 1.5Q_l \qquad \textbf{Equation 7-3}$$

The dead load includes both a superimposed deal load and the self-weight of the floor:

$$G_l = SDL + G_{self} \qquad \textbf{Equation 7-4}$$

The uniformly distributed load applied to the floors is then calculated from the known tributary width of each specimen:

$$w = W_t \times E_d \qquad \textbf{Equation 7-5}$$

Where: w = Uniformly distributed load (kN/m)

From this the maximum bending moment at mid-span can be found for a simply-supported floor with a uniformly distributed load:

$$M^* = \frac{w \times L^2}{8}$$ **Equation 7-6**

Where: M^* = Moment demand (kNm)

The bending capacity of the floor section is then calculated:

$$\emptyset M_n = \emptyset k_1 k_4 k_5 k_8 f_b' Z_b$$ **Equation 7-7**

Where:
$\emptyset$ = Strength reduction factor
M_n = Nominal bending strength capacity (kNm)
k_1 = Load duration factor
k_4 = Parallel support factor
k_5 = Grid system factor
k_8 = Load sharing factor
f_b' = Characteristic bending strength (MPa)
Z_b = Elastic section modulus (mm^3)

The design capacity is then checked against the moment demand:

$$M^* \leq \emptyset M_n$$ **Equation 7-8**

The maximum shear force is found for a simply-supported floor with a uniformly distributed load:

$$V^* = \frac{w \times L}{2}$$ **Equation 7-9**

Where: V^* = Shear demand (kN)

And the shear capacity is calculated for the floor section:

$$\emptyset V_n = \emptyset k_1 k_4 k_5 f_s' A_s \quad \textbf{Equation 7-10}$$

Where:
V_n = Nominal shear strength capacity (kN)
f_s' = Characteristic shear strength (MPa)
A_s = Shear area (mm^2)

Where the shear area is defined as:

$$A_s = t_w \frac{I}{Q_{centroid}} \quad \textbf{Equation 7-11}$$

Where:
t_w = Web thickness (mm)
I = Second moment of area (mm^4)
$Q_{centroid}$ = First moment of area about the centroid (mm^3)

The design capacity is then checked against the shear demand:

$$V^* \leq \emptyset V_n \quad \textbf{Equation 7-12}$$

Considering the bearing strength of the simply-supported seating, the demand is the reaction force at the supports, which is the same as the shear demand for the simply-supported case:

$$N_b^* = \frac{w \times L}{2} \quad \textbf{Equation 7-13}$$

Where:
N_b^* = Bearing strength demand (kN)

The bearing strength of the timber floor is completely dependent on the connection type; however the bearing direction will most likely be perpendicular to the grain. For simply-supported floors the nominal bearing capacity is:

$$\emptyset N_{nb} = \emptyset k_1 k_3 f_p' A_p$$ **Equation 7-14**

Where:
N_{nb} = Nominal bearing strength capacity (kN)
k_3 = Bearing area factor
f_p' = Characteristic compression strength perpendicular to grain (MPa)
A_p = Perpendicular bearing area (mm^2)

And the design capacity is then checked against the bearing demand:

$$N_b^* \leq \emptyset N_{nb}$$ **Equation 7-15**

7.4.3 Fire Design

For the fire design of timber floor assemblies there are a number of approaches. The simplest approach is to calculate a reduced section based on the type of fire exposure present in the design, and recalculating the cold design formulae presented above to ensure the floor will adequately withstand a fire for that specified duration.

When considering floor assemblies the fire exposure originates from the underside of the floor, and any penetrations through the slab are usually considered as a special case. Therefore for unprotected floors the complete underside of the assembly is exposed to the fire and the top of the slab is left in an ambient temperature open air environment. In the case of beam type floors this translates to three-sided exposure. In the case of a cassette type floor the charring characteristics will be one-dimensional until the bottom layer has burned through, at which time the interior section of the floor is exposed and the charring behaviour will become three-sided as with a joist floor.

Care must be taken with any structural calculations to ensure that the changing section properties take account of the rising of the neutral axis as the floor loses mass from its lower extremities while disproportionately retaining the upper slab mass. This is highly dependent on the floor geometry as to how much of an effect this will have on the overall floor strength.

Implemented in a spreadsheet this method can be run as a quasi-steady state analysis, evaluating the floor failure criteria at selected time intervals (generally 1 minute intervals suffice for structural calculations). This aids greatly in recalculating the new section properties at each defined time step.

Firstly the new section properties are calculated for the reduced section at a specified duration. For the checks presented in Section 7.4.2 this involves calculating a new section modulus, shear area and bearing area for a strip of the floor. The situational fire load factor is then applied to the loading case shown in Equation 7-3, accounting for the different probabilities of the actual loading states of the building in the case of a fire.

$$E_{d,fire} = 1.0G_l + 0.4Q_l \quad \textbf{Equation 7-16}$$

After this the strength checks shown from Equation 7-4 to Equation 7-15, with modifications to the Φ and k factors for the fire case. For simplification when considering composite floor systems, some factors do not apply such as the parallel support factor, k_4, and the grid system factor, k_5. The bearing area factor, k_3, also reduces to unity when the modular floor is supported on the ends for a simply-supported system (as would usually be the case in multi-storey buildings).

For calculations resulting in very small residual sections the maximum stresses in the tension and compression zones should be checked by calculating the maximum stresses at the extreme fibres. This is of paramount importance with very thin residual member sizes as failure is likely to occur when the bottom flanges become too thin to carry the maximum tension forces in the member.

A further check to assess the integrity and insulation criteria is generally a requirement for floor assemblies, and as discussed in Section 7.3 a minimum timber slab thickness of 15 mm is specified in this research to assess both of these criteria simultaneously:

$$15mm \leq d_{slab} - d_{char} \quad \textbf{Equation 7-17}$$

Where: d_{slab} = Slab depth (mm)

Hence if the nominal charring rate comes within 15 mm of the floor slab upper surface this criterion is deemed to have failed. If all the failure criteria are satisfied then the floor assembly is

assumed to adequately resist the fire load for the specified duration. Worked examples for different floor geometries are given in Section 7.5.

A more complex method is to substitute Equation 7-1 into the cold design formulae and derive equations to solve for the time variable. This results in a cubic formulation for each strength check which can be solved to determine the exact expected fire resistance time of the floor. This method however can be time consuming and any changes in the variables require a complete recalculation of the entire formulae. Hence is best used for a one-off estimate of floor performance. Utilising spreadsheet software is a much more time efficient and user-friendly way of calculating the fire resistance, and also simplifies the tasks of error-checking and reproducing design data for different floor systems.

With the addition of a concrete slab many issues surrounding integrity and insulation can be mitigated, as the fire resistance can be obtained by adding the fire resistance rating of the concrete to that of the protective layer of wood. The required thickness of concrete slabs in NZ 3101 (2006) to achieve a specific rating is given as:

Table 7-1: Concrete thickness fire resistance ratings according to NZ 3101 (2006)

Concrete Thickness (mm)	60	80	100	120
Rating (minutes)	30	60	90	120

If the combined fire resistance rating from the wood and the concrete is insufficient, additional protection can be obtained with an additional top surface on the floor, or a fire-rated ceiling. Some protection measures for unprotected floors are described in Chapter 8.

7.5 Worked Examples

This section provides worked examples on generic floor types, including two of the designs used in the furnace testing. The examples given below reflect generic modular spacings of 1.2 metre widths and 2.4 metre widths for short and long span floors, as did the floor designs tested in the furnace.

7.5.1 Composite Joist Floor – 30 minutes

The first design example is for an unprotected composite joist floor, which is commonly specified as a solution for smaller scale applications as it is simple to design, construct and erect. These systems can perform poorly in fires compared with other design geometries due to the large amount of surface area of timber exposed to the fire. A shorter span with lower loads generally requires more slender members, which has a further detrimental impact on the fire resistance of the floors if it is left unprotected. Specimen A described in Chapter 3 is one such floor design, with optimal span lengths ranging from 4 – 7 metres. The expected fire resistance of the following section, an illustration of which is shown in Figure 7-1 with a tributary width of 1200 mm, is shown below:

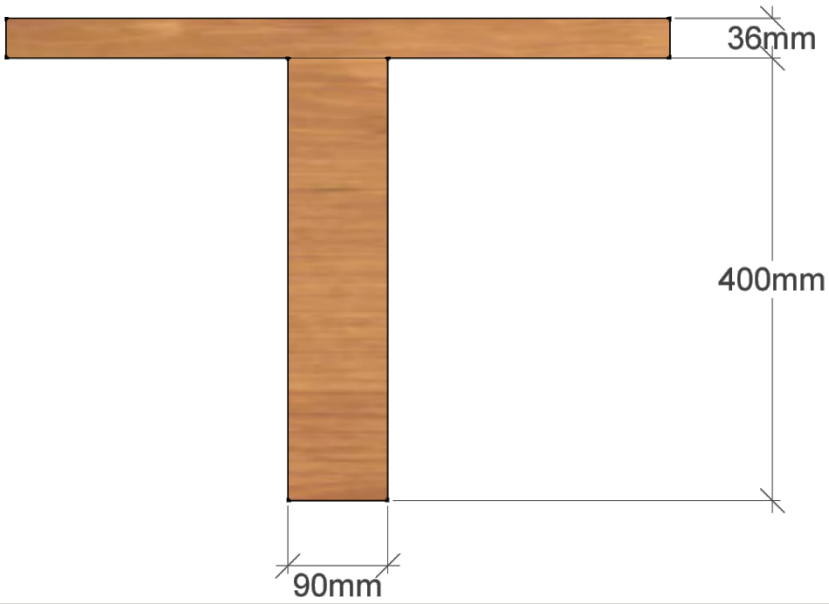

Figure 7-1: Composite joist floor design example initial dimensions

New section properties must be calculated for an expected duration of fire exposure to find the residual beam section remaining at this time. The char depth after 30 minutes fire exposure is:

$$d_{char} = 0.7mm/min \times 30min + 7mm = 28mm$$

Considering three-sided exposure of this floor from the underside, the reduced section is calculated with the nominal charring rate as shown in Figure 7-2:

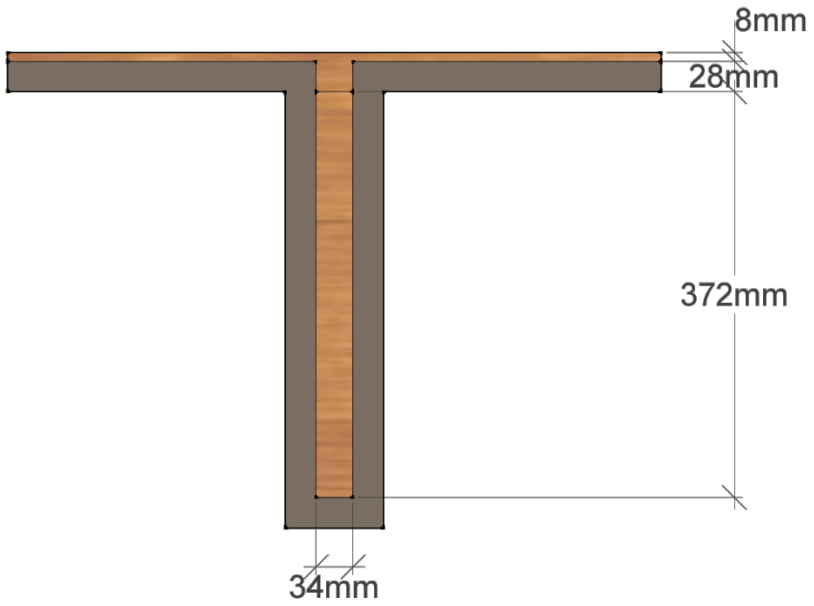

Figure 7-2: Composite joist floor design example charred dimensions

The residual section properties are then calculated as:

$$A = 23.2 \times 10^3 mm^2$$

$$Z_b = 1.48 \times 10^6 mm^3$$

$$Q_{centroid} = 1.38 \times 10^6 mm^3$$

$$I = 4.20 \times 10^8 mm^4$$

Where: A = Section area (mm²)

The external load on the floor calculated as G_l + $\psi_l Q_l$ where the coefficient for the fire case is defined as ψ_l = 0.4. Considering a normal office loading scenario of a superimposed dead load of 1.0kPa, a live load of 3.0kPa and the self-weight of the beam (which was calculated as 0.45kPa), the following loads are calculated:

$$G_l = 1.0 \times (1.0kN/m^2 + 0.45kN/m^2) = 1.45kN/m^2$$

$$\psi_l Q_l = 0.4 \times 3.0kN/m^2 = 1.2kN/m^2$$

Where: ψ_l = Load reduction factor

For the ease of transition from the ambient temperature calculations, the original self-weight of the floor is used in the load calculations. This assumption is conservative as the beam will only reduce in mass over the duration of a fire.

The uniformly distributed load applied to the floors is then calculated from the known tributary width of the floor, in this case it is 1.2 metres:

$$w = 1.2m \times (1.45kN/m^2 + 1.2kN/m^2) = 3.18kN/m$$

From this the maximum demands are then calculated for a seven metre span:

$$M^* = \frac{wL^2}{8} = \frac{3.18 \times 7^2}{8} = 19.5kNm$$

$$V^* = \frac{wL}{2} = \frac{3.18 \times 7}{2} = 11.1kN$$

$$N_b^* = \frac{wL}{2} = \frac{3.18 \times 7}{2} = 11.1kN$$

As the floor chars the neutral axis depth of the section changes. In this case the neutral axis depth measured from the top of the floor section is reduced then increases as mass is lost from the joist and the underside of the slab. The bending strength of the section is:

$$\emptyset M_n = \emptyset k_1 k_8 k_{24} f_b' Z_b = 1.0 \times 1.0 \times 1.0 \times \left(\frac{95}{408}\right)^{0.167} \times 38MPa \times 1.48 \cdot 10^6 mm^3 = 44.0kNm$$

Where: k_{24} = Size factor

Checking bending:

$$M^* \leq \emptyset M_n$$

$$19.5 \leq 44.0 \rightarrow OK$$

The shear strength of the section is:

$$A_s = t_w \frac{I}{Q_{centroid}} = 34mm \times \frac{4.20 \cdot 10^8 mm^4}{1.38 \cdot 10^6 mm^3} = 10.3 \cdot 10^3 mm^2$$

$$\emptyset V_n = \emptyset k_1 f_s' A_s = 1.0 \times 1.0 \times 5.0MPa \times 10.3 \cdot 10^3 mm^2 = 51.7kN$$

Checking the shear:

$$V^* \leq \emptyset V_n$$

$$11.1 \leq 51.7 \rightarrow OK$$

The bearing strength of the section is (assuming a bearing length of the floor of 50mm):

$$A_p = t_b L_b = 34mm \times 50mm = 1.7 \cdot 10^3 mm^2$$

$$\emptyset N_{nb} = \emptyset k_1 k_3 f_p' A_p = 1.0 \times 1.0 \times 1.0 \times 10MPa \times 1.7 \cdot 10^3 mm^2 = 17kN$$

Where: t_b = Bearing thickness (mm)

L_b = Bearing length (mm)

Checking the bearing perpendicular to the grain:

$$N_b^* \leq \emptyset N_{nb}$$

$$11.1 \leq 17 \rightarrow OK$$

All design checks for stability are OK.

Back calculations can be made to determine the actual fire resistance of the floor by deriving the section modulus or area required in each strength check and then substituting the charring equation into these. This gives a cubic formulation which when solved will give the expected fire resistance time of the member. The above equations can also be put into an excel spreadsheet and a solver used to find the expected fire resistance.

The design should consider the duration required to sufficiently heat the top of the timber slab to untenable conditions. If an insulation failure can be avoided, good construction detailing will ensure that the integrity criterion is satisfied. For insulation, checking the thickness of the slab will ensure that the top surface of the slab is still at a low temperature with regards to the failure criterion. For the purposes of this design example a value of 15 mm is specified. Checking the top slab for an insulation failure:

$$d_{slab} - d_{char} = 36mm - 28mm = 8mm$$

$$8 < 15 \rightarrow Not\ OK$$

As this design example is based on Specimen A tested in the furnace experiments the top slab thickness was very small at 36 mm, and the failure criterion is quite conservative on comparison

with the temperature readings shown in Sections 3.6.4 and 3.7.4 for tests A and B. With small slab thicknesses such as this it is common that a concrete slab would be incorporated into the design for floor durability. In this case the failure criterion would most likely be satisfied with a simple check of slab thickness from Table 7-1.

In the case that the floor passes the insulation failure criterion, the floor has been shown to withstand 30 minutes of fire exposure without failure.

7.5.2 Cassette Floor – 60 minutes

Now the case of a cassette floor system is shown, designed for approximately 60 minutes standard fire endurance while unprotected. Cassette floors are a more ideal case for fire resistance when compared with the joist floor example, as the surface area of timber exposed to the fire is greatly reduced. This results in a major reduction in the overall cross-sectional area lost to the fire, and an increased structural longevity. Mechanically they are also an optimised design of floor; hence section depths are generally lower, making this type of modular floor ideal for multi-storey applications where inter-storey depth is of paramount importance when designing tall buildings. The example shown is a generic design with optimal span lengths ranging from 6 – 9 metres. Checking the expected fire resistance of the following section shown in Figure 7-3 with a tributary width of 1000 mm:

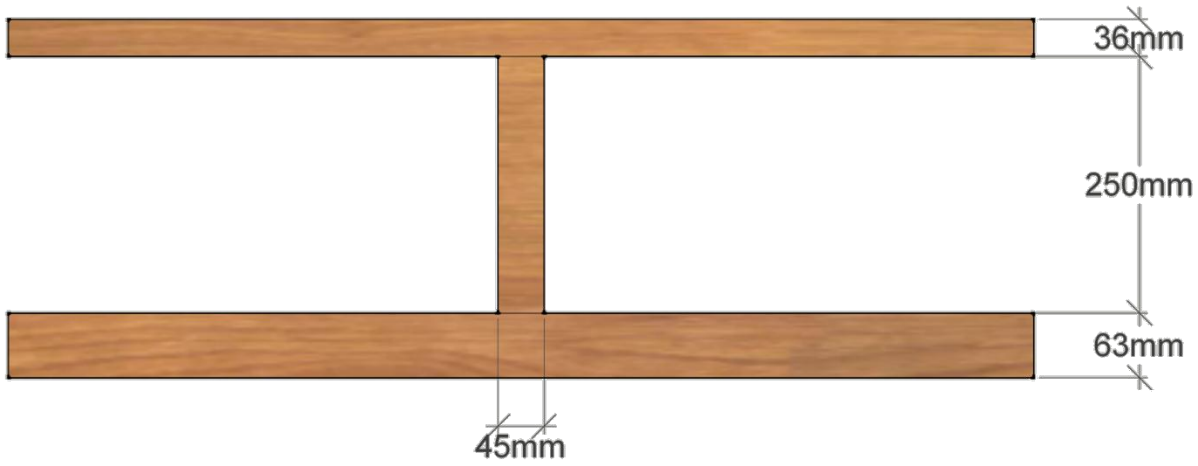

Figure 7-3: Cassette floor design example initial dimensions

The floor consists of 63 mm bottom flange, with a 36 mm top flange and 250 mm deep intermediate beams of 45 mm thickness. New section properties must be calculated for an

expected duration of fire exposure to find the residual beam section remaining at this time. The char depth after 60 minutes fire exposure is:

$$d_{char} = 0.7mm/min \times 60min + 7mm = 49mm$$

Considering one-sided exposure of this floor from the underside, the reduced section is calculated with the nominal charring rate as shown in Figure 7-4:

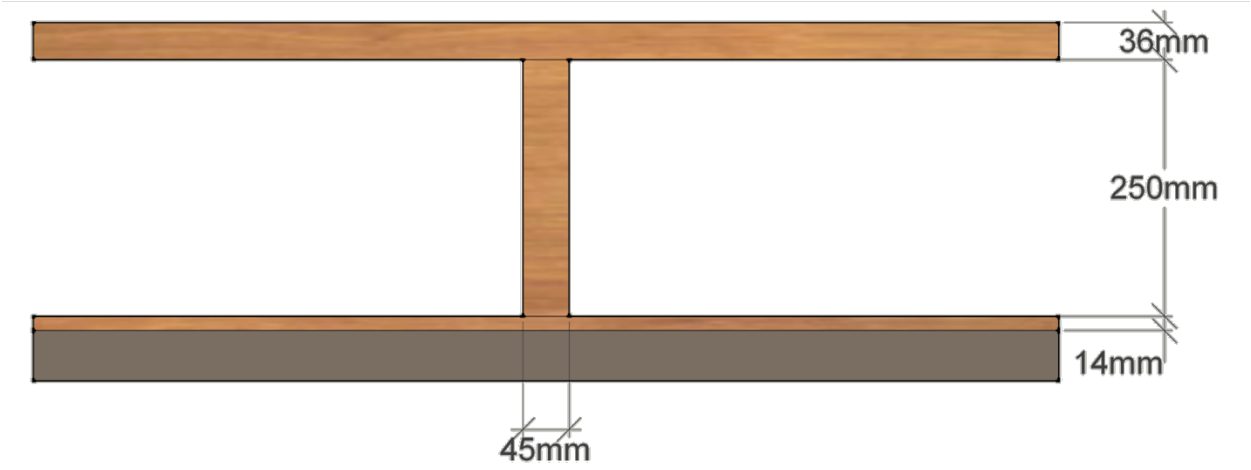

Figure 7-4: Cassette floor design example charred dimensions

The residual section properties are then calculated as:

$$A = 61.3 \times 10^3 mm^2$$

$$Z_b = 4.25 \times 10^6 mm^3$$

$$Q_{centroid} = 3.62 \times 10^6 mm^3$$

$$I = 8.75 \times 10^8 mm^4$$

Considering a normal office loading scenario of a superimposed dead load of 1.0kPa, a live load of 3.0kPa and the self-weight of the beam (which was calculated as 0.6kPa), the following loads are calculated:

$$G_l = 1.0 \times (1.0kN/m^2 + 0.63kN/m^2) = 1.63kN/m^2$$

$$\psi_l Q_l = 0.4 \times 3.0kN/m^2 = 1.2kN/m^2$$

The uniformly distributed load applied to the floors is then calculated from the known tributary width of the floor, in this case it is 1.0 metres:

$$w = 1.0m \times (1.63kN/m^2 + 1.2kN/m^2) = 2.83kN/m$$

From this the maximum demands are then calculated for an eight metre span:

$$M^* = \frac{wL^2}{8} = \frac{2.83 \times 8^2}{8} = 22.6kNm$$

$$V^* = \frac{wL}{2} = \frac{2.83 \times 8}{2} = 11.3kN$$

$$N_b^* = \frac{wL}{2} = \frac{2.83 \times 8}{2} = 11.3kN$$

As the floor chars the neutral axis depth of the section changes. In this case the neutral axis depth measured from the top of the floor section is reduced as mass is lost from the bottom flange of the floor. The bending strength of the section is:

$$\emptyset M_n = \emptyset k_1 k_8 k_{24} f_b' Z_b = 1.0 \times 1.0 \times 1.0 \times \left(\frac{95}{300}\right)^{0.167} \times 38MPa \times 4.25 \cdot 10^6 mm^3 = 133kNm$$

Checking the bending:

$$M^* \leq \emptyset M_n$$

$$22.6 \leq 133 \rightarrow OK$$

The shear strength of the section is:

$$A_s = t_w \frac{I}{Q_{centroid}} = 45mm \times \frac{8.75 \cdot 10^8 mm^4}{3.62 \cdot 10^6 mm^3} = 10.9 \cdot 10^3 mm^2$$

$$\emptyset V_n = \emptyset k_1 f_s' A_s = 1.0 \times 1.0 \times 5.0MPa \times 10.9 \cdot 10^3 mm^2 = 54.4kN$$

Checking the shear:

$$V^* \leq \emptyset V_n$$

$$11.3 \leq 54.4 \rightarrow OK$$

The bearing strength of the section is (assuming a bearing length of the floor of 50mm):

$$A_p = t_b L_b = 1000mm \times 50mm = 50.0 \cdot 10^3 mm^2$$

$$\emptyset N_{nb} = \emptyset k_1 k_3 f_p' A_p = 1.0 \times 1.0 \times 1.0 \times 10MPa \times 50.0 \cdot 10^3 mm^2 = 500kN$$

Checking the bearing perpendicular to the grain:

$$N_b^* \leq \emptyset N_{nb}$$

$$11.3 \leq 500 \rightarrow OK$$

All design checks for stability are OK. Hence the floor can withstand 60 minutes of fire exposure without failure.

Issues arise with a cassette floor when the bottom flange burns through. A simplified method of solution to this problem is to calculate when the char depth is equivalent to the bottom chord thickness, and then apply any additional charring depth to the entire inside surfaces of the exposed timber section as with the joist floor method. For the above example, the 63 mm thick bottom chord will burn through after 80 minutes of fire exposure. Considering 85 minutes of standard fire exposure, the charring profile considered is shown in Figure 7-5.

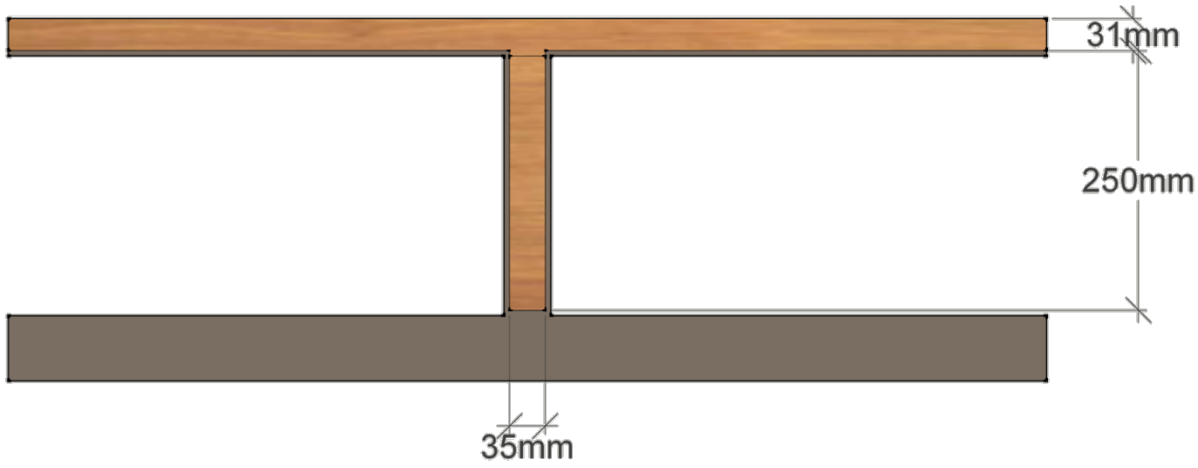

Figure 7-5: Cassette floor design example bottom chord burnout dimensions

The char thickness can be calculated by assuming the bottom layer has burned through at 80 minutes, hence the level of char on the formerly protected interior members is for 5 minutes:

$$d_{char} = 0.7mm/min \times 5min + (5 \div 20) \times 7mm = 5.3mm$$

Failure by insulation and integrity are not a major issue for cassette floors, as the charring damage is not directly applied to the top slab until latter stages of burning. For this example the insulation check should be made only if the bottom chord has burned away. As the interior members are generally very slender, once the bottom chord is gone the remaining structural

resistance of the floor will be greatly depleted, and failure would likely occur by collapse soon after this.

7.5.3 Composite Box Floor – 90 minutes

Due to some of the physical characteristics of designing unprotected timber floors, larger span floors will have much larger section sizes and hence tend to have higher expected fire resistance ratings than smaller span floors. Specimen D described in Chapter 3 is one such floor, with optimal span lengths ranging from 8 – 10 metres. Checking the expected fire resistance of the following section shown in Figure 7-6 with a tributary width of 800 mm:

Figure 7-6: Composite box floor design example initial dimensions

New section properties must be calculated for an expected duration of fire exposure to find the residual beam section remaining at this time. The char depth after 90 minutes fire exposure is:

$$d_{char} = 0.7mm/min \times 90min + 7mm = 70mm$$

Considering three-sided exposure of this floor from the underside, the reduced section is calculated with the nominal charring rate as shown in Figure 7-7:

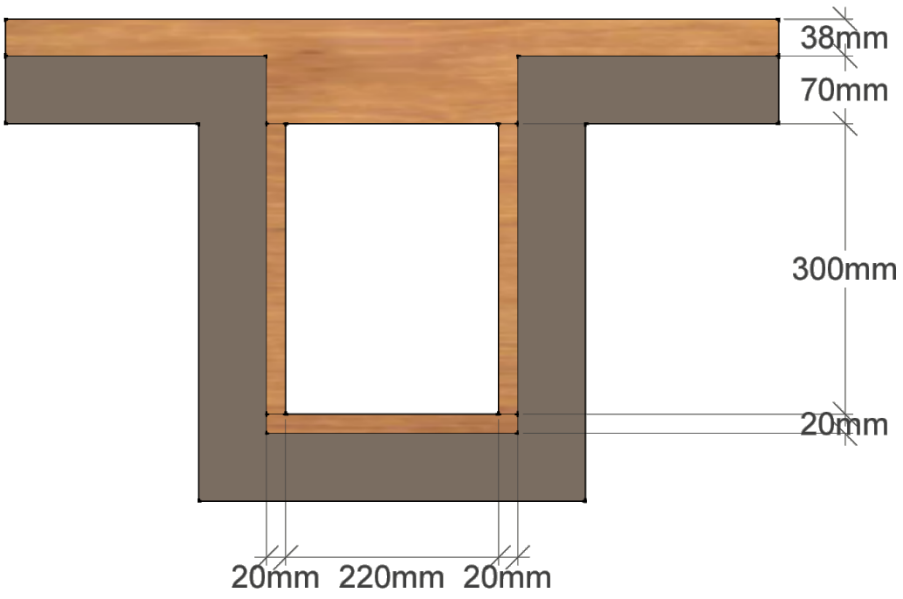

Figure 7-7: Composite box floor design example charred dimensions

The residual section properties are then calculated as:

$$A = 65.8 \times 10^3 mm^2$$

$$Z_b = 3.56 \times 10^6 mm^3$$

$$Q_{centroid} = 3.39 \times 10^6 mm^3$$

$$I = 1.13 \times 10^9 mm^4$$

Considering a normal office loading scenario of a superimposed dead load of 1.0kPa, a live load of 3.0kPa and the self-weight of the beam (which was calculated as 1.0kPa), the following loads are calculated:

$$G_l = 1.0 \times (1.0kN/m^2 + 1.0kN/m^2) = 2.0kN/m^2$$

$$\psi_l Q_l = 0.4 \times 3.0kN/m^2 = 1.2kN/m^2$$

The uniformly distributed load applied to the floors is then calculated from the known tributary width of the floor, in this case it is 0.8 metres:

$$w = 0.8m \times (2.0kN/m^2 + 1.2kN/m^2) = 2.8kN/m$$

From this the maximum demands are then calculated for a nine metre span:

$$M^* = \frac{wL^2}{8} = \frac{2.8 \times 9^2}{8} = 28.4kNm$$

$$V^* = \frac{wL}{2} = \frac{2.8 \times 9}{2} = 12.6kN$$

$$N_b^* = \frac{wL}{2} = \frac{2.8 \times 9}{2} = 12.6kN$$

As the floor chars the neutral axis of the section changes. In this case the neutral axis depth measured from the top of the floor section is reduced as mass is lost from the box beam and underside of the slab. The bending strength of the section is:

$$\emptyset M_n = \emptyset k_1 k_8 k_{24} f_b' Z_b = 1.0 \times 1.0 \times 1.0 \times \left(\frac{95}{428}\right)^{0.167} \times 38MPa \times 3.56 \cdot 10^6 mm^3 = 105kNm$$

Checking the bending:

$$M^* \leq \emptyset M_n$$

$$28.4 \leq 105 \rightarrow OK$$

The shear strength of the section is:

$$A_s = 2t_w \frac{I}{Q_{centroid}} = 2 \times 20mm \times \frac{1.13 \cdot 10^9 mm^4}{3.39 \cdot 10^6 mm^3} = 13.3 \cdot 10^3 mm^2$$

$$\emptyset V_n = \emptyset k_1 f_s' A_s = 1.0 \times 1.0 \times 5.0MPa \times 13.3 \cdot 10^3 mm^2 = 66.7kN$$

Checking the shear:

$$V^* \leq \emptyset V_n$$

$$12.6 \leq 66.7 \rightarrow OK$$

The bearing strength of the section is (assuming a bearing length of the floor of 50mm):

$$A_p = t_b L_b = 260mm \times 50mm = 13.0 \cdot 10^3 mm^2$$

$$\emptyset N_{nb} = \emptyset k_1 k_3 f_p' A_p = 1.0 \times 1.0 \times 1.0 \times 10MPa \times 13.0 \cdot 10^3 mm^2 = 130kN$$

Checking the bearing perpendicular to the grain:

$$N_b^* \leq \emptyset N_{nb}$$

$$12.6 \leq 130 \rightarrow OK$$

All design checks for stability are OK. Checking the top slab for an insulation failure:

$$d_{slab} - d_{char} = 108mm - 70mm = 38mm$$

$$38 > 15 \rightarrow OK$$

Hence the floor can withstand 90 minutes of fire exposure without failure.

7.6 Results Comparison

In order to determine the adequacy of the reduced cross-section method for estimating the fire resistance of timber floor assemblies, comparisons are made in this section between the experimental, numerical and analytical results. The displacement results from previous chapters are used in conjunction with the results given from the calculation method presented in this chapter. The calculation method was implemented in a spreadsheet as a quasi-steady state analysis in order to iteratively solve for the expected failure time of the floors to the nearest minute.

As the smaller floors in Tests A and B were designed to be extremely lightweight, they had very thin top flanges acting in the structural assembly. In practice, a lightweight non-structural concrete topping or other insulating membrane would be installed atop these floors for the purposes of better acoustic, insulation and durability properties. With these points in mind, only the strength failure mode is shown on the following figure, however both strength and insulation values are reported in Table 7-2.

Table 7-2: Calculated failure times for Tests A – D

Time to Failure	Test A	Test B	Test C	Test D
Stability (minutes)	40	47	111	111
Insulation (minutes)	20	20	123	123

7.6.1 Test A

The comparison between the calculated collapse failure time to both the experimental and modelling results is shown in Figure 7-8 for Test A.

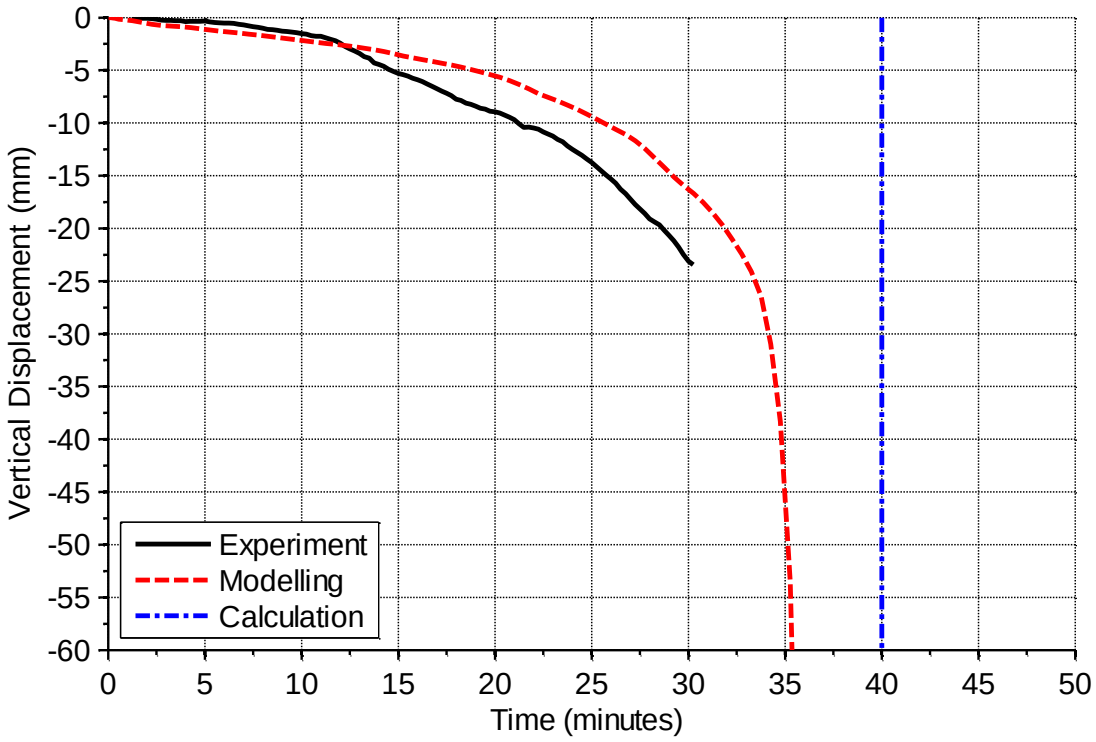

Figure 7-8: Experimental, modelling and calculation method results for Test A

For Test A the experimental results were less complete than the other records taken as the test was terminated prematurely. However observations of the displacement behaviour and from the other tests conducted suggested that a failure time for the experiment would be in the range of 33 – 37 minutes. The modelling results predicted a failure time of approximately 35 minutes.

The calculated failure time of the floor for insulation is 20 minutes, while the calculated failure time for structural collapse is 40 minutes. It can be seen from the figure that the calculation method is not conservative compared to the modelling from a structural design sense, however overall it is an acceptable level of deviation for a simplified method. It is assumed that the modelling is a good approximation to the experiment in terms of predicting failure time.

7.6.2 Test B

The comparison between the calculated collapse failure time to both the experimental and modelling results is shown in Figure 7-9 for Test B. The failure time in the experiment was 41 minutes, which was also predicted by the modelling.

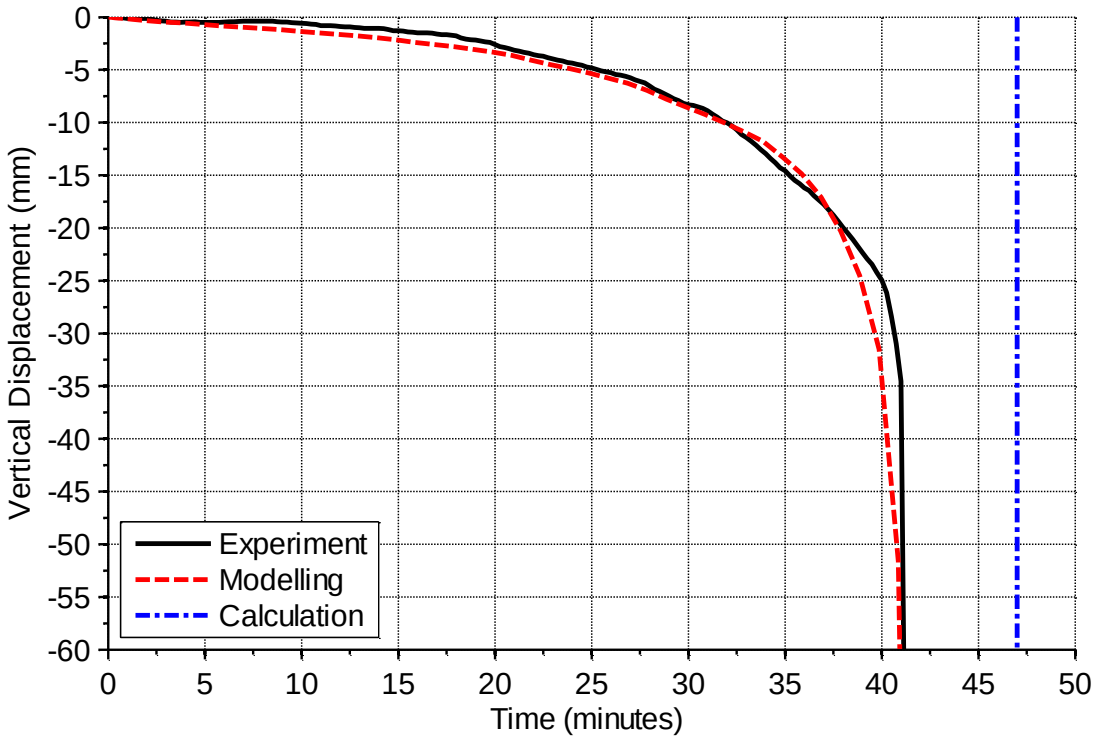

Figure 7-9: Experimental, modelling and calculation method results for Test B

The calculated failure time of the floor for insulation is 20 minutes, while the calculated failure time for structural collapse is 47 minutes. Similar to the results for Test A, the calculation method again over predicts the expected failure time of the floors. As the experimental data record is complete for Test B, these results show that the design method predicts the expected collapse time of the floor to within 6 minutes.

Although this discrepancy is notable, the amount of inputs and their subsequent complexity implemented in the simplified method serve to reduce its precision when compared with the modelling effort. Ultimately the purpose of the simplified method is to provide an adequate approximation to reality, and is meant to be applicable to a wide range of timber assemblies as opposed to simply floors. Hence deviation from the experimental and numerical results is expected. This is discussed in further detail in Section 7.6.5.

7.6.3 Test C

The comparison between the calculated collapse failure time to both the experimental and modelling results is shown in Figure 7-10 for Test C. The experiment was terminated at 105 minutes, and an expected failure time of the floor was predicted to be at 120 – 125 minutes. The modelling effort predicts the failure time of the floors at 127 minutes.

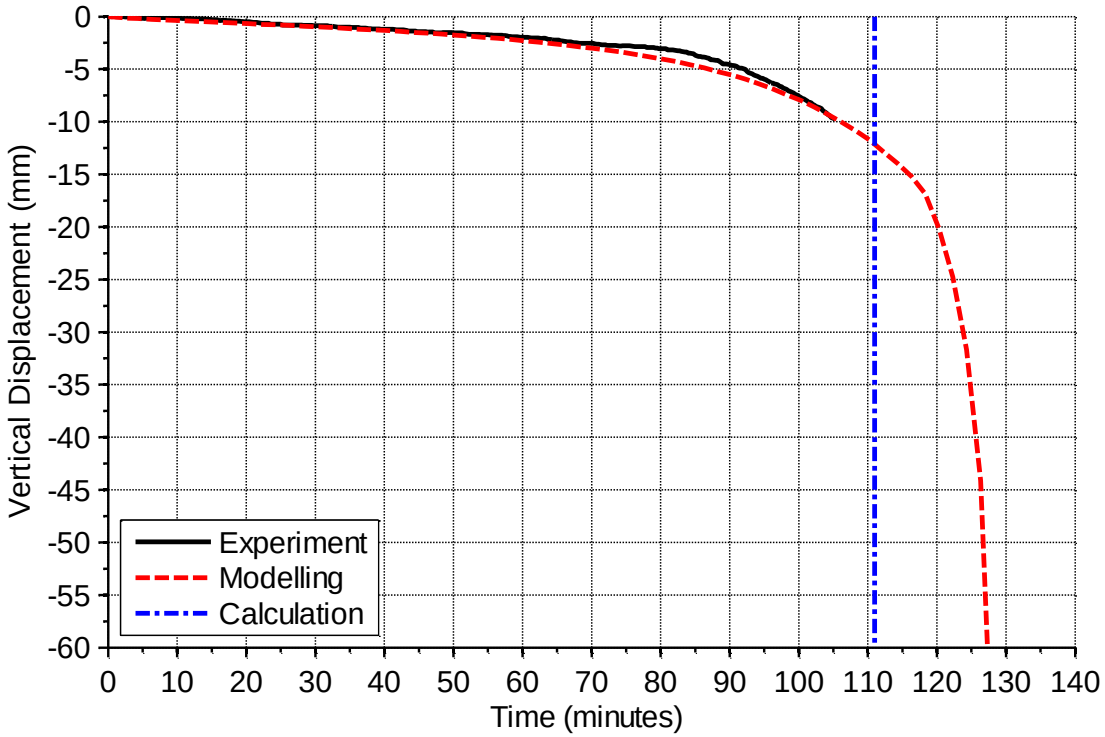

Figure 7-10: Experimental, modelling and calculation method results for Test C

The calculated failure time of the floor for insulation is 123 minutes, while the calculated failure time for structural collapse is 111 minutes as shown on the figure. Contrary to what was calculated for Tests A and B, the results suggest that the calculation method is relatively conservative from a structural design sense when considering larger floors.

7.6.4 Test D

The comparison between the calculated collapse failure time to both the experimental and modelling results is shown in Figure 7-11 for Test D. As with Test C, the experiment was terminated at 105 minutes, and an expected failure time of the floor was predicted to be at 120 – 125 minutes. The modelling effort predicts the failure time of the floors at 132 minutes.

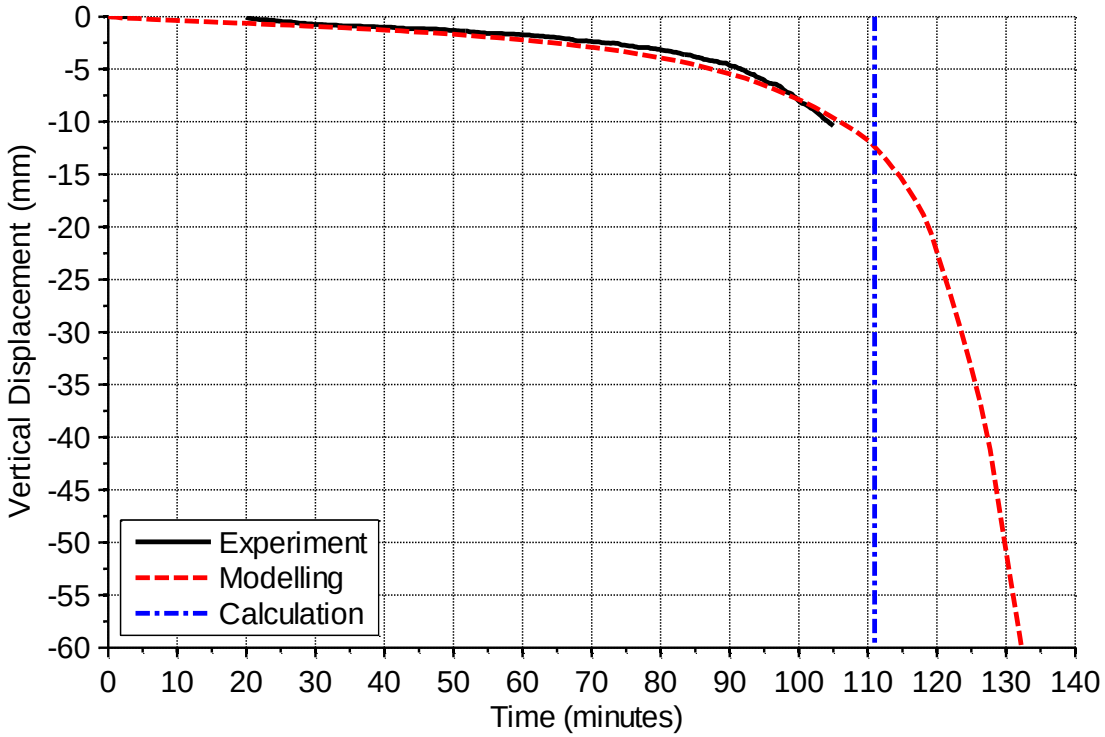

Figure 7-11: Experimental, modelling and calculation method results for Test D

The calculated failure time of the floor for insulation is 123 minutes, while the calculated failure time for structural collapse is 111 minutes. Due to the differing geometry of the composite box floor to the composite joist floor, both numerical modelling and the calculation method give higher expected failure times for this floor even though both Tests C and D were designed with an identical load ratio. This is due to the differing ratios of surface area exposed to fire, and hence a greater impact modelled on the joist floor as opposed to the composite box floor. However this was not seen in the experiments to the degree predicted by the calculations. This is most likely due to the variability of the experimental inputs with regards to the furnace temperatures, the material properties and construction of the timber assemblies, instrumentation setup, the load applied and the processes followed to achieve the results.

7.6.5 Discussion

It can be seen from the above figures that the calculation method is not conservative from a structural design sense when considering the smaller floors, however is quite conservative when considering the larger floors. This is due to many factors impacting the actual performance of floors in reality, such as the variation of the charring rate over the duration of the fire and the differing load ratio between the smaller to larger floor sizes. A much greater level of detail can be adopted in the modelling effort; hence more precise results can be achieved when simulating real experiments. However there are a number of major drawbacks to using advanced numerical methods, the most notable of which are a greater level of expertise and available time are required to conduct the modelling.

Although comparisons with the actual measured overall charring rates from the experimental testing correspond well with a nominal charring rate of 0.7 mm/min, this has shown to be slightly too crude for hand calculative methods. The simplest way of improving this calculation method is to adopt a bi-linear charring rate formulation, such that for initial modelling the charring rate is higher than prescribed by Equation 7-1, decreasing to a lower rate at the point in which the calculation method becomes conservative.

7.7 Bi-Linear Charring Rate Method

7.7.1 Proposed Formulation

When considering the results presented in Section 7.6, the proposed reduced cross-section method is under-conservative for short duration fires, and slightly over-conservative for long duration fires. This implies that initial charring rates are steeper as compared to the latter stages. To better account for this, the following bi-linear charring rate formulation is proposed:

$$d_{char} = \gamma\beta \times t + k_0 \times d_{zero}$$ **Equation 7-18**

Where: γ = Modification factor

For t < 45 minutes:

γ = 1.15

For t > 45 minutes:

γ = 0.90

This results in a charring rate which is approximately 0.81 mm/min for the initial 45 minutes, and 0.63 mm/min thereafter. It should be noted that the method is cumulative, hence the initial 45 minute char depth should be calculated and included for exposure times over 45 minutes.

7.7.2 Test Comparisons

Table 7-3 shows the comparison between the estimated failure times of Tests A to D, and the calculated results from both linear and bi-linear hand calculation methods:

Table 7-3: Comparison between estimated and calculated failure times for Tests A – D

Experiment	Failure time (minutes)		
	Estimate from Experiment	Linear Charring Rate	Proposed Bi-linear Method
Test A	33 – 37	40	35
Test B	41	47	41
Test C	120 – 125	111	123
Test D	120 – 125	111	124

It can be seen from the results that the bi-linear modification to the charring rate gives a much closer approximation to the expected failure times of the experimental tests in this research.

7.7.3 Code Comparisons

As a comparison between currently used simplified methods, calculations of char depth are made for the bi-linear method compared with a selection of regulatory codes from around the world (as described in Section 2.3) for a number of generic fire resistance times. The results are shown in Table 7-4, considering the effective charring depth (including zero strength layer approximations) of an unprotected segment of timber.

Table 7-4: Comparison between char depth calculations for the proposed and code methods

Test Method	Char depth (mm)			
	30 min	60 min	90 min	120 min
NZS 3603	20	39	59	78
AFPA Technical Report 10	26	46	64	80
AS 1720.4	27	47	67	87
Eurocode 5	28	49	70	91
Proposed Bi-linear Method	31	53	72	90

In comparison to the other code methods, the proposed bi-linear charring rate is notably more conservative for all exposures under two hours (except for two hour exposure using the Eurocode method). This is to be expected as the notional charring rate for the initial 45 minutes of exposure time is very high in comparison to other codes.

From the results it is clear that the current New Zealand standard is the least conservative in comparison to the selected group of methods, with both the AFPA and Australian methods correlating closely until high exposure times, at which the Australian method deviates in a conservative fashion. The Eurocode method is more conservative, after which the most conservative is the proposed bi-linear method. This becomes less conservative than the Eurocode method at high exposure times of two hours or more.

As these methods are all rooted in empirical findings of experimental tests, it is impossible to say which is the most appropriate for design without comparing the experiments themselves. Therefore logic dictates the most robust testing regime, coupled with the most detailed analysis should take precedence over the others. This however is not entirely true, as environmental factors with which each method has been derived have also influenced the results; the most significant being the species and therefore density of timber used. Therefore each method may be appropriate to its specific region, thus no definitive conclusion can be drawn.

With this point in mind, the maximum spread of results at 30 minutes exposure is 55%, while at two hours exposure it is approximately 15% between the New Zealand code and the new research. This indicates that the New Zealand code may require updating to include more recent fire test data for lower exposure times, or at least an assumption of a zero strength layer to bring it in line with the other accepted methods.

7.7.4 Other Experimental Comparisons

Comparisons between some recent experiments conducted on LVL members (both small and large scale furnace tests) are shown in Table 7-5. The measurements are primarily for two-dimensional exposure; the reference for each data set is noted in the table. A similar but more in-depth study was conducted by Friquin (2010). The calculated charring rate for similar exposure using the proposed bi-linear method is shown next to the experimental results, where the nominal charring rate has been used. The zero strength layer is neglected in the calculations as it is not measured in the experimental rates presented below.

It should be noted that there are a large number of studies conducted on one-dimensional charring available in the literature. However due to the calibration of the proposed method being based on the notional charring of two-dimensional surfaces, only two-dimensional test data has been presented in Table 7-5. This does not imply that the proposed bi-linear method is not appropriate for one-dimensional exposure. On the contrary, it is conservative and is meant to be applied to both cases. To aid in comparison between these specific references, only the two-dimensional test data is presented.

Table 7-5: Comparison between charring rate calculations for the proposed method and the literature

Experimental Reference Source	Charring Rate (mm/min)	
	Experimental Measurement	Proposed Bi-linear Method*
Schaffer (1967)	0.68 – 0.69	0.77 – 0.81
Frangi and Fontana (2003)	0.67 0.70	0.72 0.81
Lane (2005)	0.83 0.92	0.81 0.81
Tsai (2010)	0.70 – 0.94 0.77 – 0.80	0.81 0.76
Spellman (2012)	0.72 0.72 0.69	0.75 0.81 0.77

***The charring rate has been calculated based on the time at which the relevant data point reached 300°C to signify it had turned to char. Where this information was not available, the test duration was used for the calculation.

It can be seen from the wide range of data sourced for softwoods that the spread of measured charring rates is large, with a common rate between 0.70 – 0.80 mm/min for most test exposures. The experimental test times for the data listed ranged from 20 – 90 minutes. The proposed bi-linear method compares well with the bulk of the test data, being within 15% of the measured experimental rates. Much of the scatter seen in the results can also be attributed to variations in testing and environmental conditions, different softwood species and properties, and the level of accuracy of measurement. Despite this, the bi-linear method is still a good approximation to much of the experimental data ranging from historical to recent times.

7.7.5 Discussion

It should be noted that the floor assemblies tested may not perform in a similar manner when compared with other major structural assemblies such as walls, beams and columns. This may

have a detrimental impact on how the calculation method performs for these other assemblies, and may invalidate the requirement for a bi-linear charring rate. The load level, fire type, and surface fire exposure all play a critical role in determining the actual fire resistance of a timber assembly, and these factors can differ significantly between different types of assembly.

Despite this, the condition of the floors tested in this research should be representative of a wide range of flooring systems used in reality, in terms of load levels, cross-sectional geometries and span lengths. Thus, the bi-linear charring rate reduced cross-section method is generally applicable for these types of systems, and provides an excellent starting point for estimating their performance by hand calculation methods.

7.8 Conclusions

In conclusion, a simplified calculation method based on a reduced cross-section methodology is proposed to aid in the design of timber floor assemblies for fire resistance. A bi-linear charring rate is specified in the method:

- Using a nominal charring rate of 0.7 mm/min for all timber products, with a factor of 1.15 applied to this rate for all exposure time up to 45 minutes, and a factor of 0.9 applied for any exposure time thereafter.
- Using a zero strength layer of 7 mm.

For the design of timber floors in fire, consideration must be given to all floor components to ensure integrity or insulation failure do not occur through timber elements. This is crucial for thin exposed timber slabs with no concrete topping.

On comparison with the experimental tests, a linear charring rate calculation method was shown to be slightly under conservative for floors designed at the lower end of the endurance scale, and conservative for floors designed for much higher resistances. Thus, a bi-linear charring rate method was adopted to improve the results obtained when compared with the experiments and numerical modelling conducted in this research.

Care must be taken when using calculative methods to ensure that they are used appropriately for their intended purpose as a calculative measure, and other parts of the system which may be critical to the design are not ignored. Any other elements in the system which may cause premature failure or increased burning, such as the integrity of the connections, thin portions of slab, unprotected penetrations and holes drilled into floors, openings through wall cavities

exposing more timber surface area, and any surface treatment or covering which could have an adverse effect on the fire performance of the assembly.

As such, a greater understanding of the global behaviour of the structure and any critical elements such as connection details must be appropriately designed for fire resistance to ensure the entire system performs as desired, and a premature failure does not occur in the event of a fire. Good construction practice is also paramount to ensuring that a structural assembly performs as intended.

8 OTHER CONSIDERATIONS

8.1 Introduction

Although this research has focussed primarily on the investigation of the resistance of timber floors subjected to fires, there are a number of side issues which are related to this topic but were not analysed in detail during the research due to time constraints.

This section has been written to highlight some of the other issues involved with timber construction subjected to fire, and suggestions and references to other relevant work are made with regards to these areas of interest.

8.2 Passive Protection

The addition of passive protection is an excellent way of increasing the fire resistance of a floor. So far this research has focussed on unprotected floor assemblies; however the addition of protection to the underside of floor can have a marked improvement on the fire resistance of the assembly depending on the degree of protection applied. This section details some of the more commonly used methodologies for protecting floor assemblies from fire.

8.2.1 Full Floor Protection

Often the simplest way of protecting a floor assembly is to completely cover the exposed surfaces with a flat panel membrane system. Board type systems are commonly used for this function due to their ease of installation and relatively low costs for high area applications. A simplified section sketch of an example of this type of system is shown in Figure 8-1.

Advantages of this type of method are that the system reduces the fire impact on the assembly to a one-dimensional problem, and the ignition of the timber assembly is delayed from the time of outbreak of fire. Protective systems such as this are also relatively simple to replace after a fire event, however as with the addition of any protective measures the downside is that the costs of constructing the flooring system may increase from the unprotected state. This may be offset by the costs of timber finishing required for unprotected floors.

Figure 8-1: Joist floor with full board system protection

White (2002, 2009) discusses in detail a number of timber and plasterboard protective membranes with quantifiable levels of protection based on material thickness and product type, and an additive method for accounting for multiple layers of protection. These are an example of appropriate and simple to install claddings which are ideal for protecting the underside of timber floor assemblies. Many manufacturers of these products can also provide this information as tested to an approved standard; hence a reasonable approach is to simply add these values to the expected fire resistance time of the unprotected floor or other assembly. In this way confidence can be achieved for both the fire engineer and the regulatory body reviewing the work that the protected timber assembly in question will perform to the minimum level stated under standard fire exposure, hinging on the proper installation and function of the protective measures (which should safely be assumed in the design stage).

Work has been conducted to model the protective effects of plasterboard membranes on timber assemblies. One such study is presented by Lu et al. (2010) which models the effects of plasterboard protection on a lightweight timber joist floor in ABAQUS, and makes comparisons with experimental findings. Similarly Takeda (2010) has also studied the effect of protective membranes on timber floor assemblies and developed a simple model to estimate the mechanical failure of the floors, as discussed in Section 5.2.

A comprehensive study on the component additive model presented in Eurocode 5 (CEN, 2004) and further developments are summarised by Frangi et al. (2010). A detailed set of analyses and experimental verification have been conducted to supplement and improve the methods presented in the guidance, and fill the current gaps in knowledge. Methods for estimating the separating function of protective layers are presented, including the influence of different material types and insulations.

8.2.2 Partial Floor Protection

It can be seen that as floor dimensions become larger to accommodate higher loads and spans, the critical area of timber-only floors is the underside of the slab. To protect this vulnerable area and greatly increase the resistance of the overall assembly, it is an ideal solution to apply partial passive protective measures to these zones while leaving less vulnerable areas uncovered.

In many cases installing partial protection is a balancing act between practical installation costs and the added benefit gained from those measures in place. Trade-offs between expected fire performance and the extra incurred costs must be made to find a novel solution. When considering the floors presented in this research, Figure 8-2 shows one possible solution where a board system is installed at an intermediate level between the joists of the floor assembly. This type of installation can be cheaper than covering the entire floor with a linear system as shown in Figure 8-1, and may exhibit similar performance as a fully protected floor.

Figure 8-2: Joist floor with partial board system protection

As the height of the partial system can be altered depending on the required aesthetics, a higher degree of protection can be achieved by moving the protection system lower down the joist members. This panel insert method is applicable to a wide range of floor geometries, and is also easily installed with the use of timber blocking. With both methods, protected voids are produced which can accommodate building services and insulation. Partial protection methods are commonly employed for these reasons, to maximise the efficiency of the space and the aesthetics of the floor assembly. Issues may arise with the falling off of the plasterboard, in which it is likely that the subsequent charring rate of the freshly exposed timber may be higher than for unprotected timber (Östmann, 2010).

8.3 Penetrations

When considering the construction of a generic multi-storey building, there will invariably be penetrations and alterations to the structural system of the building to accommodate the mechanical and electrical systems required for the operational building functions. It is usual for the majority of penetrations to run through beam and floor systems, as the ventilation and electrical systems must be transferred throughout the floor plate of the building. It is not usual for columns or narrow shear walls to have any penetrations put through them due to their critical function in the building and the small physical area they encompass.

Floor systems in particular are most commonly modified to allow for services to pass through their structural system, which requires consideration as to whether remedial strengthening and extra fire safety provisions are required at these points. Ardalany (Ardalany, 2013, Ardalany et al., 2013) conducted an extensive study on the effect of penetrations through LVL beams to properly assess the strengthening techniques and design procedures required for the safe and practical use of these structural members. Although the research does not encompass fire safety, it provides an excellent summary to the major types of penetrations used in modern buildings and the remedial measures required to ensure the safe operation of the building under mechanical loading conditions. Ardalany proposes limits on the placement and maximum diameter of circular holes through beams with respect to the beam depth and span. These are to ensure that holes do not pass through areas of high stress and shear.

Ardalany also ran a parametric study on reinforcement techniques using plywood sheathing, self-tapping screws, steel brackets and epoxied to transfer the loads. A comprehensive numerical study was run to determine the effects of both unreinforced and reinforced holes through LVL beams utilising both linear elastic fracture mechanics and nonlinear fracture

mechanics in ABAQUS. The numerical study was verified in part with experimental testing. A typical shear failure of an LVL beam with hole penetrations through it, as shown in Figure 8-3.

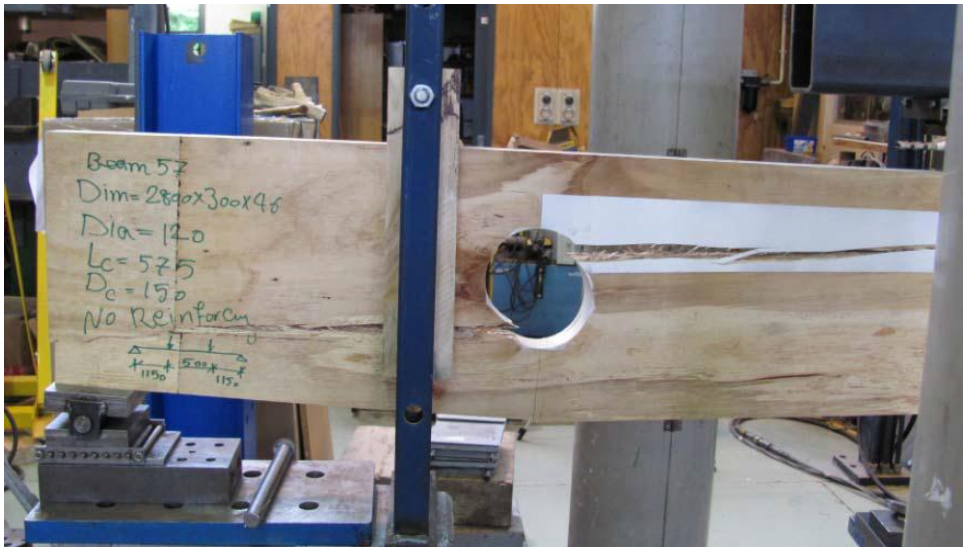

Figure 8-3: Shear failure of an LVL beam with a penetration (Ardalany, 2013)

With regards to fire safety a penetration is problematic as timber is combustible, hence a fire collar or intumescent lining will also be physically influenced by the surrounding member as it combusts during a fire. A poorly constructed penetration through a timber member will aid in heat penetration into the cold sections of the member and increase charring throughout the section. This may lead to a premature collapse as a larger proportion of the surface area of the member is exposed to the fire.

Many different fire penetration protection systems around the world are only tested when installed in non-combustible materials; hence this issue is not well documented in many countries. Many codes do not have specifications for approved solutions when considering separating timber elements in fires.

A study conducted by Werther et al. (2012) found that a major cause of early fire spread between compartments was due to inappropriately designed or installed service installations, and that over half of the services surveyed were not installed correctly or would not perform well in the case of a fire. A number of experiments were conducted on different types of penetrations through timber panels investigating different methods of sealing and protection, an example of which is shown in Figure 8-4.

Figure 8-4: Fire tests of penetrations through a timber assembly (Werther et al., 2012)

It was found that current fire sealing technologies can be applied to timber using standard procedures to ensure the adequate fire performance of the entire system. Methods are presented for better performance of timber systems with multiple types of penetrations, using different measures to seal joints and a strategy for ensuring the direct paths of heat flow are broken. This research provides a good basis for guidance on applying existing protection products to timber systems in an appropriate manner.

8.4 Connections

A significant issue with regards to the fire resistance of timber structures is the connections of any exposed primary or secondary assemblies. This may encompass beam connection, floor connections or even wall connections. The proper design and protection of exposed connections is crucial to ensuring the reliable fire performance of the entire structure. Many different types of connection system are available for timber buildings, the major ones being nails, screws, bolts and washers, rivets and toothed metal plates.

A comprehensive literature survey on the fire performance of some of the major types of connections in loadbearing timber construction has been conducted by Carling (1989). Although the construction industry is constantly flooded with new and innovative solutions to connecting

timber members together, empirical findings still hold true that exposed steel components generally have a much lower fire resistance than their respective timber components, hence when steel joint details are used to connect timber members it is usually the case that these must be protected from fire.

8.4.1 Joint Protection Systems (Carling, 1989)

Carling (1989) conducted a literature survey on the possible types of protection systems available for protecting steel joints in loadbearing timber structures, a number of these systems are summarised below:

Fire Resistant Coatings – Also known as intumescent coatings, these have the advantage of a simple painted or sprayed application method, and once heated beyond a certain temperature range (generally 100 – 150°C) they swell to many times their original thickness to provide an insulating layer. Surface preparation is essential, and it is common practice to require a number of applications to achieve the required thickness. Thicker applications will provide additional levels of protection to the degree of how much paint can practically be applied to the component. Some disadvantages of the method are that painted surfaces are prone to damage during construction and building operation, and quality control can be an issue as the process must be properly applied across the entire connection at a minimum thickness to ensure the required level of performance. For exposed members inside a building, intumescent coatings can provide an aesthetically pleasing result depending on how well they are applied.

Fire Resistant Plaster – With an application method similar to intumescent coatings, fire resistant plaster can be sprayed on to components or applied by hand. The thickness generally varies between 10 – 40 mm, with each layer being approximately 10 – 15 mm thick. Some surface preparation may be required depending on the plaster used, and the use of a steel mesh may be required in order to achieve sufficient adhesion to the component. The finish is such that this method is usually only employed when the members will be covered from view.

Sprayed Mineral Wool – Also a common protection method for steel members, sprayed mineral wool (sometimes referred to as spray-on cement) is a commonly used to protect steel connections and consists of a cementitious bonding agent mixed with mineral wool fibres, sprayed together with water in a fine particle form directly on to the component surface. The application method is simple and generally trouble free, with normal thickness of 10 – 30 mm depending on the level of insulation required. The surface must be clean however minor rusting does not impair the adhesion. A large range of spray-on products are available around the

world, hence the densities and relative insulation properties between products can vary considerably. The spray-on material itself can be very soft and prone to damage; hence during construction a quality control process is required to ensure adequate protection levels will be achieved during building operation and the damage is minimised. Due to this and the fact that sprayed mineral wool products are extremely messy to apply, they are never left exposed in a building.

Board Systems – Board systems are the most common form of protecting timber joints from fire due to their ease of installation, and are usually made from gypsum plaster, mineral wool or vermiculite. Normal application thicknesses range from 10 – 70 mm comprising of a number of boards of varying thicknesses depending on the product used. These systems are generally more resistant to damage and can be repaired easily, hence are more practical to use during construction. They also require a low level of expertise to install and are relatively cheap to produce, hence are found commonplace on most construction sites and are used regularly.

Timber Encasement – Often the most useful way of protecting timber joints is to encase the vital elements in a sacrificial layer of timber, due to the excellent insulative properties of timber and the relative ease at which a timber to timber connection can be achieved. Timber plugs are commonly used as a simple protection method for bolts and large countersunk screws, as plugs can be easily and reliably glued into small holes and openings. Full sheets of sacrificial timber can be simply fastened to existing timber members to cover entire joint details, and depending on space requirements can be extended to critical areas to greatly increase the fire resistance of whole assemblies. Another advantage of timber encasement and timber plugs are that connection details can be completely hidden in novel ways, such that the building aesthetics can be greatly improved if structural members are left exposed to the public view. Similar research on the timber encasement of whole steel members has also been conducted in the past (Twilt and Witteveen, 1974).

8.5 Openings and Gaps

For a fire to propagate through an opening it must be of a sufficient size to allow the combustion process to occur with a steady flow of air to the affected area. Aarnio (1979), and Aarnio and Kallioniemi (1983) found from experiments investigating gap widths between glulam beams that the critical width of opening was 5 mm, and timber assemblies with gaps greater than this size exhibited large amounts of char damage through the opening and hence a reduction in expected fire resistance of the assembly. Openings less than 5 mm in thickness were found to

exhibit much less char propagation through the gap, and the charring was instead more uniform across the outer surface of the timber members. This emphasises the need for proper detailing with joints in timber assemblies to ensure the specified levels of fire resistance are achieved, and appropriate quality controls are in place during the construction phase to reduce these risks.

These finding have been reinforced by post-fire investigations detailed by Babrauskas (2004) in which the presence of gaps was found to increase localised charring rates by 3 – 8 mm/min. Similarly the presence of joints or edges also increased the charring rate in these areas due to the increased exposure of timber.

8.6 Post-tensioned Timber Members

When considering post-tensioned timber members, the anchorage details are a critical point in which much contention over fire resistance of the assembly exists. Two major approaches can be taken with regards to the fire safety of post-tensioned timber structures:

Fully Protected – Protecting all of the components of the post-tensioning system prevents the steel temperature from increasing significantly for the duration of the required fire resistance time. This allows for the contribution of the post-tensioning being included in the structural fire safety design of the building, thus reducing the required sizes of members and perhaps excluding the requirement for corbels under the primary beams. This method is ideal when designing for small member sizes, or if continued lateral load resistance from the system is desired after a fire event.

Unprotected – The second strategy is to completely exclude the post-tensioning from all structural fire safety design, thus allowing for these components to be neglected and left unprotected during a fire. This means that the residual timber sections must solely resist the building loads during a fire. Care must be taken with this method to ensure the adequate lateral load resistance of the building after the fire event, which is especially important if the post-tensioning is an integral component of a lateral load resisting frame. For a multi-storey building, the fire will be contained within a single fire compartment at a single floor level, so the residual lateral load resisting capacity of the structure on the floors unaffected by fire should be able to provide sufficient residual lateral load resistance for the whole building, but this is highly dependent on the size and geometry of the building, and must be designed for carefully.

Spellman (2012) investigated the anchorage details at the ends of the beams in furnace tests at BRANZ. The experiments considered anchorages which were unprotected and protected with intumescent paint, gypsum plasterboard (shown in Figure 8-5), kaowool wrapping and a timber encasement.

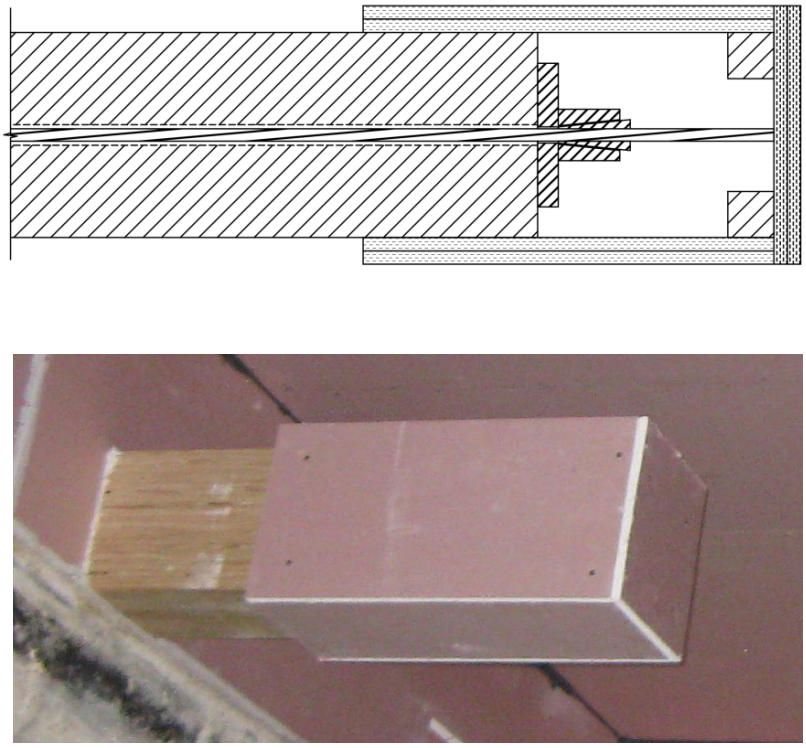

Figure 8-5: Plasterboard anchorage protection (Spellman, 2012)

From the results it was found that the temperatures in the unprotected steel anchorages increase past 200°C in a matter of minutes, and the majority of the post-tensioning force was lost within 10 minutes of testing. The intumescent paint protected the anchorage for approximately 10 minutes longer than the unprotected anchorage, and while the kaowool wrapping method provided more than 60 minutes of protection, there was no simple method of applying the protection to the anchorage suitable for practical construction applications. Both the plasterboard and timber encasement methods were found to be simple to implement and gave excellent fire protection of over 60 minutes, with relatively simple design methodologies to determine the desired level of protection to apply.

Although these results were relative to the degree of protection applied, for instance a much thicker application of intumescent paint would have given a higher fire resistance, the main observation to be made from this is the vast difference achieved between the protected and

unprotected anchorages. For a building where the anchorage connection details are exposed, located inside the firecells of the building, protection is crucial to ensure the post-tensioning system remains integral during a fire.

8.7 Exposed Timber Surfaces

As timber is combustible, the spread of flames across an exposed timber surface can cause numerous issues in building design which are not encountered with non-combustible materials and linings. The spread of flame across combustible linings and elements can have a significant impact on the growth phase of a fire, and without active suppression measures such as an automatic sprinkler system to impede this growth a fire may become more intense in a shorter period of time. For this reason, the use of combustible linings through certain areas of buildings is generally restricted depending on the firecell purpose and the protection measures in place.

Many codes use a form of a spread of flame index to quantify the flame spread across a certain material or coating. These estimates are usually based on empirical findings, and standard test methods such as the room test ISO 9705 (1993) and the calorimeter test ISO 5660 Parts 1-2 (2002) give a time to flashover group number which is a good estimate of the fire hazard present. The group numbers are measured on a scale of 1 to 4, with an increasing associated hazard as the number increases. As expected, the group number of timber depend on the species, thickness and density of the material.

Many protection methods are available from different manufacturers such as fire retardant paints and varnishes; however the absence of a widely recognised and used testing standard for these products makes their actual performance in fires difficult to quantify.

For the New Zealand building environment, a guidelines document (EXPAN^2, 2012) has been prepared to summarise the code requirements for reaction-to-fire properties of timber used in the construction of multi-storey buildings.

8.8 Tensile Membrane Action of Concrete Topping Slabs

A common question raised with regards to timber-concrete composite floors is the performance of the concrete topping slab after the timber beams have burned away; whether it is a viable assertion to assume that the slab will still carry load and deform in a way to avoid structural collapse until the fire is extinguished and repairs can be made. This question is highly dependent on the design of the concrete slab itself, and other geometric factors of the building.

There is a wealth of literature on the subject of tensile membrane action in reinforced concrete slabs and most of the underlying principles remain when comparing timber-concrete composite floors with traditional steel-concrete composite structures or solid reinforced concrete slabs.

As described by Abu et al. (2012), tensile membrane action is a loadbearing mechanism of thin slabs under large vertical displacement in which an induced radial membrane tension field in the central region of the slab is balanced by a peripheral ring of compression. Some of the requirements for this behaviour to take place are the need for vertical support around the slab edges, and slab geometry such that the outer width and length dimensions are similar (in other words slabs are squarer shaped than elongated rectangular). Larger relative areas of reinforcement in the concrete slabs are critical for larger slabs and longer fire endurances.

An obvious advantage of utilising this behaviour is the possibility of leaving all secondary beams such as the floor beams completely unprotected, with the beams fully burning away during a fire without inducing a structural collapse. This would provide cost savings and in many cases increase the expected fire resistance of the floors, however additional costs would be incurred with upgrading the reinforcement in the slab to give appropriate two-way action. In this way floors may be designed to have sacrificial timber beam elements and stronger concrete slabs, such that the overall depth of the floor assembly can be reduced while the expected fire resistance can be increased.

8.9 Construction Site Fires

Fires which occur during the construction phase of a building are common due to the nature of the works which are undertaken at this time. Rubbish piles are commonplace on many building sites during separate stages of construction, and these can usually provide the catalyst needed to start a fast growing fire. Other scenarios such as arson or accidental causes are an ever present and significant risk at this stage of the building's lifetime.

When using a combustible building material such as timber, the impact of a fire can rapidly become much more severe and result in the complete destruction of all adjoining timber construction. This is due to the combination of excessive ventilation conditions, the massive surface area of unprotected timber exposed to the fire, and the absence of any active or passive fire protection systems. Environmental conditions and the species of timber used can also play a significant role in the severity of the fire.

The increasing scope of the works being undertaken around the world on timber buildings also serves to increase the size and severity of these fires, and the economic and psychological costs of these events to the stakeholders and the public. With much taller and larger timber buildings now possible, and multiple levels being built simultaneously, the resulting fire is much larger than what has traditionally been observed in the past. The risk to neighbouring properties also increases with the size of the fire, and a fully involved multi-storey building can quickly expose adjoining properties to massive and destructive temperatures and fluxes, amplifying the associated costs of the event.

A number of key site management concepts have been identified by Bregulla et al. (2010), which states that either ignition of fires should be prevented and failing this, the impact of the fire managed to limit fire growth and spread until extinguishment by fire service intervention can take place. This management is possible by limiting ventilation (installing windows and other separating features earlier than usual in the construction process), and by compartmentalisation of the building such that incombustible separations are used to divide the building construction into a number of smaller more manageable sections. The early installation of active fire protection systems can also be used to suppress and manage construction fires if these systems are to be present in the building, sprinklers being a good example of this.

Bregulla also states that rigorous fire risk assessments should be undertaken as part of an overall fire safety plan to prevent and mitigate this risk as much as possible. This involves identifying the hazards on-site and putting procedures and training in place to ensure that the risk of a fire occurring is minimised.

Similar management procedures are also outlined in guidelines prepared for the New Zealand building environment (EXPAN[1], 2012). The major strategy involves:

- Preventing access to the building site after hours.
- Undertaking a rigorous fire assessment, as part of an overall fire safety plan.
- Planning for emergencies.
- Preventing ignition and mitigating fire risk as much as possible.
- Identifying and managing potential fuel sources.
- Implementing early installation of fire resistant construction.

Provided these simple procedures are followed, the risks of construction site fires for multi-storey timber buildings should be adequately mitigated.

9 CONCLUSIONS AND RECOMMENDATIONS

9.1 Introduction

This research was conducted as a study into the performance of timber floor systems when exposed to fires. The first major objective was to investigate the fire resistance of unprotected timber floors, focussing on composite joist floors, composite box floors and timber-concrete composite floors. The study of these floors was conducted using the finite element software ABAQUS using a thermo-stress analysis in three dimensions, and with experimental fire tests of floor assemblies. The second major objective was to develop simplified design methods for predicting the expected fire resistance of timber floors. A simplified design approach was developed which was then applied to the floor systems under study. The method of estimating of the fire resistance of unprotected floor assemblies was compared to the experimental data obtained in the research, other charring rate methodologies from around the world and other experimental data available in the literature.

9.2 Experimental Furnace Tests

Four furnace tests were conducted on unprotected timber floor systems in the full-scale furnace at the BRANZ facilities in New Zealand. The one-way strip floors had pinned support conditions and were exposed to the ISO 834 standard fire for varying durations of 30 to 105 minutes. The floors were loaded under standard office loading conditions of 3.0kPa live load and 1.0kPa superimposed dead load. The major conclusions from this work are as follows:

- Timber composite joist and box floors exhibited consistent predictable behaviour when exposed to the standard ISO 834 fire for periods of 30 to 105 minutes.
- Insulation failures were prominent with very thin timber slabs, while much thicker slabs did not suffer any failure for the duration of the tests.
- The charring rates of the timber members were found to range from 0.66 – 0.86 mm/min across all specimens.
- When designed to resist a similar load level both the composite joist and box floor types had a similar response to the fire loads, however the composite joist floors exhibited increased upward burning through the members in the latter stages of testing which may contribute to an earlier failure for smaller floor geometries.

9.3 Thermal Modelling

Numerical modelling was undertaken to approximate the thermal impact of a fire on unprotected timber members. A range of effective properties were determined for use in ABAQUS to appropriately model heat transfer through timber sections. The study focussed on both the one and two-dimensional behaviour of timber under thermal loads. The furnace experiments conducted by König and Walleij (1999) were used to validate the one-dimensional modelling, while unpublished column testing experiments from MFPA Leipzig were used for validation of the two-dimensional modelling, as discussed by Werther et al. (2012).

A sensitivity study was conducted comparing different mesh sizes, time step sizes, material model approaches and software suites to determine any shortfalls which may be encountered in the analysis.

The floor assemblies which were experimentally tested in this research were thermally modelled to validate the adequacy of the thermal parameters used for structurally modelling timber floors in fire. It was found that the thermal modelling effort predicted the charring damage of the floors to within a few millimetres of precision. This reinforced that the thermal model developed is appropriate for the sequential structural modelling conducted in this research, considering fire durations of up to 120 minutes.

For general heat transfer analyses considering structural timber members and assemblies it is recommended that:

- An initial square mesh size of 3 mm is used, with further refinement following a mesh sensitivity analysis.
- A material model adopting the latent heat approach is used.
- Simplified boundary conditions should be used describing radiative and convective heat fluxes on surfaces simulating fire conditions and convective losses on surfaces simulating an open air environment. Adiabatic surfaces should be used to simulate voids and cavities initially, with this revisited depending on the purpose of the void.
- All axes of symmetry should be utilised for applying boundary conditions, and an automatic time-stepping function should be specified if available.
- Checks are made to ensure where two-dimensional heat transfer behaviour will become significant through cross-sections, and whether this needs to be incorporated into the analysis.

9.4 Structural Modelling

In this research both one and three-dimensional structural analyses are conducted on timber floor assemblies, with varying degrees of input complexity, in order to adequately model behaviour observed in experimental tests.

The one-dimensional modelling utilised simplified wire elements to model the structural response of floors under mechanical and thermal loads. The thermal loads were input at specific points in a section profile which severely limited the applicability of the method. As the results are purely speculative and highly dependent on the temperature inputs, which are not well known, the level of input complexity is not great enough to warrant further analysis when considering timber assemblies under fire loads. A one-dimensional approach for considering timber floor assemblies in fire is not recommended.

The three-dimensional modelling utilised solid continuum brick elements and used the thermal profiles calculated in Chapter 4 to sequentially model the structural response of floors under mechanical loads subjected to a standard fire. It was found that the structural modelling effort predicted the displacement response and failure times of the floors very well, and the simplified assumptions made in relation to fire inputs, boundary conditions, mesh refinement and effective material parameters were accurate to within 20% of the experimental data obtained. A modification to the reduction in tension strength at elevated temperatures was proposed which refined the modelling results closer to the results of the experiments conducted in this research, and investigated the impact of that parameter on the overall modelling effort.

Sensitivity studies were conducted on the three-dimensional structural modelling, and for the sequential analysis of timber assemblies the following recommendations are made:

- For general analysis of floors from 5 – 10 metres in span, a general guideline of approximately 250 – 500 mm is appropriate for the mesh refinement along the span. This obviously can be reduced for floors with a less dense cross-sectional mesh, smaller cross-sectional areas, or if computational run time is not a major issue when running the simulations.
- An initial square cross-sectional mesh of 3 mm is used. A square mesh size of 5 mm was found to be adequate for this research hence further parametric studies on the mesh size are important to optimise the modelling process.

- Simplified boundary conditions such as pins and ties can be used for all major surface interactions, and all available axes of symmetry should be used to the fullest advantage. In order to avoid element distortion and stress concentrations at any support points, the bearing area of the supports should be spread across an appropriate number of nodes.
- Loads can be modelled as simple uniformly distributed loads across the top surface of the floors, although modelling exact loading points will give more precise results. Loads should be applied gradually in the initial stages of the simulation to avoid issues surrounding element distortion.
- The material model definition plays a vital role in the output of the modelling. For any simplified research considering timber assemblies in ABAQUS, the steel material model may be suitable for use as a starting point, however for implementing plasticity and more complex analyses the concrete damaged plasticity model is strongly recommended for input flexibility.
- Other parameters such as the thermal expansion coefficient can impact on the output to varying degrees. It is crucial that a parametric study on all major inputs is run for any in-depth analysis to have confidence in the results obtained.
- When modelling timber-concrete composite floors, accounting for the slip behaviour of the timber to concrete connection is paramount for confidence in the results obtained, however a simplified approach to modelling isotropic concrete can give reasonable results.

9.5 Non-Standard Fires

When modelling non-standard fires it was concluded that although it is a useful tool which will likely play a much larger role in structural fire engineering in the future, there is still much work to be done. Modelling non-standard fire exposure allows for the investigation of other scenarios not currently captured by the standard fire curves, such as differing growth rates and fire decay.

The modelling conducted suffers from some severe limitations, the least of which it is known that the material model used may not be adequate to soundly assess timber floor assemblies in its current state. The major conclusions drawn from the numerical modelling of non-standard fires were:

- The maximum temperature and growth rate of a fire has a large impact on the overall displacement response of a timber floor.

- The fire duration and decay characteristics also have a significant impact on the displacement response of the floors, and failure may be avoided provided there is adequate residual strength left in the floor once cooled.
- The modelling of continued burning of timber is important to obtain a true assessment of structural performance.

9.6 Simplified Design Methods

In conclusion, a simplified calculation method based on a reduced cross-section methodology is proposed to aid in the design of timber floor assemblies for fire resistance. A bi-linear charring rate is specified in the method:

- Using a nominal charring rate of 0.7 mm/min for all timber products, with a factor of 1.15 applied to this rate for all exposure time up to 45 minutes, and a factor of 0.9 applied for any exposure time thereafter.
- Using a zero strength layer of 7 mm.

For the design of timber floors in fire, consideration must be given to all floor components to ensure integrity or insulation failure do not occur through timber elements. This is crucial for thin exposed timber slabs with no concrete topping.

On comparison with the experimental tests, a linear charring rate calculation method was shown to be slightly under conservative for floors designed at the lower end of the endurance scale, and conservative for floors designed for much higher resistances. Thus, a bi-linear charring rate method was adopted to improve the results obtained when compared with the experiments and numerical modelling conducted in this research.

9.7 Recommendations for Future Research

As the scope of this research was broad, the main effort was focussed on the performance of timber floor systems in fire utilising both experimental testing and numerical modelling. In relation to the major divisions of the research, the following recommendations are made for future research.

9.7.1 Experimental Tests

Although furnace testing is expensive there are a multitude of different timber assemblies which could be investigated to aid in the understanding of how timber performs in real fires. Some examples of subject areas which would greatly benefit from further study are:

- Penetrations through structural timber members and assemblies.
- Exposed metal connections such as steel corbels and joist hangers.
- Specifically designed slabs to incorporate tensile membrane action.
- The performance of applied protection measures (such as intumescent paint) on floor assemblies in fire.
- Small scale testing of timber specimens to better characterise the different properties of LVL under fire loads to aid in future research. Specifically, an investigation into the plastic behaviour of timber at elevated temperatures in order to populate the numerical model with more adequate stress-strain data.
- Furnace testing of floor assemblies under real fires in order to provide comparison with the standard fires currently used as a baseline for modern day research and design.

9.7.2 Numerical Modelling

With regards to the numerical modelling conducted, there were a number of areas in which further research is warranted:

- An in-depth investigation of material properties and strength reduction factors for better characterising timber as a material in numerical software.
- Connections and boundary conditions (other than the simply-supported case).
- Tensile membrane action of timber-concrete composite floors.
- An investigation into the plastic behaviour of timber at elevated temperatures and the viability of current numerical software to adequately model such phenomena.
- Further investigation into non-standard fires, including better characterisation of the thermal properties of timber for non-standard fire exposure.

- Design for burnout of compartments, and analysis of the impact of decay phases and persistent burning on timber assemblies.

9.7.3 Other Areas of Research

A large number of other timber technologies are currently being developed, each presenting their own unique challenges when considering fire design. Further research into these areas is also paramount to ensure their implementation into the modern built environment. Some areas which require further in-depth study are:

- The fire performance of post-tensioned frames and walls in both protected and unprotected scenarios, focussing on tendon performance and global structure behaviour.
- The fire performance of timber-concrete composite floors with incorporated concrete topping slabs for the purpose of tensile membrane action in severe fires.
- The development of a comprehensive fire safety design strategy for multi-storey timber buildings.

9.8 Contribution to Fire Safety

As a final note, this section summarises the contribution of this research to the fire safety community. Recommendations are made as to the practical applications of the research with reference to some of the findings outlined in the conclusions.

It is stressed that the information presented in this section is entirely the author's personal opinion, and many factors may be present in different regulatory and political environments to promote the use of certain forms of construction or particular strands of research. It is left to the reader to draw their own conclusions from this work, with the hope that it will be a positive influence on both future research and construction of the built environment.

9.8.1 Contribution of the Research

The major contribution of this work is that it has detailed an investigative effort into both the analysis and modelling of timber floors, in the hopes of highlighting any potential pitfalls which may be encountered by other researchers and designers of such systems. This can crudely be divided into the following parts:

- Experimental furnace testing. A full set of data for four floors tested in a furnace is given which can be used as a point of reference for further investigations. This also provides a quantifiable measurement of resistance for modern LVL floor assemblies.

- Numerical modelling. A comprehensive modelling regime is documented, beginning with simplified heat transfer modelling extending to three-dimensional sequentially-coupled thermo-stress analysis. Major assumptions and limitations required for the particular software used are described, along with generalisations applicable to most advanced numerical methods.
- Analytical investigation and a critique of the available literature. Suggestions are made for improvements to current simple calculation methods.

The intention of the research was always to ensure that each part of the research could be fully reproduced by an outside party. Constraints on the general volume and readability of the research presented meant that some of the fundamentals of the research (e.g. fundamentatls of numerical modelling) have been excluded from the final dissertation. The approaches to the issues and the reasoning behind these have however been fully described.

In addition to the experimental, numerical and analytical data presented, the thesis identifies key drawbacks of the research, and where further study is required to better inform the fire safety community on the fire performance of timber floors and other timber assemblies.

The overall contribution to the fire safety community is a detailed research effort delving into an engineering field still in its infancy, which can aid others worldwide to educate the wider engineering community on timber engineering in fire conditions.

9.8.2 Practical Application

Each of the floor designs presented in Section 2 have a number of advantages and disadvantages to consider, and are suited to different types of applications. The major discerning factors influencing which floor type is most ideally suited for a particular application are:

- The intended use of the floor.
- The required loadbearing capacity.
- The required span length.
- Restrictions on absolute section depth.
- Desired aesthetic appeal.
- Economic restraints.

For an office type application, longer spanning linear composite systems (fully timber or timber-concrete composite) are ideally suited as they are economical and provide high loadbearing resistance. They are also easily retrofitted to suit multiple purposes and give high levels of operational flexibility in terms of an open plan layout.

For taller buildings where inter-storey height becomes a major issue, composite systems such as cassette floors are better suited as they have an optimised section for loadbearing. Applied passive protection would be required for this application, but would likely be easy to install considering a rectangular cross section. Concrete slabs can be added for increased acoustic or loadbearing performance.

Timber slab systems are excellent for fire and structural performance, but they can take up a lot of room and once in place generally allow for very little building modification after construction. Therefore they are well suited to residential type buildings with smaller rooms and higher aesthetic appeal, or used in smaller parts for feature floors/walls of the bottom storey of a building.

9.8.3 Concrete Toppings

A common question raised with regards to timber floors is what increase in fire performance or fire resistance is gained by the addition of a concrete topping. Albeit being a valid question, due to the very common practice of adding concrete slabs for insulation or acoustic reasons; it usually requires a complex answer. It is important to differentiate the fire performance and fire resistance of the floor assembly, as the former describes the behaviour of the floor in a fire while the latter is a measure the ability of the floor to resist the standard fire. The fire resistance is dependent on adequate fire performance of the floor, for in order to provide a resisting function it must stay in place and carry load (as simulated in experimental tests). Attention must also be paid to whether the slab contributes structurally to the floor, or if it is purely dead load which is completely supported by the floor alone.

In general terms, the addition of a non-loadbearing concrete slab will increase the fire resistance of a floor with regards to integrity and insulation, while having a detrimental effect on the loadbearing capacity by adding dead load. In terms of quantifying the contribution, the absolute thickness of the slab is generally used as a measure of the additional resistance provided.

The addition of a structural concrete slab will increase the loadbearing capacity of the floor, as the concrete will be utilised in compression while the timber mainly in tension for gravity loading,

utilising the relative strengths of both materials. This however is highly dependent on the level of reinforcement present in the slab, its relative strength, and most importantly the rigidity of the connection between the concrete and timber components of the floor. It may also allow for optimisation of floor sections to become shallower.

With regards to the fire performance of the floor however, this may be negatively impacted. As prior research (O'Neill, 2009) has shown the difference in thermal expansion between the concrete slab component and the timber component of the floor may induce either upwards or downwards thermal bowing under fire conditions due to the heating of the underside of the slab. The direction this is in depends on the relative proportional strength of each component in the floor overall, and the degree of rigidity between the connection of the components.

It should be noted that the addition of concrete slabs will increase the overall stiffness and mass of the floor, and thus the structure. This may have positive implications with regards to acoustics and thermal mass, and negative implications on seismic performance and foundation design.

9.8.4 Construction Practice

Construction practice can be loosely defined as the on-site methods which are employed to install a system as designed. A system is useless if proper expertise and measures are not in place to ensure it is installed correctly. This is especially important in the installation of timber assemblies. As the design of structural assemblies usually hinge on a number of separate components working in unison, they must be installed to specification to provide their function.

Other common site practices which cause issues later on in the construction phase are subcontractor interference with an installed system. For instance if a floor is installed correctly by a construction team, after which another subcontractor drills holes through the section to allow for services to pass through, that floor will no longer perform as designed. Remedial measures must be put in place, such as the strengthening of the penetrations through the floor, after which these must also be protected from a fire. Significant costs can be incurred when part of a structure is designed without consideration of its impact on the design of the whole project. Thus again alluding to the importance of a comprehensive design phase and appropriate construction practices to avoid these issues arising.

Common timber specific construction practices range from preventing large construction fires to adequate protection of timber on-site from the external environment.

9.8.5 Passive and Active Protection Measures

The benefits of applying passive protection to a structure which is intended to resist a fire for extended periods of time are significant. Certainly for high-rise applications of timber, or for fire protected areas such as stairwells, passageways and common lobbies, the use of passive protection on exposed timber assemblies provides a fire inhibiting function in addition to enhancing the resistance characteristics of the structure. Much of this hinges on appropriate construction of the passive protection, however with modern methods being well known and used this is usually not an area of concern.

The reliability of active systems such as sprinkler systems are also well documented and cannot be overlooked. Sprinkler systems are an excellent and rigorously tested form of active protection which should always be considered as a means of reducing the likelihood and impacts of a fire.

Irrespective of the building material involved, an increasing combination of active and passive protection should be implemented in a building as the level of risk of fire and the subsequent consequences to life safety and property protection increase. This is usually proportionate to the height and size of a structure, its historical significance and its intended function in society.

REFERENCES

Aarnio, M. "Glulam Timber Construction and the Fire Resistance Properties of the Joints", Diploma Work, Helsinki School of Technology, Division of Building Engineering, Otnas, Finland, 1979.

Aarnio, M. and Kallioniemi, P. "Fire Safety in Joints of Loadbearing Timber Construction", Research Report No. 233, VTT Technical Research Centre of Finland, Finland, 1983.

ABAQUS version 6.10. *Analysis User's Manual*, Dassault Systems Simulia Corporation, Providence, RI, USA, 2010.

ABAQUS version 6.10. *Getting Started with Abaqus – Interactive Edition*, Dassault Systems Simulia Corporation, Providence, RI, USA, 2010.

Abu, A.K., Burgess, I.W., and Plank, R.J. "The Effect of Reinforcement Ratios on Composite Slabs in Fire", *Structures and Buildings*, Institution of Civil Engineers, Volume 165, Issue SB7, pp. 385-398, 2012.

AFPA. *Calculating the Fire Resistance of Exposed Wood Members – Technical Report 10*, American Forest & Paper Association, Washington, DC, USA, 2003.

ANSYS version 12.0. *ANSYS LS-DYNA User's Guide*, ANSYS Inc., Canonsburg, PA, USA, 2009.

Ardalany, M. "Analysis and Design of Laminated Veneer Lumber Beams with Hole and Reinforcement around the Holes", Doctoral Thesis in Civil Engineering, University of Canterbury, Christchurch, New Zealand, 2013.

Ardalany, M., Fragiacomo, M., Carradine, D.M., and Moss, P.J. "Experimental behavior of Laminated Veneer Lumber (LVL) joists with holes and different methods of reinforcement", *Engineering Structures*, Volume 56, pp. 2154-2164, 2013.

ASTM. ASTM: E119-88, *Standard Test Methods for Fire Tests of Building Construction and Materials*, American Society for Testing and Materials, 1988.

Babrauskas, V. "Wood Char Depth: Interpretation in Fire Investigations", *Proc. 1st International Symposium on Fire Investigation*, Moreton-in-Marsh, United Kingdom, June 28, 2004.

Bathon, L., Bletz, O., and Schmidt, J. “Hurricane Proof Buildings – An Innovative Solution using Prefabricated Modular Wood-Concrete-Composite Elements”, *Proc. 9th World Conference on Timber Engineering*, Portland, OR, USA, August 6-10, 2006.

Beall, F.C., and Eickner, H.W. “Thermal Degradation of Wood Components: A review of the literature”, USDA Forest Service Research Paper FPL 130, Forest Products Laboratory, Madison, WI, USA, 1970.

Bobacz, D. “Behavior of Wood in Case of Fire - Proposal for a Stochastic Dimensioning of Structural Elements”, Doctoral Thesis in Civil Engineering, University of Natural Resources and Applied Life Sciences, Vienna, Austria, 2006.

Bodig, J., and Jayne, B.A. *Mechanics of Wood and Wood Composites*, Van Nostrand Reinhold Company Inc., New York, NY, USA, 1982.

Bregulla, J., Mackay, S., and Matthews, S. “Fire Safety on Timber Frame Sites during Construction”, *Proc. The 11th World Conference on Timber Engineering*, Riva del Garda, Italy, June 20-24, 2010.

Buchanan, A.H. *Structural Design for Fire Safety*, John Wiley & Sons Ltd., West Sussex, England, 2001.

Buchanan, A.H. *Timber Design Guide*, Third Edition, New Zealand Timber Industry Federation Inc., Wellington, New Zealand, 2007.

Buchanan, A.H., Deam, B., Fragiacomo, M., Pampanin, S., and Palermo, A. “Multi-Storey Prestressed Timber Buildings in New Zealand”, *Structural Engineering International*, IABSE, Special Edition on Tall Timber Buildings, 2007.

Carling, O. “Fire Resistance of Joint Details in Loadbearing Timber Construction – A Literature Survey”, [translated from Swedish by Harris, B. and Yiu, P.K.A], BRANZ Study Report SR 18, Building Research Association of New Zealand, Judgeford, New Zealand, 1989.

Ceccotti, A. “Composite Concrete-Timber Structures”, *Progress in Structural Engineering Materials*, Volume 4, Issue 3, pp. 264-275, 2002.

Ceccotti, A., Fragiacomo, M., and Giordano, S. “Behaviour of a Timber-Concrete Composite Beam with Glued Connection at Strength Limit State”, *Proc. The 9th World Conference on Timber Engineering*, Portland, OR, USA, August 6-10, 2006.

CEN. EN 1991-1-2: 2002, *Eurocode 1: Actions on Structures, Part 1-2: General Actions – Actions on Structures Exposed to Fire*, European Committee for Standardisation, Brussels, Belgium, 2002.

CEN. EN 1992-1-2: 2004, *Eurocode 2: Design of Concrete Structures, Part 1-2: General Rules – Structural Fire Design*, European Committee for Standardisation, Brussels, Belgium, 2004.

CEN. EN 1995-1-2: 2004, *Eurocode 5: Design of Timber Structures, Part 1-2: General – Structural Fire Design*, European Committee for Standardisation, Brussels, Belgium, 2004.

Chapra, S.C., and Canale, R.P. *Numerical Methods for Engineers – with Software and Programming Applications*, Fourth Edition, McGraw-Hill, New York, NY, USA, 2002.

Cook, R.D. *Finite Element Modelling for Stress Analysis*, First Edition, John Wiley and Sons, Inc., New York, NY, USA, 1995.

Cote, A.E., and Grant, C.G. *Fire Protection Handbook: Codes and Standards for the Built Environment*, Volume 1, 20th Edition, National Fire Protection Association, Quincy, MA, USA, 2008.

Craft, S.T., Desjardins, R., and Richardson, L.R. "Development of Small-Scale Evaluation Methods for Wood Adhesives at Elevated Temperatures", *Proc. The 10th World Conference on Timber Engineering*, Miyazaki, Japan, June 2-5, 2008.

Crews, K., and Shrestha, R. *Design Guide Australia and New Zealand: Design Procedures for Timber Only Composite Floor Systems*, Structural Timber Innovation Company, Christchurch, New Zealand, 2013.

EXPAN[1]. "Guidelines for Fire Safety on EXPAN Construction Sites", Technical Bulletin No. 1, December Issue, 2012.

EXPAN[2]. "Requirements Regarding Reaction-to-Fire Properties of Timber Used in the Construction and Finishing of Multi-Storey Timber Buildings in New Zealand", Technical Bulletin No. 2, December Issue, 2012.

Fleischer, H.O. "The Performance of Wood in Fire", Report No. 2202, Forest Products Laboratory, Madison, WI, USA, 1960.

Forman Building Systems. “Forman Building Systems – Kaowool Product Data Sheet”, Forman Building Systems, Auckland, New Zealand, 2010.

Fragiacomo, M., Gutkowski, R.M., Balogh, J., and Fast, R.S. “Long-term Behavior of Wood-Concrete Composite Floor/deck Systems with Shear Key Connection Detail”, *Journal of Structural Engineering*, Volume 133, Issue 9, pp. 1307-1315, 2007.

Fragiacomo, M., Menis, A., Moss, P.J., Clemente, I., and Buchanan, A.H. “Numerical and Experimental Thermal-structural Behaviour of Laminated Veneer Lumber (LVL) Exposed to Fire”, *Proc. The 11th World Conference on Timber Engineering*, Riva del Garda, Italy, June 20-24, 2010.

Fragiacomo, M., Menis, A., Moss, P.J., Buchanan, A.H., and Clemente, I. “Numerical and Experimental Evaluation of the Temperature Distribution within Laminated Veneer Lumber (LVL) Exposed to Fire”, *Journal of Structural Fire Engineering*, Volume 1, Number 3, pp. 145-159, 2010.

Fragiacomo, M., Menis, A., Clemente, I., Bochicchio, G., and Ceccotti, A. “Fire Resistance of Cross-Laminated Timber Panels Loaded Out-of-Plane”, *Journal of Structural Engineering*, online publication 7 December, 2012.

Frangi, A., and Fontana, M. “Fire Behaviour of Timber-Concrete Composite Slabs”, *Proc. The 5th World Conference on Timber Engineering*, Montreux, Switzerland, August 17-20, 1998.

Frangi, A., and Fontana, M. “A Design Model for the Fire Resistance of Timber-Concrete Composite Slabs”, *Proc. Innovative Wooden Structures and Bridges*, Lahti, Finland, August 29-31, 2001.

Frangi, A., and Fontana, M. “Charring rates and temperature profiles of wood sections”, *Fire and Materials*, Volume 27, Issue 2, pp. 91-102, 2003.

Frangi, A., Knobloch, M., and Fontana, M. “Fire Design of Timber Slabs made of Hollowcore Elements”, *Engineering Structures*, Volume 31, Issue 1, pp. 150-157, 2009.

Frangi, A., Fontana, M., Hugi, E., and Jubstl, R. “Experimental Analysis of Cross-Laminated Timber Panels in Fire”, *Fire Safety Journal*, Volume 44, Issue 8, pp. 1078-1087, 2009.

Frangi, A., Fontana, M., Hugi, E., and Wiederkehr, R. "Fire Safety of Multi Storey Timber Buildings", *Proc. The 11th World Conference on Timber Engineering*, Riva del Garda, Italy, June 20-24, 2010.

Friquin, K.L., Grimsbu, M., and Hovde, P.J. "Charring Rates for Cross-Laminated Timber Panels Exposed to Standard and Parametric Fires", *Proc. The 11th World Conference on Timber Engineering*, Riva del Garda, Italy, June 20-24, 2010.

Friquin, K.L. "Charring Rates of Heavy Timber Structures for Fire Safety Design", Doctoral Thesis in Civil and Transport Engineering, Norwegian University of Science and Technology, Trondheim, Norway, 2010.

Gagnon, S., and Pirvu, C. *Cross-Laminated Timber Handbook*, FPInnovations, Pointe-Claire, QC, Canada, 2011.

Gerber, C., Crews, K., and Shrestha, R. *Design Guide Australia and New Zealand: Timber Concrete Composite Floor Systems*, Structural Timber Innovation Company, Christchurch, New Zealand, 2012.

Gerhards, C.C. "Effect of Moisture Content and Temperature on the Mechanical Properties of Wood: An Analysis of Immediate Effects", *Wood and Fiber*, Volume 14, Issue 1, pp. 4-36, 1982.

Glass, S.V., and Zelinka, S.L. *The Wood Handbook – Wood as an Engineering Material: Moisture Relations and Physical Properties of Wood*, Centennial Edition, Forest Products Laboratory, Madison, WI, USA, 2010.

Glos, P., and Henrici, D. "Bending Strength and MoE of Structural Timber at Temperatures up to 150°C", [in German], *Holz als Roh- und Werkstoff*, Volume 49, pp. 417-422, 1991. Translated by Forest Products Laboratory, Madison, WI, USA, 1992.

Grant, G. "Evaluation of Timber Floor Systems for Fire Resistance and Other Performance Requirements", Master's Thesis in Fire Engineering, University of Canterbury, Christchurch, New Zealand, 2010.

Hadvig, S. *Charring of Wood in Building Fires: Practice, Theory, Instrumentation, Measurements*, Laboratory of Heating and Air-Conditioning, Technical University of Denmark, Lyngby, Denmark, 1981.

ISO. ISO 9705: 1993, *Fire Tests – Full Scale Room Test for Surface Products*, International Organisation for Standardisation, 1993.

ISO. ISO 834-1: 1999, *Fire Resistance Tests - Elements of Building Construction, Part 1: General Requirements*, International Organisation for Standardisation, 1999.

ISO. ISO 5660-1: 2002, *Reaction to Fire Tests – Heat Release, Smoke Production and Mass Loss Rate, Part 1: Heat Release Rate (Cone Calorimeter Method)*, International Organisation for Standardisation, 2002.

ISO. ISO 5660-2: 2002, *Reaction to Fire Tests – Heat Release, Smoke Production and Mass Loss Rate, Part 2: Smoke Production Rate (Dynamic Measurement)*, International Organisation for Standardisation, 2002.

Janssens, M.L. "Modeling of the Thermal Degradation of Structural Wood Members Exposed to Fire", *Fire and Materials*, Volume 28, Issues 2-4, pp. 199-207, 2004.

Karlsson, B., and Quintiere, J.G. *Enclosure Fire Dynamics*, CRC Press LLC, Boca Raton, FL, USA, 2000.

Khorsandnia, N., Valipour, H.R., and Crews, K. "Experimental and analytical investigation of short-term behaviour of LVL-concrete composite connections and beams", Construction and Building Materials, Volume 37, pp. 229-238, 2012.

Khorsandnia, N., Valipour, H.R., Shrestha, R., Gerber, C., and Crews, K. "Review on long-term behaviour of timber-concrete composite floors", *Proc. The 22nd Australasian Conference on the Mechanics of Structures and Materials*, Sydney, Australia, December 11-14, 2012.

Khorsandnia, N., Valipour, H.R., and Crews, K. "Nonlinear finite element analysis of timber beams and joints using the layered approach and hypoelastic constitutive law", Engineering Structures, Volume 46, pp. 606-614, 2013.

Klippel, M., Frangi, A., and Fontana, M. "Influence of the Adhesive on the Load-Carrying Capacity of Glued Laminated Timber Members in Fire", P*roc. The 10th Symposium on Fire Safety Science*, University of Maryland, MD, USA, June 19-24, 2011.

Kmiecik, P., and Kaminski, M. "Modelling of Reinforced Concrete Structures and Composite Structures with Concrete Strength Degradation taken into Consideration", *Archives of Civil and Mechanical Engineering*, Volume 11, Number 3, pp. 623-636, 2011.

Kolb, J. *Systems in Timber Engineering: Loadbearing Structures and Component Layers*, Birkhäuser Verlag AG, Basel, Switzerland, 2008.

König, J. "Fire Resistance of Timber Joists and Load Bearing Wall Frames", Report I 9412071, Swedish Institute for Wood Technology Research, Stockholm, Sweden, 1995.

König, J., and Walleij, L. "One-Dimensional Charring of Timber Exposed to Standard and Parametric Fires in Initially Unprotected and Postprotection Situations", Report I 9908029, Swedish Institute for Wood Technology Research, Stockholm, Sweden, 1999.

König, J., and Walleij, L. "Timber Frame Assemblies Exposed to Standard and Parametric Fire, Part 2: A Design Model for Standard Fire Exposure", Report I 0001001, Swedish Institute for Wood Technology Research, Stockholm, Sweden, 2000.

König, J. "Structural Fire Design according to Eurocode 5 – Design Rules and their Background", *Fire and Materials*, Volume 29, Issue 3, pp. 147-163, 2005.

König, J. "Effective Thermal Actions and Thermal Properties of Timber Members in Natural Fires", *Fire and Materials*, Volume 30, Issue 1, pp. 51-63, 2006.

König, J., and Schmidt, J. "Bonded Timber Deck Plates in Fire", *Proc. The 40th CIB-W18 Meeting on Timber Structures*, Bled, Slovenia, 2007.

Kretschmann, D.E. *The Wood Handbook – Wood as an Engineering Material: Mechanical Properties of Wood*, Centennial Edition, Forest Products Laboratory, Madison, WI, USA, 2010.

Kuhlmann, U., and Michelfelder, B. "Optimized design of grooves in timber-concrete composite slabs", *Proc. The 9th World Conference on Timber Engineering*, Portland, OR, USA, August 6-10, 2006.

Lane, W.P. "Ignition, Charring and Structural Performance of Laminated Veneer Lumber", Fire Engineering Research Report, School of Engineering, University of Canterbury, 2005.

Lie, T.T. *The SFPE Handbook of Fire Protection Engineering: Fire Temperature-Time Relations*, National Fire Protection Association, Quincy, MA, USA, 2002.

Lignatur Product Guide. *Lignatur Workbook*, Lignatur AG, Waldstatt, Switzerland, 2011.

Lu, L., Isgor, O.B., and Hadjisophocleous, G. “A Computer Model for Light-Frame Wood Floor Assemblies under Fire Attack”, *Proc. The 11th World Conference on Timber Engineering*, Riva del Garda, Italy, June 20-24, 2010.

Lukaszewska, E., Fragiacomo, M., and Frangi, A. “Evaluation of the slip modulus for ultimate limit state verifications of timber-concrete composite structures”, *Meeting forty of the Working Commission W18-Timber Structures*, CIB, International Council for Research and Innovation, Bled (Slovenia), August 28-31, paper No. CIB-W18/40-7-5, 14 pp., 2007.

Menis, A., Fragiacomo, M., and Clement, I. “Numerical Investigation of the Fire Resistance of Protected Cross-Laminated Timber Floor Panels”, *Structural Engineering International*, Volume 22, Number 4, pp. 523-532, 2012.

Mikkola, E. “Fire Safety in Timber Buildings: Fire safety in buildings”, SP Report 2010:19, SP Technical Research Institute of Sweden, Stockholm, Sweden, 2010.

Nelson Pine LVL. *Nelson Pine Laminated Veneer Lumber – Specific Engineering Guide*, Nelson Pine Industries Ltd, Nelson, New Zealand, 2012.

O'Neill, J.W. “The Fire Performance of Timber-Concrete Composite Floors”, Master's Thesis in Fire Engineering, University of Canterbury, Christchurch, New Zealand, 2009.

O’Neill, J.W. “Modelling the Fire Performance of Structural Timber Floors”, *Proc. 7th International Conference on Structures in Fire*, Zurich, Switzerland, June 6-8, 2012.

Östmann, B.A. “Wood Tensile Strength at Temperatures and Moisture Contents Simulating Fire Conditions”, *Wood and Science Technology*, Volume 19, Issue 2, pp. 103-116, 1985.

Östmann, B.A. “Fire Safety in Timber Buildings: European requirements”, SP Report 2010:19, SP Technical Research Institute of Sweden, Stockholm, Sweden, 2010.

Pau, D. “A Comparative Study on Combustion Behaviours of Polyurethane Foams with Numerical Simulations using Pyrolysis Models”, Doctoral Thesis in Fire Engineering, University of Canterbury, Christchurch, New Zealand, 2013.

Peng, L. “Performance of Heavy Timber Connections in Fire”, Doctoral Thesis in Civil and Environmental Engineering, Carleton University, Ottawa, Ontario, Canada, 2010.

SA. AS 1530.4: 2005, *Methods for Fire Tests on Building Materials, Components and Structures, Part 4: Fire Resistance Test of Elements of Construction*, Standards Australia, 2005.

SA. AS 1720.4: 2006, *Timber Structures – Fire Resistance for Structural Adequacy of Timber Members*, Standards Australia, 2006.

SAFIR. *User's Manual for SAFIR – A Computer Program for Analysis of Structures Subjected to Fire*, University of Liège, Liège, Belgium, 2011.

Saito, Y., Harada, K., Sakaguchi, A., Nakaue, K., Tsuchihashi, T., Tanaka, Y., Tasaka, S., and Yoshida, M. "Burning of Laminated Wood Assembly after Intense Heat Exposure by Fire Resistance Furnace", *Proc. The 7th Asia-Oceania Symposium on Fire Science and Technology*, Hong Kong, China, September 20-22, 2007.

Schaffer, E.L. "Charring Rate of Selected Woods – Transverse to Grain", US Forest Service Research Paper FPL69, Forest Products Laboratory, Madison, WI, USA, 1967.

Schaffer, E.L. "Effect of Pyrolitic Temperature on the Longitudinal Strength of Dry Douglas Fir", *Journal of Testing and Evaluation*, Volume 1, Issue 4, pp. 319-329, 1973.

Schmid, J., König, J., and Köhler, J. "Fire-Exposed Cross-Laminated Timber – Modelling and Tests", *Proc. The 11th World Conference on Timber Engineering*, Riva del Garda, Italy, June 20-24, 2010.

SNZ. NZS 3603: 1993, *Timber Structures Standard*, Standards New Zealand, 1993.

SNZ. AS/NZS 1328.1: 1998, *Glued Laminated Structural Timber, Part 1: Performance Requirements and Minimum Protection Requirements*, Standards New Zealand, 1998.

SNZ. AS/NZS 1328.2: 1998, *Glued Laminated Structural Timber, Part 2: Guidelines for AS/NZS 1328.1 for the Selection, Production and Installation of Glued Laminated Structural Timber*, Standards New Zealand, 1988.

SNZ. AS/NZS 1170.0: 2002, *Structural Design Actions, Part 0: General Principles*, Standards New Zealand, 2002.

SNZ. AS/NZS 1170.1: 2002, *Structural Design Actions, Part 1: Permanent, Imposed and Other Actions*, Standards New Zealand, 2002.

SNZ. NZS 3101: 2006, *Concrete Structures Standard, Part 1: The Design of Concrete Structures*, Standards New Zealand, 2006.

SNZ. AS/NZS 2754.1: 2008, *Adhesives for Timber and Timber Products, Part 1: Adhesives for Manufacture of Plywood and Laminated Veneer Lumber (LVL)*, Standards New Zealand, 2008.

SNZ. AS/NZS 2098.2: 2012, *Methods of Test for Veneer and Plywood, Method 2: Bond Quality of Plywood (Chisel Test)*, Standards New Zealand, 2012.

SNZ. AS/NZS 2269.0: 2012, *Plywood – Structural, Part 0: Specifications*, Standards New Zealand, 2012.

Spellman, P.M. "The Fire Performance of Post-Tensioned Timber Beams", Master's Thesis in Civil Engineering, University of Canterbury, Christchurch, New Zealand, 2012.

STIC. Structural Timber Innovation Company Summary Document, www.stic.co.nz, accessed August, 2009.

Tabaddor, M. "Modeling the Thermal and Structural Behavior of Wood Beams in a Fire Environment", Corporate Research Report, Underwriters Laboratories Inc., Northbrook, IL, USA, 2011.

Takeda, H. "Effect of Insulation on the Fire Resistance of Wood-Framed Floor Assembly", *Proc. The 11th World Conference on Timber Engineering*, Riva del Garda, Italy, June 20-24, 2012.

Thomas, G.C. "Fire Resistance of Light Timber Framed Walls and Floors", Doctoral Thesis in Fire Engineering, University of Canterbury, Christchurch, New Zealand, 1996.

Tsai, K., Buchanan, A.H., Moss, P.J., and Carradine, D.M. "Charring Rates for Different Cross Sections of Laminated Veneer Lumber (LVL)", Master's Thesis in Civil Engineering, University of Canterbury, Christchurch, New Zealand, 2010.

Tsai, K., Carradine, D.M., Moss, P.J., and Buchanan, A.H. "Charring rates for double beams made from laminated veneer lumber (LVL)", *Fire and Materials*, Volume 37, Issue 1, pp. 58-74, 2013.

Twilt, L., and Witteveen, J. "The fire resistance of wood-clad steel columns", *Fire Prevention Science and Technology*, Volume 11, pp. 14-20, 1974.

Van Beerschoten, W.A. "Structural Performance of Post-Tensioned Timber Frames in Non-Seismic Areas", Doctoral Thesis in Civil Engineering, University of Canterbury, Christchurch, New Zealand, 2013.

Weatherwax, R.C., and Stamm, A.J. "The Coefficients of Thermal Expansion of Wood and Wood Products", Report No. 1487, Forest Products Laboratory, Madison, WI, USA, 1956.

Werther, N., Merk, M., Stein, R., and Winter, S. "Fire Safe Service Installations in Timber Buildings", *Proc. The 12th World Conference on Timber Engineering*, Auckland, New Zealand, July 16-19, 2012.

Werther, N., O'Neill, J.W., Spellman, P.M., Abu, A.K., Moss, P.J., Buchanan, A.H., and Winter, S. "Parametric Study of Modelling Structural Timber in Fire with Different Software Packages", *Proc. 7th International Conference on Structures in Fire*, Zurich, Switzerland, June 6-8, 2012.

Williams, M.S., and Todd, J.D. *Structures – Theory and Analysis*, Palgrave Macmillan, New York, NY, USA, 2000.

White, R.H. "Charring Rates of Different Wood Species", Doctoral Thesis in Forestry, University of Wisconsin, Madison, WI, USA, 1988.

White, R.H. *The SFPE Handbook of Fire Protection Engineering: Analytical Methods for Determining Fire Resistance of Timber Members*, National Fire Protection Association, Quincy, MA, USA, 2002.

White, R.H. "Fire Resistance of Wood Members with Directly Applied Protection", *Wood Design Focus*, Volume 19, No. 2, pp. 13-19, 2009.

White, R.H., and Dietenberger, M.A. *The Wood Handbook – Wood as an Engineering Material: Fire Safety of Wood Construction*, Centennial Edition, Forest Products Laboratory, Madison, WI, USA, 2010.

Wiedenhoeft, A. *The Wood Handbook – Wood as an Engineering Material: Structure and Function of Wood*, Centennial Edition, Forest Products Laboratory, Madison, WI, USA, 2010.

Yeoh, D. "Behaviour and Design of Timber-Concrete Composite Floor System", Doctoral Thesis in Civil Engineering, University of Canterbury, Christchurch, New Zealand, 2010.